DIPLOMARBEIT

Harmonic Scattering of Multi Phase Integer and Fractional Slot Windings

eingereicht an der
Technischen Universität Wien
Fakultät für Elektrotechnik und Informationstechnik

zur Erlangung des akademischen Grades eines
Diplomingenieurs

unter der Leitung durch

Ao.Univ.Prof. Dipl.-Ing. Dr.techn. Erich Schmidt
Institut für Energiesysteme und Elektrische Antriebe

von

David Alexander Lackner BSc
Matr.Nr. 01325072
Rautenstrauchgasse 5, 1110 Wien

Wien, im Mai 2022

Erklärung

Hiermit erkläre ich, dass die vorliegende Arbeit ohne unzulässige Hilfe Dritter und ohne Benutzung anderer als der angegebenen Hilfsmittel angefertigt wurde. Die aus anderen Quellen direkt oder indirekt übernommenen Daten und Konzepte sind unter Angabe der Quelle gekennzeichnet.

Die Arbeit wurde bisher weder im In- noch im Ausland in gleicher oder in ähnlicher Form in anderen Prüfungsverfahren vorgelegt.

Wien, im Mai 2022

David Alexander Lackner BSc

Kurzfassung

Die Diplomarbeit beschäftigt sich mit der mathematischen Formulierung der Oberwellenstreuung von Wicklungen elektrischer Maschinen mit ausgeprägten Strängen für eine variable Strang- und Lochzahl. Die Oberwellenstreuung ist ein bedeutender Parameter für Vorausberechnung und Entwurf von Ankerwicklungen sowie auch für die Beschreibung des räumlichen Verlaufs der Felderregerkurve im Luftspalt einer elektrischen Maschine mit ausgeprägten Strängen. Im Rahmen der Arbeit liegt der Schwerpunkt auf Wicklungen mit zwei Strängen und weiter bei beliebig ungeraden Strangzahlen. Ziel ist es, sofern möglich, eine allgemein analytische Methode zur Beschreibung der Oberwellenstreuung solcher Wicklungen aufzustellen. Dies wird für Ganzlochwicklungen analytisch und Bruchlochwicklungen algorithmisch entwickelt.

Nach einer Einführung in die Grundlagen der Ankerwicklungen mit ausgeprägten Strängen folgt eine ausführliche Beschreibung des Wicklungsfaktors, insbesondere die Grundwellen im Luftspalt betreffend, weil dieser eine wichtige Funktion bei der Berechnung der Oberwellenstreuung einnimmt. Für die mathematische Formulierung der Oberwellenstreuung werden mehrere Ansätze aus der älteren Literatur für zwei- und dreisträngige Anordnungen verglichen und in einer einheitlichen Nomenklatur neu beschrieben. Eine verallgemeinerte Form, insbesondere für beliebig ungerade Strangzahlen, basierend auf den Nutdurchflutungen der Ankerwicklung und dem *Görges Polygon* ermöglicht für strangsymmetrische Ganzlochwicklungen die direkte Berechnung der Oberwellenstreuung in Abhängigkeit der Parameter Strangzahl, Lochzahl, Schichtzahl, Zonenbreite und Sehnung der Spulen. Für Bruchlochwicklungen mit deren vielfältigen Parametern hingegen errechnet ein Algorithmus die Oberwellenstreuung über eine Bestimmung der Nutdurchflutungen ausgehend vom *Tingley-Schema* und dann wiederum mittels des *Görges Polygons*.

Im Rahmen einer Auswertung werden die Strangzahlen zwei, drei, fünf und sieben für Ganzlochwicklungen und Bruchlochwicklungen einschließlich einiger ausgewählter Zahnspulenwicklungen untersucht. Eine Evaluierung der Ergebnisse zeigt, dass eine große Lochzahl einerseits und eine erhöhte Strangzahl andererseits signifikanten Einfluss auf die Verringerung der Oberwellenstreuung haben.

Abstract

This diploma thesis deals with the mathematical formulation of the harmonic scattering of electric machines with an poly-phase armature winding with a various number of phases as well as a variable number of slots per pole and phase. The harmonic scattering is one of the most important parameter with the preliminary calculations and the design of armature windings as well as for describing the distribution of field exciter curve along the circumference within the air-gap of poly-phase electrical machines. Within the thesis, the focus is set on windings with two phases and with an arbitrary odd number of phases. The aim is to establish a general analytical method for describing the harmonic scattering phenomenon of such windings. This is carried out fully analytical for integer slot windings and by introducing an algorithmic method for fractional slot windings.

The thesis starts with an introduction to the basics of armature windings with distinct phases. Subsequently, a detailed description of the winding factor, in particular for the fundamental harmonics, is given because of the important role for calculating the harmonic scattering coefficient. For the mathematical formulation of the harmonic scattering coefficient, several approaches from older literature for two and three phase systems were compared and described in a uniform nomenclature. A generalized form, partiscularly for an arbitrary odd number of phases, based on the magnetomotive force in the slots and the *Görges Polygon* is established to calculate the harmonic scattering coefficient. For integer slot windings, various values of the number of phases, number of slots per pole and phase, number of layers, zone span as well as pitch of the winding coils are considered. For fractional slot windings with their manifold parameters, an algorithm is solving the harmonic scattering via a determination of the magnetomotive force of the slots based on the *Tingley-Scheme* and then again via the *Görges Polygon*.

In the course of an evaluation, phase numbers of two, three, five and seven are investigated for integer and fractional slot windings, thereby including some selected tooth coil windings. A conclusion of the results shows that a larger number of slots per pole and phase on the one hand and an increased number of phases on the other hand have significant effects on the reduction of the harmonic scattering.

Acknowledgements

I would like to thank Ao.Univ.Prof. Dipl.-Ing. Dr.techn. Erich Schmidt from the Institute of Energy Systems and Electrical Drives at the Vienna University of Technology for giving me the opportunity to write a diploma thesis in the field of electrical machines. His lectures influenced my interest in electric machines significantly. During the course of my work I was able to expand and deepen the knowledge gained there enormously through numerous conversations with him and explanations, tips and feedback from him.

Of course, a special thank you goes to my mother and father, who made it possible for me to complete my studies in electrical engineering and who supported me in all the time wherever possible.

An important constant from the time of my studies should also be mentioned: The study group that existed practically from the beginning with my colleagues Andreas, Clara, Daniela and Peter and also many other friends as well as colleagues from my studies. Together we were able to complete some exam preparations as a team – Thank you all!

Life is and will ever remain an equation incapable of solution,
but it contains certain known factors.
Nikola Tesla (1856 – 1943).

Table of Contents

Mathematical Symbols

Symbol	Definition	Unit
$\mathscr{A}$	surface	m^2
A	current sheet density	$\mathrm{A\,m^{-1}}$
a	number of parallel winding branches	1
B	magnetic flux density	T
B_Q	magnetic flux density of a slot	T
$\hat{B}_\delta$	amplitude of B in the air-gap	T
$\mathscr{C}$	curve	m
c	wave velocity	$\mathrm{m\,s^{-1}}$
D	diameter of the armature	m
E	electric field strength	$\mathrm{V\,m^{-1}}$
f	frequency	Hz
f	slot spacing between coils	1
G	number of coil groups of the winding	1
g	integer value	1
H	magnetic field strength	$\mathrm{A\,m^{-1}}$
I	electric current	A
$\hat{I}$	amplitude of the electric current	A
I_k	electric current of the k-th phase	A
i	count variable	1
J	electric current density	$\mathrm{A/m^2}$
j	imaginary unit	1
k	count variable	1
L	inductance	H

Symbol	Definition	Unit
l_{Fe}	active length of the iron core	m
m	number of phases	1
N	turns of a coil	1
N_S	number of turns of a phase	1
n	maximum number of count	1
n_S	number of coils per phase	1
p	number of pole pairs	1
Q	total number of slots	1
q	number of slots per pole and phase	1
q_e	proper nominator of q	1
q_g	integer part of q	1
q_n	denominator of q	1
q_z	improper nominator of q	1
R	resistance	Ω
R_g	diameter of inertia of the *Görges Polygon*	1
R_ν	diameter of inertia of the ν-th harmonic	1
$r_{polycirc}$	radius of the *Görges Polygon*	1
s	length	m
T	number of non equal phasors	1
t	time	s
t	number of equal phasor positions	1
t	number of zones within a coil group	1
t'	auxiliary quantity for the *Tingley-Scheme*	1
U	electric voltage	V
U_{coil}	coil voltage	V
U_{cs}	coil side coltage	V
U_G	voltage of a coil group	V
U_Z	voltage of a winding zone	V
U_{phase}	voltage of a phase	V
$U_{polygon}$	circumference of the *Görges Polygon*	1
$\mathscr{V}$	volume	m^3
V	magnetomotive force	A
V_{AF}	auxiliary factor of V in slots	1
V_{max}	maximum value of V	A
V_Q	magnetomotive force of a slot	A
$\hat{V}_{k,\nu}$	$\hat{V}$ for the k-th phase and ν-th harmonic	A
W	coil width	m

Symbol	Definition	Unit
W	magnetic energy	W s
W_1	magnetic energy of the fundamental wave	W s
X_h	main reactance	Ω
X_o	scattering reactance	Ω
X_δ	air-gap reactance	Ω
x	coordinate in direction of propagation	m
x	part of α_Q	rad
y_G	slot step between two coil groups	1
y_Q	slot step	1
y_ε	shortening step	1
y_σ	coil step	1
z	nuber of coil groups	1
z_Q	number of conductors per slot	1
z_W	number of conductors of the armature	1
α	angle between phasors of adjacent slots	rad
α	phase shift of coil voltages	rad
α	pivot angle	rad
α'	angle between T phasors	rad
α_e	electric angle of a phase	rad
α_Q	slot angle	rad
α_z	zone angle	rad
α_ν	angle between phases of ν-th harmonic	rad
$\alpha + \beta$	pivot angle	rad
γ	number of coils per phase	1
δ	air-gap of the machine	m
ε	complementary number to σ	1
ζ_i	certain coil group	1
Θ	magnetomotive force	A
λ	wave length	m
μ_0	permeability of free space	(Vs)/(Am)
ν	wave order	1
ξ_ν	total winding factor	1
ξ_σ	pitch factor	1
$\xi_{\sigma,\nu}$	pitch factor of the ν-th harmonic	1
$\xi_{D,\nu}$	distribution factor of the ν-th harmonic	1

Symbol	Definition	Unit
$\xi_{G,\nu}$	group factor of the ν-th harmonic	1
$\xi_{Z,\nu}$	zone factor of the ν-th harmonic	1
$\xi_{ZV,\nu}$	zone reduction factor of the ν-th harmonic	1
$\xi_{phase,\nu}$	phase factor of the ν-th harmonic	1
σ	coil pitch	1
σ_o	harmonic scattering coefficient	1
τ_P	pole pitch	m
τ_Q	slot pitch	m
Φ	magnetic flux	Wb
Φ_{pole}	magnetic pole flux	Wb
Φ_{coil}	magnetic coil flux	Wb
Φ_V	magnetic linkage flux	Wb
φ_U	phase angle of the electric voltage	rad
ω	angular frequency	1/s
ω_1	angular frequency of the fundamental wave	1/s
$\mathbb{N}$	set of natural numbers	
$\mathbb{N}_{even}$	set of natural even numbers	
$\mathbb{N}_{odd}$	set of natural odd numbers	
$\mathbb{N}_0$	set of natural numbers including 0	
$\mathbb{Q}$	set of rational numbers	

1 Introduction and Motivation

The subject of scattering phenomenons of electric machines plays an important role in their design. The term can be divided mainly into slot scattering, tooth head scattering, end winding scattering, pole scattering and harmonic scattering. The latter will be the main topic of this thesis.

The harmonic scattering can be seen as one of the most important parameter to describe the courses of the magnetomotive force in the air-gap of an electrical machine. Further, the harmonic scattering depends on the winding factors of all harmonics and therefore also on the design of the windings.

While electric drives were used for many years on two and three phased designs, recent reports repeatedly point to considerations of multi phase arrangements of odd phase numbers for vehicle drives. It is expected to reduce the acoustic properties of a machine in addition to a quieter run (lower vibration torque) if properly designed.

Preliminary calculations are necessary for an assessment of possible benefits, including evaluations of the harmonic scattering coefficients.

1.1 Definition of Task

The aim of this work is to reroll the topic around the term of harmonic scattering. On the one hand, the notation of literature, some of which dates back many years, should be standardized and rewritten in accordance with today's standard.

On the other hand, it shall be tried to apply the formal approaches previously established only for two and three phased machines with integer slot windings for five and seven phased arrangements, or to obtain a general, closed form for any odd number of phases.

The third part of this work is dedicated to selected fractional slot windings. It is investigated to what extent closed solutions for the harmonic scattering can be specified at all.

In addition to the determination of the formal correlations, a detailed evaluation of the coefficients of the harmonic wave scattering for the odd phase numbers three, five, seven and - due to the wide spread - also for the phase number of two can be found in the appendix.

1.2 Literature Review

The basic literature relevant to electrical machinery is covered by Rudolf Richter in five volumes. One part deals exclusively with the windings of electric machines (Richter (1952)). A detailed description of scattering phenomena is given in the volume "Induktionsmaschinen" (Richter (1954)).

Of particular importance are the four books on windings of electrical machines written by Heinrich Sequenz in the 1950s. In particular, the volume "Wechselstromwicklungen" (Sequenz (1950)) was of interest in which, starting from single layer integer slot windings, moves on to selected relevant three phase fractional slot windings, which are presented in addition to the analytical side also via corresponding winding schemes.

The book of Wladimir Schuisky "Berechnung elektrischer Maschinen" (Schuisky (1960)) offers a compact summary on the subject of calculating electric machines, in particular scattering phenomena.

Among more modern works, the works of Germar Müller, Karl Vogt and Bernd Ponick (Müller et al. (2007)) are mentioned, as well as the book published in English by Juha Pyrhönen, Tapani Jokinen and Valéria Hrabovcová (Pyrhönen et al. (2008)).

With regard to the basics of windings of electric machines in general, mention should be made of the already older works of Franz Heiles (Heiles (1953)) and Theodor Königshofer (Königshofer (1956)).

A broad overview of feasible winding designs including the corresponding winding schemes can be found in the book "Der Katechismus für die Ankerwickelei" by Fritz Raskop (Raskop (1964)). However, newer technologies such as tooth winding designs are not represented here.

In addition to the above mentioned works, the publications of Robert Baffrey (Baffrey (1926)) and Milan Krondl (Krondl (1928)) were an important support for the abstraction of the harmonic scattering coefficient of phase numbers greater than three.

The wide scope of fractional slot windings cannot be fully dealt with in this thesis. Some restrictions will be made in this respect in later chapters. In addition to the literature mentioned so far, it is worth mentioning the elaborations of Michael Liwschitz (Liwschitz (1946) and Liwschitz (1949)), who dealt intensively with this type of winding in the 1940s. With regard to works from today's time, mention should also be made of the studies by Antonio Di Tommaso (Di Tommaso et al. (2018)).

Finally, the basic literature of electrical engineering by Adalbert Prechtl (Prechtl (1994)), which was frequently used in the course of studies, as well as the lecture notes on electrical machines by the supervisor of this thesis, Erich Schmidt (Schmidt (2020) and Schmidt (2021)), should not be unmentioned.

2 AC Armature Windings

2.1 Electric Conductors and their Magnetic Field

If a current passes through an electrical conductor, a magnetic field is set around the conductor. The direction of the field lines depends on the direction of the current. The magnetic field lines always enclose the conductor to the right in relation to the current direction, see figure 2.1. By convention, the direction of the current is understood as coming out of the plane by the symbol $\odot$ and as flowing into the plane by the symbol of $\otimes$ (Königshofer (1956)).

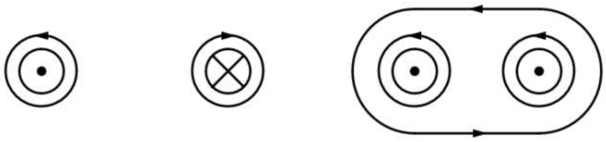

Figure 2.1: The relationship between the direction of the current and the resulting magnetic field (Königshofer (1956)).

In the case of two conductors not flowing in the same direction, the field lines between the conductors are identical – the conductors repel each other. If two (or more) conductors have flowed in the same direction by the current, the field lines between the conductors show different directions – the conductors attract each other. Because of this force effect, the coils of an armature must have sufficient mechanical strength.

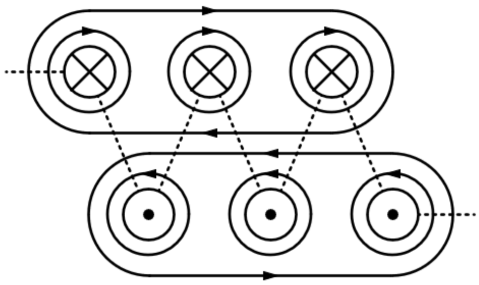

Figure 2.2: Simplified illustration of the magnetic field of a cylinder coil according to Königshofer (1956).

When a loop is formed out of a conductor, a coil is created. Depending on the number of loops a number of coils result in a winding. Inside the coil, a uniform magnetic field is created. Its field lines close on the outside of the coil (figure 2.2). The effect of the magnetic field is significantly enhanced when the magnetic field lines are passed over a laminated iron core.

2.2 Symmetrical Poly Phase Systems

With electric rotary field machines, a distinction is made between temporal and spatial phase shifts $\Delta\alpha_e = \pm\pi$. However, since spatial phase shifts do not represent an effect of their own, they are not included in the phase number. The following is an overview of possible cases of phase numbers:

- Windings with an **odd number of phases** ($\mathbf{m \geq 3}$) always result in so called complete systems. In time harmonic operation, the common star point wire does not link current and can therefore be omitted.
- Windings with **even number of phases** and whose phase number has at least one **odd divisor** ($\mathbf{m \geq 6}$) can be described by spatially phase shifted complete subsystems. In time harmonic operation, the common star point wire is regrettably powerless and can therefore also be omitted with this variant.
- Windings with **even number of phases** and whose phase number **does not have an odd divisor** (**exponentiations of two**) necessarily require a star point wire for the formation of the independent phases. Here, the star point wire leads current also in time harmonic operation.

From these three variants, the spatial phase shift can generally be determined as a function of the number of phases. Thus, for an odd number of phases

$$\Delta\alpha_e = \frac{2\pi}{m} \quad , \quad m \in \mathbb{N}_{odd} \tag{2.1}$$

is valid (Schmidt (2021)), while for an even number of phases

$$\Delta\alpha_e = \frac{\pi}{m} \quad , \quad m \in \mathbb{N}_{even} \tag{2.2}$$

is valid (Schmidt (2021)).

In the course of this work systems with odd phase numbers are primarily investigated. An exception here is the phase number of two, which is also examined because of its practical importance.

2.3 Basics of Armature Windings

The windings of armatures play an essential role in electric machines. From a mathematical point of view, the function and effect of the windings are described by the *Faraday's law of induction* on the one hand and the *Ampère's circuital law* on the other. Particularly important in windings regarding voltage and current is the concept of the interconnection of individual coils (in series or parallel) to a winding – thus a coil is the original form of a winding. In addition, there are some concepts and mathematical approaches to the design of the windings which serve to describe the different types of windings in detail. This chapter introduces the most important terms for AC windings.

2.3.1 Faraday's Law

The law of induction describes the relationship between the magnetic flux Φ and the electric voltage U of a conductor loop. With a time-changing magnetic flux (change of the flux itself or movement of the conductor loop) passing through a surface $\mathscr{A}$ the electric voltage is equal to its negative rate of change and is right-handed assigned to the shape of the surface $\partial\mathscr{A}$ (Prechtl (1994)).

In mathematical terms in global form by the use of U and Ψ:

$$U\left(\partial\mathscr{A}\right) = -\frac{d\Phi\left(\mathscr{A}\right)}{dt} \tag{2.3}$$

And in local form, for non moving arrangements, by the use of the electric field strength E and the magnetic flux density B:

$$\nabla \times \mathbf{E} = -\frac{\partial \mathbf{B}}{\partial t} \tag{2.4}$$

The flux given in equation (2.3) corresponds to the magnetic linkage flux Φ_V. Its rate of change depends on the time-varying air-gap field between stator and rotor. According to Prechtl (1994), equation (2.5) and figure 2.3 show the situation by means of a winding simplified as a conductor loop with a resistance R.

$$U = R\,I + \frac{d\Phi_V}{dt} \tag{2.5}$$

Herein, the voltage U must reside outside of the region of the time-varying magnetic field.

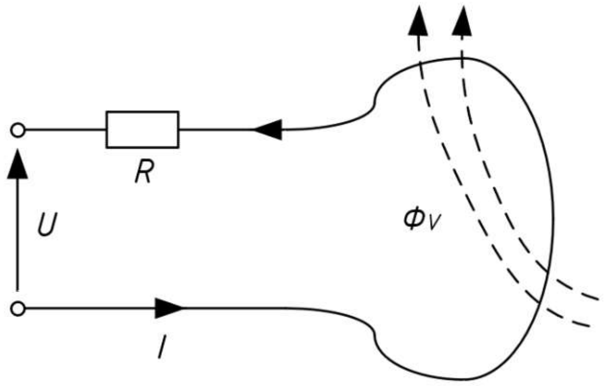

Figure 2.3: Assignment of the sign convention in the sense of equation (2.5) for a conductor loop traversed by a chaining flow. Voltage U, current I and flux linkage Φ_V are arranged right-handed according to the passive sign convention.

2.3.2 Ampère's Law

The Ampère's circuital law is valid for current distributions when the effects of time-varying charge distributions can be neglected. This means, on the one hand, that any change in the electric field does not affect the magnetic field, and on the other hand, possible displacement currents are disregarded. In words the law means that magnetomotive force V along the edge of a surface $\mathscr{C} = \partial\mathscr{A}$ is equal to the total value of the current I passing through a surface $\mathscr{A}$ (Prechtl (1994)). The direction of circulation of the area corresponds to a right-handed assignment with respect to the current, see figure 2.4. The geometric shape of the surface $\mathscr{A}$ is irrelevant, any surface with an equivalent edge carries the same current.

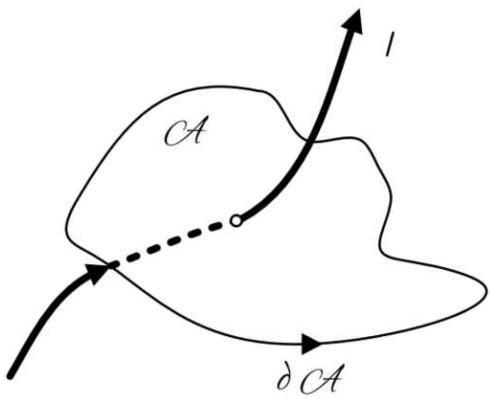

Figure 2.4: Illustration of the Ampère's circuital law. The random shaped surface $\mathscr{A}$ is forced by the current I. The magnetomotive force is given by the right-handed shape $\partial\mathscr{A}$.

In mathematical terms in global form by the use of V and I:

$$V(\partial\mathscr{A}) = I(\mathscr{A}) \tag{2.6}$$

And in local form, for non moving arrangements, by the use of the magnetic field strength H and the current density J:

$$\nabla \times \mathbf{H} = \mathbf{J} \tag{2.7}$$

In terms of windings, the total current through a surface means a coil with N turns and is represented by the magnetomotive force with:

$$\Theta = N\, I \tag{2.8}$$

A coil, depending on its number of turns N, is in general forced through several times by a magnetic flux which does not necessarily have to be the same magnetic flux with each turn. Thus, the magnetomotive force Θ acts as an excitation for the total linkage flux Φ_V. But the assumption that this linkage flux is proportional to the number of turns is only an approximation.

2.3.3 Terms for Coils and Armature Windings

Armature windings of AC machines are designed as distributed windings which are inserted into the slots of an armature. The armature is mostly laminated using high-permebale iron sheets. Those parts of the coil that are located in the slots are referred to as *coil sides*, those outside, called *end winding region*, are referred to as *coil ends* or *end winding*. The geometric centerline of a coil is called *coil axis*. A coil always exists out of two coil sides and at least one end winding (Heiles (1953)).

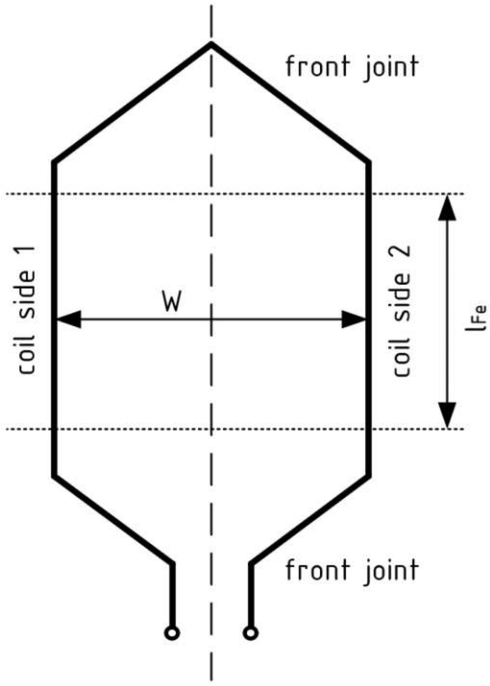

Figure 2.5: Sketch of a coil for armature windings according to Schmidt (2021).

As pictured in figure 2.5, the distance between the two coil sides is referred to as *coil width* W. In case of a *full pitched* coil, the coil width is equal to the *pole pitch*

$$\tau_P = \frac{\pi\, D}{p}, \tag{2.9}$$

where p is representing the number of *pole pairs* and D is the *diameter of the armature*. The length of a coil side in a slot is named *active length* of the iron core l_{Fe} and is responsible, among other things, for the induction of the voltage. The direction of the current of the first coil side is always in opposite direction to the curent of the second coil side.

As an armature usually consists of more than one coil or two slots, coils are distributed equally spaced along the circumferential direction according to the *slot pitch*

$$\tau_Q = \frac{\pi\, D}{Q}, \tag{2.10}$$

while Q is the total number of slots of an armature. In symmetrical structures, armature windings have (phasewise) the same number of turns N (Schmidt (2021)).

The coil width can also be expressed equally via the slot step $y_Q \in \mathbb{N}$. This indicator describes the progress of the coils in perimeter direction with respect to the total number of slots Q.

2.4 Layers of Windings and Winding Zones

The terms *winding layers* and *winding zones* also play an important role in the description and dimensioning of armature windings. While the selection of the number of layers directly describes a constructive property, the assignment of winding zones facilitates the conception of the mathematical description of the winding.

2.4.1 Number of Layers

In general, a distinction is made between single and double layer armature windings. Windings with more than two layers are rarely performed and are not discussed here.

With an ordinary single layer winding there is only one coil side per slot (figure 2.6 left). The number of conductors per slot is therefore $z_Q = N$, where N is the number of turns of a coil (Schmidt (2021)).

Double layer windings always carry two coil sides, which are arranged on top of each other (figure 2.6 right), the number of conductors per slot is usually $z_Q = 2\,N$ (Schmidt (2021)). A distinction is made between the bottom layer (side of the coil lying at the ground of the slot) and the upper layer (side on the top of the slot). Each coil always has one coil side in the upper and one in the bottom layer. The mean coil width is therefore usually always constant (Heiles (1953)). The big advantage over single layer winding is the possibility of an easy pitching (equal to a shift of upper layer against the bottom layer) resulting in a zone shift.

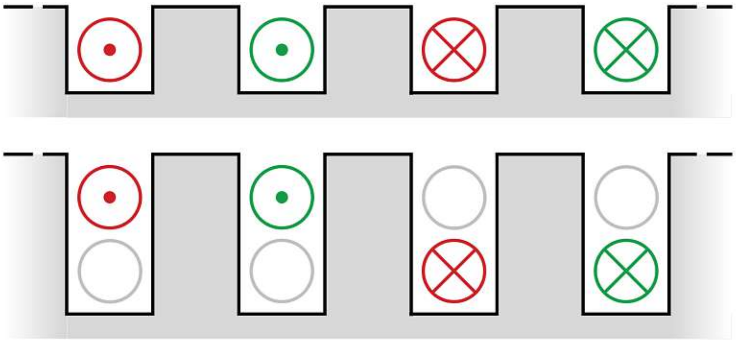

Figure 2.6: Linear sketch of the slots of an armature winding with single layer (top) and double layer (bottom) windings.

2.4.2 Winding Zones

When connecting several coils to a coil group, all coils of the coil group must be connected in series due to the spatial phase shift between the coils. The coil sides of such a coil group with the same current orientation in one direction form a so called *winding zone*. Furthermore, the term of winding zone can be divided into the types of windings with *normal zone span* and windings with *double zone span*. For simplicity, integer slot windings are considered for the description of normal and double zone spans.

Normal Zone Span

Windings with normal zone span are interpreted in such a way that each of the m phases has two zones within each layer along one pole pair, which are always spatially offset to each other by a pole pitch τ_P. Within each zone there is a coil group with a certain, equal, number of q coils. This results in a natural division of zones.

In the case of double layer windings, there is also the possibility of pitching (see chapter 2.6). This is achieved by a shortening step y_ε which twists the two layers to each other without changing the distribution of the zones in the layers. Thus, the symmetry axes of the phases between each other are retained.

Windings with an even number of phases m can only be realized as windings with a normal zone span due to their angular offset of the phases α_e, see equation (2.2).

Double Zone Span

Windings with double zone span are interpreted in such a way that for each of the m phases there is only one zone within each layer along one pole pair with a coil group consisting of $2q$ coils available. Here, a natural zoning is created, too. A special feature compared to windings with normal zone span is that phases with the same direction always follow one another.

Windings with double zone span can only be executed as double layer windings, again with the possibility of pitching (see chapter 2.6). This is again achieved by a shortening step $|y_\varepsilon|$ which twists the two layers to each other. The immanent antisymmetry between the poles of one pole pair τ_P of a double zone span winding gets lost when pitching is applied.

2.4.3 Examples for Winding Zone Plans

Zone plans can also be displayed ring shaped or flat, as the following part will show – the information content is the same (Heiles (1953)). For integer slot windings, each zone plan extends over the double pole pitch $2\,\tau_P$. The coil width W is always the same for each phase and therefore always drawn only for the first phase. For the examples in figures 2.7 to 2.11 with $m = 2$ and 3, each phase has its own colour (1 = red, 2 = green, 3 = yellow) and each zone is also marked with its direction of the current.

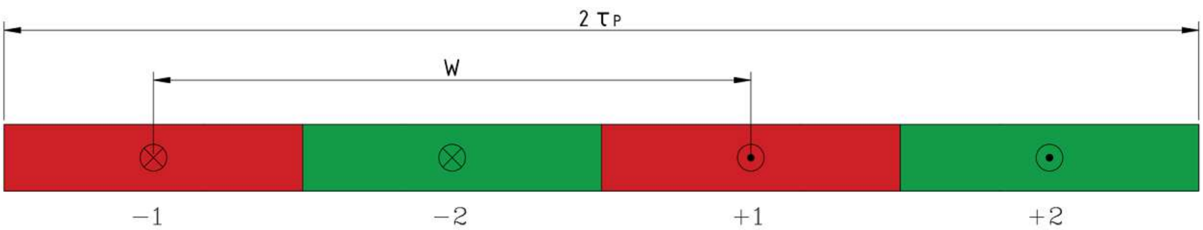

Figure 2.7: Flat zone plan of a single layer armature winding with two phases, full pitch and normal zone span.

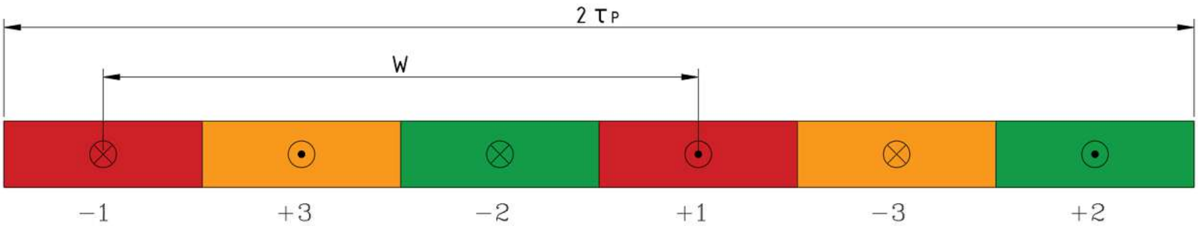

Figure 2.8: Flat zone plan of a single layer armature winding with three phases, full pitch and normal zone span.

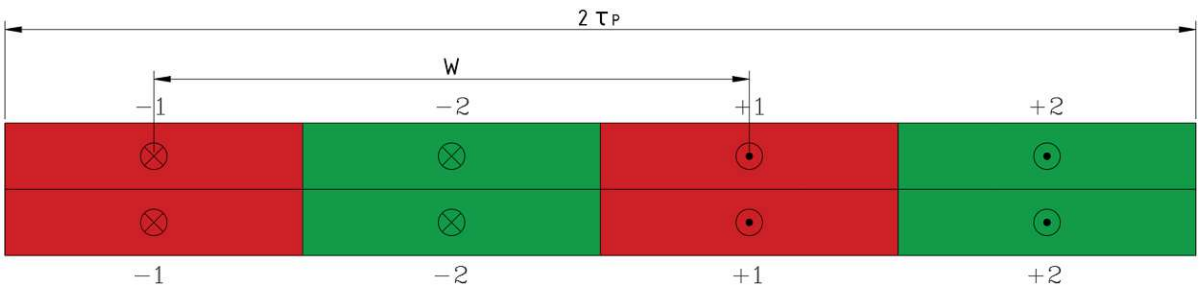

Figure 2.9: Flat zone plan of a double layer armature winding with two phases, full pitch and normal zone span.

2.5 Number of Slots per Pole and Phase

The number of slots per pole and phase q is mostly used to characterize poly phase windings. It is defined as the quotient of the amount of slots Q of the armature by the number of poles $2p$ and phases m:

$$q = \frac{Q}{2p\,m} \tag{2.11}$$

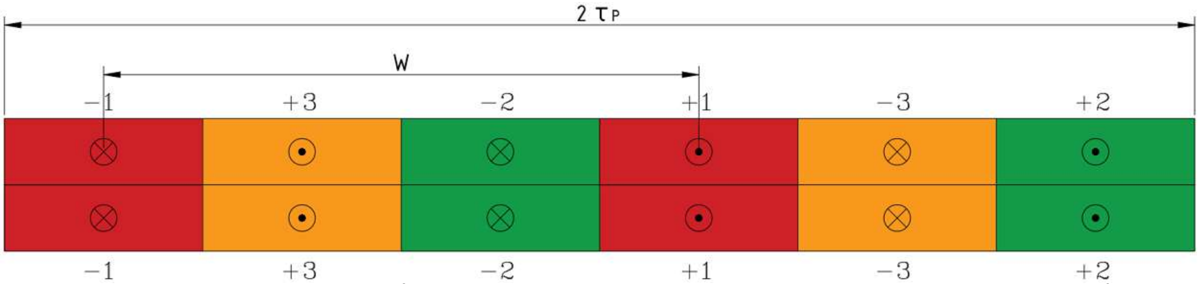

Figure 2.10: Flat zone plan of a double layer armature winding with three phases, full pitch and normal zone span.

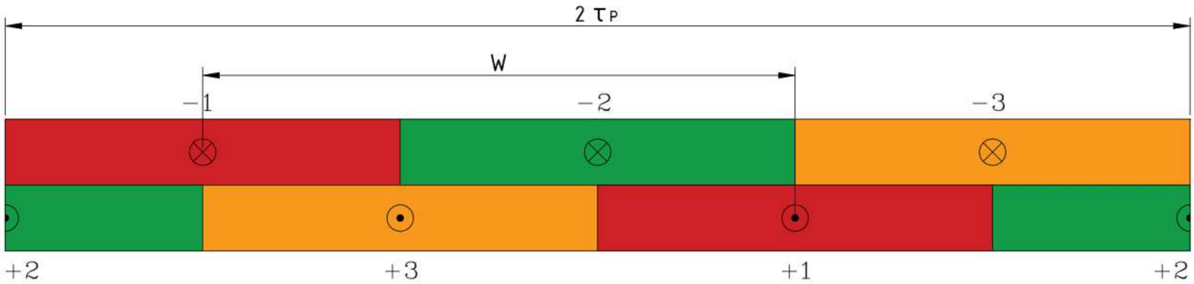

Figure 2.11: Flat zone plan of a double layer armature winding with three phases, full pitch and double zone span.

2.5.1 Integer Slot Windings

If equation (2.11) yields an integer, $q \in \mathbb{N}$, the winding is called an *integer slot winding*. Hereby hold $mq \in \mathbb{N}$ and $2mq \in \mathbb{N}_{even}$. Integer slot windings are the most commonly used for AC windings.

Due to symmetry conditions, not every slot number is possible. The interplay of the numbers of phases, poles and slots must therefore always satisfy the following equation (Schmidt (2021)):

$$\frac{Q}{m} = 2\,p\,q \begin{cases} \in \mathbb{N}_{even} & \text{, single layer} \\ \in \mathbb{N} & \text{, double layer} \end{cases} \tag{2.12}$$

An integer slot winding can be build up symmetrically for any number of pole pairs. The repetition of the slot pattern (base distribution) results for each natural number of slots per pole pair. The m phases can thus be distributed symmetrically along the circumference of the armature with an even number of slots ($2q \in \mathbb{N}_{even}$). The periodic pattern of the repetition also allows a simple implementation of parallel winding branches (Schmidt (2021)).

In practice, integer slot windings can be easily realized. As will be shown in the course of the work, the harmonic scattering is particularly easy to minimise. However, distortions of the magnetomotive force and especially of the induced voltages are a disadvantage.

2.5.2 Fractional Slot Windings

Fractional slot windings have no integer value for q, the number of holes per phase and pole pair is defined as

$$q = \frac{q_z}{q_n} = q_g + \frac{q_e}{q_n} \tag{2.13}$$

with the properties $q \in \mathbb{Q} \setminus \mathbb{N}$, $q_g \in \mathbb{N}_0$ and $(q_e\,,\,q_n) \in \mathbb{N}$ (Schmidt (2021)).

Thereby, the condition

$$\gcd(q_z, q_n) = \gcd(q_e, q_n) = 1 \tag{2.14}$$

must be fulfilled (Müller et al. (2007)). In order to generate a harmonic wave along two pole pitches, in addition

$$\gcd(m, q_n) = 1. \tag{2.15}$$

must be satisfied (Krall (2015)).

With regard to the divisor q_n, there are two types to be distinguished: If q_n is an odd number, this means a *fractional slot winding of first kind*; if q_n is an even number, the winding is called a *fractional slot winding of second kind*. The number of slots per pole and phase must not be a natural number ($mq \notin \mathbb{N}$).

In contrast to integer slot windings, fractional slot windings can only be realized as phase symmetric windings under certain additional conditions. According to Schmidt (2021), these conditions are:

$$\text{possible numbers of } Q \begin{cases} \dfrac{Q}{2m} \in \mathbb{N} & \text{, single layer} \\[2ex] \dfrac{Q}{m} \in \mathbb{N} & \text{, double layer} \end{cases} \tag{2.16}$$

$$\text{possible numbers of } q \begin{cases} \dfrac{p}{q_n} \in \mathbb{N} & \text{, single layer} \\[2ex] \dfrac{2p}{q_n} \in \mathbb{N} & \text{, double layer} \end{cases} \tag{2.17}$$

The big advantage of fractional slot windings is that even with small slot numbers and despite a distorted curve of the magnetomotive force, the induced voltages of the windings have a smoothed, more sinusodial form (Richter (1952)). Furthermore, this also results in a suppression of slot harmonics with open slots (Kucera and Hapl (1956)).

2.5.3 Base Distribution and Base Winding

A base distribution indicates the smallest unit in which the slot distribution is electrically equivalent along the circumference of the armature. For integer slot windings this is given by a pole pair. In contrast to them, the base distribution of fractional slot windings does not necessarily repeat after each pole pair. An exception is given by windings with $q_n = 2$. The following table according to Schmidt (2021) summarizes, sorted by type of winding, the number of base distributions as well as the corresponding number of slots per phase and base distribution.

Table 2.1: Base distribuions of windings.

		number of base distribution	**slots per phase and base distribution**
integer slot winding	$q \in \mathbb{N}$	p	$2q \in \mathbb{N}_{even}$
fractional slot winding first kind	$q_n \in \mathbb{N}_{odd}$	$\frac{p}{q_n} \in \mathbb{N}$	$2q_z \in \mathbb{N}_{even}$
fractional slot winding second kind	$q_n \in \mathbb{N}_{even}$	$\frac{2p}{q_n} \in \mathbb{N}$	$q_z \in \mathbb{N}_{odd}$

A base winding on the other hand describes the smallest unit in which the winding distribution is electrically equivalent. A base winding requires in most cases only one base distribution. However, the exception of this rule are single layer fractional slot windings of the second kind. Due to the fact of $q_z \in \mathbb{N}_{odd}$, a base winding of such fractional slot windings always asks for two base distributions.

2.5.4 Tooth Coil Windings

AC windings with a coil width W of only one slot pitch τ_Q are called *tooth coil windings*. Their number of slots per pole and phase is always smaller than 1 due to their design and therefore belong at all times to fractional slot windings.

Tooth coil windings can be realized in single layer and double layer versions. The single layer winding has one coil side in each slot, the double layer winding two coil sides. Here, the layers are not placed on top of each other as for common double layer windings, but next to each other – a winding always includes one stator tooth (figure 2.12).

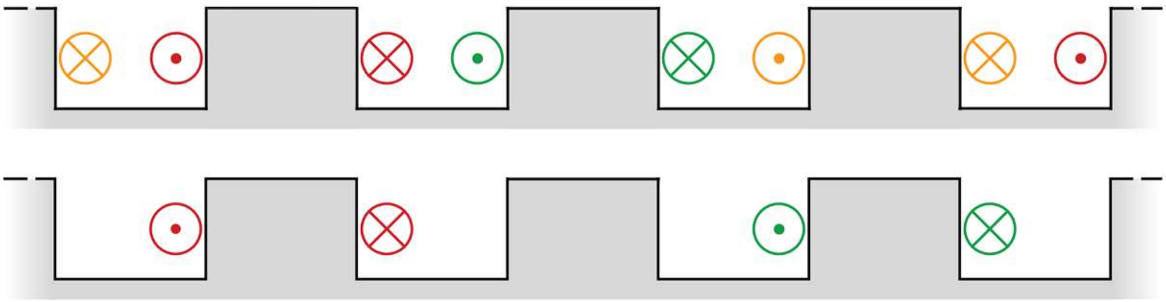

Figure 2.12: Example of the coil arrangement for tooth coil windings as a double layer winding (top) and single layer winding (bottom).

In the case of single layer windings, the following conditions must also be met, which differentiate between even and odd phase numbers (Krall (2015)):

$$\frac{Q}{4\,m} \in \mathbb{N}\,,\; m \in \mathbb{N}_{even} \qquad\qquad \frac{Q}{2\,m} \in \mathbb{N}\,,\; m \in \mathbb{N}_{odd} \tag{2.18}$$

Tooth coil windings are simple and compact to realize. They are widely used in permanent magnet synchronous machines with a high number of pole pairs (Rader (2013)). It should be mentioned beforehand that tooth coil windings generally result in a significantly higher harmonic scattering than conventional distributed windings.

2.6 Coil Pitch

The coil width W of a winding shall always be designed in a way to maximise the utilization of the pole flux. The extent of enclosure is described by the pitch of a coil σ. This can be expressed as a ratio by

$$\sigma = \frac{W}{\tau_P} \tag{2.19}$$

and is limited by the range of $0 < \sigma < 2$. The values $\sigma = 0$ and $\sigma = 2$ are theoretical values. In case of integer slot windings, they represent the case of no enclosure of a magnetic flux, also no harmonics. The value of $\sigma = 1$ is the ideal case with the highest utilization of the pole flux and is called *full pitched*. While values of $1 < \sigma < 2$ mark *long pitched* coils, a value of $0 < \sigma < 1$ stands for *short pitched* coils which is the usual variant of pitching.

According to literature it is also common to use the complementary number to one of σ:

$$\varepsilon = 1 - \sigma \tag{2.20}$$

The range of this definition is given by $-1 < \varepsilon < 1$.

The pitch of a coil can also be expressed by the shortening step y_ε. This is defined by the difference of the product of the number of phases m and the number of slots per pole and phase q minus the slot step y_Q,

$$y_\varepsilon = m\,q - y_Q. \tag{2.21}$$

For integer slot windings $y_\varepsilon \in \mathbb{N}$ and for fractional slot windings $y_\varepsilon \in \mathbb{Q} \setminus \mathbb{N}$ is valid.

Accordingly, the following relationships apply by introducing the coil step y_σ:

$$\begin{aligned} y_\sigma = \sigma\,m\,q \quad &, \quad y_\varepsilon = \varepsilon\,m\,q \\ \sigma + \varepsilon = 1 \quad &, \quad y_\sigma + y_\varepsilon = m\,q \end{aligned} \tag{2.22}$$

For pitching integer slot windings by shifting the winding zones against each other (corresponding to a twist of the two layers to each other), the symmetry axes of the phases between each other are retained. Therefore both signs of y_ε are valid. So for any further calculations $|y_\varepsilon|$ is applied.

It should be mentioned here that the shortening step y_ε is intented to be an integer in the definition just given. But this is not a mandatory condition for the correlations derived in chapter 5 for the calculation of the harmonic scattering coefficient σ_o. Ironless machines are an example of applications of non integer values of the shortening step, even with integer slot windings.

As a supplement with regard to fractional slot windings, the following applies: As given from equation (2.15), such windings must always be pitched. The base distributions of fractional slot windings extend over several polar pairs according to the divisor q_n. When considering two pole pairs with an exception of $q_n = 2$, this necessarily results in a non integer number of slots. As the range for shortening steps y_σ depends on q_n, it is much larger than for integer slot windings. The pitch of the coils can therefore theoretically assume values greater than the classical limit of $\sigma = 2$. As will be shown in the course of the work (see chapter 6.2), there is a theoretically possible pitching range of $0 < \sigma < 2\,q_n$ and a symmetry of the harmonic scattering in relation to the half base winding.

Consequently, tooth coil windings with their coil step $y_\sigma = 1$ are also always pitched (Krall (2015) and Schmidt (2021)). Their coil pitch with regard to the utilization of the pole flux will be limited practically in the range

$$\frac{2}{3} \leq \sigma = \frac{1}{m\,q} \leq \frac{4}{3} \tag{2.23}$$

or rearranged for the number of slots per pole and phase

$$\frac{3}{4\,m} \leq q \leq \frac{3}{2\,m} \tag{2.24}$$

Table 2.2: Number of slots per pole and phase of tooth coil windings.

m	2	3	5	7
$\mathbf{q}_{\min}$	$\frac{3}{8}$	$\frac{1}{4}$	$\frac{3}{20}$	$\frac{3}{28}$
$\mathbf{q}_{\max}$	$\frac{3}{4}$	$\frac{1}{2}$	$\frac{3}{10}$	$\frac{3}{14}$

as listed in table 2.2 in more detail.

When choosing the number of slots per pole and phase in accordance with table 2.1, equation (2.15) has to be observed always. Consequently, among others the following numbers for q are commonly utilized: With two phases $q = 2/3$, $2/5$, $3/5$, $3/7$, $4/7$, $5/7$, $4/9$, $5/9$ and with three phases $q = 1/2$, $1/4$, $2/5$, $2/7$, $3/7$, $3/8$, $3/10$. However, with five phases $q = 1/4$, $1/6$, $2/7$, $2/9$, $2/11$, $3/11$ and with seven phases $q = 1/5$, $1/6$, $1/8$, $1/9$, $2/11$ can be realized.

2.7 Pole Flux and Induced Voltage

For an optimum utilization of the magnetic flux Φ along the pole pitch τ_P and the active length l_{Fe}, a corresponding coil width W is required. In case of electric rotary field machines, the magnetic flux density $B(x)$ of the fundamental wave is spatially harmonious over the entire circumference of the armature. With its wavelength $\lambda = 2\,\tau_P$ the fundamental part of the flux density can be described according to Schmidt (2021):

$$B(x) = \hat{B}_\delta \cos\left(\frac{\pi\, x}{\tau_P}\right) \tag{2.25}$$

In equation (2.25), $\hat{B}_\delta$ represents the amplitude of the magnetic flux density in the air-gap of the machine. The magnetic pole flux Φ_{pole} can now be calculated by integrating the magnetic flux density:

$$\Phi_{pole} = \int_{-\frac{\tau_P}{2}}^{\frac{\tau_P}{2}} B(\tilde{x})\, l_{Fe}\; d\tilde{x} = \frac{2}{\pi}\, \hat{B}_\delta\, l_{Fe}\, \tau_P \tag{2.26}$$

In electric rotating machines, the coil (or winding) moves relative to the distribution of the magnetic flux density with a velocity of $c = \lambda\, f$ corresponding to an angular frequency of $\omega = 2\pi\, f$. According to a coil pitch as defined in equation (2.19) and the pitch factor ξ_σ of chapter 3.1, the magnetic flux of a coil Φ_{coil} can be written as (Schmidt (2021))

$$\Phi_{coil}(x,t) = \int\limits_{ct-\frac{W}{2}}^{ct+\frac{W}{2}} B(\tilde{x})\, l_{Fe}\; d\tilde{x} = \Phi_{pole}\, \xi_\sigma\, \cos(\omega\, t) \tag{2.27}$$

For a coil with N turns and the use of equation (2.3) the voltage of a coil can be derived by (Schmidt (2021)):

$$U_{coil}(t) = -\omega\, N\, \Phi_{pole}\, \xi_\sigma\, \sin(\omega\, t) \tag{2.28}$$

2.8 Voltage Phasor Diagram

By assuming that a sinusoidal shaped voltage is induced within armature windings (or single coils) of a rotary field machine, these can be displayed as phasors for each slot. Each phasor usually has the same absolute value of the voltage, but a different phase position. If the number

$$t = \gcd(Q, p) \tag{2.29}$$

is defined as the greatest common divisor of the number of slots Q and the amount of pole pairs p, t phasors along the whole circumference have the same phase position (Sequenz (1950)). Therefore the phasor diagram consists of

$$T = \frac{Q}{t} \tag{2.30}$$

non phase-equal phasors (Richter (1952)). These phasors have an angle to each other within the diagram of

$$\alpha' = 2\pi\, \frac{t}{Q}. \tag{2.31}$$

The angle between two phasors, which are located in two directly adjacent slots of the armature, is calculated to:

$$\alpha = 2\pi\, \frac{p}{Q} = \alpha'\, \frac{p}{t}. \tag{2.32}$$

The individual phasors for the fundamental wave ($\nu = 1$) are numbered continuously counter-clockwise by a freely chosen first phasor according to the angle α. The circulation is going through t times. For harmonics of the order ν, α is calculated by

$$\alpha_\nu = \nu\, \alpha. \tag{2.33}$$

Figures 2.13 and 2.14 show examples for voltage phasor diagrams.

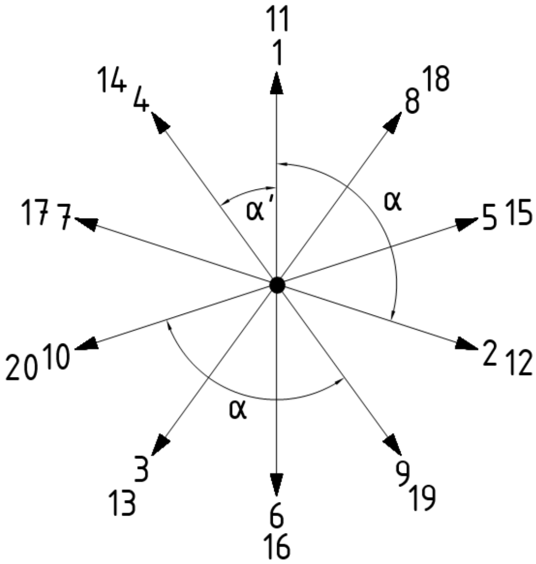

Figure 2.13: Phasor diagram of an armature with $Q = 20$, $T = 10$, $2p = 12$ and $t = 2$. Each line stands for two phasors (two numbers at arrowhead).

2.8.1 Assignment to Phases

The individual coil sides, which are located in the slots of the armature, must be connected to coils (possibly with several turns) via a chosen coil width W. Each coil has a positive and a negative coil side. For an m phase construction, m winding phases must be created. The number of coils per winding phase γ is according to Sequenz (1950):

$$\gamma = \frac{Q}{2\,m} \tag{2.34}$$

For interconnection, the combination shall be selected in such a way that those coils of the same phase have as little phase difference as possible. This achieves the highest possible voltage induced by the coils. An analogous procedure is used for the coil sides of the other phases. In case of an odd number, they are shifted by $2\pi/m$, ..., $(m-1)\,2\pi/m$ relative to the first phase. In case of an even number, they are shifted by half. Figure 2.14 shows an example of building phases.

2.9 Field Exciter Curve

For the investigation of the field exciter curve of an armature winding, only the normal component of the field within the air-gap between stator and rotor is of interest (figure 2.15). The properties of the field within the iron core are mostly neglected (Sequenz (1950)). Graphically, the field exciter curve is mostly shown as a stepped graph.

The excitation of the windings by a time harmonic current for an m phased system can be given as follows (Schmidt (2021)):

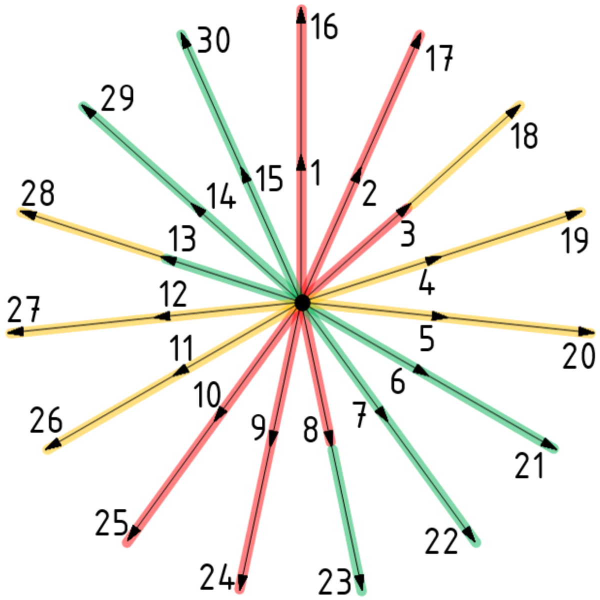

Figure 2.14: Phasor diagram of a three-phase (red, green and yellow) fractional slot winding ($Q = 30$, $2p = 8$, $q = 2,5$).

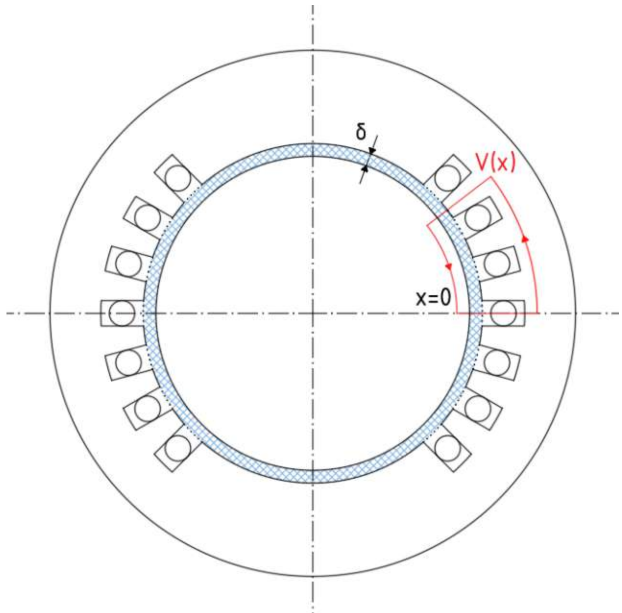

Figure 2.15: Graphical explanation of the definition of the field exciter curve. The point $x = 0$ can be chosen freely due to symmetry.

$$I_k\,(t) = \hat{I}\,\cos\left(\omega_1\,t - (k-1)\,\frac{2\,\pi}{m}\right) \tag{2.35}$$

In equation (2.35) $\hat{I}$ is the amplitude of the current, ω_1 the angular frequency of a symmetrical poly phase system and $k = 1, 2, ..., m$ a certain phase of the system. The zero position of the first phase is freely chosen as zero.

2.9.1 Surface Current Density

If considering a current in the two dimensional plane in relation to a length lying transversely to the direction of the current, this quantity is called the surface current density A, sometimes also denoted as the current sheet (Sequenz (1950)).

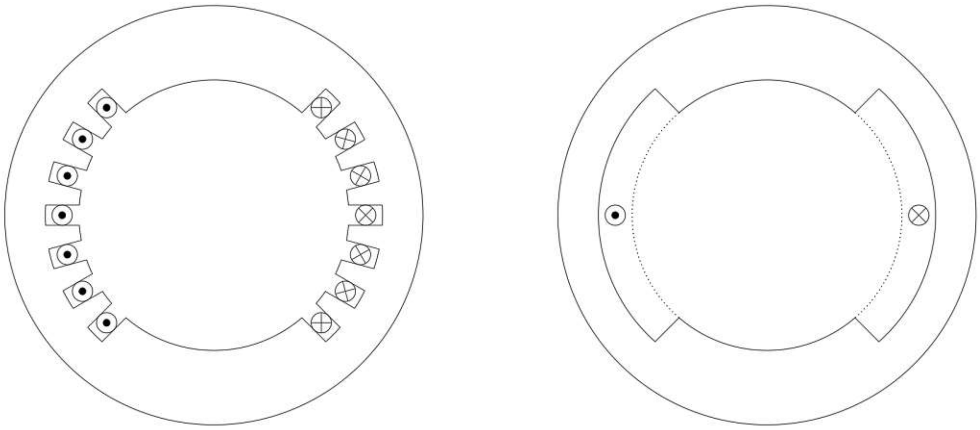

Figure 2.16: Transition from distributed individual conductors (left) to continuous distribution as a condition for the definition of the surface current density (right).

The conductors of an armature winding are usually in slots around the armature circumference, so they are not evenly distributed (figure 2.16, left). The course of the field then corresponds to a stepped shape. Assuming an infinitely large number of slots $q \to \infty$, the current is theoretically evenly distributed within a winding zone along the circumference. Then it is possible to introduce, as mentioned above, A as a current related to a length (figure 2.16, right).

2.9.2 Windings with Normal Zone Span

When considering full pitch windings with normal zone span, no matter whether single layer or double layer version, each zone has the total amount of $q\,z_Q$ conductors, flooded by a current of $I_k\left(t\right)/a$ each. z_Q marks the amount of conductors per slot. According to the "law of winding",

$$z_W = z_Q\,Q = 2\,m\,a\,N_S, \tag{2.36}$$

with the total amount of conductors of the armature winding z_W, the number of parallel conductor branches a and the number of turns of a phase N_S. The maximum value of the magnetomotive force can be written as

$$V_{max} = \frac{q\,z_Q}{2}\,\frac{\hat{I}}{a} = \frac{N_S}{2\,p}\,\hat{I}. \tag{2.37}$$

If the function of the magnetomotive force is subjected to a *Fourier Analysis*, equation (2.38), the amplitudes of the magnetomotive force for the fundamental wave and also the harmonics of the first phase even considering pitching can be expressed according to Schmidt (2021) as in equation (2.39).

$$V_1(x) = \sum_{\nu=1}^{\infty} \hat{V}_{1,\nu} \cos\left(-\frac{\nu\,\pi\,x}{\tau_P}\right) \tag{2.38}$$

$$\hat{V}_{1,\nu} = \frac{2}{\pi}\,\frac{N_S}{p}\,\frac{\xi_\nu}{\nu}\,\hat{I} \tag{2.39}$$

The meaning of the winding factor ξ_ν in equation (2.39) is explained in detail in chapter 3. Furthermore, it is important to mention that due to the antisymmetry between the respective poles of a pole pair mainly only odd numbers of harmonics are possible, $\nu \in \mathbb{N}_{odd}$. Figure 2.17 shows the exemplary course of a field exciter curve.

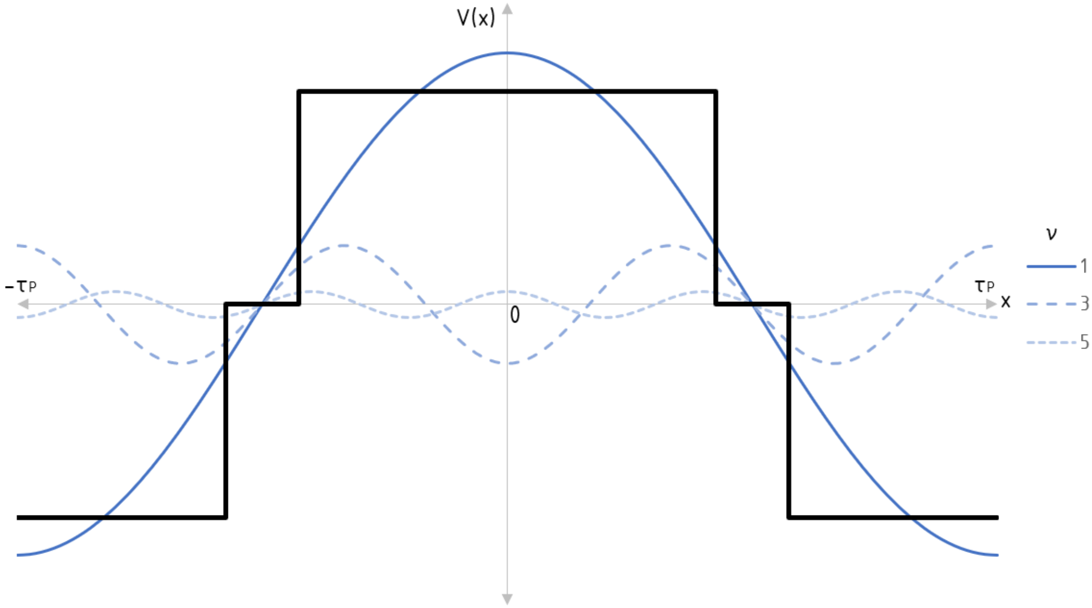

Figure 2.17: Example of a field exciter curve of a single phase of a full pitched winding with normal zone span. For $m = 3$, $q = 2$ and $\omega_1\,t = 0$ the stepped course and the single waves for $\nu = 1, 3, 5$ are shown.

2.9.3 Windings with Double Zone Span

Full pitch winding with double zone span can only be executed as double layer windings. Each zone has a total amount of $(2\,q)\;z_Q/2$ conductors, flooded by a current of $I_k\,(t)\,/a$ each.

Now, the maximum value of the magnetomotive force is

$$V_{max} = \frac{2\,q\,z_Q}{4}\,\frac{\hat{I}}{a} = \frac{N_S}{2\,p}\,\hat{I}. \tag{2.40}$$

A *Fourier Analysis* of the magnetomotive force like in equation (2.38) leads to the same amplitudes as in equation (2.39), Schmidt (2021). However, the winding factor ξ_ν gets calculated in a different way (see chapter 3). While for full pitched windings with double zone span only odd numbers of harmonics occur due to the antisymmetry of the poles, in case of pitching and the loss of antisymmetry also even harmonic order numbers result, $\nu \in \mathbb{N}$.

2.9.4 Cumulative Effect of m Phases

The total effect of all phases must always be taken into account for the complete field excitation curve. With a symmetric winding, the axes of the windings are always distributed in length at a distance of $\Delta x_m = 2\,\tau_P/m$ to each other over the circumference of the armature.

In addition to the approach of the magnetomotive force for the first phase in equation (2.38), the following applies to the k^{th} subsequent phase:

$$V_k\,(x) = V_1\left[x - (k-1)\,\frac{2\,\tau_P}{m}\right] \tag{2.41}$$

Inserting the current of equation (2.35) leads to

$$\begin{aligned} V_k\,(x,t) &= \sum_{\nu=1}^{\infty} \hat{V}_{1,\nu}\,\cos\left(\omega_1\,t - (k-1)\,\frac{2\,\pi}{m}\right)\cos\left((k-1)\,\nu\frac{2\,\pi}{m} - \frac{\nu\,\pi\,x}{\tau_P}\right) \\ &= \sum_{\nu=1}^{\infty} \frac{\hat{V}_{1,\nu}}{2}\,\cos\left(\omega_1\,t - \frac{\nu\,\pi\,x}{\tau_P} - (k-1)\,(1-\nu)\,\frac{2\,\pi}{m}\right) \\ &+ \sum_{\nu=1}^{\infty} \frac{\hat{V}_{1,\nu}}{2}\,\cos\left(\omega_1\,t + \frac{\nu\,\pi\,x}{\tau_P} - (k-1)\,(1+\nu)\,\frac{2\,\pi}{m}\right). \end{aligned} \tag{2.42}$$

According to equation (2.42), each phase has two waves running against each other at the same velocity per an order of a harmonic. These waves also have the same amplitude. The following applies to the function of the magnetomotive force in the air-gap according to Schmidt (2021):

$$V\,(x,t) = \sum_{k=1}^{m} V_k\,(x,t) = V_+\,(x,t) + V_-\,(x,t) \tag{2.43}$$

$$V_+(x,t) = \sum_{g=0}^{\infty} \frac{m}{2} \hat{V}_{1,\nu} \cos\left(\omega_1 t - \frac{\nu \pi x}{\tau_P}\right) \quad , \quad \nu - 1 = g\, m \tag{2.44a}$$

$$V_-(x,t) = \sum_{g=1}^{\infty} \frac{m}{2} \hat{V}_{1,\nu} \cos\left(\omega_1 t + \frac{\nu \pi x}{\tau_P}\right) \quad , \quad \nu + 1 = g\, m \tag{2.44b}$$

Equation (2.44) shows that in case of a symmetric poly phase system ultimately only certain numbers of ν occur in the field exciter curve. If negative numbers for the orders of the harmonics were taken into consideration, equation (2.43) can be given in a compact form as follows:

$$V(x,t) = \sum_{g=-\infty}^{\infty} \frac{m}{2} \hat{V}_{1,\nu} \cos\left(\omega_1 t - \frac{\nu \pi x}{\tau_P}\right) \quad , \quad \nu = 1 + g\, m \tag{2.45}$$

According to Schmidt (2021), therefore, the ν-th harmonic of the magnetomotive force is

$$V_\nu(x,t) = \hat{V}_\nu \cos\left(\omega_1 t - \frac{\nu \pi x}{\tau_P}\right), \tag{2.46}$$

with amplitudes of

$$\hat{V}_\nu = \frac{m}{2} \hat{V}_{1,\nu} = \frac{1}{\pi} \frac{m\, N_S}{p} \frac{\xi_\nu}{\nu} \hat{I} \tag{2.47}$$

The possible numbers of harmonics orders are $\nu = 1 + 2\, g\, m$ for windings with normal zone span and $\nu = 1 + g\, m$ for windings with double zone span, where the condition of $g \in \mathbb{Z}$ always has to be valid. Positive orders of ν mean a wave running with respect to the fundamental wave, negative orders of ν mean a wave running against the fundamental wave. Figure 2.18 shows the exemplary course of a field exciter curve.

2.10 Polygon of the Magnetomotive Force

In the general case of an AC machine, the armature is provided with a finite number of slots. The magnetomotive force V of the air-gap between rotor and stator is constant at each tooth. Until the next tooth, the magnetomotive force increases by current powered conductors with a surface current density A lying in a slot. Assuming an infinitely narrow slot, the increase of the magnetomotive force V corresponds to a jump function. The relationship between A and V as an integral can therefore be written as a sum (Sequenz (1950)):

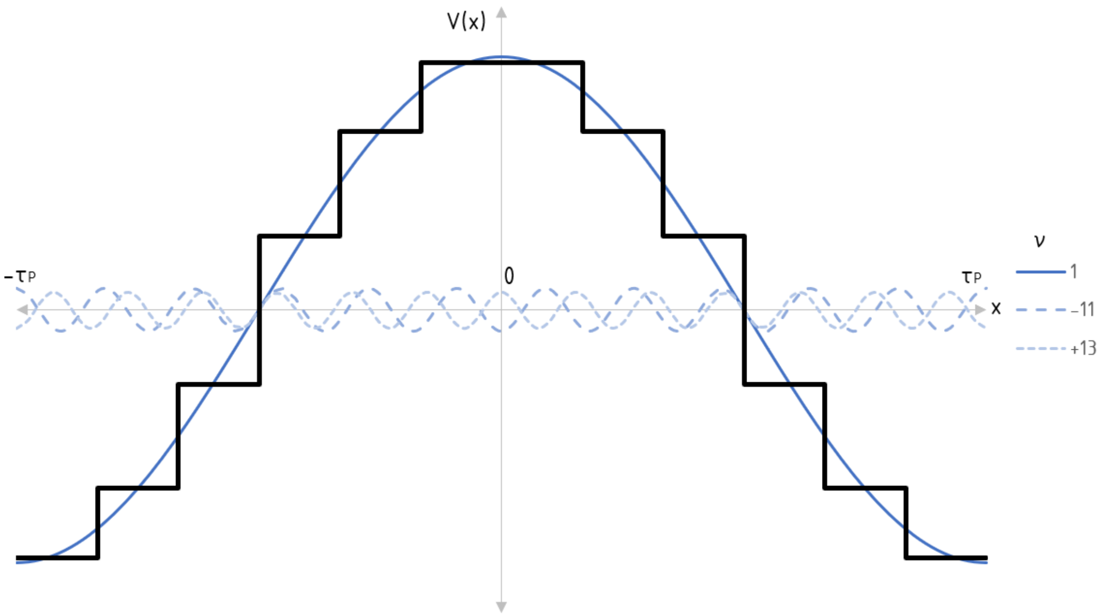

Figure 2.18: Example of a cumulative field exciter curve of a pitched winding with normal zone span. For $m = 3$, $q = 2$, $\sigma = 5/6$ and $\omega_1 t = 0$ the stepped course and the single waves for $\nu = 1, -11, 13$ are shown.

$$V(x) = -\int_{\mathscr{C}} A \, dx \quad \Rightarrow \quad V(x) = -\sum_{i=1}^{n} A_i \tag{2.48}$$

For a display as a pointer model, pointers of A_i are plotted phasewise to the corresponding currents of the conductor in the case of its peak value, see figure 2.19. The geometric addition of A_i provides the pointers of the magnetomotive forces V_i. The first pointer V_0 can be selected freely to define the origin.

The pointers of V_i give the ordinates of the field exciter curve $V(x)$ of the corresponding slots. A complete rotation along the armature always results in a closed polygon due to the *Kirchhoff Law*. In case of a repetitive section of the winding within a natural part of the whole circumference, the polygon is identically passed through more than once. This polygon of the magnetomotive force is also known as *Görges Polygon*.

The corners of the polygon represent the slots, while the edges are determined by the magnetomotive force of the slots. By projecting the pointers of V on a timeline (freely selectable), the values of the field exciter curve in the air-gap at different points of the armature are obtained.

2.11 The Tingley-Scheme

The *Tingley-Scheme* is a linear representation of the winding arrangement of a machine and equivalent to the phasor diagram of the slots by its meaning. The table-like structure

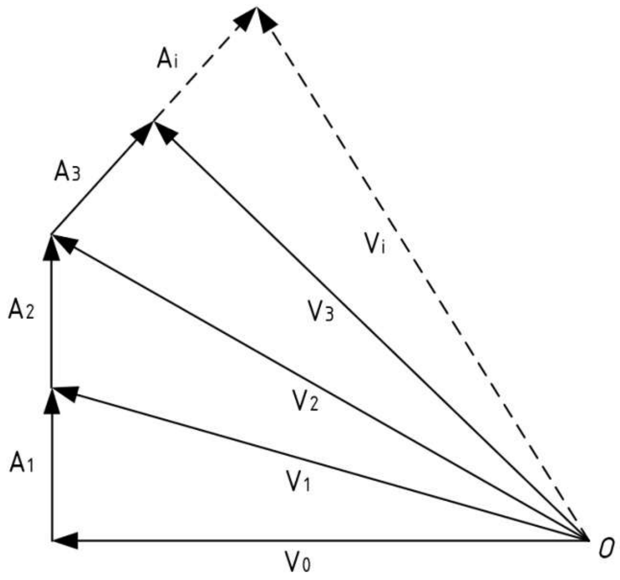

Figure 2.19: Basic correlation of the current powered conductors A with the magnetomotive force V for illustration of the field exciter curve in pointer representation (Sequenz (1950)).

allows an easy assignment of the coil groups of the phases to the slots of the armature even for more complicated windings, especially fractional slot windings.

The table consists at maximum of as many rows as the machine has pole pitches. Practically, the scheme can be reduced to the repetitive section of the winding. The columns of the table represent slots and teeth of the armature. The sum of the columns corresponds to a pole pitch τ_P (Kucera and Hapl (1956)).

By defining

$$t' = \gcd(Q, 2p) \tag{2.49}$$

as the greatest common divider of the total number of slots Q and the number of poles $2p$, the *Tingley-Scheme* has $Q/t' \in \mathbb{N}$ columns for one pole pitch τ_P. A single slot pitch τ_Q is represented by $2p/t'$ columns. Thus, one column stands for a slot and the rest builds the tooth of τ_Q. According to Sequenz (1950), for a complete representation of the winding, $2p/t$ pole pitches should always be indicated.

After completion of the table, the slots must still be assigned to the m phases. This is relatively easy to do by splitting the total number of columns into sections according to the zone plan. Thus, windings with normal zone span will form $2m$ sections along two pole pitches, whereas windings with double zone span will form only m sections along two pitches. The slots located in the respective areas (including coil sides) are then assigned to the corresponding phase.

Figure 2.20 shows an example of a single layer fractional slot winding with $m = 3$, $Q = 78$, $2p = 4$ and $q = 13/2$. Here $t' = 2$ and also $t = 2$. So the table has $N/t' = 39$ columns per pole divison and $2p/t' = 2$ columns per slot pitch. Due to the single layer winding and consequently the necessity of an even number of slots per phase, the number of rows corresponds to the full machine with $2p = 4$.

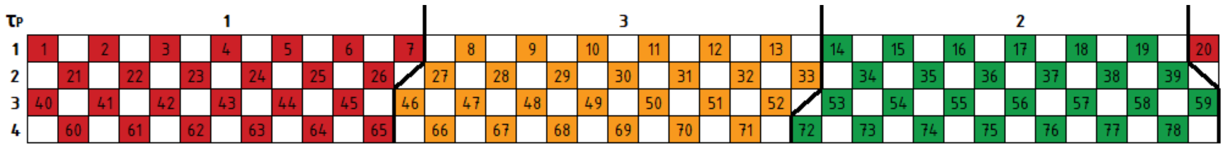

Figure 2.20: Example for a Tingley-Scheme of a fractional slot winding (Sequenz (1950)). The corresponding phases are assigned.

3 Winding Factor

3.1 Pitch Factor

Armature windings with a width W that is smaller than the pole pitch τ_P are called pitched windings, represented by the coil pitch σ. The effect of σ is expressed via the *pitch factor* ξ_σ of a coil. For the determination of the pitch factor, it is advantageous to derive its importance via the voltage of the coil sides. The voltage of a coil $\underline{U}_{coil}$ gets calculated by the geometric difference of the coil side voltages $\underline{U}_{cs1}$ and $\underline{U}_{cs2}$ that have a same absolute value $|\underline{U}_{cs1}| = |\underline{U}_{cs2}|$:

$$\underline{U}_{coil} = \underline{U}_{cs1} - \underline{U}_{cs2}. \tag{3.1}$$

Figure 3.1 shows the relationship of equation (3.1) in the form of a phasor diagram. The phasors of the voltages of the two coil sides are phase shifted to each other by the angle of $\pi\,\sigma$. If $\sigma = 1$ (full pitched coil), the coil voltage $\underline{U}_{coil}$ reaches its maximum value.

The application of geometric and angular functions leads to an equation for the coil voltage induced from the fundamental wave as a function of the coil pitch (figure 3.1, Sequenz (1950)):

$$|\underline{U}_{coil}| = 2\,|\underline{U}_{cs1}|\,\cos\left(\frac{1}{2}\,(\pi - \pi\,\sigma)\right) \tag{3.2}$$

Using the angle sum theorem for cos functions,

$$\cos(\alpha - \beta) = \cos(\alpha)\,\cos(\beta) + \sin(\alpha)\,\sin(\beta)\,, \tag{3.3}$$

and under analysis of calculable expressions follows it is possible to write equation (3.2) as

$$|\underline{U}_{coil}| = 2\,|\underline{U}_{cs1}|\,\sin\left(\frac{\pi}{2}\sigma\right) \tag{3.4}$$

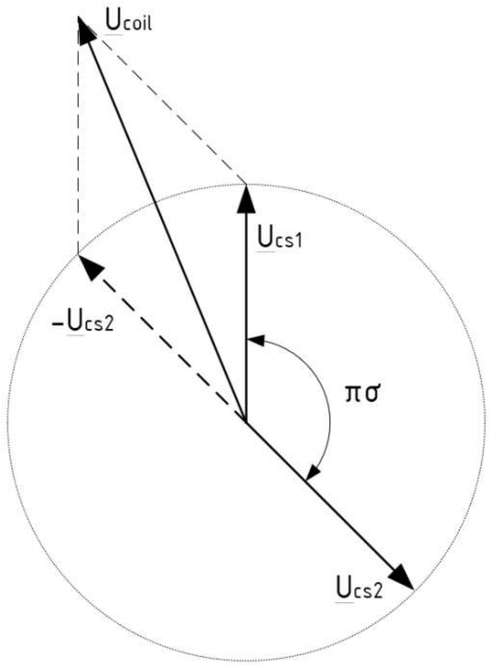

Figure 3.1: Phasor diagram to derive the pitch factor ξ_σ.

From equation (3.4), the pitch factor ξ_σ of the fundamental wave can now be defined by the ratio

$$\frac{\text{geometric sum of the coil side voltages}}{\text{algebraic sum of the coil side voltages}} \tag{3.5}$$

after Sequenz (1950) as:

$$\xi_\sigma = \frac{|\underline{U}_{coil}|}{2\,|\underline{U}_{cs1}|} = \sin\left(\frac{\pi}{2}\sigma\right) \tag{3.6}$$

When looking at harmonics, the pitch factor expands. The numerical value of the harmonic wave goes into the calculation and requires a separate treatment of even and odd harmonic numbers ν. According to Sequenz (1950), for odd values of ν, the pitch factor gets calculated by

$$\xi_{\sigma,\nu=odd} = \sin\left(\nu\frac{\pi}{2}\right)\sin\left(\nu\frac{\pi}{2}\sigma\right), \tag{3.7}$$

and applying to even values of ν

$$\xi_{\sigma,\nu=even} = -\cos\left(\nu\frac{\pi}{2}\right)\sin\left(\nu\frac{\pi}{2}\sigma\right). \tag{3.8}$$

The first factors in equations (3.8) and (3.7) determine only the sign of the pitch factor. The sign describes how the induced voltage of a certain harmonic wave is relative to the field curve. Harmonic waves with odd order are in phase (positive sign of the pitch factor) or counterphase (negative sign of the pitch factor). Harmonic waves of even order are shifted by 90° of a diameter coil ($\sigma = 1$). A positive sign of the coil factor means a negative phase-shift, a negative sign means a positive phase-shift.

The main advantage of pitched coils is the possibility of a suppression of distinct harmonics. The aim would be a complete suppression of all harmonics with the maximum value of the fundamental wave at the same time. Figures 3.2 and 3.3 show the ratio of the pitch factor of several numbers of ν to the pitch ratio of the basic wave over the range of the coil pitch from $0,15$ to 1. Each zero passage of a characteristic line represents the suppression of the respective harmonic to a certain value of σ.

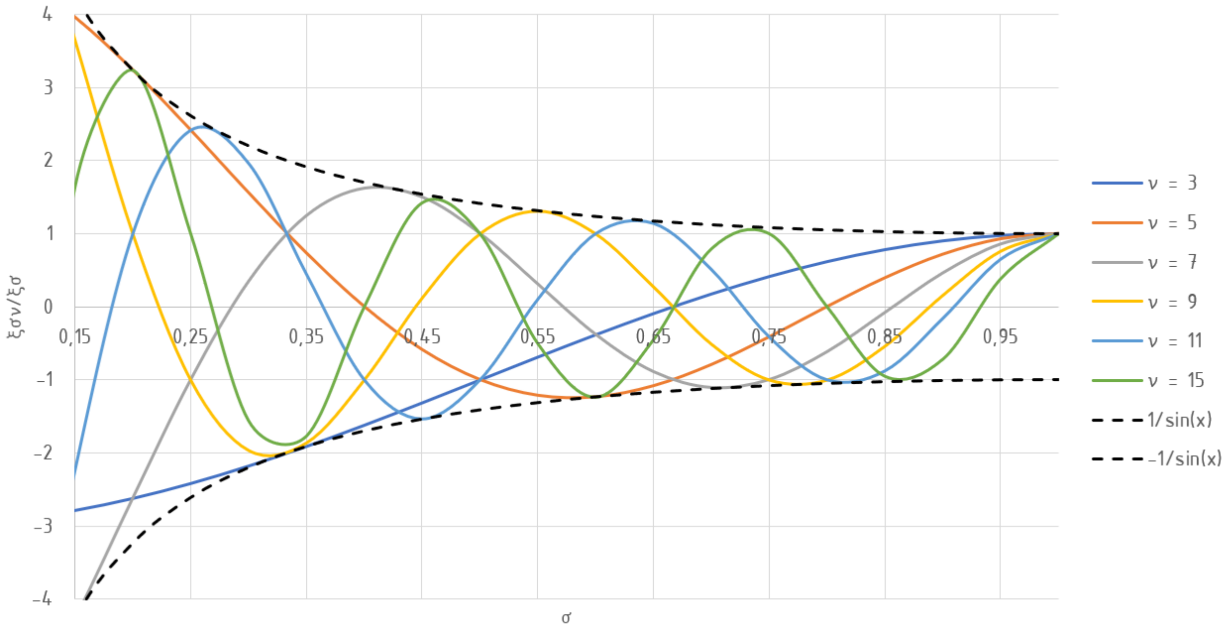

Figure 3.2: Ratio of the pitch factor for odd numbers of ν ($\xi_{\sigma,\nu=odd}$) to the pitch factor of the basic wave (ξ_σ) in the range from $\sigma = 0,15...1$.

As the characteristics show, it is not possible to suppress all harmonics by a single choice of σ. A suppression can always only be done for a certain harmonic wave. The conditions for suppressing a certain harmonic wave following Sequenz (1950) are:

$$\frac{1}{2}\,\nu\,\sigma = g \tag{3.9}$$

The variables g represents any integer values.

According to Müller et al. (2007), the pitch factor for harmonics can also be written in a closed form as a complex function. Mostly, however, the absolute value of the pitch factor $|\xi_{\sigma,\nu}|$ is sufficient for calculations and it is the same for even and odd orders of harmonics:

$$|\xi_{\sigma,\nu}| = \left|\sin\left(\nu\,\frac{\pi}{2}\,\sigma\right)\right| \tag{3.10}$$

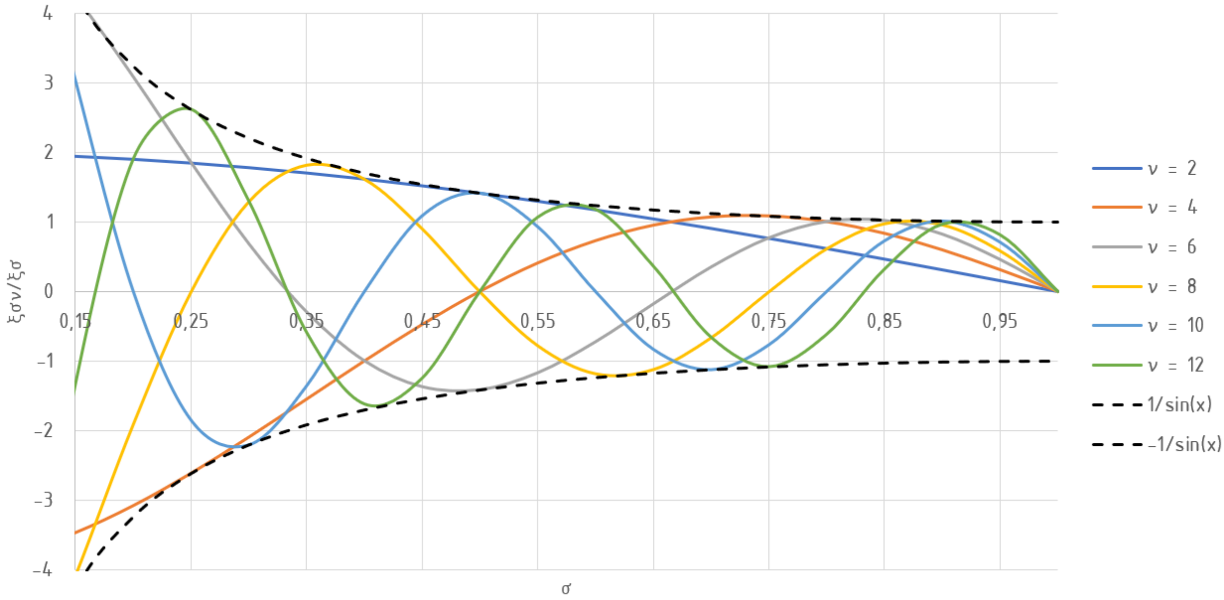

Figure 3.3: Ratio of the pitch factor for odd numbers of ν ($\xi_{\sigma,\nu=even}$) to the pitch factor of the basic wave (ξ_σ) in the range from $\sigma = 0,15...1$.

3.2 Group Factor

If several coils are connected together in series, these connections form so called coil groups. The voltage of a coil group U_G is represented by the geometrical sum of the voltages of each single coil $U_{cs,i}$. In most cases they all have the same amplitude, but always a phase shift according to the slot pitch. The *group factor* of a coil group is now defined by the ratio of U_G to the algebraic sum of $U_{cs,i}$.

Coils of the same width W have the same absolute value of the voltage, but are phase shifted. The phase shift between the coil voltages $U_{cs,i}$ gets calculated by an angle reflecting the slot pitch,

$$\alpha = \frac{p}{Q} 2\pi \tag{3.11}$$

As usual, p denotes the number of pole pairs and Q the number of slots of the armature in equation (3.11). For a consideration of harmonics, equation (3.11) must be multiplied on the right hand side by ν, leading to phase angle $\alpha_\nu = \nu\alpha$. Voltages of coils that are induced by harmonics have a different phase angle and their group voltage can be smaller than the absolute value of the voltage of a single coil.

If there are n_S coils with a slot spacing f in between them, using geometric and angular functions delivers to the equation for the group voltage of the fundamental wave:

$$U_G = U_{coil} \frac{\sin\left(n_S\, f\, \frac{\alpha}{2}\right)}{n_S \, \sin\left(f\, \frac{\alpha}{2}\right)} \tag{3.12}$$

With equation (3.12), the group factor ξ_G can be formed by the ratio of the voltages. If harmonics are taken into account, the group factor for any harmonic order ν can be defined, according to Sequenz (1950), by

$$\xi_{G,\nu} = \frac{\sin\left(\nu\, n_S\, f\, \pi\, \frac{p}{Q}\right)}{n_S \, \sin\left(\nu\, f\, \pi\, \frac{p}{Q}\right)} \tag{3.13}$$

Equation (3.13) shows that $\xi_{G,\nu}$ does not depend on σ anyway. If Q, $n_S \to \infty$, the equation can be interpreted geometrically as the ratio of circular chord and arch length reflecting the part of the circumference covered by the coil group.

3.3 Zone Factor

A series circuit of z coil groups results in a winding zone. Each of the groups is necessarily formed by the same number of coil sides. The geometric sum of the group voltages $U_{G,i}$ is the zone voltage U_Z of a winding zone. Equation (3.14) is derived from (3.12). z represents the amount of coil groups within a winding zone and y_G stands for the slot distance (step) between these coil groups.

$$U_{Z,\nu} = U_{G,\nu} \frac{\sin\left(\nu\, z\, y_G\, \frac{p}{G}\, \pi\right)}{\sin\left(\nu\, y_G\, \frac{p}{G}\, \pi\right)} \tag{3.14}$$

According to the definition of the group factor, the zone factor $\xi_{Z,\nu}$ can be written after Sequenz (1950) as

$$\xi_{Z,\nu} = \frac{\sin\left(\nu\, z\, y_G\, \frac{p}{G}\, \pi\right)}{z\, \sin\left(\nu\, y_G\, \frac{p}{G}\, \pi\right)}. \tag{3.15}$$

3.4 Phase Factor

A winding phase is created by two coil groups (ζ_1, ζ_2), with t zones each, connected against each other. According to Sequenz (1950) the voltage of a phase can be derived to

$$U_{phase,\nu} = \sqrt{U^2_{\zeta_1,\nu} + U^2_{\zeta_2,\nu} - 2\,U_{\zeta_1,\nu}\,U_{\zeta_2,\nu}\,\cos\left(\frac{1}{2}\,\frac{G}{t}\,y_G\,\frac{p}{G}\,2\pi\right)}. \tag{3.16}$$

Inserting equation (3.14) for the voltages $U_{\zeta_1,\nu}$ and $U_{\zeta_2,\nu}$ yields a form that includes the *phase factor* $\xi_{phase,\nu}$.

$$U_{phase,\nu} = (\zeta_1 + \zeta_2)\,U_{G,\nu}\,\xi_{phase,\nu} \tag{3.17}$$

If $\nu p/t$ is an integer, the phase factor equals (Sequenz (1950))

$$\xi_{phase,\nu} = \underbrace{\frac{\cos\left(\dfrac{\pi}{3}\,\nu\,y_G\,\dfrac{p}{t}\right)}{\dfrac{1}{6}\,\dfrac{G}{t}\,\sin\left(\nu\,y_G\,\dfrac{p}{G}\,\pi\right)}}_{\xi_{D,\nu}}\;\underbrace{\sin\left(\frac{\dfrac{G}{t} \mp (\zeta_1 - \zeta_2)}{\dfrac{G}{t}}\,\frac{\pi}{2}\,\nu\,y_G\,\frac{p}{t}\right)}_{\xi_{ZV,\nu}} \tag{3.18}$$

Equation (3.18) can be split up into a *distribution factor* $\xi_{D,\nu}$ and a *zone reduction factor* $\xi_{ZV,\nu}$. $\xi_{D,\nu}$ takes the influence of the distribution of coil group voltages $U_{G,\nu}$ into account and does not depend on the amount of coil groups (z) within the zone. $\xi_{ZV,\nu}$ describes the influence of unequal zones (distorted voltage phasor diagram) on the winding factor. A zone reduction is finally equivalent to a shortening step y_ε.

3.5 Total Winding Factor

Assuming that all coils are connected in series and $\nu p/t$ is an integer, the total winding factor is calculated from the product of the pitch factor, the group factor and the zone factor.

$$\xi_\nu = \xi_{\sigma,\nu}\,\xi_{G,\nu}\,\xi_{Z\nu} \tag{3.19}$$

With applications, this winding factor will be complemented in case of skewed slots by a *skew factor* and in case of tooth coil windings by a *slot opening factor*.

3.6 Winding Factor in Application

3.6.1 Single Layer Integer Slot Winding

Assuming an m phased symmetric single-layer integer slot winding with $Q/pm = 2q \in \mathbb{N}_{even}$, a slot distance $f = 1$ and coil count equal to the number of pole pairs ($n_S = p$), the winding factor can be expressed as (Schmidt (2020)):

$$\xi_\nu = \frac{\sin\left(\nu \dfrac{\pi}{2\,m}\right)}{q \sin\left(\nu \dfrac{\pi}{2\,q\,m}\right)} \tag{3.20}$$

Due to symmetry, all p coil groups have the same absolute valued and phased voltages. This results in the winding factor in equation (3.20) being equivalent to the group factor $\xi_{G,\nu}$ from equation (3.13).

When considering a base winding, it can also be assumed that all zones have the same zone angle α_z. In this case equation (3.20) is also equivalent to the zone factor $\xi_{Z,\nu}$ of equation (3.15).

Using the definition of zone angle α_z

$$\alpha_z = q\,\alpha_Q = \frac{\pi}{m} \tag{3.21}$$

with the slot angle α_Q, equation (3.20) can be also written as

$$\xi_\nu = \frac{\sin\left(\nu \dfrac{q\,\alpha_Q}{2}\right)}{q\,\sin\left(\nu \dfrac{\alpha_Q}{2}\right)}. \tag{3.22}$$

In case of a (theoretically) infinite number of slots per pole and phase ($q \to \infty$), equation (3.20) is

$$\xi_{\nu,q\to\infty} = \frac{\sin\left(\nu \dfrac{\pi}{2m}\right)}{\nu\,\dfrac{\pi}{2m}}. \tag{3.23}$$

Single layer integer slot windings can not be pitched, therefore ξ_σ is always 1.

3.6.2 Single Layer Fractional Slot Winding

In extension to equation (3.20), the winding factor for *odd numbers of harmonics* of a m-phased general fractional slot winding can be written after Sequenz (1950) as follows:

$$\xi_\nu = \frac{\sin\left(\nu \frac{\pi}{2\,m}\right)}{q_n\,q\,\sin\left(\nu \frac{\pi}{2\,q_n\,q\,m}\right)} \cos\left(\nu\,x\,\frac{p}{Q}\,2\pi\right) \tag{3.24}$$

The variable x denotes a part of the phase angle α between adjacent slots and represents the inevitable difference between an averaged coil pitch against the pole pitch. The basic period of this winding factor is determined by a multiple of $2mq$.

For *even numbers of harmonics* the winding factor is equal to those with odd numbers of harmonics that are an extension of a multiple of $2mq$ (Sequenz (1950)).

Winding factors with a *fractional number of harmonics* are equal to those of integer numbers of harmonics that are an extension of a multiple of a part of $2mq$.

3.6.3 Double Layer Integer Slot Winding

Assuming that all coil groups G have the same number of coils q with $f = 1$, the winding factor is according to Sequenz (1950) a product of the pitch factor $\xi_{\sigma,\nu}$ and the group factor $\xi_{G,\nu}$

$$\xi_\nu = \xi_{\sigma,\nu}\,\xi_{G,\nu} = \sin\left(\nu\,\frac{\pi}{2}\,\sigma\right)\,\sin^2\left(\nu\,\frac{\pi}{2}\right)\frac{\sin\left(\nu\,\frac{\pi}{2m}\right)}{q\,\sin\left(\nu\,\frac{\pi}{2\,q\,m}\right)} \tag{3.25}$$

When considering a base winding, it can also be assumed that all zones have the same zone angle α_z. In this case the second term of equation (3.25) is also equivalent to the zone factor $\xi_{Z,\nu}$ of equation (3.15).

For the variant of an armature winding with double zone span the winding factor is according to Schmidt (2020)

$$\xi_\nu = \xi_{\sigma,\nu}\,\xi_{G,\nu} = \sin\left(\nu\,\frac{\pi}{2}\,\sigma\right)\frac{\sin\left(\nu\,\frac{\pi}{m}\right)}{2\,q\,\sin\left(\nu\,\frac{\pi}{2\,q\,m}\right)} \tag{3.26}$$

In case of a (theoretically) infinite number of slots per pole and phase ($q \to \infty$), equation (3.25) is

$$\xi_{\nu,q\to\infty} = \sin\left(\nu\,\frac{\pi}{2}\right)\frac{2\,m}{\nu\,\pi}\,\sin\left(\nu\,\frac{\pi}{2\,m}\right)\,\sin^2\left(\nu\frac{\pi}{2}\right), \tag{3.27}$$

and for equation (3.26)

$$\xi_{\nu,q\to\infty} = \sin\left(\nu\,\frac{\pi}{2}\right)\frac{m}{\nu\,\pi}\,\sin\left(\nu\,\frac{\pi}{m}\right). \tag{3.28}$$

3.6.4 Double Layer Fractional Slot Winding

In order of equation (2.13), the winding factor for *odd numbers of harmonics* is written after Sequenz (1950) as

$$|\xi_\nu| = \left|\sin\left(\nu\,\frac{\pi}{2}\,\sigma\right)\frac{\sin\left(\nu\,\dfrac{\pi}{2m}\right)}{q_n\,q\,\sin\left(\nu\,\dfrac{\pi}{2\,q_n\,m\,q}\right)}\right| \tag{3.29}$$

For calculating the fractional slot winding factor of *harmonics with even or fractional numbers* the winding factor of a reference integer slot winding with $q_g = q_n\,q$ is necessary. For q_n slot harmonics, the q_n-th slot harmonic is defined by

$$\nu = \pm\,2\,q_n\,m\,Q_g + 1. \tag{3.30}$$

Between the fundamental wave and the q_n-th slot harmonic there are $0 < q_g < q_n$ slot harmonics. The graph of the absolute value of the winding factor over the harmonic order ν corresponds to $1/\sin(x)$ curves - the absolute value of the winding factor of the basic wave is always the same as the absolute value at a certain slot harmonic. Slot harmonics can be of an even, odd or a fractional order. The principal course of the winding factor ξ_ν is shown in figure 3.4.

However, due to the large number of possible variants, it is not possible to specify a closed formulation for calculating the winding factor for any fractional slot winding. While it is possible to derive a formula for most double layer lap windings with coils of equal coil pitches, it is rather impossible to derive a formula for double layer wave windings or for all kinds of single layer windings. Therefore, the determination of the winding factor for the fundamental harmonic will be afterwards performed by means of an algorithm based on the voltage phasor diagram of the slots, which can be specified by the *Tingley-Scheme*.

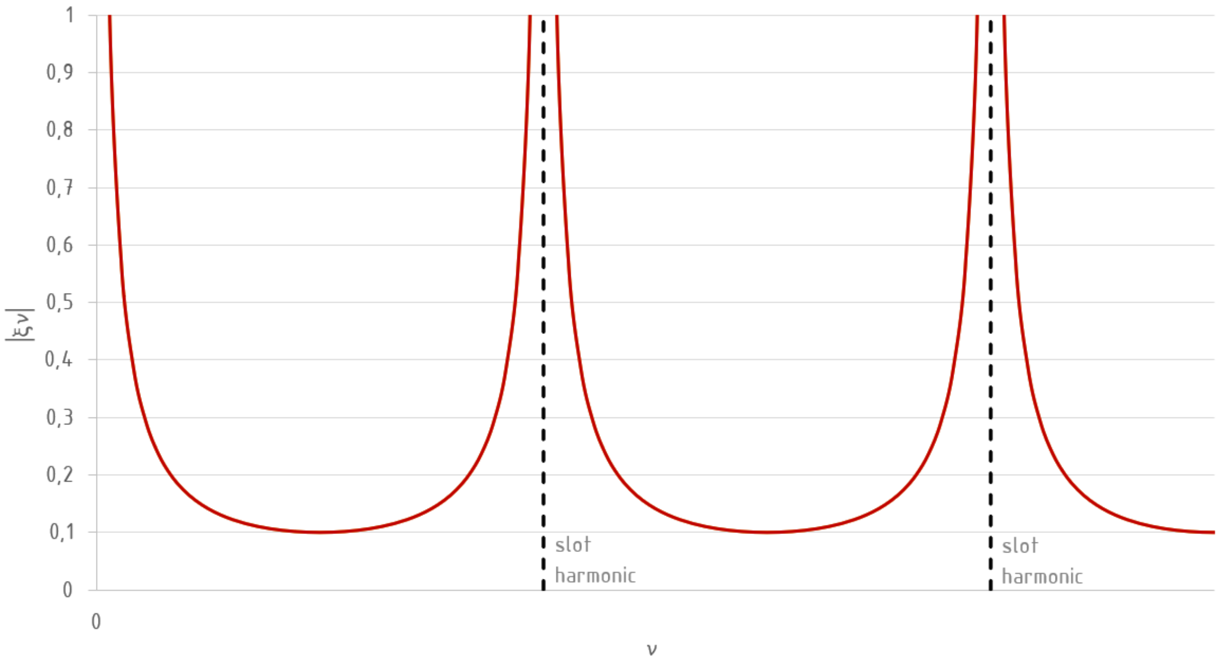

Figure 3.4: Course of the winding factor ξ_ν of fractional slot windings as a function of ν. The absolute values of ξ_ν are repeating, ground wave and slot harmonics have the same value.

4 Harmonic Scattering

The term of *harmonic scattering*, sometimes also called *gap scattering*, describes all phenomenons of scattering of the air-gap of electrical machines. The harmonic wave scattering can be assigned to the windings of the stator side as well as those of the rotor side.

In case of induction machines with a running rotor, additional torques are generated by the harmonics, which have a negative effect on the start-up of the machine. This will almost disappear in the range of the rated speed. Therefore, the main reactance X_h is only attributed to the fundamental wave and the other harmonics are summarized by the scattering reactance X_o, (Richter (1954)).

For the following treatise only one winding side (stator or rotor) is considered – unless explicitly described. Furthermore, reactions of slots or saturation effects of the iron core are not taken into account. The slot width is assumed to be ideal and therefore set to zero. As mentioned before, the real slot width can be represented by a slot opening factor.

4.1 Calculation by Reactances

If X_δ is the total air-gap reactance of the machine, the following relationship is valid in respect to the main reactance X_h and scattering reactance X_o:

$$X_\delta = X_h - X_o \tag{4.1}$$

For the connection of the main reactance X_h with the scattering reactance X_o, the harmonic scattering is introduced by the coeficient σ_o in equation (4.2):

$$X_o = \sigma_o \, X_h \tag{4.2}$$

Thus, harmonic wave scattering is defined by the ratio of scattering reactance and main reactance. Equation (4.2) can be transformed (Richter (1954)) with the use of equation (4.1) to

$$\sigma_o = \frac{X_\delta}{X_h} - 1. \tag{4.3}$$

Assuming this ratio, an approach using the magnetic energy of the air-gap field leads to the coefficitent of σ_o according to Richter (1954)

$$\sigma_o = \sum_{\nu \setminus \{1\}} \left(\frac{\xi_\nu}{\nu\, \xi_1} \right)^2 \tag{4.4}$$

As shown before, the magnitude of the harmonics within the air-gap field are scaled by the quotient ξ_ν/ν. Consequently, the coefficitent σ_o has to include the energy of all harmonics with the exception of the fundamental wave. The meaning of equation (4.4) is a sum of the quadratic ratio of the scale of a specific harmonic ξ_ν/ν with regard to the scale of the fundamental wave given by ξ_1. The occuring orders of harmonics due to a sinusodial excitation can be calculated (Richter (1954)) by

$$\nu = 1 + k\, m \tag{4.5}$$

In equation (4.5), k represents any number out of $\mathbb{Z}$ and m is the number of phases. For fractional slot windings also fractional numbers of ν must be taken into account.

Equation (4.4) consists of an infinite series, its calculation looks rather simple. But on the one hand, there is a lack of a closed and compact general formulation for this sum. And on the other hand, the convergence of this infinite series is rather slow. Therefore, this laborious method of calculation is impractical in general.

4.2 Calculation by the Magnetic Energy

The required reactance X_δ, which includes the fundamental wave as well as all harmonics, and the main reactance X_h can be calculated using the magnetic energy W considering only the fundamental wave. For an m phased winding, the averaged magnetic energy along a fundamental period of the excitating symmetric poly phase currents can be written as

$$W_m = \frac{1}{4}\, m\, L\, \hat{I}^2 \tag{4.6}$$

or in integral form via the magnetic flux density $\mathbf{B}$, the magnetic field strength $\mathbf{H}$ and the permeability of air $\mu \approx \mu_0$

$$W_m = \frac{1}{4} \int_{\mathscr{V}} \mathbf{H} \cdot \mathbf{B}\;\, d\mathscr{V} = \frac{1}{4} \int_{\mathscr{V}} \mu_0\, H^2\;\, d\mathscr{V}. \tag{4.7}$$

Due to assuming an infinite permeability of the iron parts $\mu_{Fe} \to \infty$, the integral extends only over the volume $\mathscr{V}$, which describes the entire region of the air-gap.

According to Richter (1954) the reactance of the air-gap can be described with the use of equations (4.6) and (4.7) as

$$X_\delta = 2\pi\, f\, L = \frac{2\pi\, f}{m\, \hat{I}^2} \int_{\mathscr{V}} \mu_0\, H^2 \;\, d\mathscr{V}. \tag{4.8}$$

Since the volume of the gap $\mathscr{V}$ is defined by the geometry of the machine, it can be written as the following product:

$$\mathscr{V} = 2p\, \tau_P\, l_{Fe}\, \delta, \tag{4.9}$$

whereby $2p$ represents the number of poles, τ_P the pole pitch, l_{Fe} the effective iron length of the machine and δ the length of the air-gap.

As far as the magnetomotive force V is defined by

$$V = \int_{\mathscr{C}} \mathbf{H}\; d\mathbf{s} \quad \Leftrightarrow \quad \mathbf{H} = \frac{dV}{d\mathbf{s}}, \tag{4.10}$$

the magnetic field density H in equation (4.8) can be replaced by V. The field exciting curve corresponds to a step wise function. Therefore the integral in equation (4.8) is equal to a sum over the whole amount of slots Q:

$$X_\delta = \frac{2\pi\, f}{m\, \hat{I}^2}\, \frac{2p\, \tau_P\, l_{Fe}}{\delta}\, \mu_0\, \frac{\sum \hat{V}_Q^2}{Q} \tag{4.11}$$

This formulation is valid for all kinds of armature windings. With regard to the repetitive section of an armature winding, this formula can be reduced to the slots only of the repetitive section. For integer slot windings, this results in the sum along the number of Q/p slots.

For the main reactance X_h, just the amplitude $\hat{V}_1$ of the fundamental wave of V is relevant (Richter (1954))

$$\hat{V}_1 = \frac{m\, N_S\, \xi_1}{\pi\, p}\, \hat{I} \tag{4.12}$$

finally yielding

$$X_h = \frac{2\pi\, f}{m\, \hat{I}^2}\, \frac{2p\, \tau_P\, l_{Fe}}{\delta}\, \mu_0\, \frac{m^2\, N_S^2\, \xi_1^2}{\pi^2\, p^2}\, \hat{I}^2. \tag{4.13}$$

The application of equations (4.11) and (4.13) to equation (4.3) gives the result for the factor of the harmonic scattering σ_o (Richter (1954)).

$$\sigma_o = \left(\frac{\pi\, p}{m\, \xi_1\, N_S\, \hat{I}}\right)^2 \frac{\sum \hat{V}_Q^2}{Q} - 1 \tag{4.14}$$

4.3 Calculation by the Polar Moment of Inertia

The harmonic scattering coefficient σ_o of stator and rotor can also be calculated according to the following formula (4.15), Heller and Kauders (1935). It is defined as the ratio of the *polar moment of inertia on points of the Görges Polygon* to the *polar moment on the perimeter of the fundamental wave* minus 1. The variables R_g and R_1 in equation (4.15) represent the corresponding diameters to the polar moments of inertia.

$$\sigma_o = \left(\frac{R_g}{R_1}\right)^2 - 1 \tag{4.15}$$

For the variable R_g^2 it is necessary to sum up the squared absolute values of all pointers of the magnetomotive force of the *Görges Polygon* and divide it by the amount of pointers,

$$R_g^2 = \frac{\sum\limits_{i=1}^{n} \left|\hat{V}_i\right|^2}{n} \tag{4.16}$$

The diameter R_1 can be equated by the value of the total circumference of the *Görges Polygon* and the ratio of the winding factor,

$$R_1 = \frac{U_{polygon}}{2\pi}\, \xi_1 \tag{4.17}$$

4.4 Calculation in Practice

The problem with the calculation of σ_o for all presented variants is the calculation of the respective summation term. The lengthy determination of the amplitudes of the magnetomotive forces of slots and teeth can be circumvented by a graphical determination with the help of the *Görges Polygon*.

The application of equation (4.14) according to Richter (1954) still requires a modification for a use of the *Görges Polygon*. With an auxiliary factor V_{AF} in the form of,

$$V_{AF} = \frac{1}{2\, q^2} \frac{\sum \left|\hat{V}_Q\right|^2}{Q}, \tag{4.18}$$

the harmonic scattering coefficient can be written as

$$\sigma_o = \left(\frac{\pi}{m\,\xi_1}\right)^2 V_{AF} - 1. \tag{4.19}$$

V_{AF} can be determined directly out of the *Görges Polygon*.

For phase numbers of two and three as well as single layer and double layer integer slot windings, closed solutions for the auxiliary factor - also including short pitched coils - can be found already in the existing literature.

5 Calculation of the Harmonic Scattering Coefficient

The following chapter deals with the analytical calculation of the harmonic scattering coefficient σ_o in general for any odd amount of phases. In detail calculation solutions for two-, three-, five- and seven-phased windings are shown afterwards. Based on integer slot windings in different variants, also selected fractional slot windings are discussed. All calculations are based on a zone plan of each winding.

The major calculation steps in determining the harmonic scattering coefficient are the determination of the winding factor of the fundamental wave as well as the auxiliary factor of equation (4.18).

5.1 Integer Slot Windings

According to equation (2.11), an integer slot winding is characterized by $q \in \mathbb{N}$ and can be made up of a single layer or a double layer.

5.1.1 Single Layer Windings

The characteristic of common single layer windings is that there is only one coil side in each slot. The zone plan therefore contains only one ring, and pitching is not possible with a fixed number of zones.

Consequently, the harmonic scattering coefficients σ_o of single layer windings are identical to those of full pitched double layer windings with the same number of phases m. This is because of the equivalent zone plans for $\xi_\sigma = 1$ for both kinds of windings.

Figure 5.1 in principle shows the resulting *Görges Polygons* for such windings. In general, any *Görges Polygon* is a regular one and has a number of edges as well as corners according to two times the number of phases.

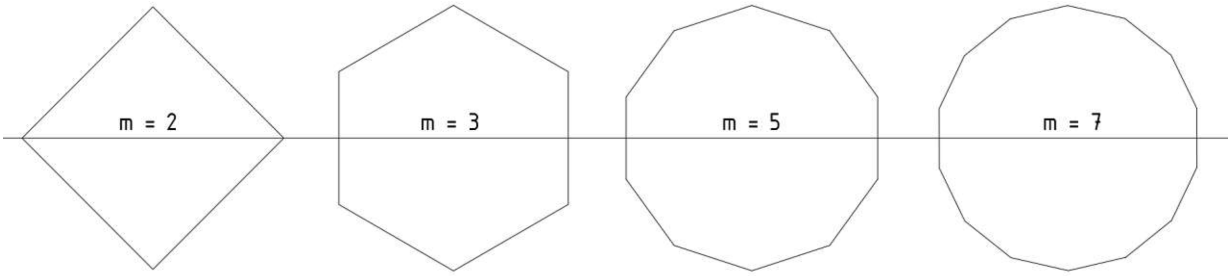

Figure 5.1: *Görges Polygons* for full pitched integer slot windings with $m = 2$, 3, 5 and 7.

5.1.1.1 Auxiliary Factor of odd numbered Poly Phase Windings

Closed solutions for the harmonic scattering coefficient for phase numbers of two and three can be found in literature (Richter (1954) and Schuisky (1960)). These are valid for full pitched single layer and double layer windings. These approaches are also used in the following chapters. For any odd numbered poly phase windings a general, closed form for single layer windings and full pitched double layer windings is given below.

The derivation is made by using the *Görges Polygon* based on the notations of Heller and Kauders (1935) and Richter (1954).

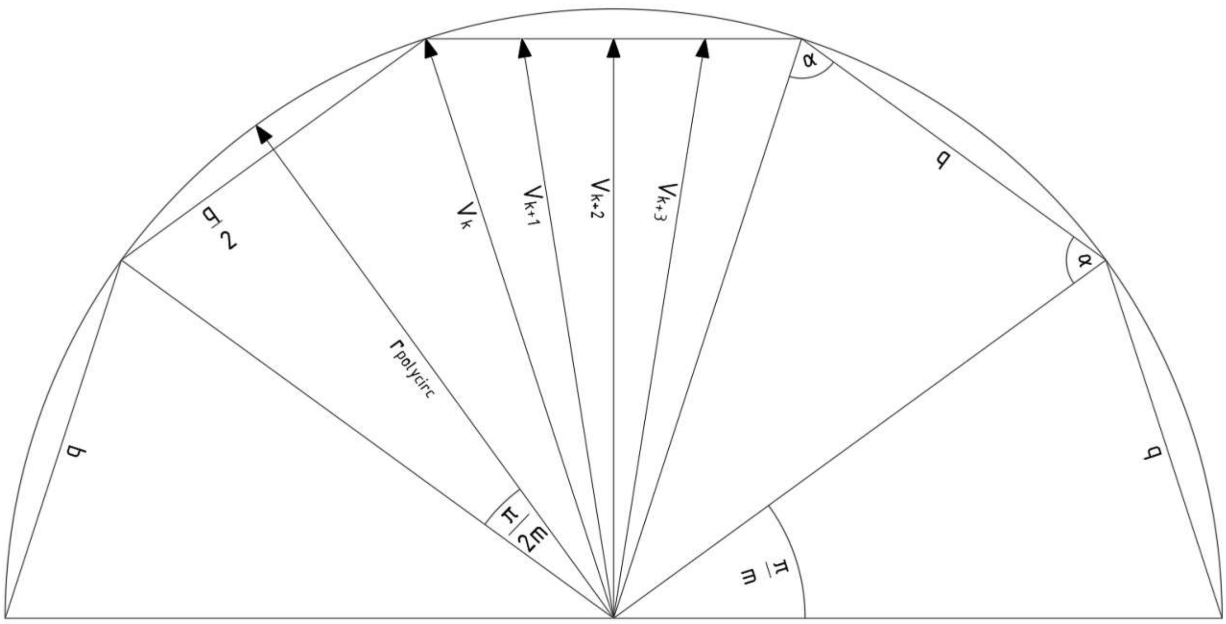

Figure 5.2: Half *Görges Polygon* of an $m = 5$ winding including exemplary phasors of the magnetomotive force V.

Starting from an example of a winding with a phase number of $m = 5$, the upper half of the *Görges Polygon* is shown in figure 5.2 by a symmetrical decagon. The following formal approaches, however, satisfy a general symmetrical polygon and are therefore applicable to randomly odd phase numbers. The edge length of the polygon always represents the number of slots per pole and phases q, the absolute value of the magnetomotive force per slot is $|V_N| = 1$. The angle between the circumcircle radius and the polygon tendon (pivot angle) therefore corresponds to the difference

$$2\,\alpha = \pi - \frac{\pi}{m}. \tag{5.1}$$

The geometry of a symmetrical polygon leads to the following equation with connection to the radius of the circumcircle of the polygon:

$$\cos\left(\alpha\right) = \frac{q}{2\,r_{polycirc}} \tag{5.2}$$

$$r_{polycirc}^2 = \frac{q^2}{4}\,\frac{1}{\sin^2\left(\dfrac{\pi}{2\,m}\right)} \tag{5.3}$$

Applying the law of cosines, a general formulation of the pointers of the magnetomotive force over the individual q lengths is possible as follows,

$$V_Q^2 = r^2 + k^2 - 2\,r\,k\,\cos\left(\alpha\right), \tag{5.4}$$

with $k = 1, 2, ..., q$. The formation of the mean value of V over the total number of slots Q results in the expression in the form:

$$\frac{\sum V_Q^2}{Q} = \frac{1}{q}\sum_{k=1}^{q}\left(r^2 + k^2 - 2\,r\,k\,\cos\left(\alpha\right)\right) \tag{5.5}$$

The growth of the mean value of equation (5.5) is thus quadratic with the number of slots per pole and phase q, the radii of the magnetomotive force phasors are proportional to the edge length of the polygon and this in turn proportional to the number of slots per pole and phase q.

The general solution of the summation terms provide:

$$\sum_{k=1}^{n} k = \frac{1}{2}\,n\,\left(n+1\right) \tag{5.6a}$$

$$\sum_{k=1}^{n} k^2 = \frac{1}{6}\,n\,\left(n+1\right)\left(2\,n+1\right) \tag{5.6b}$$

$$\sum_{k=1}^{n}\left(n\,k - k^2\right) = \frac{1}{6}\,n\,\left(n^2+1\right) \tag{5.6c}$$

With equations (5.5) and (5.6) the auxiliary factor can be solved in closed form using the cosecans function by:

$$\frac{\sum V_Q^2}{Q} = \frac{1}{12}\left[q^2\left(3\,\csc^2\left(\frac{\pi}{2\,m}\right)-2\right)+2\right] \tag{5.7}$$

Via equations (5.7), (4.18) and (4.19), the harmonic scattering coefficient σ_o for full pitched single and double layer windings of poly phase systems can be calculated comfortably. The following chapters deal with the calculation of the harmonic scattering coefficient for phase numbers $m = 2, 3, 5$ and 7.

5.1.2 Full Pitched Double Layer Windings with Double Zone Span

The unmentioned case of full pitched windings with double zone span shall be dealt with here.

The ratio of the winding factor of windings with double zone span $\xi_{1,dzs}$ (3.26) to the winding factor with normal zone span $\xi_{1,nzs}$ (3.25) - both for the fundamental wave - for any number of slots results by the use of trigonometric identities always to:

$$\frac{\xi_{1,dzs}}{\xi_{1,nzs}} = \frac{\dfrac{\sin\left(\dfrac{\pi}{m}\right)}{2\,q\,\sin\left(\dfrac{\pi}{2\,q\,m}\right)}}{\dfrac{\sin\left(\dfrac{\pi}{2\,m}\right)}{q\,\sin\left(\dfrac{\pi}{2\,q\,m}\right)}} = \cos\left(\frac{\pi}{2\,m}\right) \tag{5.8}$$

As the example of figure 5.3 shows, there are always two different phases in the upper layer and bottom layer whose zones overlap symmetrically. Considering the total circumference there are thus as many zones as for full pitched windings with normal zone span.

The ratio from equation (5.8) also requires that the total magnetomotive force of all slots of a winding with double zone span is smaller by the factor of $\cos(\pi/(2m))$ compared to those with a normal zone span, and additionally that it is phase-shifted by the angle $\pi/(2m)$.

Focusing on the formulas of the harmonic scattering coefficient σ_o and the auxiliary factor V_{AF}, this results in a smaller sum of the magnetomotive force of the slots, equation (4.18), on the one hand and a smaller square of the winding factor ξ_1 in the denominator of equation (4.19) on the other.

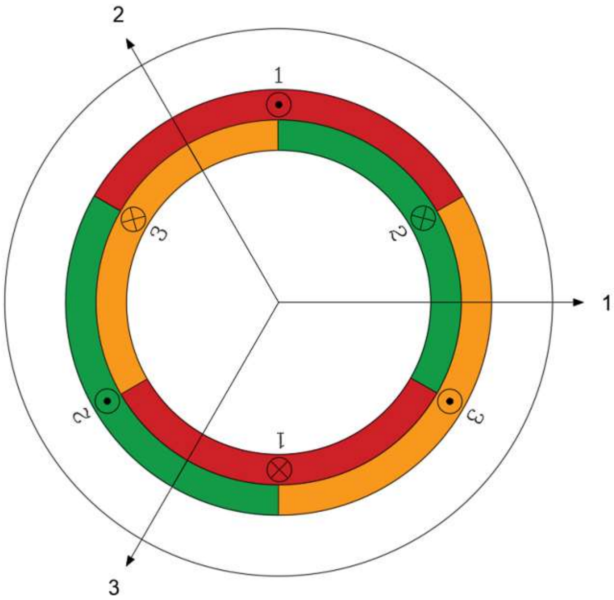

Figure 5.3: Zone diagram of a full pitched double layer winding with three phases and double zone span.

This leads to the interesting fact that phase symmetric full pitched integer slot windings always have the same harmonic scattering factor σ_o, no matter if a single layer winding, a double layer winding with normal zone span or a double layer winding with double zone span.

5.1.3 Pitched Double Layer Windings

The characteristic of common double layer windings is that there are two coil sides in each slot which are usually on top of each other. The zone plan therefore contains two rings. The main advantage of double layer windings is the possibility of pitching. Via the coil pitch σ the zone rings can be shifted against each other. A normal zone span can be made with each number of phases, a double zone span however only with odd numbers of phases. In the following chapter, the general calculation for these variants is given separately.

In addition to full pitched windings, closed solutions for pitched windings can be found in existing literature for the calculation of the harmonic scattering factor at least for two phase and three phase windings (Baffrey (1926), Richter (1954) and Schuisky (1960)). It is important to mention here the restriction of their ranges of validity to $0 \leq |y_\varepsilon| \leq q$.

For shortening steps $|y_\varepsilon| > q$, corresponding approaches of the summed magnetomotive forces have to be defined in the respective steps of the multiple of q to get the auxiliary factor V_{AF}.

The determination of the auxiliary factor for pitched windings is more complicated than the determination of full pitched windings. Furthermore, it plays a significant role in the case of pitching whether the winding is carried out in a normale zone span or a double zone span.

5.1.3.1 Normal Zone Span

The *Görges Polygon* for a winding with normal zone span is formed according to the fourfold number of phases and has a periodicity according to the double number of phases (figure 5.1). Consequently, there are two ray lengths, which represent the magnetomotive force of the slots. This results in two edge lengths of the polygon.

The number of the ranges for the shortening step $|y_\varepsilon|$ is directly depending on the number of phases: m phases require m pitching ranges. This is due to the fact that, as already given by Richter (1954) and reflected with this thesis for all pitching regions, the scattering is symmetric to $|y_\varepsilon| = 0$ for each winding.

When classifying the pitching ranges the last range must be considered in particular. In the region $|y_\varepsilon|$ up to $m\,q$ contributions to the magnetomotive force in some slots disappear due to the high pitch value. In other words, affected edges of the *Görges Polygon* disappear, too, and become “zero length edges”. Thus, the polygon obviously has only the number of edges corresponding to two times the number of phases, while the number of rays to the edges is kept constant to four times the number of phases. In the extreme case of $|y_\varepsilon| = m\,q$, the total magnetomotive force in the slots and thus also the entire *Görges Polygon* disappear. This shortening step also results in vanishing winding factors for all harmonics and is therefore irrelevant.

The disappearance of the magnetomotive force in the slots does <u>not</u> mean a disappearance of those in the teeth of the armature. Contrarily, they remain constant and must be taken into account in the calculation of the auxiliary factor. In the elaboration, this fact is taken into account by the cos term. On the one hand it is possible to realize ”zero length edges” and on the other hand the angle β is fixed to $\pi/2$ to create a triangle with two edge lengths $r_{polycirc}$ and the third edge length of 0. The magnetomotive force of the teeth are superimposed rays with the same length $r_{polycirc}$ in the *Görges Polygon* and are also counted according to their multiplicity.

In the following, the approaches of the summation term of the magnetomotive forces of the slots for a general number of m phases are derived. Due to the detailed treatment of phase numbers 2, 3, 5 and 7, the approaches for the mean values of the magnetomotive force of the slots for seven sub areas are given. It has to be mentioned that the maximum shortening step is always given by $m\,q$. Therefore, different regions equal to the number of phases have to be discussed.

Range: $\mathbf{0 \leq |y_\varepsilon| \leq q}$

Absolute values of the magnetomotive forces of the slots (rays of the polygon):

$$|V_N| = 1 \quad , \quad |V_N| = \cos\left(\frac{\pi}{2\,m}\right) \tag{5.9}$$

Edge lengths:

$$(q - |y_\varepsilon|) \quad , \quad |y_\varepsilon| \cos\left(\frac{\pi}{2\,m}\right) \tag{5.10}$$

The angle of pivot of the polygon can be represented as a sum by

$$\alpha + \beta = \pi - \frac{\pi}{2\,m}. \tag{5.11}$$

This results in the following aggregations with respect to the radius of the circumcircle of the polygon

$$\cos(\alpha) = \frac{q - |y_\varepsilon|}{2\,r_{polycirc}} \quad , \quad \cos(\beta) = \frac{|y_\varepsilon|}{2\,r_{polycirc}} \cos\left(\frac{\pi}{2\,m}\right), \tag{5.12}$$

and finally an expression for the radius of the circumcircle

$$r^2_{polycirc} = \frac{q^2 - |y_\varepsilon|\,(2\,q - |y_\varepsilon|)\,\sin^2\left(\frac{\pi}{2\,m}\right)}{4\,\sin^2\left(\frac{\pi}{2\,m}\right)}. \tag{5.13}$$

Figure 5.4 shows the relationships of edge lengths and angles for this pitching range.

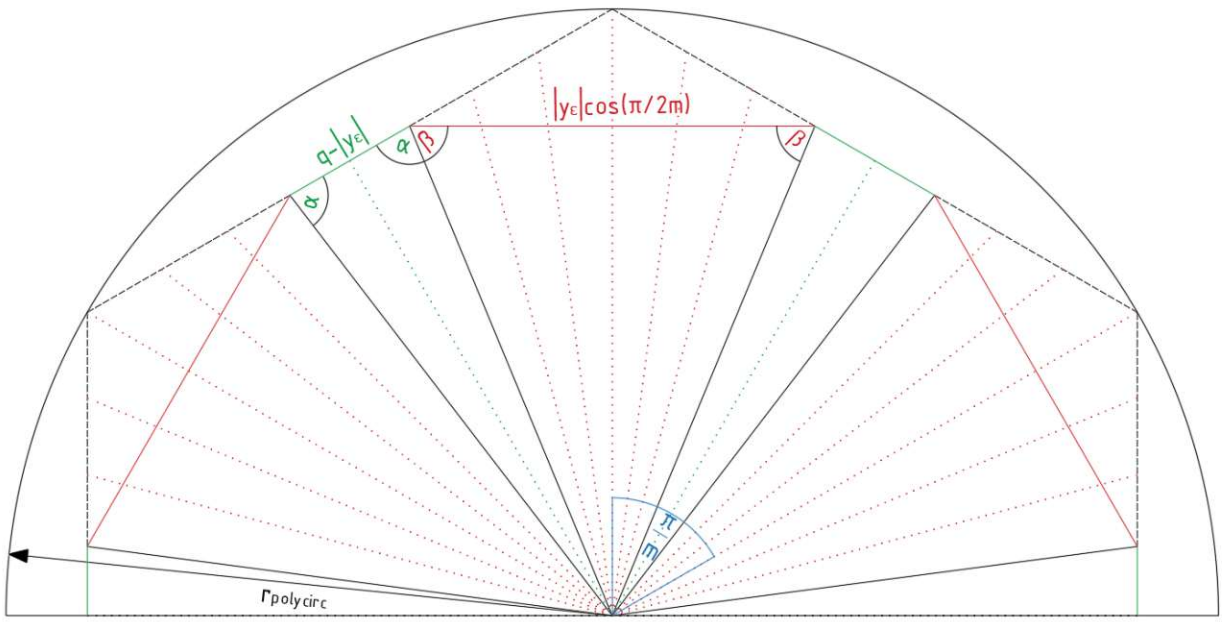

Figure 5.4: Half *Görges Polygon* of a winding with $m = 3$ for an exemplarily pitch of the range $0 \leq y_\varepsilon \leq q$.

The mean value of the magnetomotive force of the slots is calculated in the same way as in section 5.1.1.1.

$$\begin{aligned}\frac{\sum V_Q^2}{Q} &= \frac{1}{q}\sum_{k=1}^{q-|y_\varepsilon|}\left[r_{polycirc}^2 + k^2 - 2\,r_{polycirc}\,k\,\cos(\alpha)\right] \\ &+ \frac{1}{q}\sum_{k=1}^{|y_\varepsilon|}\left[r_{polycirc}^2 + k^2\,\cos^2\left(\frac{\pi}{2\,m}\right) - 2\,r_{polycirc}\,k\,\cos\left(\frac{\pi}{2\,m}\right)\,\cos(\beta)\right] \\ &= r_{polycirc}^2 - \frac{1}{6\,q}\left[(q-|y_\varepsilon|) - \left((q-|y_\varepsilon|)^2 - 1\right) + |y_\varepsilon|\,\left(y_\varepsilon^2 - 1\right)\,\cos^2\left(\frac{\pi}{2\,m}\right)\right]\end{aligned} \tag{5.14}$$

Range: $\mathbf{q \le |y_\varepsilon| \le 2\,q}$

Absolute values of the magnetomotive forces of the slots (rays of the polygon):

$$|V_N| = \cos\left(\frac{\pi}{2\,m}\right) \quad , \quad |V_N| = \cos\left(\frac{2\,\pi}{2\,m}\right) \tag{5.15}$$

Edge lengths:

$$(2\,q - |y_\varepsilon|)\,\cos\left(\frac{\pi}{2\,m}\right) \quad , \quad (|y_\varepsilon| - q)\,\cos\left(\frac{2\,\pi}{2\,m}\right) \tag{5.16}$$

The angle of pivot of the polygon is the same as in equation (5.11). This results in the following aggregations with respect to the radius of the circumcircle of the polygon

$$\cos(\alpha) = \frac{2\,q - |y_\varepsilon|}{2\,r_{polycirc}}\,\cos\left(\frac{\pi}{2\,m}\right) \quad , \quad \cos(\beta) = \frac{|y_\varepsilon| - q}{2\,r_{polycirc}}\,\cos\left(\frac{2\,\pi}{2\,m}\right), \tag{5.17}$$

and finally an expression for the radius of the circumcircle

$$r_{polycirc}^2 = \frac{q^2 + 4\,q\,(|y_\varepsilon| - q)\,\sin^4\left(\frac{\pi}{2\,m}\right) + (4\,q^2 - 6\,q\,|y_\varepsilon| + y_\varepsilon^2)\,\sin^2\left(\frac{\pi}{2\,m}\right)}{4\,\sin^2\left(\frac{\pi}{2\,m}\right)}. \tag{5.18}$$

The mean value of the magnetomotive force of the slots is calculated in the same way as in section 5.1.1.1.

$$
\begin{aligned}
\frac{\sum V_Q^2}{Q} &= \frac{1}{q}\sum_{k=1}^{2q-|y_\varepsilon|}\left[r_{polycirc}^2 + k^2\,\cos^2\left(\frac{\pi}{2\,m}\right) - 2\,r_{polycirc}\,k\,\cos\left(\frac{\pi}{2\,m}\right)\cos\left(\alpha\right)\right]\\
&+ \frac{1}{q}\sum_{k=1}^{|y_\varepsilon|-q}\left[r_{polycirc}^2 + k^2\,\cos^2\left(\frac{2\,\pi}{2\,m}\right) - 2\,r_{polycirc}\,k\,\cos\left(\frac{2\,\pi}{2\,m}\right)\cos\left(\beta\right)\right]\\
&= r_{polycirc}^2 - \frac{1}{6\,q}\left(2\,q-|y_\varepsilon|\right)\left[\left(2\,q-|y_\varepsilon|\right)^2-1\right]\,\cos^2\left(\frac{\pi}{2\,m}\right)\\
&- \frac{1}{6\,q}\left(|y_\varepsilon|-q\right)\left[\left(|y_\varepsilon|-q\right)^2-1\right]\,\cos^2\left(\frac{2\,\pi}{2\,m}\right)
\end{aligned}
\tag{5.19}
$$

Range: $\mathbf{2\,q \leq |y_\varepsilon| \leq 3\,q\ ,\ m \geq 3}$

Absolute values of the magnetomotive forces of the slots (rays of the polygon):

$$|V_N| = \cos\left(\frac{2\,\pi}{2\,m}\right)\quad,\quad |V_N| = \cos\left(\frac{3\,\pi}{2\,m}\right) \tag{5.20}$$

Edge lengths:

$$\left(3\,q-|y_\varepsilon|\right)\,\cos\left(\frac{2\,\pi}{2\,m}\right)\quad,\quad \left(|y_\varepsilon|-2\,q\right)\,\cos\left(\frac{3\,\pi}{2\,m}\right) \tag{5.21}$$

The angle of pivot of the polygon is the same as in equation (5.11). This results in the following aggregations with respect to the radius of the circumcircle of the polygon

$$\cos\left(\alpha\right) = \frac{3\,q-|y_\varepsilon|}{2\,r_{polycirc}}\,\cos\left(\frac{2\,\pi}{2\,m}\right)\quad,\quad \cos\left(\beta\right) = \frac{|y_\varepsilon|-2\,q}{2\,r_{polycirc}}\,\cos\left(\frac{3\,\pi}{2\,m}\right), \tag{5.22}$$

and finally an expression for the radius of the circumcircle

$$
\begin{aligned}
r_{polycirc}^2 &= \frac{\left(3\,q-|y_\varepsilon|\right)^2\,\cos^2\left(\frac{2\,\pi}{2\,m}\right) + \left(|y_\varepsilon|-2\,q\right)^2\,\cos^2\left(\frac{3\,\pi}{2\,m}\right)}{4\,\sin^2\left(\frac{\pi}{2\,m}\right)}\\
&+ \frac{2\,\left(3\,q-|y_\varepsilon|\right)\left(|y_\varepsilon|-2\,q\right)\,\cos\left(\frac{2\,\pi}{2\,m}\right)\,\cos\left(\frac{3\,\pi}{2\,m}\right)\,\cos\left(\frac{\pi}{2\,m}\right)}{4\,\sin^2\left(\frac{\pi}{2\,m}\right)}.
\end{aligned}
\tag{5.23}
$$

The mean value of the magnetomotive force of the slots is calculated in the same way as in section 5.1.1.1.

$$\begin{aligned}\frac{\sum V_Q^2}{Q} &= \frac{1}{q}\sum_{k=1}^{3\,q-|y_\varepsilon|}\left[r_{polycirc}^2 + k^2\,\cos^2\left(\frac{2\,\pi}{2\,m}\right) - 2\,r_{polycirc}\,k\,\cos\left(\frac{2\,\pi}{2\,m}\right)\,\cos\left(\alpha\right)\right]\\ &+ \frac{1}{q}\sum_{k=1}^{|y_\varepsilon|-2\,q}\left[r_{polycirc}^2 + k^2\,\cos^2\left(\frac{3\,\pi}{2\,m}\right) - 2\,r_{polycirc}\,k\,\cos\left(\frac{3\,\pi}{2\,m}\right)\,\cos\left(\beta\right)\right]\\ &= r_{polycirc}^2 - \frac{1}{6\,q}\left(3\,q-|y_\varepsilon|\right)\left[\left(3\,q-|y_\varepsilon|\right)^2-1\right]\,\cos^2\left(\frac{2\,\pi}{2\,m}\right)\\ &- \frac{1}{6\,q}\left(|y_\varepsilon|-2\,q\right)\left[\left(|y_\varepsilon|-2\,q\right)^2-1\right]\,\cos^2\left(\frac{3\,\pi}{2\,m}\right)\end{aligned} \tag{5.24}$$

Range: $\mathbf{3\,q \leq |y_\varepsilon| \leq 4\,q\ ,\ m \geq 5}$

Absolute values of the magnetomotive forces of the slots (rays of the polygon):

$$|V_N| = \cos\left(\frac{3\,\pi}{2\,m}\right)\quad,\quad |V_N| = \cos\left(\frac{4\,\pi}{2\,m}\right) \tag{5.25}$$

Edge lengths:

$$\left(4\,q-|y_\varepsilon|\right)\,\cos\left(\frac{3\,\pi}{2\,m}\right)\quad,\quad \left(|y_\varepsilon|-3\,q\right)\,\cos\left(\frac{4\,\pi}{2\,m}\right) \tag{5.26}$$

The angle of pivot of the polygon is the same as in equation (5.11). This results in the following aggregations with respect to the radius of the circumcircle of the polygon

$$\cos\left(\alpha\right) = \frac{4\,q-|y_\varepsilon|}{2\,r_{polycirc}}\,\cos\left(\frac{3\,\pi}{2\,m}\right)\quad,\quad \cos\left(\beta\right) = \frac{|y_\varepsilon|-3\,q}{2\,r_{polycirc}}\,\cos\left(\frac{4\,\pi}{2\,m}\right), \tag{5.27}$$

and finally an expression for the radius of the circumcircle

$$\begin{aligned}r_{polycirc}^2 &= \frac{\left(4\,q-|y_\varepsilon|\right)^2\,\cos^2\left(\frac{3\,\pi}{2\,m}\right) + \left(|y_\varepsilon|-3\,q\right)^2\,\cos^2\left(\frac{4\,\pi}{2\,m}\right)}{4\,\sin^2\left(\frac{\pi}{2\,m}\right)}\\ &+ \frac{2\,\left(4\,q-|y_\varepsilon|\right)\left(|y_\varepsilon|-3\,q\right)\,\cos\left(\frac{3\,\pi}{2\,m}\right)\,\cos\left(\frac{4\,\pi}{2\,m}\right)\,\cos\left(\frac{\pi}{2\,m}\right)}{4\,\sin^2\left(\frac{\pi}{2\,m}\right)}.\end{aligned} \tag{5.28}$$

The mean value of the magnetomotive force of the slots is calculated in the same way as in section 5.1.1.1.

$$\begin{aligned}\frac{\sum V_Q^2}{Q} &= \frac{1}{q}\sum_{k=1}^{4\,q-|y_\varepsilon|}\left[r_{polycirc}^2 + k^2\,\cos^2\left(\frac{3\,\pi}{2\,m}\right) - 2\,r_{polycirc}\,k\,\cos\left(\frac{3\,\pi}{2\,m}\right)\,\cos(\alpha)\right]\\ &+ \frac{1}{q}\sum_{k=1}^{|y_\varepsilon|-3\,q}\left[r_{polycirc}^2 + k^2\,\cos^2\left(\frac{4\,\pi}{2\,m}\right) - 2\,r_{polycirc}\,k\,\cos\left(\frac{4\,\pi}{2\,m}\right)\,\cos(\beta)\right]\\ &= r_{polycirc}^2 - \frac{1}{6\,q}\,(4\,q-|y_\varepsilon|)\,\left[(4\,q-|y_\varepsilon|)^2-1\right]\,\cos^2\left(\frac{3\,\pi}{2\,m}\right)\\ &- \frac{1}{6\,q}\,(|y_\varepsilon|-3\,q)\,\left[(|y_\varepsilon|-3\,q)^2-1\right]\,\cos^2\left(\frac{4\,\pi}{2\,m}\right)\end{aligned} \tag{5.29}$$

Range: $\mathbf{4\,q \leq |y_\varepsilon| \leq 5\,q}$, $\mathbf{m \geq 5}$

Absolute values of the magnetomotive forces of the slots (rays of the polygon):

$$|V_N| = \cos\left(\frac{4\,\pi}{2\,m}\right) \quad , \quad |V_N| = \cos\left(\frac{5\,\pi}{2\,m}\right) \tag{5.30}$$

Edge lengths:

$$(5\,q-|y_\varepsilon|)\,\cos\left(\frac{4\,\pi}{2\,m}\right) \quad , \quad (|y_\varepsilon|-4\,q)\,\cos\left(\frac{5\,\pi}{2\,m}\right) \tag{5.31}$$

The angle of pivot of the polygon is the same as in equation (5.11). This results in the following aggregations with respect to the radius of the circumcircle of the polygon

$$\cos(\alpha) = \frac{5\,q-|y_\varepsilon|}{2\,r_{polycirc}}\,\cos\left(\frac{4\,\pi}{2\,m}\right) \quad , \quad \cos(\beta) = \frac{|y_\varepsilon|-4\,q}{2\,r_{polycirc}}\,\cos\left(\frac{5\,\pi}{2\,m}\right), \tag{5.32}$$

and finally an expression for the radius of the circumcircle

$$\begin{aligned} r_{polycirc}^2 &= \frac{(5\,q-|y_\varepsilon|)^2\,\cos^2\left(\frac{4\,\pi}{2\,m}\right) + (|y_\varepsilon|-4\,q)^2\,\cos^2\left(\frac{5\,\pi}{2\,m}\right)}{4\,\sin^2\left(\frac{\pi}{2\,m}\right)}\\ &+ \frac{2\,(5\,q-|y_\varepsilon|)\,(|y_\varepsilon|-4\,q)\,\cos\left(\frac{4\,\pi}{2\,m}\right)\,\cos\left(\frac{5\,\pi}{2\,m}\right)\,\cos\left(\frac{\pi}{2\,m}\right)}{4\,\sin^2\left(\frac{\pi}{2\,m}\right)}.\end{aligned} \tag{5.33}$$

Figure 5.5 shows the relationships of edge lengths and angles for this pitching range.

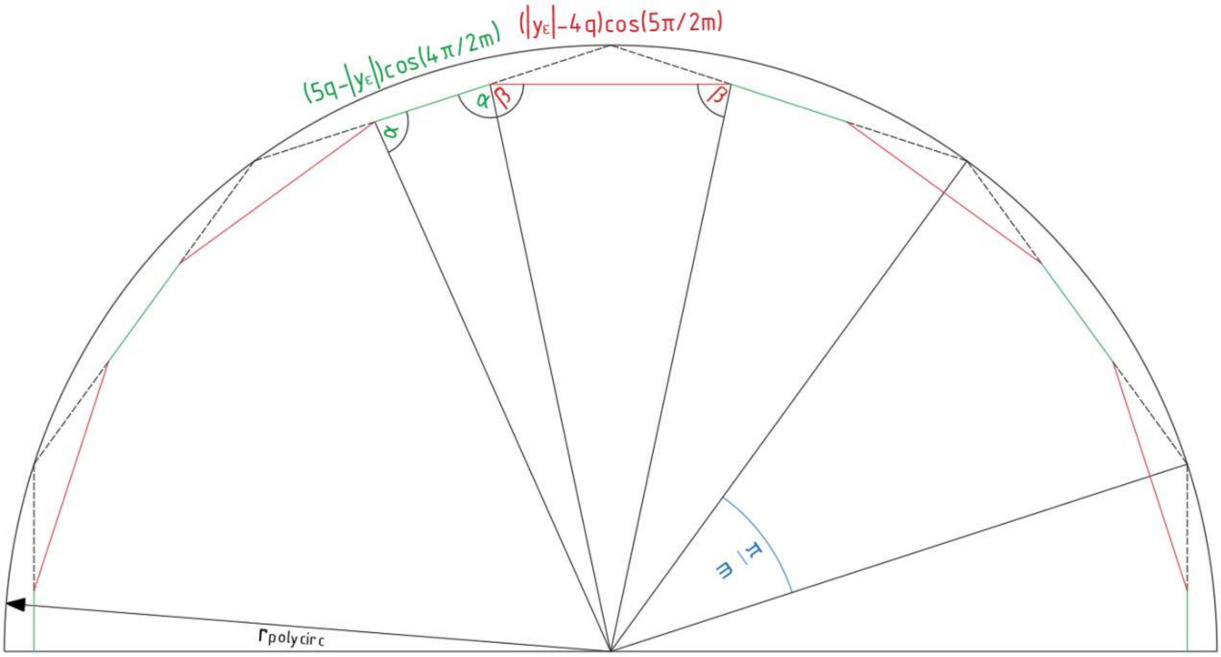

Figure 5.5: Half *Görges Polygon* of a winding with $m = 5$ for an exemplary pitch of the range $4\,q \leq y_\varepsilon \leq 5\,q$.

The mean value of the magnetomotive force of the slots is calculated in the same way as in section 5.1.1.1.

$$\begin{aligned}\frac{\sum V_Q^2}{Q} &= \frac{1}{q}\sum_{k=1}^{5\,q-|y_\varepsilon|}\left[r_{polycirc}^2 + k^2\,\cos^2\left(\frac{4\,\pi}{2\,m}\right) - 2\,r_{polycirc}\,k\,\cos\left(\frac{4\,\pi}{2\,m}\right)\,\cos(\alpha)\right]\\ &+ \frac{1}{q}\sum_{k=1}^{|y_\varepsilon|-4\,q}\left[r_{polycirc}^2 + k^2\,\cos^2\left(\frac{5\,\pi}{2\,m}\right) - 2\,r_{polycirc}\,k\,\cos\left(\frac{5\,\pi}{2\,m}\right)\,\cos(\beta)\right]\\ &= r_{polycirc}^2 - \frac{1}{6\,q}\,(5\,q-|y_\varepsilon|)\left[(5\,q-|y_\varepsilon|)^2-1\right]\,\cos^2\left(\frac{4\,\pi}{2\,m}\right)\\ &- \frac{1}{6\,q}\,(|y_\varepsilon|-4\,q)\left[(|y_\varepsilon|-4\,q)^2-1\right]\,\cos^2\left(\frac{5\,\pi}{2\,m}\right)\end{aligned} \tag{5.34}$$

Range: $\mathbf{5\,q \leq |y_\varepsilon| \leq 6\,q}$, $\mathbf{m \geq 7}$

Absolute values of the magnetomotive forces of the slots (rays of the polygon):

$$|V_N| = \cos\left(\frac{5\,\pi}{2\,m}\right) \quad , \quad |V_N| = \cos\left(\frac{6\,\pi}{2\,m}\right) \tag{5.35}$$

Edge lengths:

$$(6\,q-|y_\varepsilon|)\,\cos\left(\frac{5\,\pi}{2\,m}\right) \quad , \quad (|y_\varepsilon|-5\,q)\,\cos\left(\frac{6\,\pi}{2\,m}\right) \tag{5.36}$$

The angle of pivot of the polygon is the same as in equation (5.11). This results in the following aggregations with respect to the radius of the circumcircle of the polygon

$$\cos(\alpha)=\frac{6\,q-|y_\varepsilon|}{2\,r_{polycirc}}\,\cos\left(\frac{5\,\pi}{2\,m}\right) \quad , \quad \cos(\beta)=\frac{|y_\varepsilon|-5\,q}{2\,r_{polycirc}}\,\cos\left(\frac{6\,\pi}{2\,m}\right), \tag{5.37}$$

and finally an expression for the radius of the circumcircle

$$\begin{aligned} r^2_{polycirc} &= \frac{(6\,q-|y_\varepsilon|)^2\,\cos^2\left(\frac{5\,\pi}{2\,m}\right)+(|y_\varepsilon|-5\,q)^2\,\cos^2\left(\frac{6\,\pi}{2\,m}\right)}{4\,\sin^2\left(\frac{\pi}{2\,m}\right)} \\ &+\frac{2\,(6\,q-|y_\varepsilon|)\,(|y_\varepsilon|-5\,q)\,\cos\left(\frac{5\,\pi}{2\,m}\right)\,\cos\left(\frac{6\,\pi}{2\,m}\right)\,\cos\left(\frac{\pi}{2\,m}\right)}{4\,\sin^2\left(\frac{\pi}{2\,m}\right)}. \end{aligned} \tag{5.38}$$

The mean value of the magnetomotive force of the slots is calculated in the same way as in section 5.1.1.1.

$$\begin{aligned} \frac{\sum V_Q^2}{Q} &= \frac{1}{q}\sum_{k=1}^{6\,q-|y_\varepsilon|}\left[r^2_{polycirc}+k^2\,\cos^2\left(\frac{5\,\pi}{2\,m}\right)-2\,r_{polycirc}\,k\,\cos\left(\frac{5\,\pi}{2\,m}\right)\,\cos(\alpha)\right] \\ &+\frac{1}{q}\sum_{k=1}^{|y_\varepsilon|-5\,q}\left[r^2_{polycirc}+k^2\,\cos^2\left(\frac{6\,\pi}{2\,m}\right)-2\,r_{polycirc}\,k\,\cos\left(\frac{6\,\pi}{2\,m}\right)\,\cos(\beta)\right] \\ &= r^2_{polycirc}-\frac{1}{6\,q}\,(6\,q-|y_\varepsilon|)\left[(6\,q-|y_\varepsilon|)^2-1\right]\,\cos^2\left(\frac{5\,\pi}{2\,m}\right) \\ &-\frac{1}{6\,q}\,(|y_\varepsilon|-5\,q)\left[(|y_\varepsilon|-5\,q)^2-1\right]\,\cos^2\left(\frac{6\,\pi}{2\,m}\right) \end{aligned} \tag{5.39}$$

Range: $\mathbf{6\,q \le |y_\varepsilon| \le 7\,q}$, $\mathbf{m \ge 7}$

Absolute values of the magnetomotive forces of the slots (rays of the polygon):

$$|V_N|=\cos\left(\frac{6\,\pi}{2\,m}\right) \quad , \quad |V_N|=\cos\left(\frac{7\,\pi}{2\,m}\right) \tag{5.40}$$

Edge lengths:

$$(7\,q - |y_\varepsilon|)\,\cos\left(\frac{6\,\pi}{2\,m}\right) \quad , \quad (|y_\varepsilon| - 6\,q)\,\cos\left(\frac{7\,\pi}{2\,m}\right) \tag{5.41}$$

The angle of pivot of the polygon is the same as in equation (5.11). This results in the following aggregations with respect to the radius of the circumcircle of the polygon

$$\cos(\alpha) = \frac{7\,q - |y_\varepsilon|}{2\,r_{polycirc}}\,\cos\left(\frac{6\,\pi}{2\,m}\right) \quad , \quad \cos(\beta) = \frac{|y_\varepsilon| - 6\,q}{2\,r_{polycirc}}\,\cos\left(\frac{7\,\pi}{2\,m}\right), \tag{5.42}$$

and finally an expression for the radius of the circumcircle

$$\begin{aligned} r_{polycirc}^2 = & \frac{(7\,q - |y_\varepsilon|)^2\,\cos^2\left(\frac{6\,\pi}{2\,m}\right) + (|y_\varepsilon| - 6\,q)^2\,\cos^2\left(\frac{7\,\pi}{2\,m}\right)}{4\,\sin^2\left(\frac{\pi}{2\,m}\right)} \\ & + \frac{2\,(7\,q - |y_\varepsilon|)\,(|y_\varepsilon| - 6\,q)\,\cos\left(\frac{6\,\pi}{2\,m}\right)\,\cos\left(\frac{7\,\pi}{2\,m}\right)\,\cos\left(\frac{\pi}{2\,m}\right)}{4\,\sin^2\left(\frac{\pi}{2\,m}\right)}. \end{aligned} \tag{5.43}$$

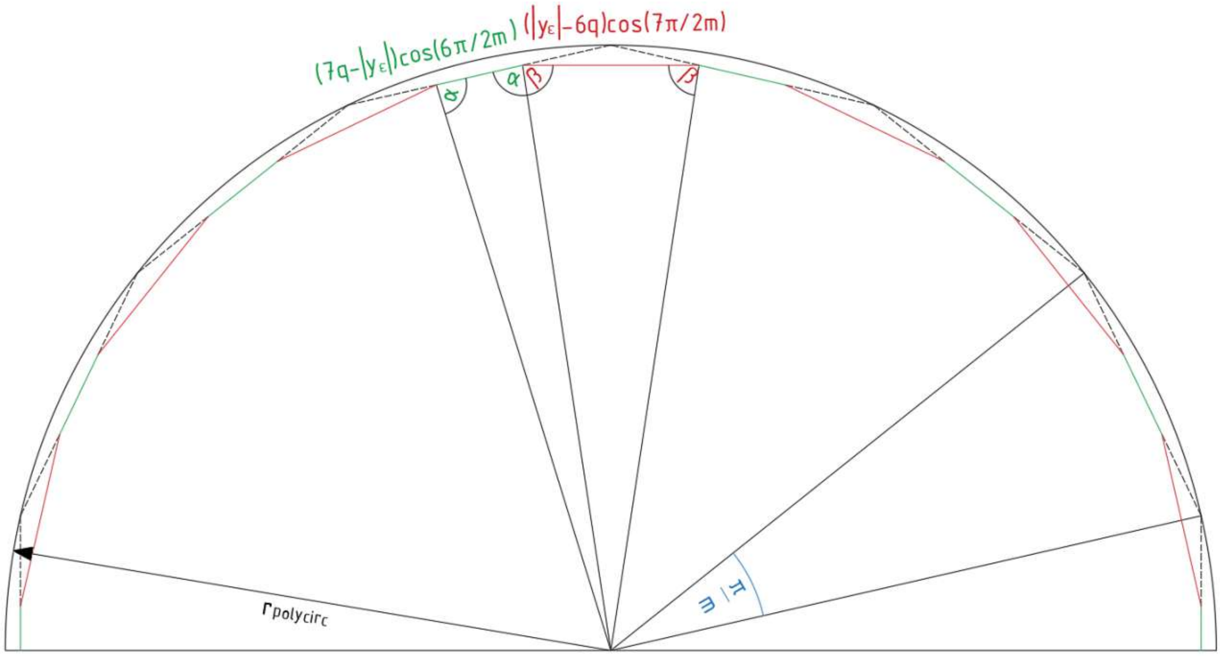

Figure 5.6: Half *Görges Polygon* of a winding with $m = 7$ for an exemlarily pitch of the range $6\,q \leq y_\varepsilon \leq 7\,q$.

The mean value of the magnetomotive force of the slots is calculated in the same way as in section 5.1.1.1.

$$\begin{aligned}
\frac{\sum V_Q^2}{Q} &= \frac{1}{q}\sum_{k=1}^{7\,q-|y_\varepsilon|}\left[r_{polycirc}^2 + k^2\,\cos^2\left(\frac{6\,\pi}{2\,m}\right) - 2\,r_{polycirc}\,k\,\cos\left(\frac{6\,\pi}{2\,m}\right)\,\cos\left(\alpha\right)\right] \\
&+ \frac{1}{q}\sum_{k=1}^{|y_\varepsilon|-6\,q}\left[r_{polycirc}^2 + k^2\,\cos^2\left(\frac{7\,\pi}{2\,m}\right) - 2\,r_{polycirc}\,k\,\cos\left(\frac{7\,\pi}{2\,m}\right)\,\cos\left(\beta\right)\right] \\
&= r_{polycirc}^2 - \frac{1}{6\,q}\left(7\,q-|y_\varepsilon|\right)\left[\left(7\,q-|y_\varepsilon|\right)^2-1\right]\,\cos^2\left(\frac{6\,\pi}{2\,m}\right) \\
&- \frac{1}{6\,q}\left(|y_\varepsilon|-6\,q\right)\left[\left(|y_\varepsilon|-6\,q\right)^2-1\right]\,\cos^2\left(\frac{7\,\pi}{2\,m}\right)
\end{aligned} \tag{5.44}$$

Range: $\mathbf{(l-1)\;q \leq |y_\varepsilon| \leq l\,q}$

The recurring pattern allows a general approach to the l^{th} pitching range of a winding with m phases.

Absolute values of the magnetomotive forces of the slots (rays of the polygon):

$$|V_N| = \cos\left(\frac{(l-1)\;\pi}{2\,m}\right) \quad , \quad |V_N| = \cos\left(\frac{l\,\pi}{2\,m}\right) \tag{5.45}$$

Edge lengths:

$$\left(l\,q-|y_\varepsilon|\right)\,\cos\left(\frac{(l-1)\;\pi}{2\,m}\right) \quad , \quad \left(|y_\varepsilon|-(l-1)\;q\right)\,\cos\left(\frac{l\,\pi}{2\,m}\right) \tag{5.46}$$

The angle of pivot of the polygon is the same as in equation (5.11). This results in the following aggregations with respect to the radius of the circumcircle of the polygon

$$\cos\left(\alpha\right) = \frac{l\,q-|y_\varepsilon|}{2\,r_{polycirc}}\,\cos\left(\frac{(l-1)\;\pi}{2\,m}\right) \quad , \quad \cos\left(\beta\right) = \frac{|y_\varepsilon|-(l-1)\;q}{2\,r_{polycirc}}\,\cos\left(\frac{l\,\pi}{2\,m}\right), \tag{5.47}$$

and finally an expression for the radius of the circumcircle

$$\begin{aligned}
r_{polycirc}^2 &= \frac{\left(l\,q-|y_\varepsilon|\right)^2\,\cos^2\left(\frac{(l-1)\;\pi}{2\,m}\right) + \left(|y_\varepsilon|-(l-1)\;q\right)^2\,\cos^2\left(\frac{l\,\pi}{2\,m}\right)}{4\,\sin^2\left(\frac{\pi}{2\,m}\right)} \\
&+ \frac{2\,\left(l\,q-|y_\varepsilon|\right)\left(|y_\varepsilon|-(l-1)\;q\right)\,\cos\left(\frac{(l-1)\;\pi}{2\,m}\right)\,\cos\left(\frac{l\,\pi}{2\,m}\right)\,\cos\left(\frac{\pi}{2\,m}\right)}{4\,\sin^2\left(\frac{\pi}{2\,m}\right)}.
\end{aligned} \tag{5.48}$$

The mean value of the magnetomotive force of the slots is calculated in the same way as in section 5.1.1.1.

$$
\begin{aligned}
\frac{\sum V_Q^2}{Q} &= \frac{1}{q} \sum_{k=1}^{l\,q-|y_\varepsilon|} \left[r_{polycirc}^2 + k^2 \cos^2\left(\frac{(l-1)\,\pi}{2\,m}\right) - 2\,r_{polycirc}\,k\,\cos\left(\frac{(l-1)\,\pi}{2\,m}\right)\cos(\alpha) \right] \\
&+ \frac{1}{q} \sum_{k=1}^{|y_\varepsilon|-(l-1)\,q} \left[r_{polycirc}^2 + k^2 \cos^2\left(\frac{l\,\pi}{2\,m}\right) - 2\,r_{polycirc}\,k\,\cos\left(\frac{l\,\pi}{2\,m}\right)\cos(\beta) \right] \\
&= r_{polycirc}^2 - \frac{1}{6\,q}\,(l\,q-|y_\varepsilon|)\left[(l\,q-|y_\varepsilon|)^2-1\right]\cos^2\left(\frac{(l-1)\,\pi}{2\,m}\right) \\
&- \frac{1}{6\,q}\,(|y_\varepsilon|-(l-1)\,q)\left[(|y_\varepsilon|-(l-1)\,q)^2-1\right]\cos^2\left(\frac{l\,\pi}{2\,m}\right)
\end{aligned}
\tag{5.49}
$$

5.1.3.2 Double Zone Span

The *Görges Polygon* for a winding with double zone span is formed according to the double number of phases and has a periodicity according to the number of phases. Consequently, there is only one ray length for the first range and two each for every other range, which represent the magnetomotive force of the slots. This results in two edge lengths of the polygon.

The number of the ranges for the shortening step y_ε directly depends on the odd number of phases: m phases require $\lfloor m/2 \rfloor + 1$ pitching ranges.

Like for normal zone span, when classifying the pitching ranges, the last range must be considered as well. In the area $|y_\varepsilon|$ up to $m\,q$ contributions to the magnetomotive force in the slots disappear due to the high pitch value. In other words, affected edges of the *Görges Polygon* disappear and become "zero length edges". Thus, the polygon has only the number of edges which correspond to the number of phases.

Below are the approaches of the summation term of the magnetomotive forces of the slots for a general, odd number of m phases.

Range: $\mathbf{0 \le |y_\varepsilon| \le q}$

Absolute value of the magnetomotive force of the slots (ray of the polygon):

$$
|V_N| = \cos\left(\frac{\pi}{2\,m}\right) \tag{5.50}
$$

Edge lengths:

$$(q - |y_\varepsilon|)\ \cos\left(\frac{\pi}{2\,m}\right) \quad , \quad (q + |y_\varepsilon|)\ \cos\left(\frac{\pi}{2\,m}\right) \tag{5.51}$$

The angle of pivot of the polygon can be represented as a sum by

$$\alpha + \beta = \pi - \frac{\pi}{m}. \tag{5.52}$$

This results in the following aggregations with respect to the radius of the circumcircle of the polygon

$$\cos(\alpha) = \frac{q - |y_\varepsilon|}{2\,r_{polycirc}}\ \cos\left(\frac{\pi}{2\,m}\right) \quad , \quad \cos(\beta) = \frac{q + |y_\varepsilon|}{2\,r_{polycirc}}\ \cos\left(\frac{\pi}{2\,m}\right), \tag{5.53}$$

and finally an expression for the radius of the circumcircle

$$r_{polycirc}^2 = \frac{q^2\ \cos^2\left(\frac{\pi}{2\,m}\right) + y_\varepsilon^2\ \sin^2\left(\frac{\pi}{2\,m}\right)}{4\ \sin^2\left(\frac{\pi}{2\,m}\right)}. \tag{5.54}$$

The mean value of the magnetomotive force of the slots is calculated in the same way as in section 5.1.1.1.

$$\begin{aligned}\frac{\sum V_Q^2}{Q} &= \frac{1}{2\,q}\sum_{k=1}^{q-|y_\varepsilon|}\left[r_{polycirc}^2 + k^2\ \cos^2\left(\frac{\pi}{2\,m}\right) - 2\,r_{polycirc}\,k\ \cos\left(\frac{\pi}{2\,m}\right)\ \cos(\alpha)\right] \\ &+ \frac{1}{2\,q}\sum_{k=1}^{q+|y_\varepsilon|}\left[r_{polycirc}^2 + k^2\ \cos^2\left(\frac{\pi}{2\,m}\right) - 2\,r_{polycirc}\,k\ \cos\left(\frac{\pi}{2\,m}\right)\ \cos(\beta)\right] \\ &= r_{polycirc}^2 - \frac{1}{6}\left(q^2 + 3\,y_\varepsilon^2 - 1\right)\ \cos^2\left(\frac{\pi}{2\,m}\right)\end{aligned} \tag{5.55}$$

Range: $\mathbf{q \le |y_\varepsilon| \le 3\,q\ ,\ m \ge 3}$

Absolute values of the magnetomotive force of the slots (rays of the polygon):

$$|V_N| = \cos\left(\frac{\pi}{2\,m}\right) \quad , \quad |V_N| = \cos\left(\frac{3\,\pi}{2\,m}\right) \tag{5.56}$$

Edge lengths:

$$(3\,q - |y_\varepsilon|)\,\cos\left(\frac{\pi}{2\,m}\right) \quad , \quad (|y_\varepsilon| - q)\,\cos\left(\frac{3\,\pi}{2\,m}\right) \tag{5.57}$$

The angle of pivot of the polygon is the same as in equation (5.52). This results in the following aggregations with respect to the radius of the circumcircle of the polygon

$$\cos(\alpha) = \frac{3\,q - |y_\varepsilon|}{2\,r_{polycirc}}\,\cos\left(\frac{\pi}{2\,m}\right) \quad , \quad \cos(\beta) = \frac{|y_\varepsilon| - q}{2\,r_{polycirc}}\,\cos\left(\frac{3\,\pi}{2\,m}\right), \tag{5.58}$$

and finally an expression for the radius of the circumcircle

$$\begin{aligned} r_{polycirc}^2 &= \frac{(3\,q - |y_\varepsilon|)^2\,\cos^2\left(\frac{\pi}{2\,m}\right) + (|y_\varepsilon| - q)^2\,\cos^2\left(\frac{3\,\pi}{2\,m}\right)}{4\,\sin^2\left(\frac{\pi}{m}\right)} \\ &+ \frac{2\,(3\,q - |y_\varepsilon|)\,(|y_\varepsilon| - q)\cos\left(\frac{\pi}{2\,m}\right)\,\cos\left(\frac{3\,\pi}{2\,m}\right)\,\cos\left(\frac{\pi}{m}\right)}{4\,\sin^2\left(\frac{\pi}{m}\right)}. \end{aligned} \tag{5.59}$$

The mean value of the magnetomotive force of the slots is calculated in the same way as in section 5.1.1.1.

$$\begin{aligned} \frac{\sum V_Q^2}{Q} &= \frac{1}{2\,q}\sum_{k=1}^{3\,q-|y_\varepsilon|}\left[r_{polycirc}^2 + k^2\,\cos^2\left(\frac{\pi}{2\,m}\right) - 2\,r_{polycirc}\,k\,\cos\left(\frac{\pi}{2\,m}\right)\,\cos(\alpha)\right] \\ &+ \frac{1}{2\,q}\sum_{k=1}^{|y_\varepsilon|-q}\left[r_{polycirc}^2 + k^2\,\cos^2\left(\frac{3\,\pi}{2\,m}\right) - 2\,r_{polycirc}\,k\,\cos\left(\frac{3\,\pi}{2\,m}\right)\,\cos(\beta)\right] \\ &= r_{polycirc}^2 - \frac{1}{12\,q}\,(3\,q - |y_\varepsilon|)\left((3\,q - |y_\varepsilon|)^2 - 1\right)\,\cos^2\left(\frac{\pi}{2\,m}\right) \\ &- \frac{1}{12\,q}\,(|y_\varepsilon| - q)\left((|y_\varepsilon| - q)^2 - 1\right)\,\cos^2\left(\frac{3\,\pi}{2\,m}\right) \end{aligned} \tag{5.60}$$

Range: $\mathbf{3\,q \leq |y_\varepsilon| \leq 5\,q\ ,\ m \geq 5}$

Absolute values of the magnetomotive force of the slots (rays of the polygon):

$$|V_N| = \cos\left(\frac{3\,\pi}{2\,m}\right) \quad , \quad |V_N| = \cos\left(\frac{5\,\pi}{2\,m}\right) \tag{5.61}$$

Edge lengths:

$$(5\,q - |y_\varepsilon|)\,\cos\left(\frac{3\,\pi}{2\,m}\right) \quad , \quad (|y_\varepsilon| - 3\,q)\,\cos\left(\frac{5\,\pi}{2\,m}\right) \tag{5.62}$$

The angle of pivot of the polygon is the same as in equation (5.11). This results in the following aggregations with respect to the radius of the circumcircle of the polygon

$$\cos(\alpha) = \frac{5\,q - |y_\varepsilon|}{2\,r_{polycirc}}\,\cos\left(\frac{3\,\pi}{2\,m}\right) \quad , \quad \cos(\beta) = \frac{|y_\varepsilon| - 3\,q}{2\,r_{polycirc}}\,\cos\left(\frac{5\,\pi}{2\,m}\right), \tag{5.63}$$

and finally an expression for the radius of the circumcircle

$$\begin{aligned} r^2_{polycirc} = &\frac{(5\,q - |y_\varepsilon|)^2\,\cos^2\left(\frac{3\,\pi}{2\,m}\right) + (|y_\varepsilon| - 3\,q)^2\,\cos^2\left(\frac{5\,\pi}{2\,m}\right)}{4\,\sin^2\left(\frac{\pi}{m}\right)} \\ &+ \frac{2\,(5\,q - |y_\varepsilon|)\,(|y_\varepsilon| - 3\,q)\cos\left(\frac{3\,\pi}{2\,m}\right)\,\cos\left(\frac{5\,\pi}{2\,m}\right)\,\cos\left(\frac{\pi}{m}\right)}{4\,\sin^2\left(\frac{\pi}{m}\right)}. \end{aligned} \tag{5.64}$$

The mean value of the magnetomotive force of the slots is calculated in the same way as in section 5.1.1.1.

$$\begin{aligned} \frac{\sum V_Q^2}{Q} &= \frac{1}{2\,q}\sum_{k=1}^{5\,q-|y_\varepsilon|}\left[r^2_{polycirc} + k^2\,\cos^2\left(\frac{3\,\pi}{2\,m}\right) - 2\,r_{polycirc}\,k\,\cos\left(\frac{3\,\pi}{2\,m}\right)\,\cos(\alpha)\right] \\ &+ \frac{1}{2\,q}\sum_{k=1}^{|y_\varepsilon|-3\,q}\left[r^2_{polycirc} + k^2\,\cos^2\left(\frac{5\,\pi}{2\,m}\right) - 2\,r_{polycirc}\,k\,\cos\left(\frac{5\,\pi}{2\,m}\right)\,\cos(\beta)\right] \\ &= r^2_{polycirc} - \frac{1}{12\,q}\,(5\,q - |y_\varepsilon|)\left((5\,q - |y_\varepsilon|)^2 - 1\right)\,\cos^2\left(\frac{3\,\pi}{2\,m}\right) \\ &- \frac{1}{12\,q}\,(|y_\varepsilon| - 3\,q)\left((|y_\varepsilon| - 3\,q)^2 - 1\right)\,\cos^2\left(\frac{5\,\pi}{2\,m}\right) \end{aligned} \tag{5.65}$$

Range: $\mathbf{5\,q \leq |y_\varepsilon| \leq 7\,q}$, $\mathbf{m \geq 7}$

Absolute values of the magnetomotive force of the slots (rays of the polygon):

$$|V_N| = \cos\left(\frac{5\,\pi}{2\,m}\right) \quad , \quad |V_N| = \cos\left(\frac{7\,\pi}{2\,m}\right) \tag{5.66}$$

Edge lengths:

$$(7\,q - |y_\varepsilon|)\,\cos\left(\frac{5\,\pi}{2\,m}\right) \quad , \quad (|y_\varepsilon| - 5\,q)\,\cos\left(\frac{7\,\pi}{2\,m}\right) \tag{5.67}$$

The angle of pivot of the polygon is the same as in equation (5.11). This results in the following aggregations with respect to the radius of the circumcircle of the polygon

$$\cos(\alpha) = \frac{7\,q - |y_\varepsilon|}{2\,r_{polycirc}}\,\cos\left(\frac{5\,\pi}{2\,m}\right) \quad , \quad \cos(\beta) = \frac{|y_\varepsilon| - 5\,q}{2\,r_{polycirc}}\,\cos\left(\frac{7\,\pi}{2\,m}\right), \tag{5.68}$$

and finally an expression for the radius of the circumcircle

$$\begin{aligned} r_{polycirc}^2 = &\frac{(7\,q - |y_\varepsilon|)^2\,\cos^2\left(\frac{5\,\pi}{2\,m}\right) + (|y_\varepsilon| - 5\,q)^2\,\cos^2\left(\frac{7\,\pi}{2\,m}\right)}{4\,\sin^2\left(\frac{\pi}{m}\right)} \\ &+ \frac{2\,(7\,q - |y_\varepsilon|)\,(|y_\varepsilon| - 5\,q)\cos\left(\frac{5\,\pi}{2\,m}\right)\,\cos\left(\frac{7\,\pi}{2\,m}\right)\,\cos\left(\frac{\pi}{m}\right)}{4\,\sin^2\left(\frac{\pi}{m}\right)}. \end{aligned} \tag{5.69}$$

The mean value of the magnetomotive force of the slots is calculated in the same way as in section 5.1.1.1.

$$\begin{aligned} \frac{\sum V_Q^2}{Q} &= \frac{1}{2\,q}\sum_{k=1}^{7\,q-|y_\varepsilon|}\left[r_{polycirc}^2 + k^2\,\cos^2\left(\frac{5\,\pi}{2\,m}\right) - 2\,r_{polycirc}\,k\,\cos\left(\frac{5\,\pi}{2\,m}\right)\,\cos(\alpha)\right] \\ &+ \frac{1}{2\,q}\sum_{k=1}^{|y_\varepsilon|-5\,q}\left[r_{polycirc}^2 + k^2\,\cos^2\left(\frac{7\,\pi}{2\,m}\right) - 2\,r_{polycirc}\,k\,\cos\left(\frac{7\,\pi}{2\,m}\right)\,\cos(\beta)\right] \\ &= r_{polycirc}^2 - \frac{1}{12\,q}\,(7\,q - |y_\varepsilon|)\left((7\,q - |y_\varepsilon|)^2 - 1\right)\,\cos^2\left(\frac{5\,\pi}{2\,m}\right) \\ &- \frac{1}{12\,q}\,(|y_\varepsilon| - 5\,q)\left((|y_\varepsilon| - 5\,q)^2 - 1\right)\,\cos^2\left(\frac{7\,\pi}{2\,m}\right) \end{aligned} \tag{5.70}$$

Range: $(\mathbf{l}-\mathbf{2})\,\mathbf{q} \le |\mathbf{y}_\varepsilon| \le \mathbf{l}\,\mathbf{q}$

The recurring pattern allows a general approach to the l-th pitching range of a winding with m phases and double zone span. It is important to note that this general approach is only applicable to the condition $l \ge 3$.

Absolute values of the magnetomotive force of the slots (rays of the polygon):

$$|V_N| = \cos\left(\frac{(l-2)\,\pi}{2\,m}\right) \quad , \quad |V_N| = \cos\left(\frac{l\,\pi}{2\,m}\right) \tag{5.71}$$

Edge lengths:

$$(l\,q - |y_\varepsilon|)\,\cos\left(\frac{(l-2)\,\pi}{2\,m}\right) \quad , \quad (|y_\varepsilon| - (l-2)\,q)\,\cos\left(\frac{l\,\pi}{2\,m}\right) \tag{5.72}$$

The angle of pivot of the polygon is the same as in equation (5.11). This results in the following aggregations with respect to the radius of the circumcircle of the polygon

$$\cos(\alpha) = \frac{l\,q - |y_\varepsilon|}{2\,r_{polycirc}}\,\cos\left(\frac{(l-2)\,\pi}{2\,m}\right) \quad , \quad \cos(\beta) = \frac{|y_\varepsilon| - (l-2)\,q}{2\,r_{polycirc}}\,\cos\left(\frac{l\,\pi}{2\,m}\right), \tag{5.73}$$

and finally an expression for the radius of the circumcircle

$$\begin{aligned} r^2_{polycirc} &= \frac{(l\,q - |y_\varepsilon|)^2\,\cos^2\left(\frac{(l-2)\,\pi}{2\,m}\right) + (|y_\varepsilon| - (l-2)\,q)^2\,\cos^2\left(\frac{l\,\pi}{2\,m}\right)}{4\,\sin^2\left(\frac{\pi}{m}\right)} \\ &+ \frac{2\,(l\,q - |y_\varepsilon|)\,(|y_\varepsilon| - (l-2)\,q)\cos\left(\frac{(l-2)\,\pi}{2\,m}\right)\,\cos\left(\frac{l\,\pi}{2\,m}\right)\,\cos\left(\frac{\pi}{m}\right)}{4\,\sin^2\left(\frac{\pi}{m}\right)}. \end{aligned} \tag{5.74}$$

The mean value of the magnetomotive force of the slots is calculated in the same way as in section 5.1.1.1.

$$\begin{aligned} \frac{\sum V_Q^2}{Q} &= \frac{1}{2\,q}\sum_{k=1}^{l\,q-|y_\varepsilon|}\left[r^2_{polycirc} + k^2\,\cos^2\left(\frac{(l-2)\,\pi}{2\,m}\right) - 2\,r_{polycirc}\,k\,\cos\left(\frac{(l-2)\,\pi}{2\,m}\right)\,\cos(\alpha)\right] \\ &+ \frac{1}{2\,q}\sum_{k=1}^{|y_\varepsilon|-(l-2)\,q}\left[r^2_{polycirc} + k^2\,\cos^2\left(\frac{l\,\pi}{2\,m}\right) - 2\,r_{polycirc}\,k\,\cos\left(\frac{l\,\pi}{2\,m}\right)\,\cos(\beta)\right] \\ &= r^2_{polycirc} - \frac{1}{12\,q}\,(l\,q - |y_\varepsilon|)\left((l\,q - |y_\varepsilon|)^2 - 1\right)\,\cos^2\left(\frac{(l-2)\,\pi}{2\,m}\right) \\ &- \frac{1}{12\,q}\,(|y_\varepsilon| - (l-2)\,q)\left((|y_\varepsilon| - (l-2)\,q)^2 - 1\right)\,\cos^2\left(\frac{l\,\pi}{2\,m}\right) \end{aligned} \tag{5.75}$$

5.2 Fractional Slot Windings

Fractional slot windings have a wide variety of designs that cannot be combined in a single closed solution. Therefore the topic cannot be fully dealt with in this thesis. Here, some restrictions are thus made with regard to the investigation of the harmonic scattering of fractional slot windings. First, it is assumed that only coils of the same width occur, thus only lap windings are considered. Secondly, all slots of the armature are occupied and no nesting of zones or phases is applied. Additionally, for the first calculations, only double layer windings with slot numbers greater than 1 are considered. These restrictions are fulfilled by most of the practically used lap windings of fractional slot windings.

The calculation of the harmonic scattering coefficients is based on algorithms in this chapter and is done via the *Görges Polygon*. The flow chart shown in figure 5.7 describes the procedure for determining the harmonic scattering coefficient of a fractional slot winding. The algorithms were programmed using MATLAB®.

A brief description of the individual processes of the flowchart from figure 5.7 follows here:

The second process box has the task of establishing the general phasor star of currents of an m phased system (for odd or even numbers). This is the only parameter for this process. For further calculations these phasors must be available as complex values:

$$\begin{aligned} \underline{I}_k &= \underline{I}_1\, e^{-j(k-1)\frac{2\pi}{m}} \quad , \quad k = 1, ..., m \\ \underline{I}_1 &= I_1\, e^{j\varphi_I} \end{aligned} \tag{5.76}$$

The third process box leads to the *Tingley-Scheme* (see chapter 2.11). Necessary parameters are the zone span, again the number of phases m, the number of slots per pole and phase $q \in \mathbb{Q}$, the coil step y_σ and the total number of slots Q. The program code finally returns the slots with the corresponding phases according to the *Tingley-Scheme* in sorted order of the slot numbers of the armature and as far as the bottom layer and upper layer is concerned. Two examples are shown in figure 5.8.

Due to the availability of the current phasors and their assignments to certain slots, the complex valued magnetomotive force V_i of each slot can be calculated within the fourth process box. Figure 5.9 shows two examples for a winding with $m = 5$.

Process box five is responsible for the *Görges Polygon* and is an integral part of the calculation of the harmonic scattering coefficient. The required parameters are the phasors of the magnetomotive force and the total number of slots Q. As a result, the process returns the vertices of the *Görges Polygon*, for which

$$\sum \underline{V}_i = 0, \tag{5.77}$$

is always valid. This makes it easy to visualize the corresponding polygon, see figure 5.10.

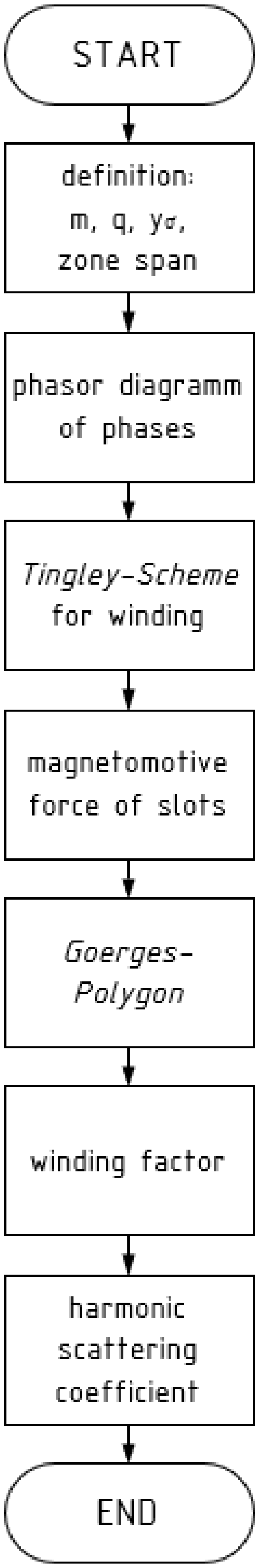

Figure 5.7: Flow chart oft the algorithm for a calculation of the harmonic scattering coefficient of fractional slot windings.

	1	2	3	4	5	6	7	8	9	10	11	12	13	14	15
UL	-1	-1	+4	-2	-2	+5	-3	-3	+1	-4	-4	+2	-5	-5	+3
BL	-2	+5	+5	-3	+1	+1	-4	+2	+2	-5	+3	+3	-1	+4	+4

	1	2	3	4	5	6	7	8	9	10	11	12	13	14	15	16	17	18	19	20	21	22	23	24	25	26	27	28	29	30
UL	-1	-1	-1	-2	-2	-2	-3	-3	-3	-4	-4	-4	-5	-5	-5	-1	-1	-1	-2	-2	-2	-3	-3	-3	-4	-4	-4	-5	-5	-5
BL	+4	+5	+5	+5	+1	+1	+1	+2	+2	+2	+3	+3	+3	+4	+4	+4	+5	+5	+5	+1	+1	+1	+2	+2	+2	+3	+3	+3	+4	+4

Figure 5.8: Examples of sorted *Tingley-Schemes* for a double layer fractional slot winding with $m = 5$, $q = 3/2$ and $y_\sigma = 4$ out of the progam code. On top for normal zone span and below for double zone span.

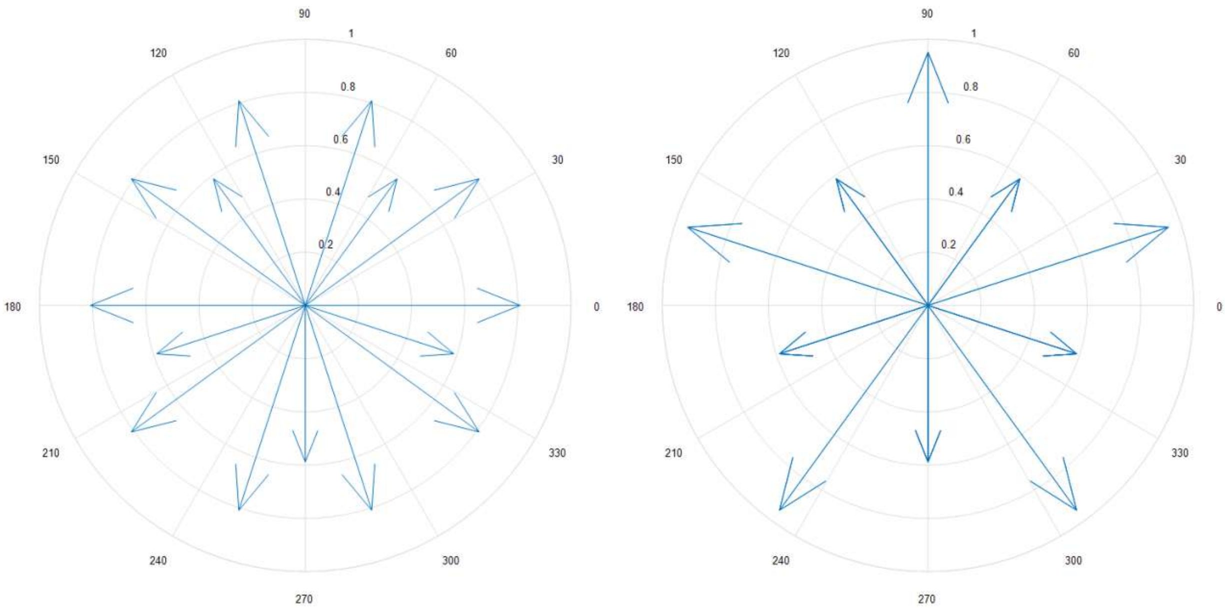

Figure 5.9: Examples of phasors of the magnetomotive forces V_i in for a double layer fractional slot winding with $m = 5$, $q = 3/2$ and $y_\sigma = 4$ out of the progam code. On the left for normal zone span (15 phasors) and on the right for double zone span (30 phasors, some may overlap each other).

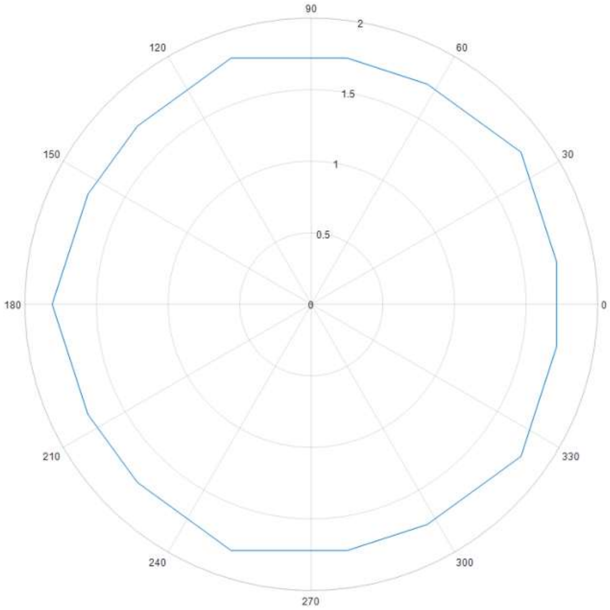

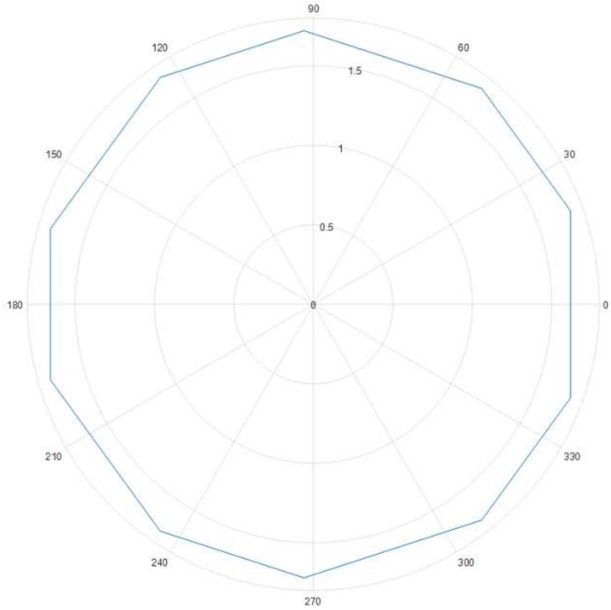

Figure 5.10: Examples of *Görges Polygons* for a double layer fractional slot winding with $m = 5$, $q = 3/2$ and $y_\sigma = 4$ out of the progam code. On the left for normal zone span and on the right for double zone span.

The calculation of the winding factors ξ_1 of the fundamental wave is done in the sixth process box using the equations from chapter 3.6.

Finally, the determination of the harmonic scattering coefficient σ_o within the seventh process box following all necessary parameters is now available and can be evaluated exactly according to the following equation:

$$\sigma_o = \frac{\pi^2}{m^2\, q^2\, \xi_1^2} \frac{\sum \left| \underline{V}_Q^2 \right|}{Q} - 1 \tag{5.78}$$

6 Evaluation of Harmonic Scattering Coefficients

6.1 Integer Slot Windings

6.1.1 Single Layer Windings

Winding with two Phases

A winding of two phases and one layer is characterized by four zones which each occupy a quarter of the two poles pitches along the circumference (figure 6.1).

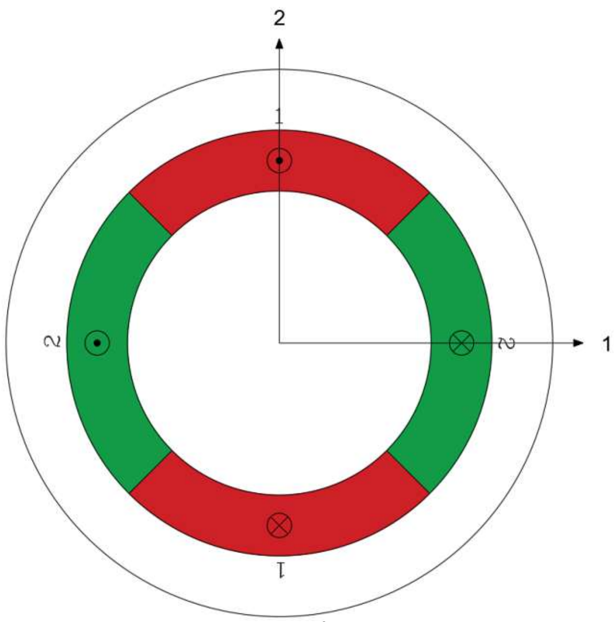

Figure 6.1: Zone diagram of a winding with two phases.

The winding factor for the fundamental wave ξ_1 gets calculated by equation (3.20) with $m = 2$ and $\nu = 1$. For the calculation of the harmonic scattering coefficient σ_o according to formula (4.19) it is necessary to calculate the auxiliary factor V_{AF}. According to equations (5.7) and (4.18) or Richter (1954), the closed solution as a function of the number of slots per pole and phase is:

$$V_{AF} = \frac{2\,q^2 + 1}{12\,q^2} \tag{6.1}$$

Table 6.1 contains solutions for ξ_1 and σ_o for several numbers of q and for the borderline case of an infinite number of slots. Figure 6.3 shows the course of the harmonic scattering coefficient σ_o as a function of the number of slots per pole and phase q. Due to its very high value, the point of $q = 1$ was not included in the diagram.

Table 6.1: Winding factor ξ_1 and harmonic scattering factor σ_o of a single layer armature winding with $m = 2$.

q	ξ_1	σ_o
1	1	0,233701
2	0,92388	0,084028
3	0,91068	0,046802
4	0,90613	0,033008
5	0,90403	0,026487
6	0,90289	0,022908
10	0,90124	0,017656
20	0,90055	0,015424
100	0,90033	0,014710
∞	0,90032	0,014678

Winding with three Phases

A winding of three phases and one layer is characterized by six zones which each occupy a sixth of two pole pitches along the circumference (figure 6.2).

The winding factor for the fundamental wave ξ_1 gets calculated by equation (3.20) with $m = 3$ and $\nu = 1$. For the calculation of the harmonic scattering coefficient σ_o according to formula (4.19) it is necessary to calculate the auxiliary factor V_{AF}. According to equations (5.7) and (4.18) or Richter (1954), the closed solution as a function of the number of slots per pole and phase is:

$$V_{AF} = \frac{5\,q^2 + 1}{12\,q^2} \tag{6.2}$$

Table 6.2 contains solutions for ξ_1 and σ_o for several numbers of q and for the borderline case of an infinite number of slots. Figure 6.4 shows the course of the harmonic scattering coefficient σ_o as a function of the number of slots per pole and phase q. Due to its very high value, the point of $q = 1$ was not included in the diagram.

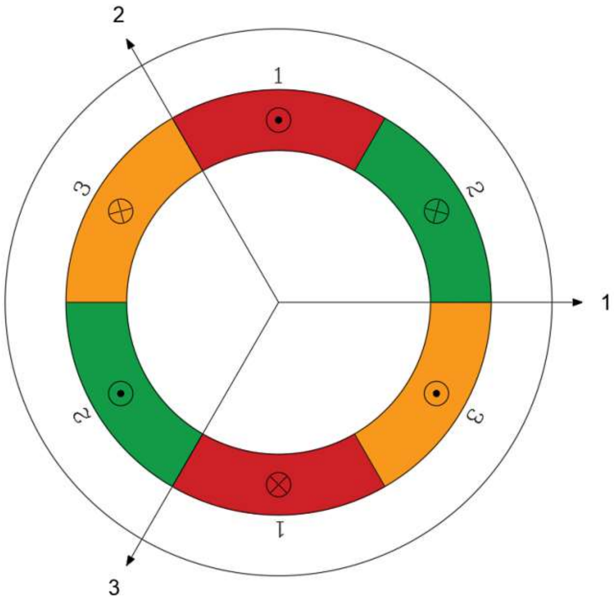

Figure 6.2: Zone diagram of a winding with three phases.

Table 6.2: Winding factor ξ_1 and harmonic scattering factor σ_o of a single layer armature winding with $m = 3$.

q	ξ_1	σ_o
1	1	0,096620
2	0,96593	0,028437
3	0,95980	0,014061
4	0,95766	0,008896
5	0,95668	0,006481
6	0,95614	0,005163
10	0,95537	0,003238
20	0,95504	0,002423
100	0,95493	0,002162
∞	0,95493	0,002151

Winding with five Phases

A winding of five phases and one layer is characterized by ten zones which each occupy a tenth of two pole pitches along the circumference (figure 6.5).

The winding factor for the fundamental wave ξ_1 gets calculated by equation (3.20) with $m = 5$ and $\nu = 1$. For the calculation of the harmonic scattering coefficient σ_o according to formula (4.19) it is necessary to calculate the auxiliary factor V_{AF}. According to equations (5.7) and (4.18), the closed solution as a function of the number of slots per pole and phase is:

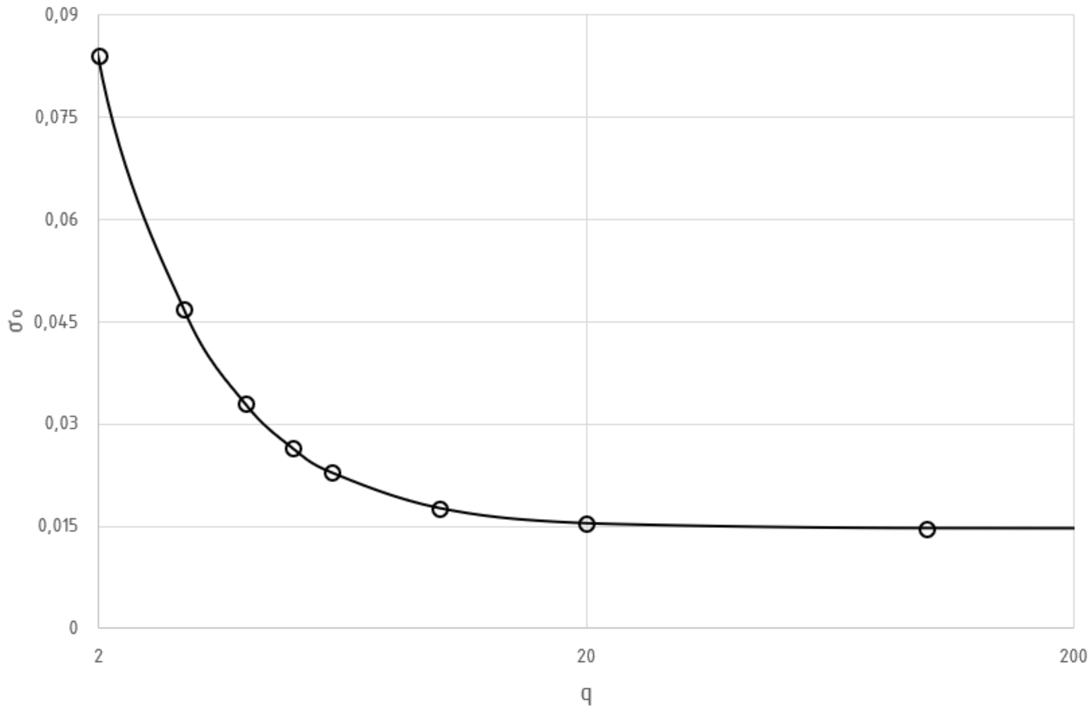

Figure 6.3: Course of the harmonic scattering coefficient σ_o over the number of slots per pole and phase q (logarithmic scale) of a single layer winding with $m = 2$.

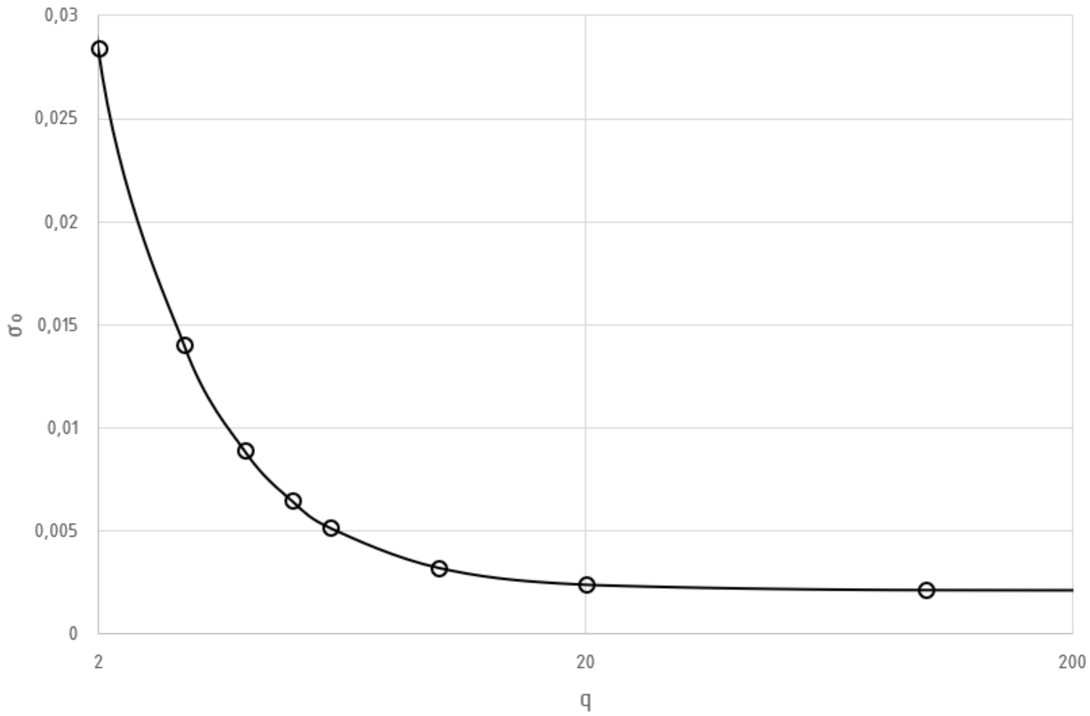

Figure 6.4: Course of the harmonic scattering coefficient σ_o over the number of slots per pole and phase q (logarithmic scale) of a single layer winding with $m = 3$.

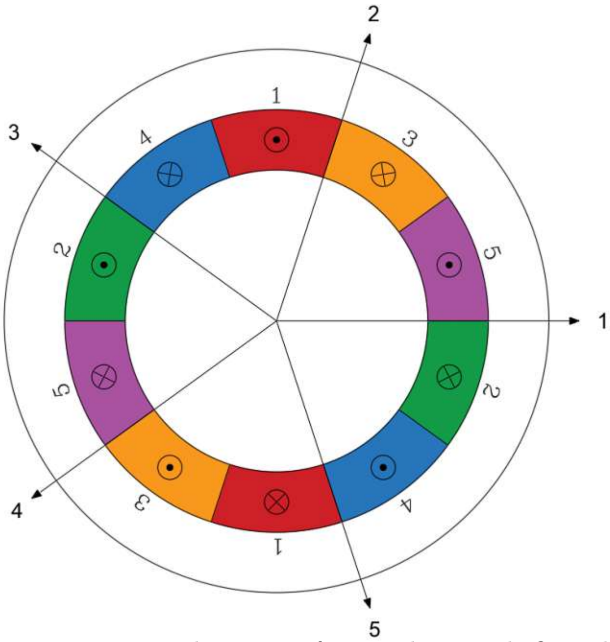

Figure 6.5: Zone diagram of a winding with five phases.

$$V_{AF} = \frac{\left(8 + 3\sqrt{5}\right) q^2 + 1}{12\, q^2} \tag{6.3}$$

Table 6.3 contains solutions for ξ_1 and σ_o for several numbers of q and for the borderline case of an infinite number of slots. Figure 6.7 shows the course of the harmonic scattering coefficient σ_o as a function of the number of slots per pole and phase q.

Table 6.3: Winding factor ξ_1 and harmonic scattering factor σ_o of a single layer armature winding with $m = 5$.

q	ξ_1	σ_o
1	1	0,033558
2	0,98769	0,008900
3	0,98543	0,004115
4	0,98464	0,002424
5	0,98428	0,001639
6	0,98408	0,001211
10	0,98379	0,000588
20	0,98367	0,000325
100	0,98363	0,000241
∞	0,98363	0,000238

Winding with seven Phases

A winding of seven phases and one layer is characterized by fourteen zones which each occupy a fourteenth of two pole pitches along the circumference (figure 6.6).

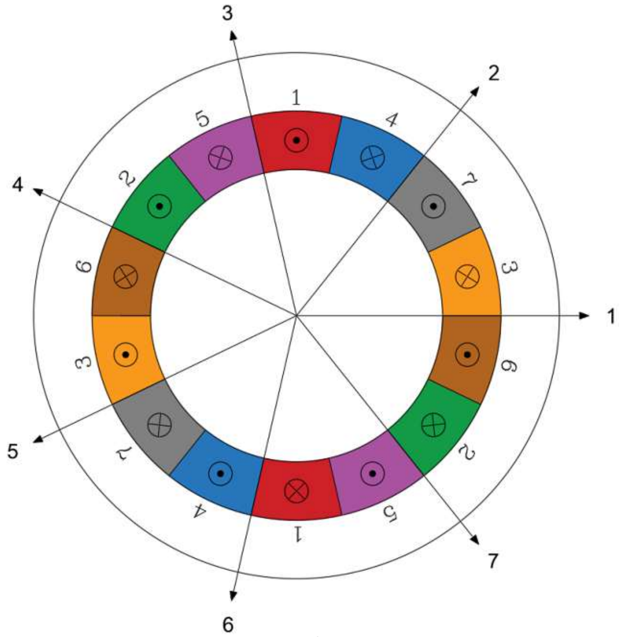

Figure 6.6: Zone diagram of a winding with seven phases.

The winding factor for the fundamental wave ξ_1 gets calculated by equation (3.20) with $m = 7$ and $\nu = 1$. For the calculation of the harmonic scattering coefficient σ_o according to formula (4.19) it is necessary to calculate the auxiliary factor V_{AF}. According to equations (5.7) and (4.18), the closed solution as a function of the number of slots per pole and phase is:

$$V_{AF} = \frac{\left(\frac{3}{2}\csc^2\left(\frac{\pi}{14}\right) - 1\right) q^2 + 1}{12\, q^2} \tag{6.4}$$

Table 6.4 contains solutions for ξ_1 and σ_o for several numbers of q and for the borderline case of an infinite number of slots. Figure 6.8 shows the course of the harmonic scattering coefficient σ_o as a function of the number of slots per pole and phase q.

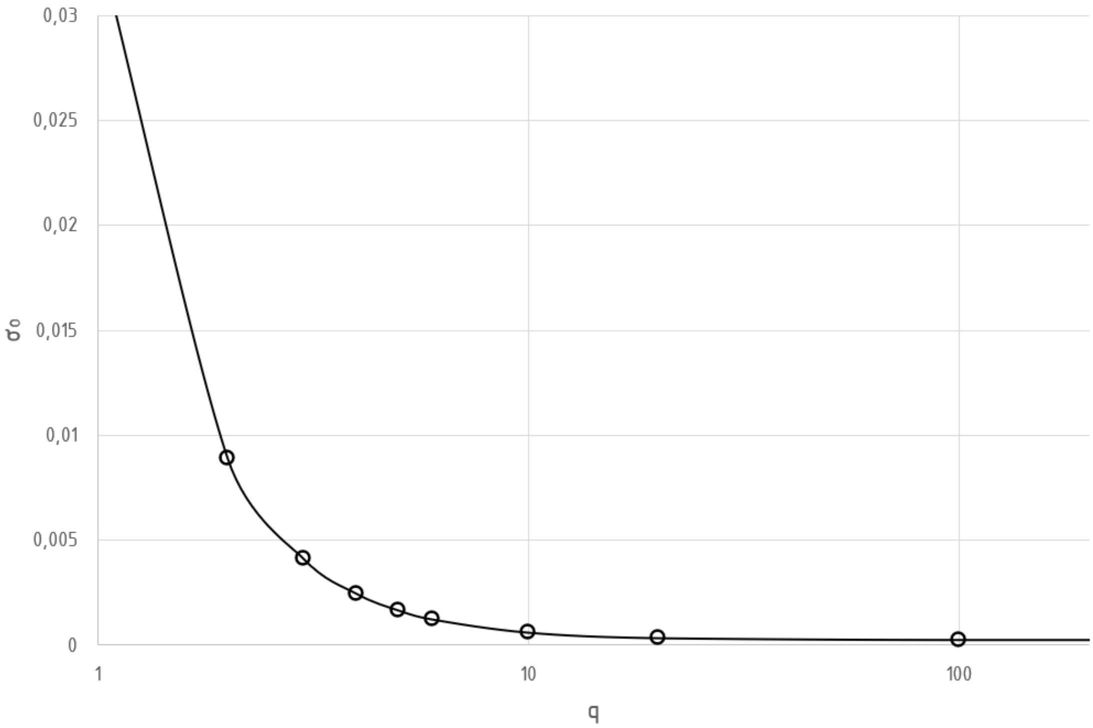

Figure 6.7: Course of the harmonic scattering coefficient σ_o over the number of slots per pole and phase q (logarithmic scale) of a single layer winding with $m = 5$.

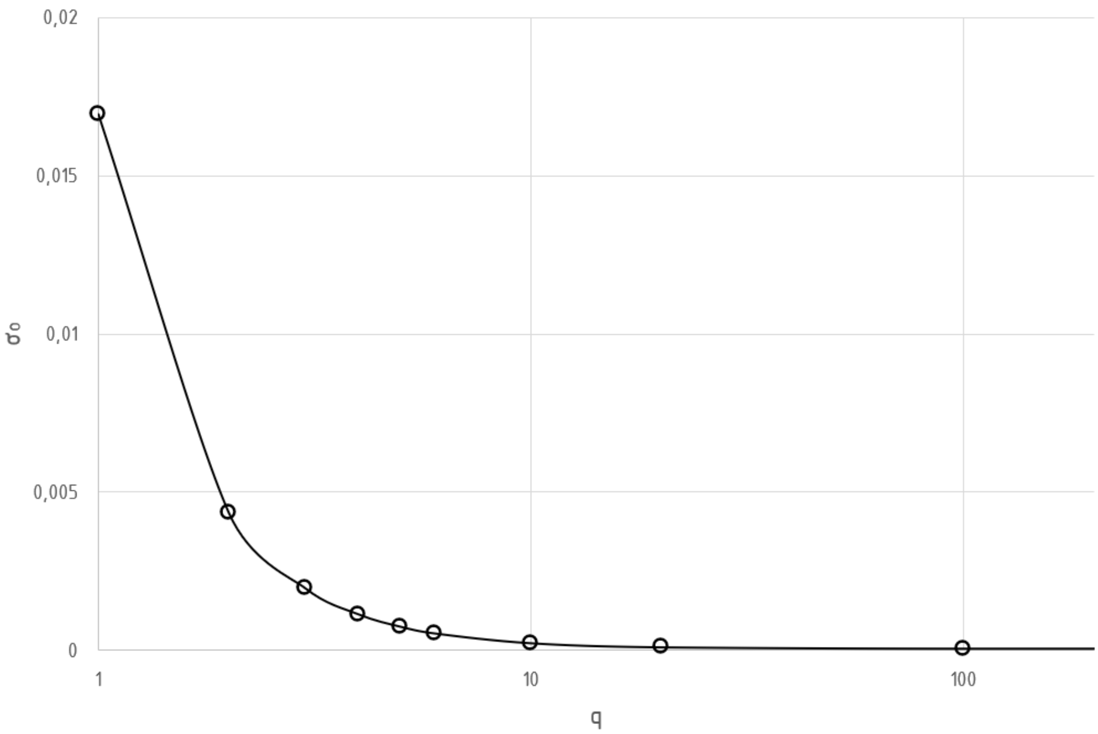

Figure 6.8: Course of the harmonic scattering coefficient σ_o over the number of slots per pole and phase q (logarithmic scale) of a single layer winding with $m = 7$.

Table 6.4: Winding factor ξ_1 and harmonic scattering factor σ_o of a single layer armature winding with $m = 7$.

q	ξ_1	σ_o
1	1	0,016955
2	0,99371	0,004369
3	0,99255	0,001982
4	0,99215	0,001142
5	0,99196	0,000752
6	0,99186	0,000541
10	0,99171	0,000233
20	0,99165	0,000102
100	0,99163	0,000061
∞	0,99163	0,000059

6.1.2 Double Layer Windings

6.1.2.1 Normal Zone Span

Winding with two Phases

A double layer winding of two phases is characterized by eight zones (four per layer) which each occupy a quarter of two pole pitches along the circumference (figure 6.9).

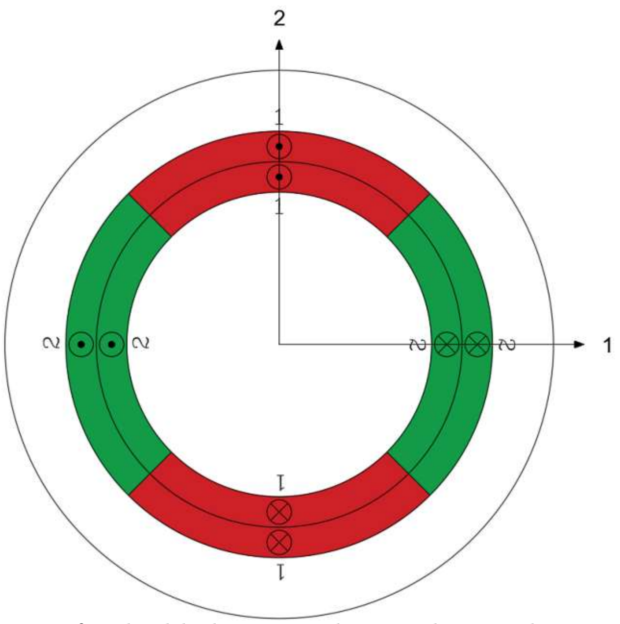

Figure 6.9: Zone diagram of a double layer winding with two phases and a coil pitch of $\sigma = 1$.

The winding factor for the fundamental wave ξ_1 gets calculated by equation (3.25) with $m = 2$, $\nu = 1$ and a certain coil pitch σ. For the calculation of the harmonic scattering coefficients, a winding with $m = 2$ needs two pitching ranges.

According to Baffrey (1926), the closed solution as a function of the number of slots per pole and phase and the shortening step for the range of $0 \leq |y_\varepsilon| \leq q$ is:

$$V_{AF} = \frac{2\,q^2 + 1 + \dfrac{|y_\varepsilon|^3}{2\,q} - \dfrac{3\,|y_\varepsilon|^2}{2} - \dfrac{y_\varepsilon}{2\,q}}{12\,q^2} \tag{6.5}$$

The same result for V_{AF}, of course, also yields the relationship derived from equation (5.14).

The auxiliary factor for the second range $q \leq |y_\varepsilon| \leq 2q$ gets calculated by equation (5.19) and can be written as:

$$V_{AF} = \frac{2\,q^3 + q + (|y_\varepsilon| - q)\left[(|y_\varepsilon| - q)^2 - 3\,q^2 - 1\right]}{24\,q^3} \tag{6.6}$$

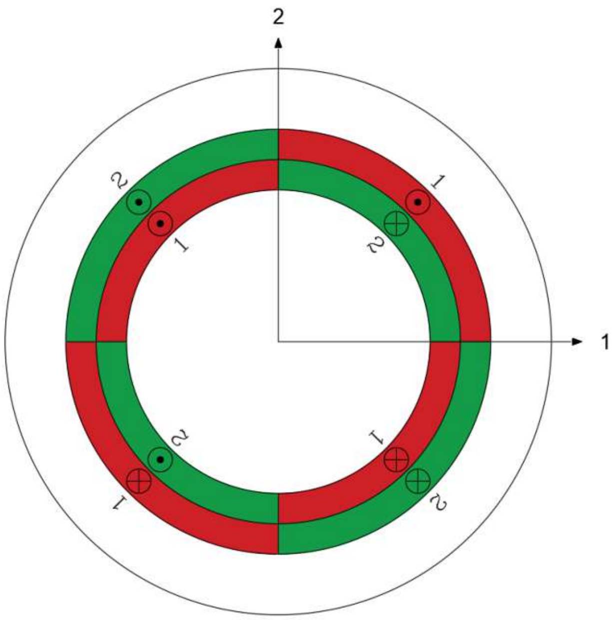

Figure 6.10: Zone diagram of a double layer winding with two phases and a coil pitch of $\sigma = 1/2$.

Table A.1 in the appendix gives the harmonic scattering coefficients for possible shortening steps of a winding with two phases. Figure 6.11 shows the progression of the harmonic scattering coefficient as a function of the coil pitch ($0 \leq \sigma \leq 1$). It is clear to see that from a slot number of $q = 5$, σ_o no longer significantly decreases. The vertical lines indicate the limits of the pitching ranges, figure 6.10 corresponds to the zone plan at the intersection of the pitching ranges. Here, the zones of the bottom layer and upper layer do not show overlaps of different phases.

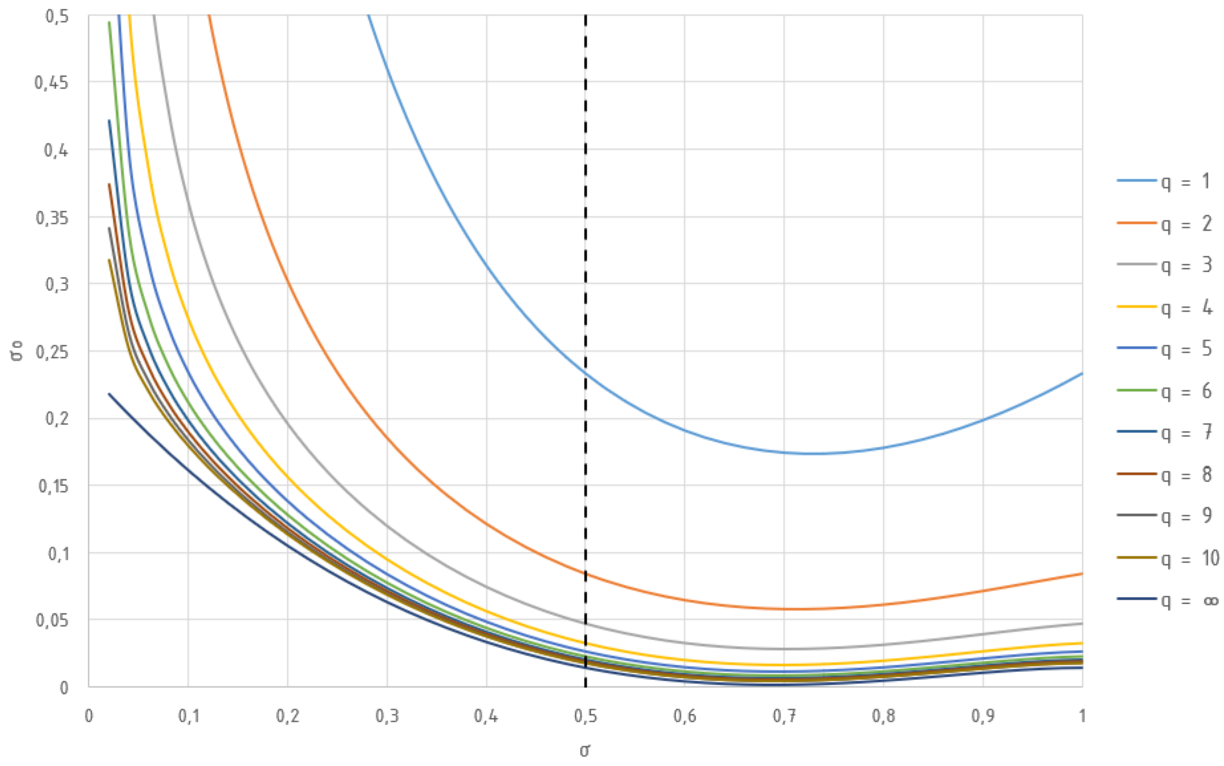

Figure 6.11: Courses of the harmonic scattering coefficient σ_o over the coil pitch $0 \leq \sigma \leq 1$ of a double layer winding with normal zone span and $m = 2$ for several numbers of slots q.

Winding with three Phases

A double layer winding of three phases is characterized by twelve zones (six per layer) which each occupy a sixth of two pole pitches along the circumference (figure 6.12).

The winding factor for the fundamental wave ξ_1 gets calculated by equation (3.25) with $m = 3$, $\nu = 1$ and a certain coil pitch σ. For the calculation of the harmonic scattering coefficients, a winding with $m = 3$ needs three pitching ranges.

According to Richter (1954), the closed solution as a function of the number of slots per pole and phase and the shortening step for the range of $0 \leq |y_\varepsilon| \leq q$ is:

$$V_{AF} = \frac{5\,q^2 + 1 + \dfrac{|y_\varepsilon|^3}{4\,q} - \dfrac{3\,|y_\varepsilon|^2}{2} - \dfrac{|y_\varepsilon|}{4\,q}}{12\,q^2} \tag{6.7}$$

The same result for V_{AF}, of course, also yields the relationship derived from equation (5.14).

The auxiliary factor for the second range $q \leq |y_\varepsilon| \leq 2q$ gets calculated by Baffrey (1926):

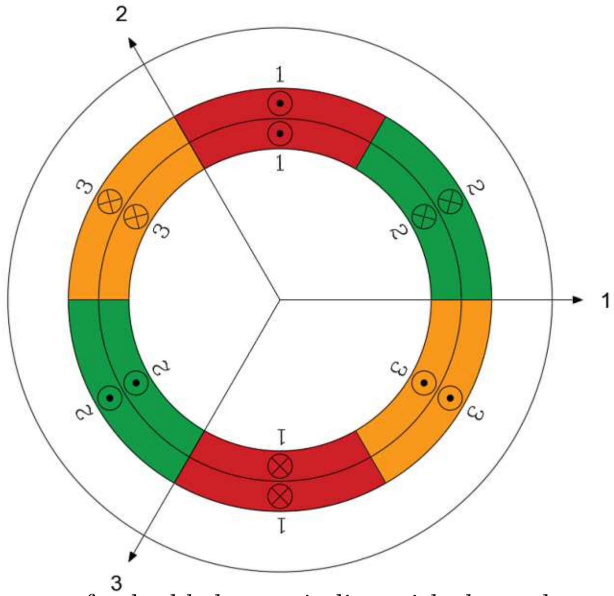

Figure 6.12: Zone diagram of a double layer winding with three phases and a coil pitch of $\sigma = 1$.

$$V_{AF} = \frac{5\,q^2 + 1 + \dfrac{2\,(|y_\varepsilon| - q)^3}{3\,q} - (|y_\varepsilon| - q)^2 - 3\,q\,(|y_\varepsilon| - q) - \dfrac{2\,(|y_\varepsilon| - q)}{3\,q}}{16\,q^2} \tag{6.8}$$

The same result for V_{AF}, of course, also yields the relationship derived from equation (5.19).

According to equation (5.24), the auxiliary factor for the third pitching range is:

$$V_{AF} = \frac{3\,\left[9\,q^3 - 3\,q^2\,|y_\varepsilon| + q\,\left(1 - |y\varepsilon|^2\right)\right] + |y_\varepsilon|^3 - |y_\varepsilon|}{48\,q^3} \tag{6.9}$$

Table A.2 in the appendix gives the harmonic scattering coefficients for possible shortening steps of a winding with three phases. Figure 6.14 shows the progression of the harmonic scattering coefficient as a function of the coil pitch ($0 \leq \sigma \leq 1$). It is clear to see that from a slot number of $q = 2$, σ_o no longer significantly decreases. The vertical lines indicate the limits of the pitching ranges, figure 6.13 corresponds to the zone plans at the intersection of the pitching ranges. The zones of the bottom layer and upper layer do not show overlaps of different phases.

Winding with five Phases

A double layer winding of five phases is characterized by twenty zones (ten per layer) which each occupy a tenth of two pole pitches along the circumference (figure 6.15).

The winding factor for the fundamental wave ξ_1 gets calculated by equation (3.25) with $m = 5$, $\nu = 1$ and a certain coil pitch σ. For the calculation of the harmonic scattering coefficients, a winding with $m = 5$ needs five pitching ranges.

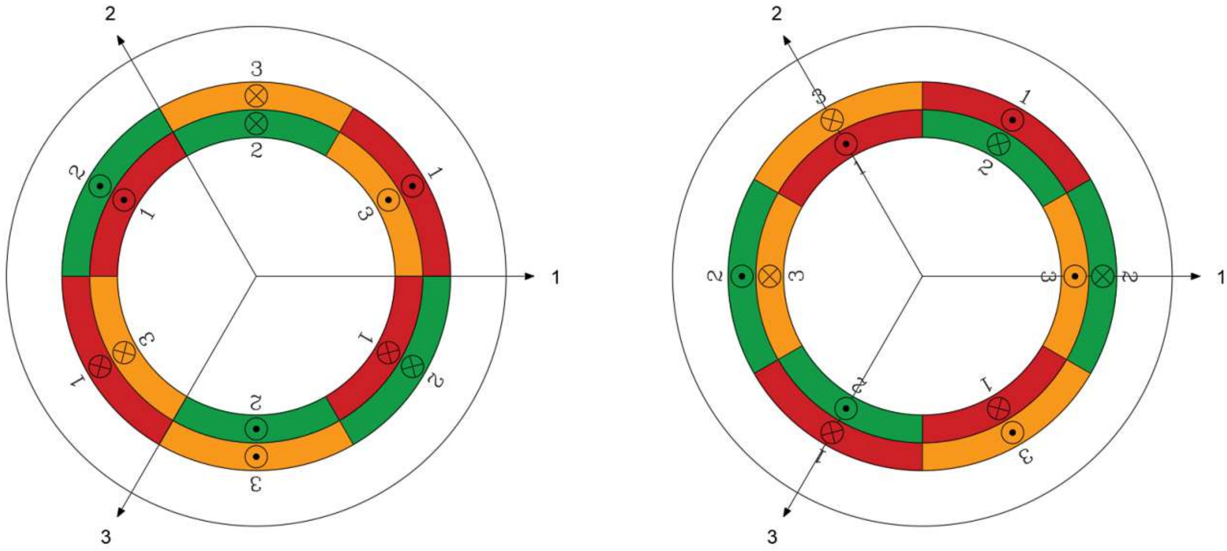

Figure 6.13: Zone diagrams of a double layer winding with three phases and a coil pitches of $\sigma = 1/3$ (left) and $\sigma = 2/3$ (right).

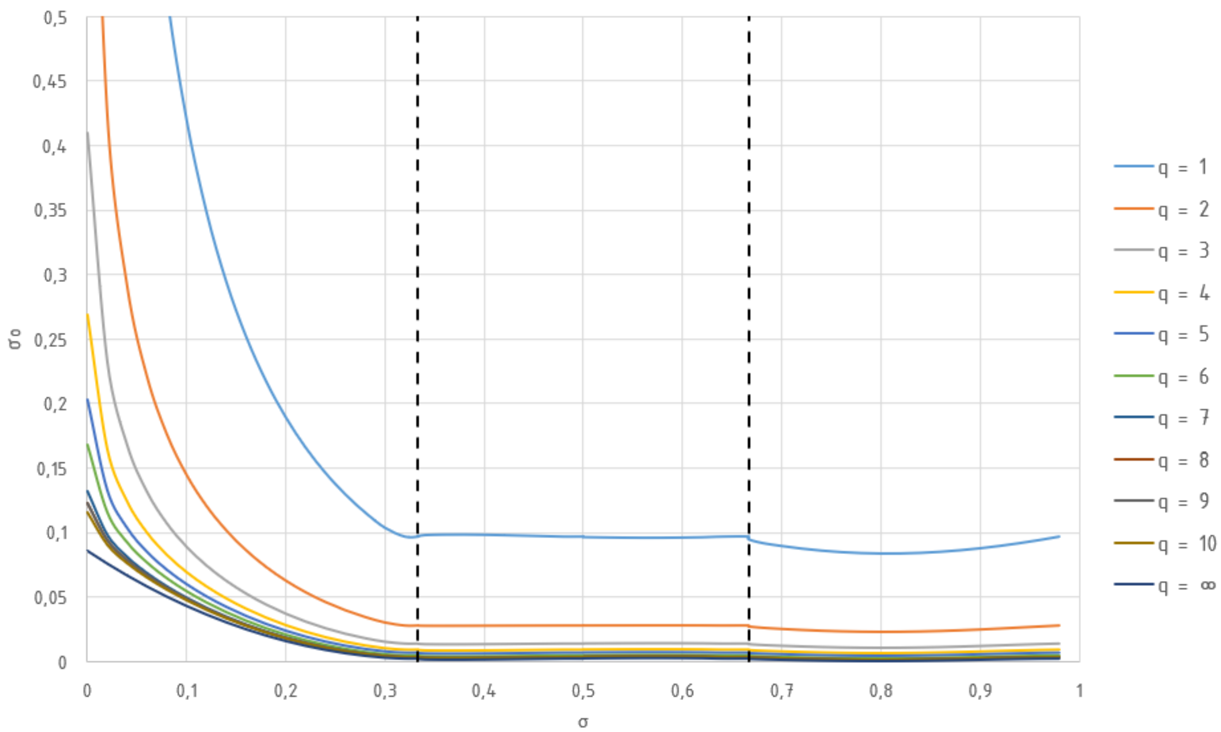

Figure 6.14: Courses of the harmonic scattering coefficient σ_o over the coil pitch $0 \leq \sigma \leq 1$ of a double layer winding with normal zone span and $m = 3$ for several numbers of slots q.

The calculation of the auxiliary factor V_{AF} for the individual pitching ranges is done according to the formulae in chapter 5.1.3.1. A simplification of the expressions is no longer possible or useful. A separate written solution will therefore be omitted. The following

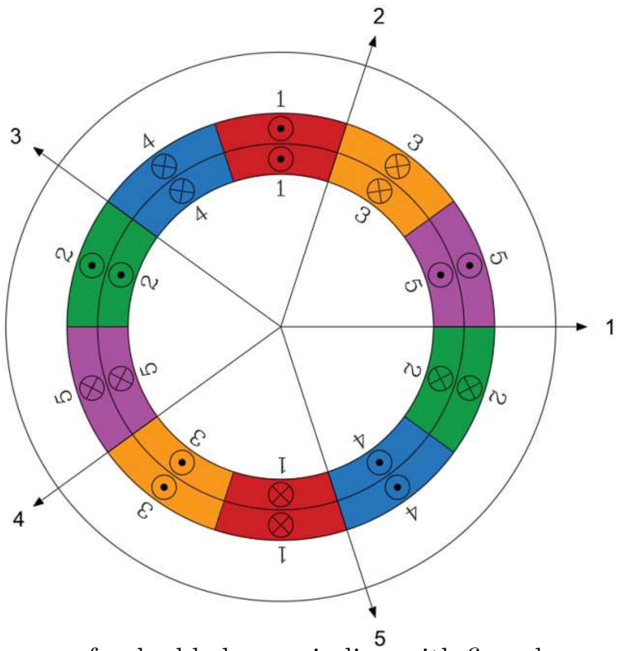

Figure 6.15: Zone diagram of a double layer winding with five phases and a coil pitch of $\sigma = 1$.

assignments to the pitching ranges apply:

$$
\begin{array}{rclcl}
1 \leq \sigma \leq 4/5 & \text{resp.} & 0 \leq |y_\varepsilon| \leq q & \rightarrow & (5.14) \\
4/5 \leq \sigma \leq 3/5 & \text{resp.} & q \leq |y_\varepsilon| \leq 2\,q & \rightarrow & (5.19) \\
3/5 \leq \sigma \leq 2/5 & \text{resp.} & 2\,q \leq |y_\varepsilon| \leq 3\,q & \rightarrow & (5.24) \\
2/5 \leq \sigma \leq 1/5 & \text{resp.} & 3\,q \leq |y_\varepsilon| \leq 4\,q & \rightarrow & (5.29) \\
1/5 \leq \sigma \leq 0 & \text{resp.} & 4\,q \leq |y_\varepsilon| \leq 5\,q & \rightarrow & (5.34)
\end{array}
$$

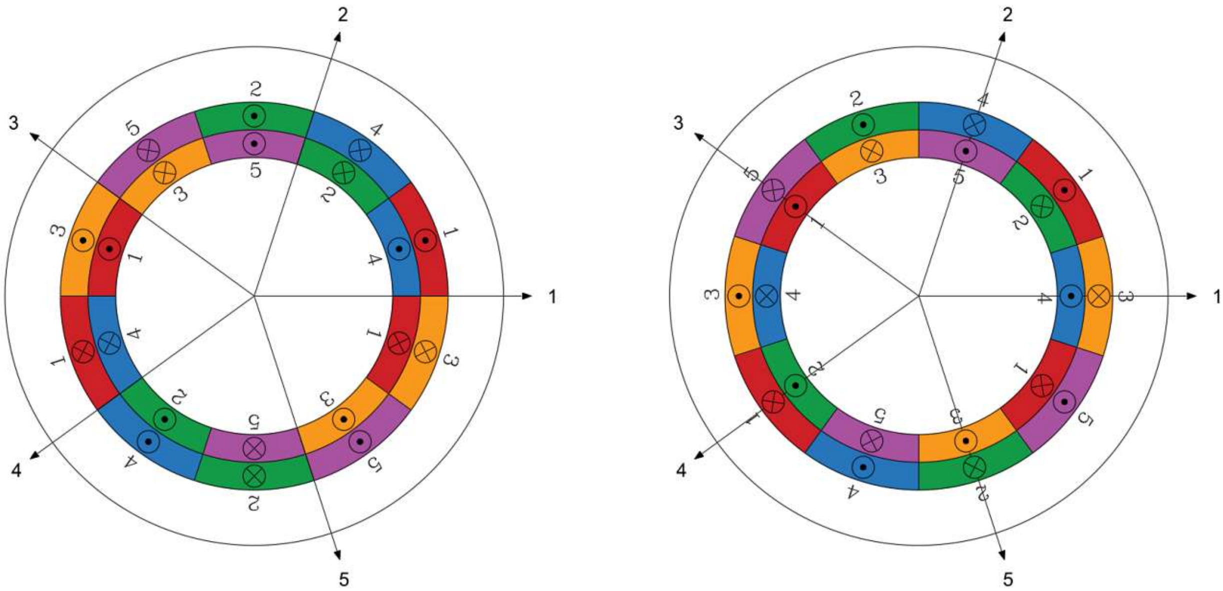

Table A.3 in the appendix gives the harmonic scattering coefficients for possible shortening steps of a winding with three phases. Figure 6.17 shows the progression of the harmonic

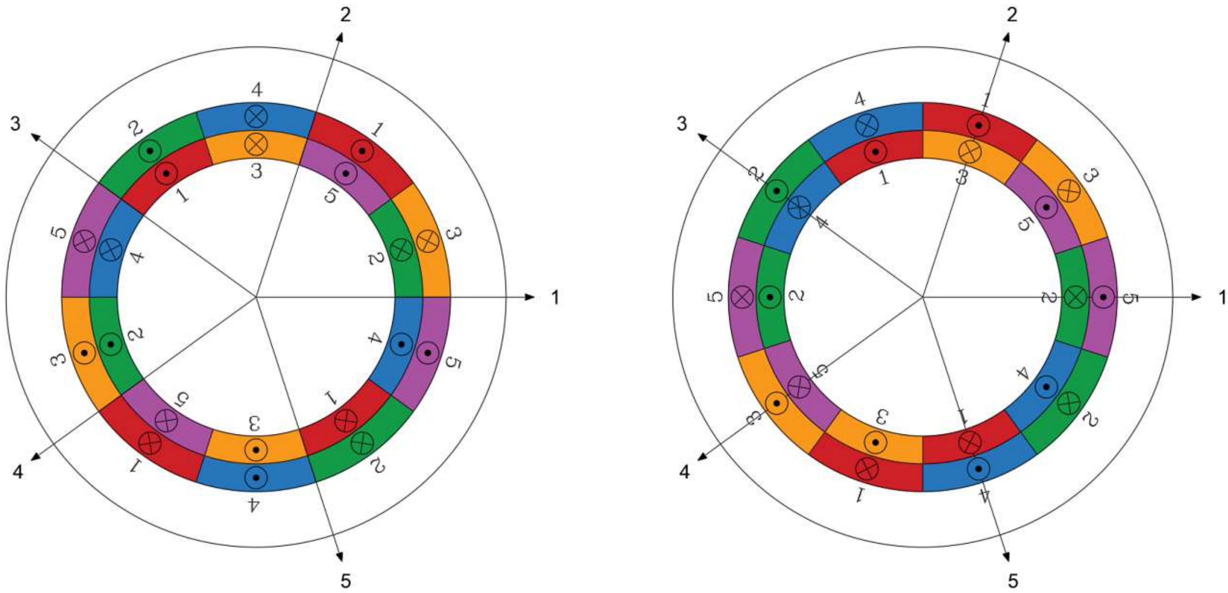

Figure 6.16: Zone diagrams of a double layer winding with five phases and a coil pitch of $\sigma = 1/5$ (top left), $\sigma = 2/5$ (top right), $\sigma = 3/5$ (bottom left) and $\sigma = 4/5$ (bottom right).

scattering coefficient as a function of the coil pitch ($0 \leq \sigma \leq 1$). It is clear to see that from a slot number of $q = 3$, σ_o no longer significantly decreases. The vertical lines indicate the limits of the pitching ranges, figure 6.16 corresponds to the zone plans at the intersection of the pitching ranges. The zones of the bottom layer and upper layer do not show overlaps of different phases.

Winding with seven Phases

A double layer winding of seven phases is characterized by twenty-eight zones (fourteen per layer) which each occupy a fourteenth of two pole pitches along the circumference (figure 6.18).

The winding factor for the fundamental wave ξ_1 gets calculated by equation (3.25) with $m = 7$, $\nu = 1$ and a certain coil pitch σ. For the calculation of the harmonic scattering coefficients, a winding with $m = 7$ needs seven pitching ranges.

The calculation of the auxiliary factor V_{AF} for the individual pitching ranges is done according to the formulae in chapter 5.1.3.1. A simplification of the expressions is no longer possible or useful. A separate written solution will therefore be omitted. The following assignments to the pitching ranges apply:

Table A.4 in the appendix gives the harmonic scattering coefficients for possessive shortening steps of a winding with three phases. Figure 6.22 shows the progression of the harmonic scattering coefficient as a function of the coil pitch ($0 \leq \sigma \leq 1$). It is clear to see that from a slot number of $q = 3$, σ_o no longer significantly decreases. The vertical lines indicate the limits of the pitching ranges. Figures 6.19 and 6.20 correspond to the zone plans at the

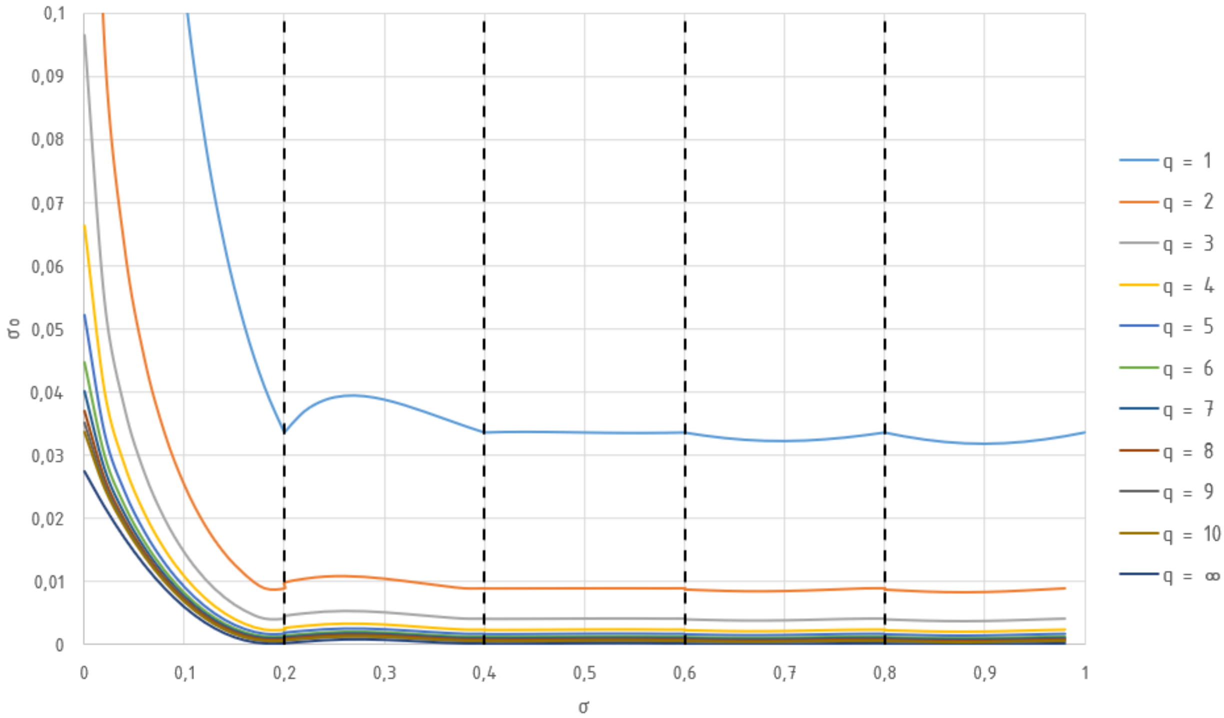

Figure 6.17: Courses of the harmonic scattering coefficient σ_o over the coil pitch $0 \leq \sigma \leq 1$ of a double layer winding with normal zone span and $m = 5$ for several numbers of slots q.

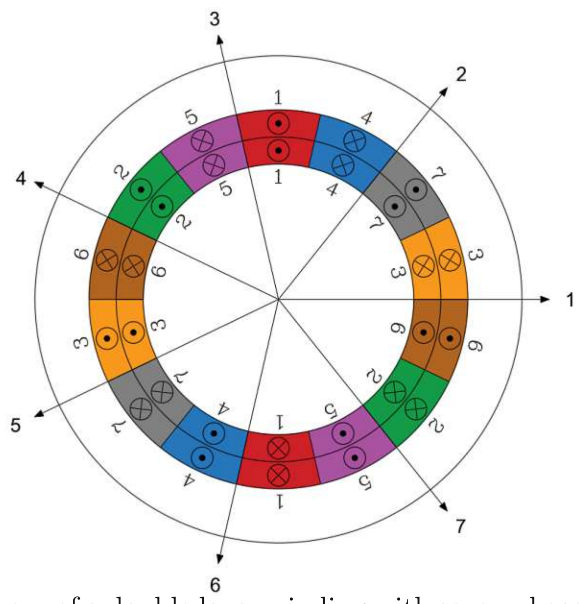

Figure 6.18: Zone diagram of a double layer winding with seven phases and a coil pitch of $\sigma = 1$.

intersection of the pitching ranges. The zones of the bottom layer and upper layer do not show overlaps of different phases.

$$
\begin{array}{ccccc}
1 \le \sigma \le 6/7 & \text{resp.} & 0 \le |y_\varepsilon| \le q & \rightarrow & (5.14) \\
6/7 \le \sigma \le 5/7 & \text{resp.} & q \le |y_\varepsilon| \le 2\,q & \rightarrow & (5.19) \\
5/7 \le \sigma \le 4/7 & \text{resp.} & 2\,q \le |y_\varepsilon| \le 3\,q & \rightarrow & (5.24) \\
4/7 \le \sigma \le 3/7 & \text{resp.} & 3\,q \le |y_\varepsilon| \le 4\,q & \rightarrow & (5.29) \\
3/7 \le \sigma \le 2/7 & \text{resp.} & 4\,q \le |y_\varepsilon| \le 5\,q & \rightarrow & (5.34) \\
2/7 \le \sigma \le 1/7 & \text{resp.} & 5\,q \le |y_\varepsilon| \le 6\,q & \rightarrow & (5.39) \\
1/7 \le \sigma \le 0 & \text{resp.} & 6\,q \le |y_\varepsilon| \le 7\,q & \rightarrow & (5.44)
\end{array}
$$

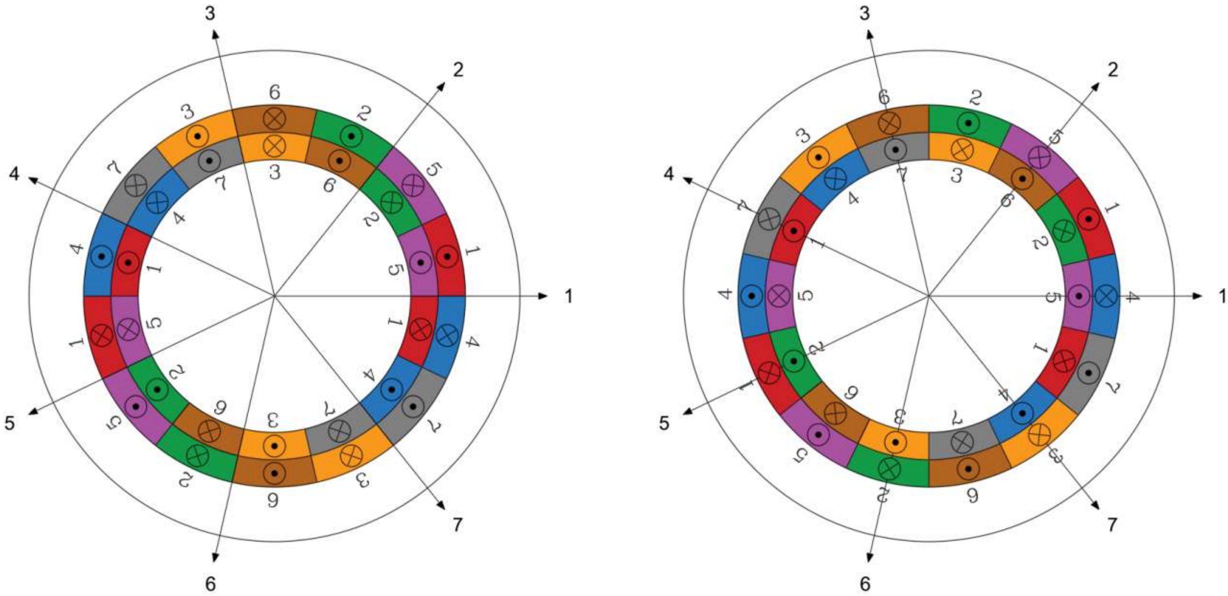

Figure 6.19: Zone diagrams of a double layer winding with five phases and coil pitches of $\sigma = 1/7$ (left), $\sigma = 2/7$ (right).

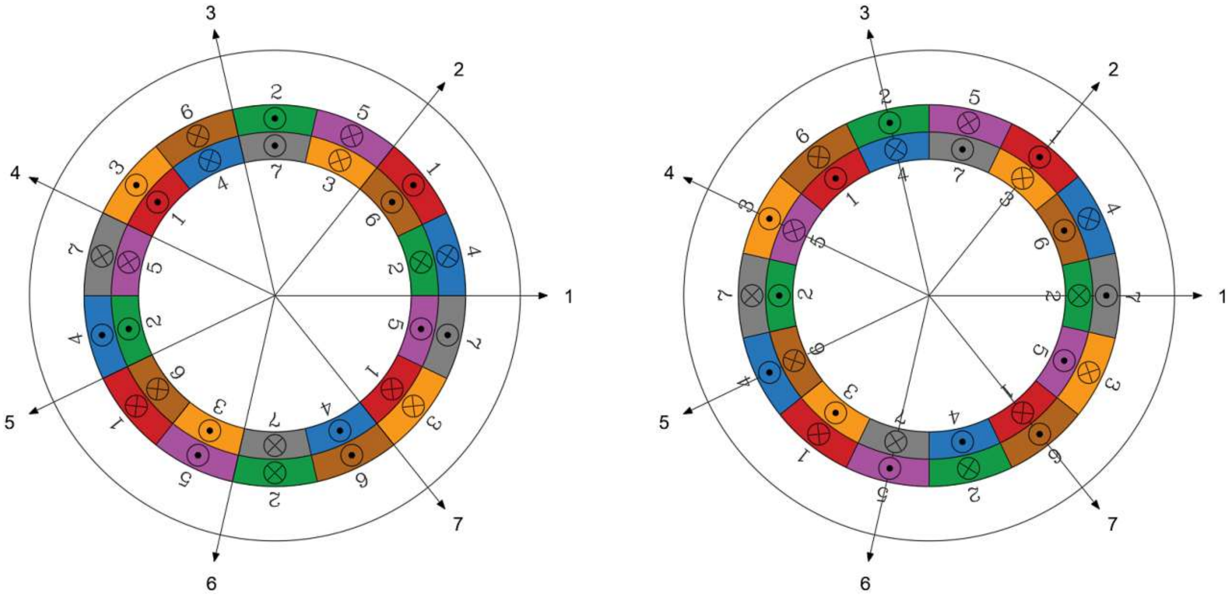

Figure 6.20: Zone diagrams of a double layer winding with seven phases and coil pitches of $\sigma = 3/7$ (left), $\sigma = 4/7$ (right).

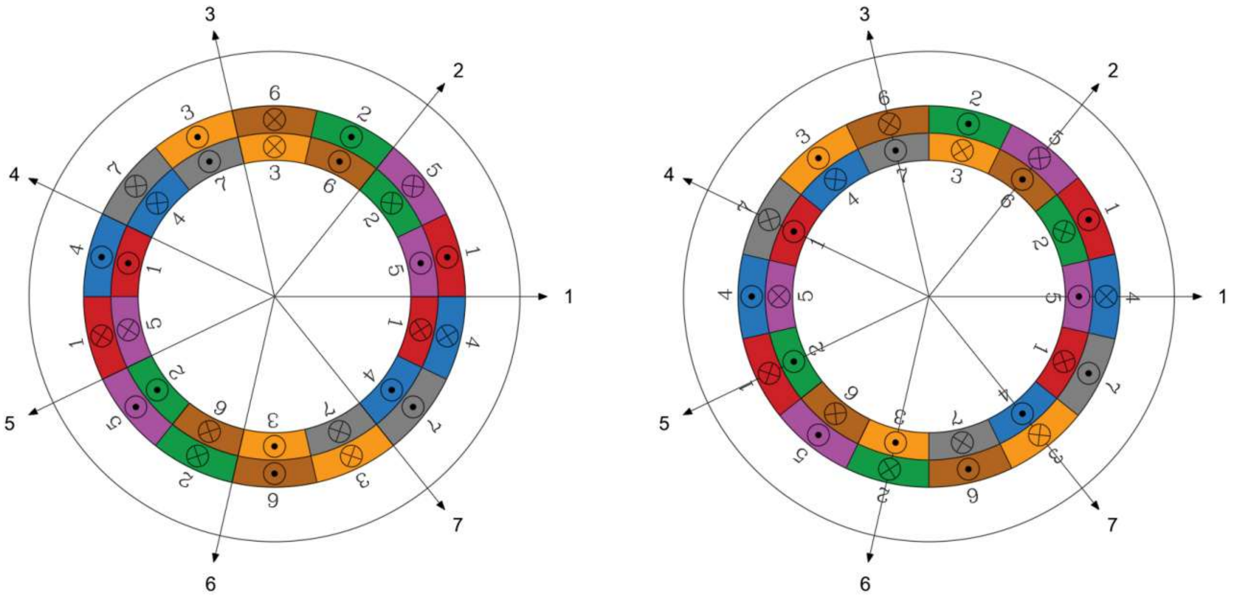

Figure 6.21: Zone diagrams of a double layer winding with seven phases and coil pitches of $\sigma = 5/7$ (left) and $\sigma = 6/7$ (right).

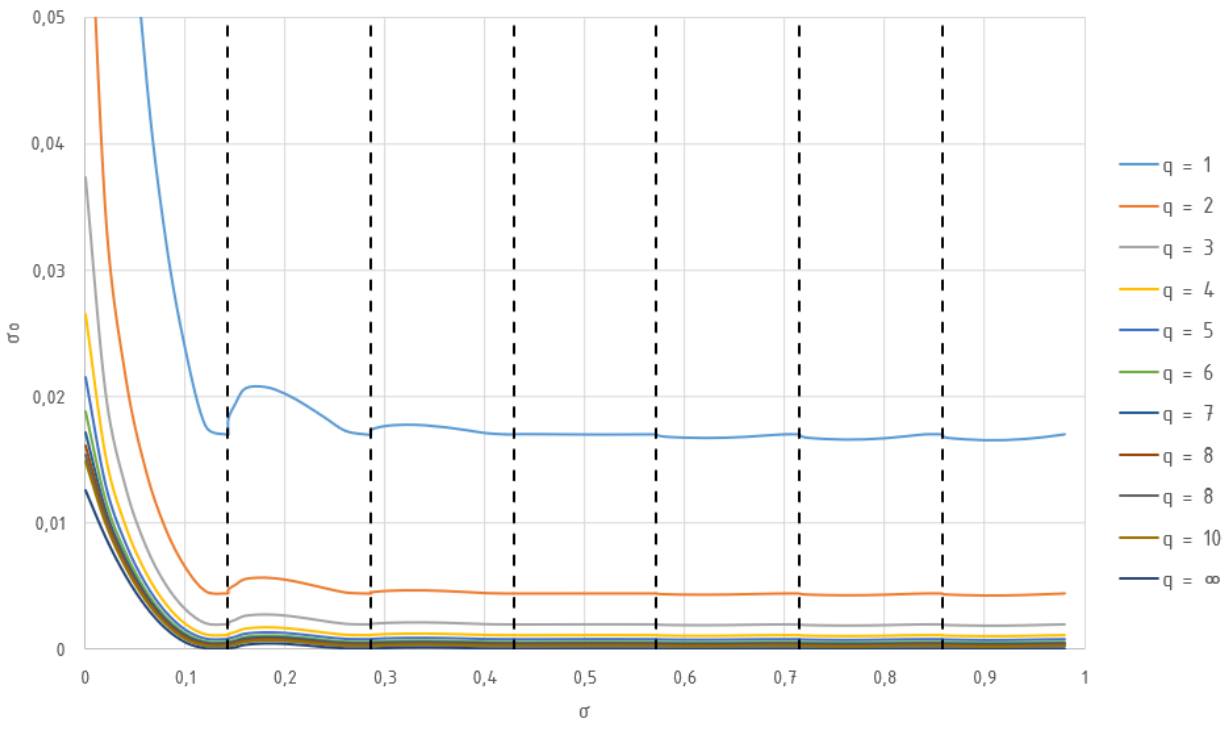

Figure 6.22: Courses of the harmonic scattering coefficient σ_o over the coil pitch $0 \leq \sigma \leq 1$ of a double layer winding with normal zone span and $m = 7$ for several numbers of slots q.

6.1.2.2 Double Zone Span

Winding with three Phases

A double layer winding of three phases and double zone span is characterized by six zones (three per layer) which each occupy a third of two pole pitches along the circumference (figure 6.23).

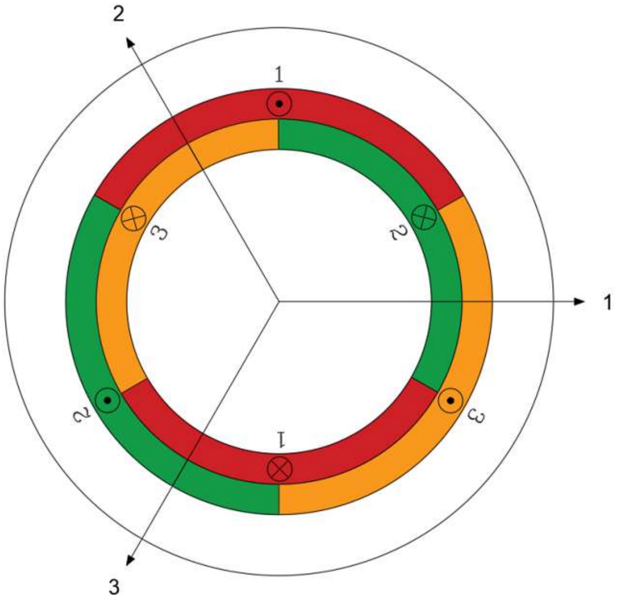

Figure 6.23: Zone diagram of a double layer winding with three phases and double zone span at a coil pitch of $\sigma = 1$.

The winding factor for the fundamental wave ξ_1 gets calculated by equation (3.26) with $m = 3$, $\nu = 1$ and a certain coil pitch σ. For the calculation of the harmonic scattering coefficients, a winding with $m = 3$ needs two pitching ranges.

The first pitching range is equal to windings with normal zone span. Equation (5.55) leads to the auxiliary factor:

$$V_{AF} = \frac{15\,q^2 - 3\,|y_\varepsilon|^2 + 9}{48\,q^2} \tag{6.10}$$

According to equation (5.60), the auxiliary factor for the second pitching range is:

$$V_{AF} = \frac{9\,q^3 + 3\,q^2\;|y_\varepsilon| - 7\,q\,|y_\varepsilon|^2 + 3\,q - |y_\varepsilon^3| - |y_\varepsilon|}{32\,q^3} \tag{6.11}$$

Table A.5 in the appendix provides the harmonic scattering coefficients for possible shortening steps of a winding with three phases. Figure 6.25 shows the progression of the harmonic scattering coefficient as a function of the coil pitch ($0 \leq \sigma \leq 1$). The vertical lines indicate the limits of the pitching ranges, figure 6.24 corresponds to the zone plans

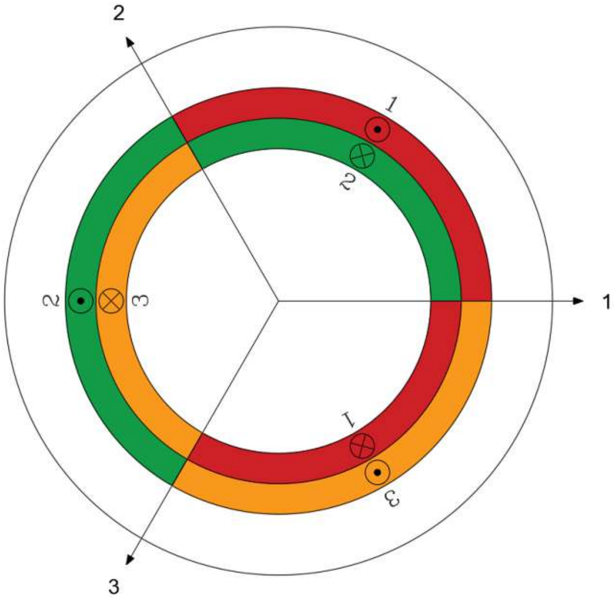

Figure 6.24: Zone diagram of a double layer winding with three phases and double zone span for a coil pitch of $\sigma = 2/3$.

at the intersection of the pitching ranges. The zones of the bottom layer and upper layer do not show overlaps of different phases.

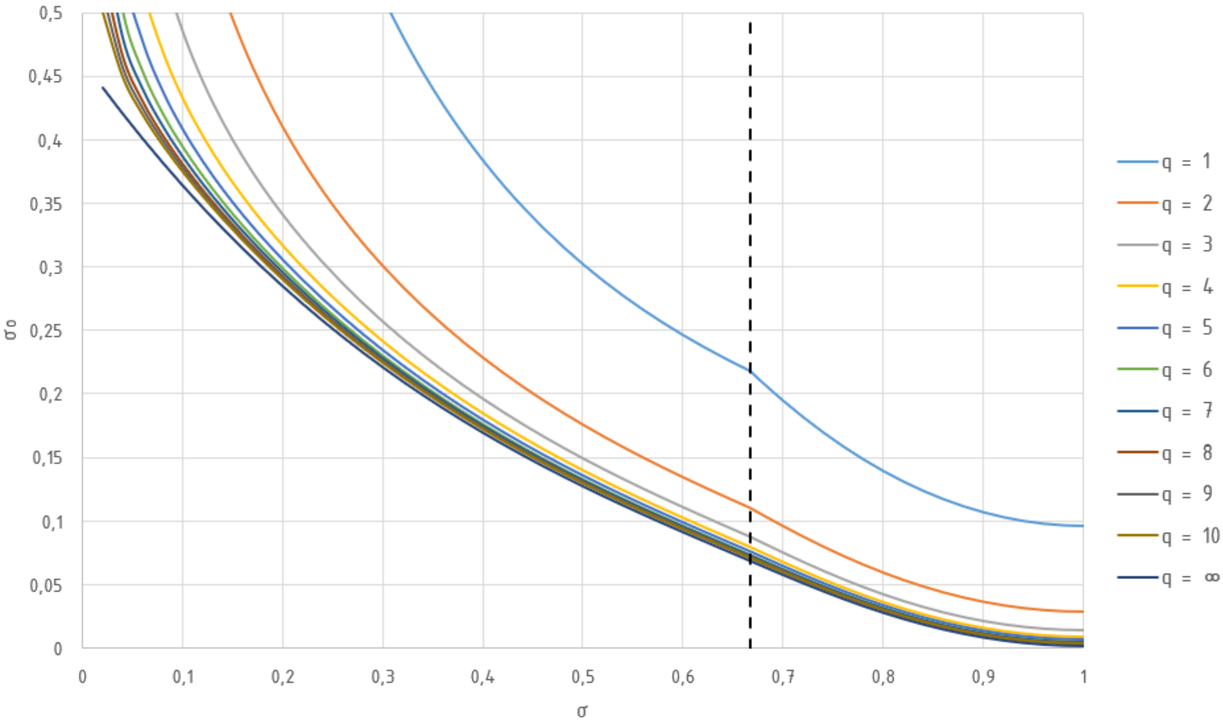

Figure 6.25: Courses of the harmonic scattering coefficient σ_o over the coil pitch $0 \leq \sigma \leq 1$ of a double layer winding with normal zone span and $m = 3$ for several numbers of slots q.

Winding with five Phases

A double layer winding of five phases and double zone span is characterized by ten zones (five per layer) which each occupy a fifth of two pole pitches along the circumference (figure 6.26).

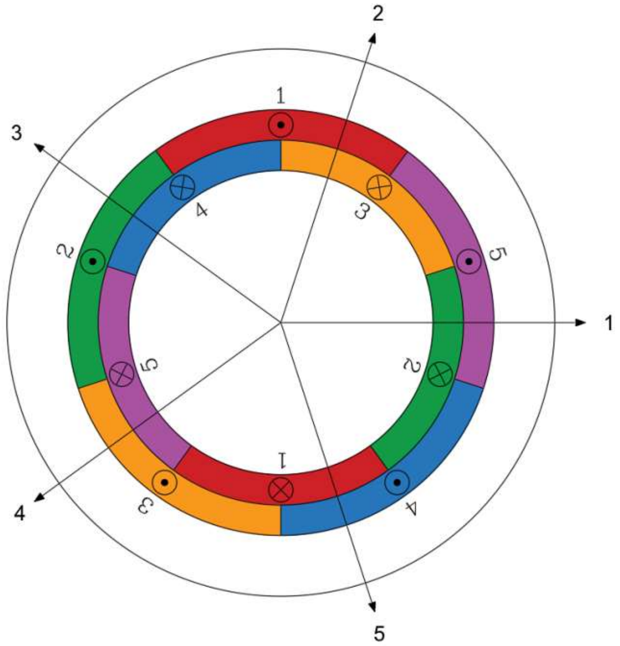

Figure 6.26: Zone diagram of a double layer winding with five phases and double zone span at a coil pitch of $\sigma = 1$.

The winding factor for the fundamental wave ξ_1 gets calculated by equation (3.26) with $m = 5$, $\nu = 1$ and a certain coil pitch σ. For the calculation of the harmonic scattering coefficients, a winding with $m = 5$ needs three pitching ranges.

The calculation of the auxiliary factor V_{AF} for the individual pitching ranges is done according to the formulae in chapter 5.1.3.2. A simplification of the expressions is no longer possible or useful. A separate written solution will therefore be omitted. The following assignments to the pitching ranges apply:

$$\begin{array}{lccc} 4/5 \leq \sigma \leq 1 & \text{resp.} & 0 \leq |y_\varepsilon| \leq q & \rightarrow \quad (5.55) \\ 2/5 \leq \sigma \leq 4/5 & \text{resp.} & q \leq |y_\varepsilon| \leq 3\,q & \rightarrow \quad (5.60) \\ 0 \leq \sigma \leq 2/5 & \text{resp.} & 3\,q \leq |y_\varepsilon| \leq 5\,q & \rightarrow \quad (5.65) \end{array}$$

Table A.6 in the appendix provides the harmonic scattering coefficients for possible shortening steps of a winding with three phases. Figure 6.28 shows the progression of the harmonic scattering coefficient as a function of the coil pitch ($0 \leq \sigma \leq 1$). The vertical lines indicate the limits of the pitching ranges, figure 6.27 corresponds to the zone plans at the intersection of the pitching ranges. The zones of the bottom layer and upper layer do not show overlaps of different phases.

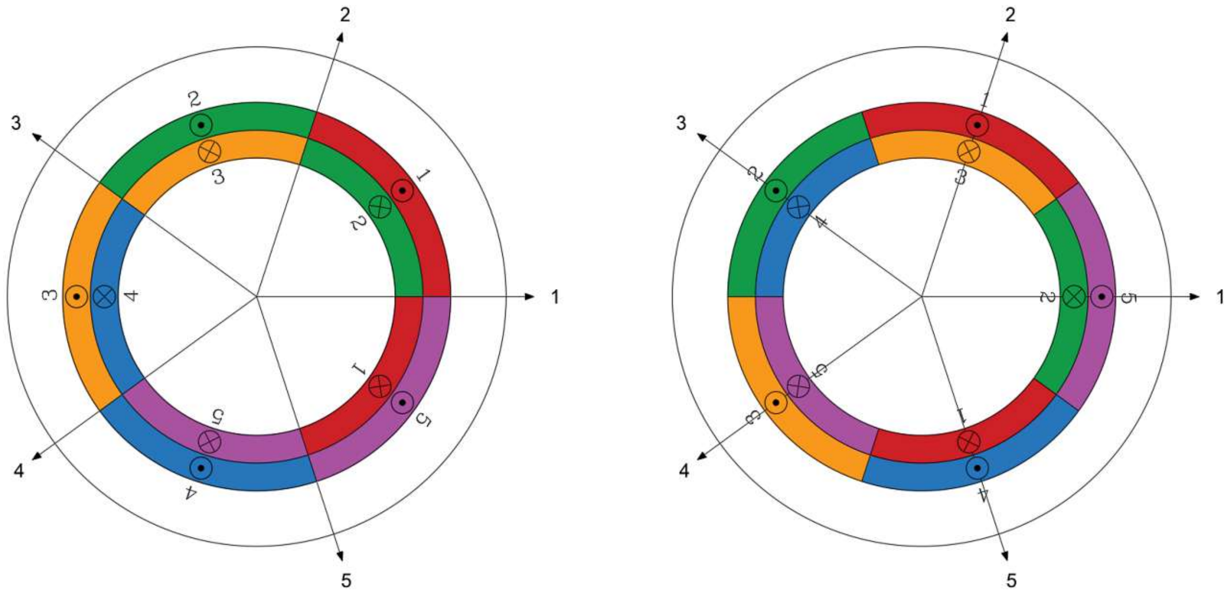

Figure 6.27: Zone diagrams of a double layer winding with five phases and double zone span for coil pitches of $\sigma = 2/5$ (left) and $\sigma = 4/5$ (right).

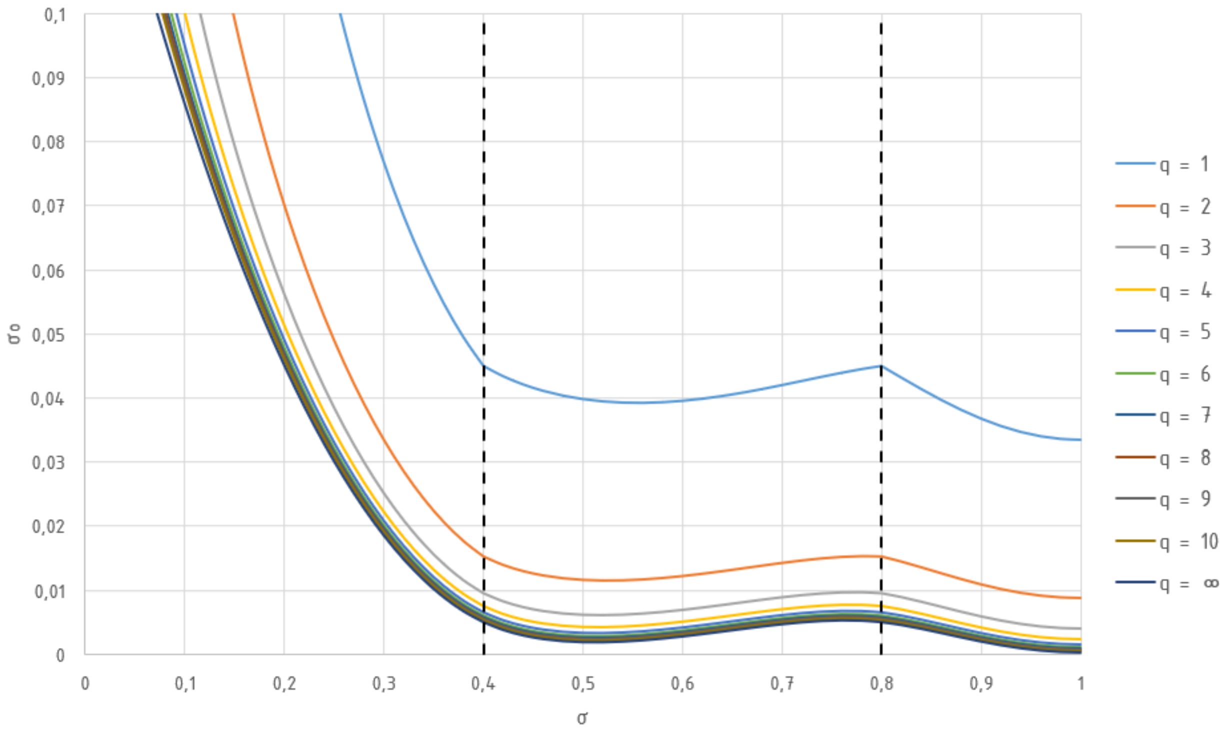

Figure 6.28: Courses of the harmonic scattering coefficient σ_o over the coil pitch $0 \leq \sigma \leq 1$ of a double layer winding with normal zone span and $m = 5$ for several numbers of slots q.

Winding with seven Phases

A double layer winding of seven phases and double zone span is characterized by fourteen zones (seven per layer) which each occupy a seventh of two pole pitches along the circumference (figure 6.29).

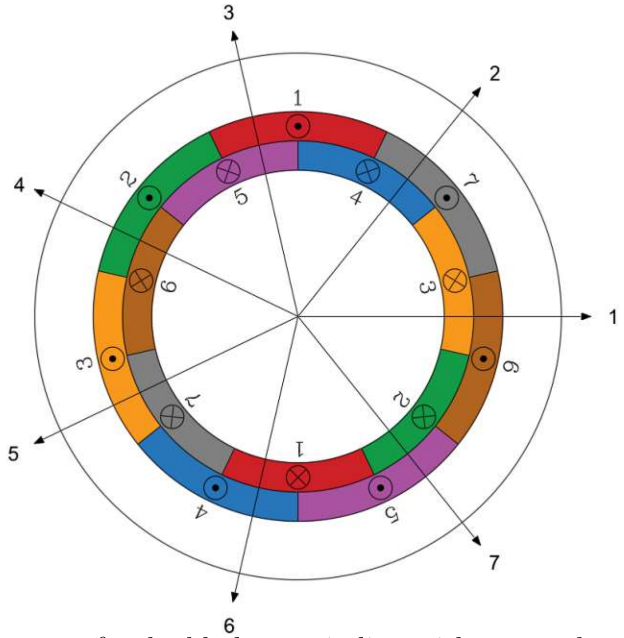

Figure 6.29: Zone diagram of a double layer winding with seven phases and double zone span at a coil pitch of $\sigma = 1$.

The winding factor for the fundamental wave ξ_1 gets calculated by equation (3.26) with $m = 7$, $\nu = 1$ and a certain coil pitch σ. For the calculation of the harmonic scattering coefficients, a winding with $m = 7$ needs four pitching ranges.

The calculation of the auxiliary factor V_{AF} for the individual pitching ranges is done according to the formulae in chapter 5.1.3.2. A simplification of the expressions is no longer possible or useful. A separate written solution will therefore be omitted. The following assignments to the pitching ranges apply:

$$\begin{array}{rcrcl} 6/7 \leq \sigma \leq 1 & \text{resp.} & 0 \leq |y_\varepsilon| \leq q & \rightarrow & (5.55) \\ 4/5 \leq \sigma \leq 6/7 & \text{resp.} & q \leq |y_\varepsilon| \leq 3\,q & \rightarrow & (5.60) \\ 2/7 \leq \sigma \leq 4/7 & \text{resp.} & 3\,q \leq |y_\varepsilon| \leq 5\,q & \rightarrow & (5.65) \\ 0 \leq \sigma \leq 2/7 & \text{resp.} & 5\,q \leq |y_\varepsilon| \leq 7\,q & \rightarrow & (5.70) \end{array}$$

Table A.7 in the appendix provides the harmonic scattering coefficients for possible shortening steps of a winding with three phases. Figure 6.32 shows the progression of the harmonic scattering coefficient as a function of the coil pitch ($0 \leq \sigma \leq 1$). The vertical lines indicate the limits of the pitching ranges, figures 6.30 and 6.31 correspond to the zone plans at the intersection of the pitching ranges. The zones of the bottom layer and upper layer do not show overlaps of different phases.

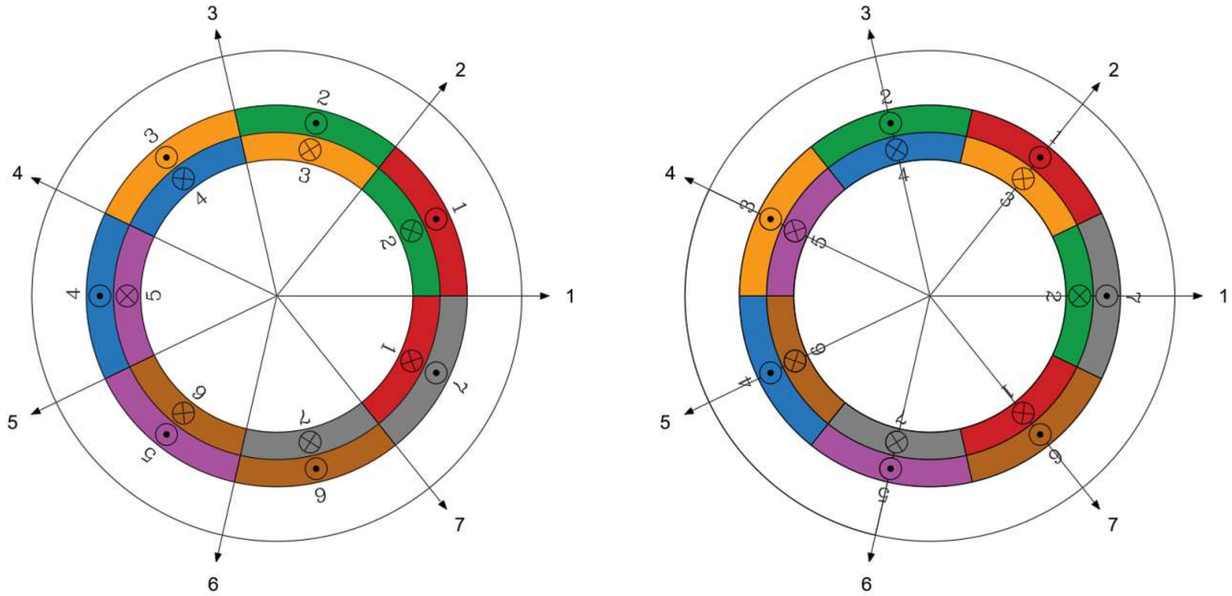

Figure 6.30: Zone diagrams of a double layer winding with seven phases and double zone span for coil pitches of $\sigma = 2/7$ (left) and $\sigma = 4/7$ (right).

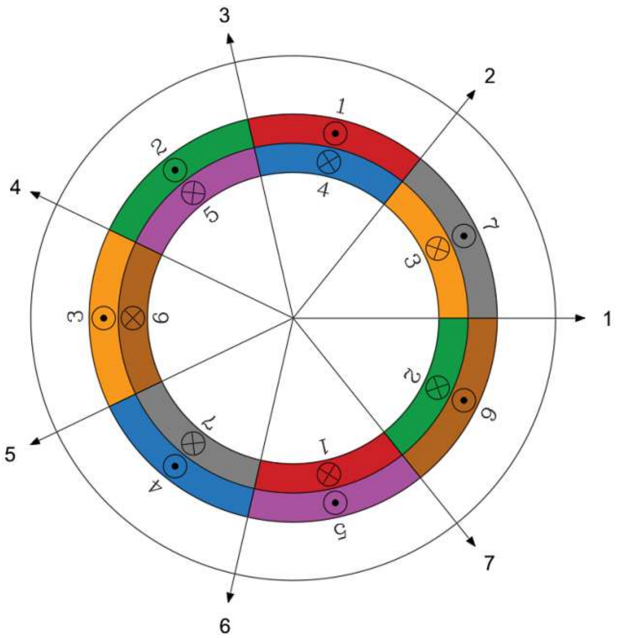

Figure 6.31: Zone diagram of a double layer winding with seven phases and double zone span for a coil pitch of $\sigma = 6/7$.

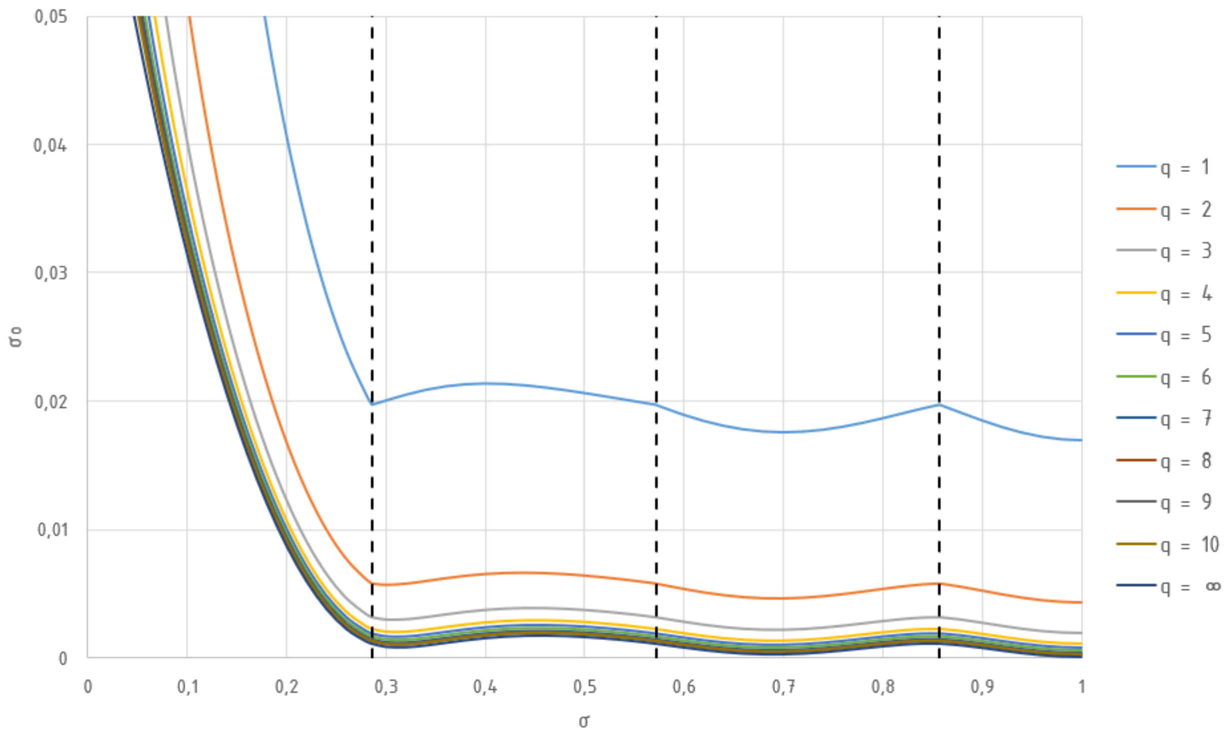

Figure 6.32: Courses of the harmonic scattering coefficient σ_o over the coil pitch $0 \leq \sigma \leq 1$ of a double layer winding with normal zone span and $m = 7$ for several numbers of slots q.

6.1.3 Correlation for a Constant Product of m q

In order to illustrate the advantages of a higher number of phases in terms of a decreasing harmonic scattering, the following correlations of the harmonic scattering coefficients σ_o of two phase numbers each for a constant product of $m\,q$ are given. Both normal zone span and double zone span windings are considered.

The data basis for the correlations is derived from the values calculated in the previous sub chapters (see also appendix tables). The vertically dashed lines in the diagrams represent the boundaries of the pitching ranges and are always kept in the color corresponding to the respective phase number.

$\mathbf{m\,q = 6}$

The product $m\,q = 6$ allows combinations for $m = 2$ with $q = 3$ and $m = 3$ with $q = 2$. The graphs are shown in figure 6.33. Here the pitch of $\sigma = 2/3$, as both winding variants have almost the same harmonic scattering factor. The two phase winding experiences a stronger increase of σ_o against $\sigma = 1$.

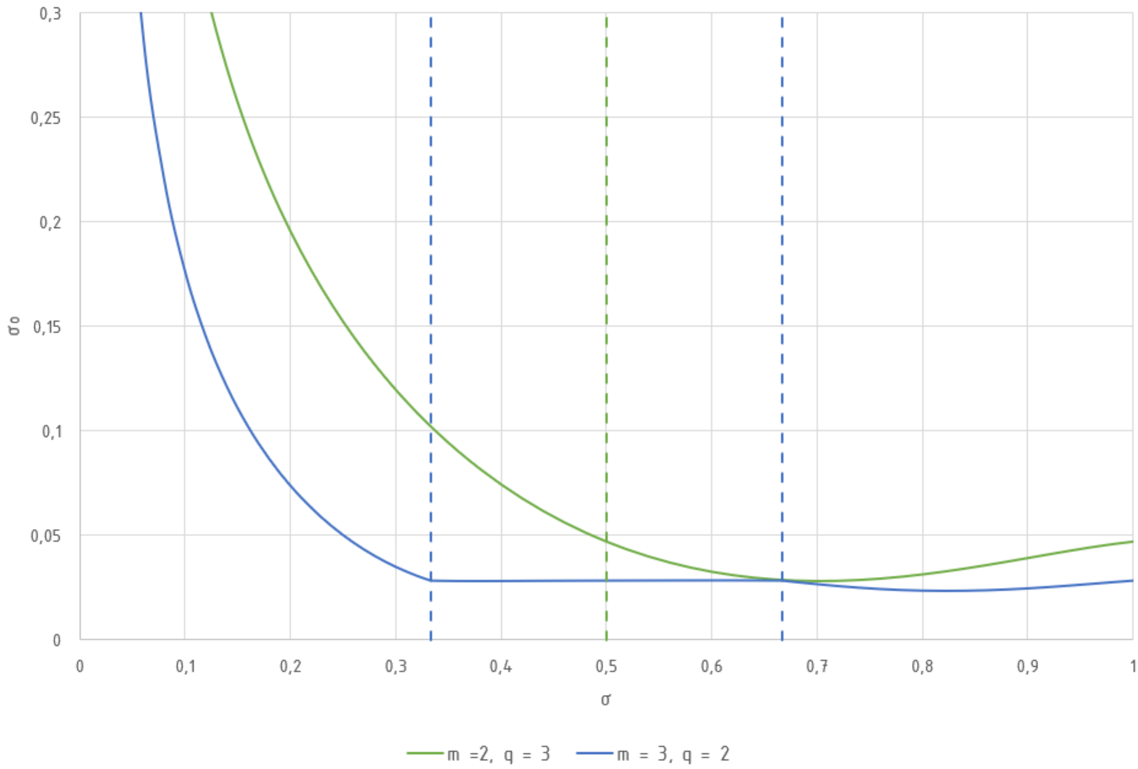

Figure 6.33: Correlation of the harmonic scattering coefficient σ_o of windings with two and three phases for $m\,q = 6$.

$\mathbf{m\,q = 10}$

The product $m\,q = 10$ allows combinations for $m = 2$ with $q = 5$ and $m = 5$ with $q = 2$. The graphs are shown in figure 6.34. Compared to the two phase winding, the five phase winding offers a significant reduction in harmonic scattering over almost the entire considered pitching range from $0 \leq \sigma \leq 1$.

$\mathbf{m\,q = 14}$

The product $m\,q = 14$ allows combinations for $m = 2$ with $q = 7$ and $m = 7$ with $q = 2$. The graphs are shown in figure 6.35. Compared to the two phase winding, the seven phase winding offers an even stronger reduction in harmonic scattering. In this correlation, the seven phase winding seems to have a quasi constant harmonic scattering within the pitching range $1/7 \leq \sigma \leq 1$ compared to the two phase winding.

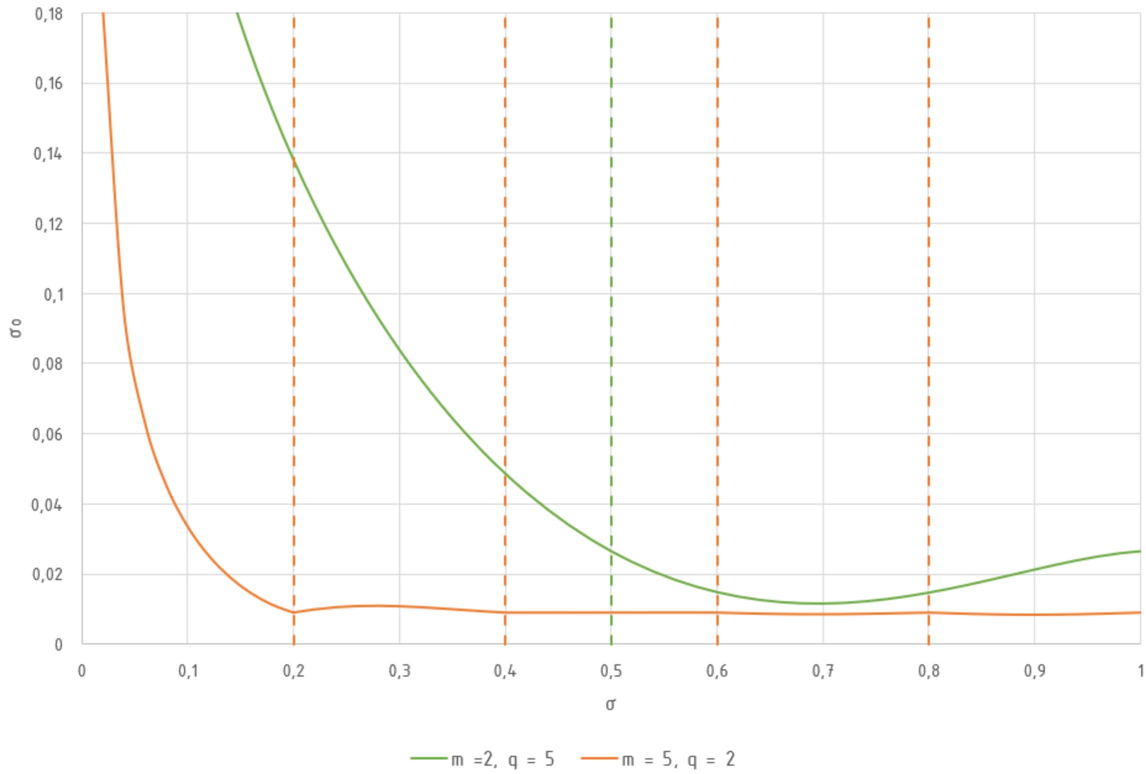

Figure 6.34: Correlation of the harmonic scattering coefficient σ_o of windings with two and five phases for $m\,q = 10$.

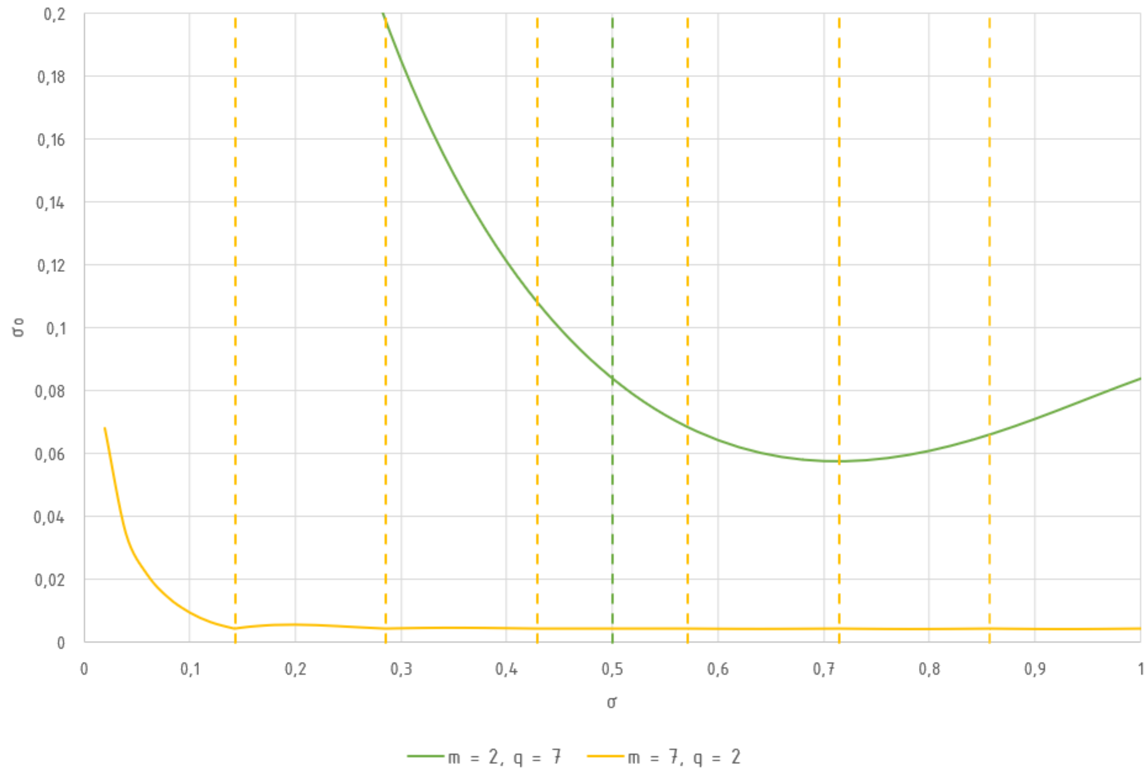

Figure 6.35: Correlation of the harmonic scattering coefficient σ_o of windings with two and seven phases for $m\,q = 14$.

$\mathbf{m\,q = 15}$

The product $m\,q = 15$ allows combinations for $m = 3$ with $q = 5$ and $m = 5$ with $q = 3$, either with normal zone span or double zone span. The graphs are shown in figure 6.36. Whereas relatively similar values of the harmonic scattering coefficients can be achieved with normal zone span starting from a pitch of approximately $\sigma = 1/3$, with double zone span (with already higher harmonic scattering) the difference between three phase and five phase windings is practically only reached to some extent from $\sigma = 0,9$ – before that the difference between three phase and five phase windings is considerable.

$\mathbf{m\,q = 21}$

The product $m\,q = 21$ allows combinations for $m = 3$ with $q = 7$ and $m = 7$ with $q = 3$, either with normal zone span or double zone span. The graphs are shown in figure 6.37. The qualitative evaluation is practically the same as for $m\,q = 15$, except for the even lower harmonic scattering for the seven phase armature winding.

$\mathbf{m\,q = 35}$

The product $m\,q = 35$ allows combinations for $m = 5$ with $q = 7$ and $m = 7$ with $q = 5$, either with normal zone span or double zone span. The graphs are shown in figure 6.38. This comparison allows a more detailed examination and scaling of the diagrams due to the low values of the harmonic scattering. Obviously, the courses for normal zone span (top of figure 6.38) show that the harmonic scattering of the seven phase winding is not always smaller for each pitch σ than that of the five phase winding, once around the pitch of approximately $\sigma = 0,2$ and once approximately between $0,85 \leq \sigma \leq 0,9$.

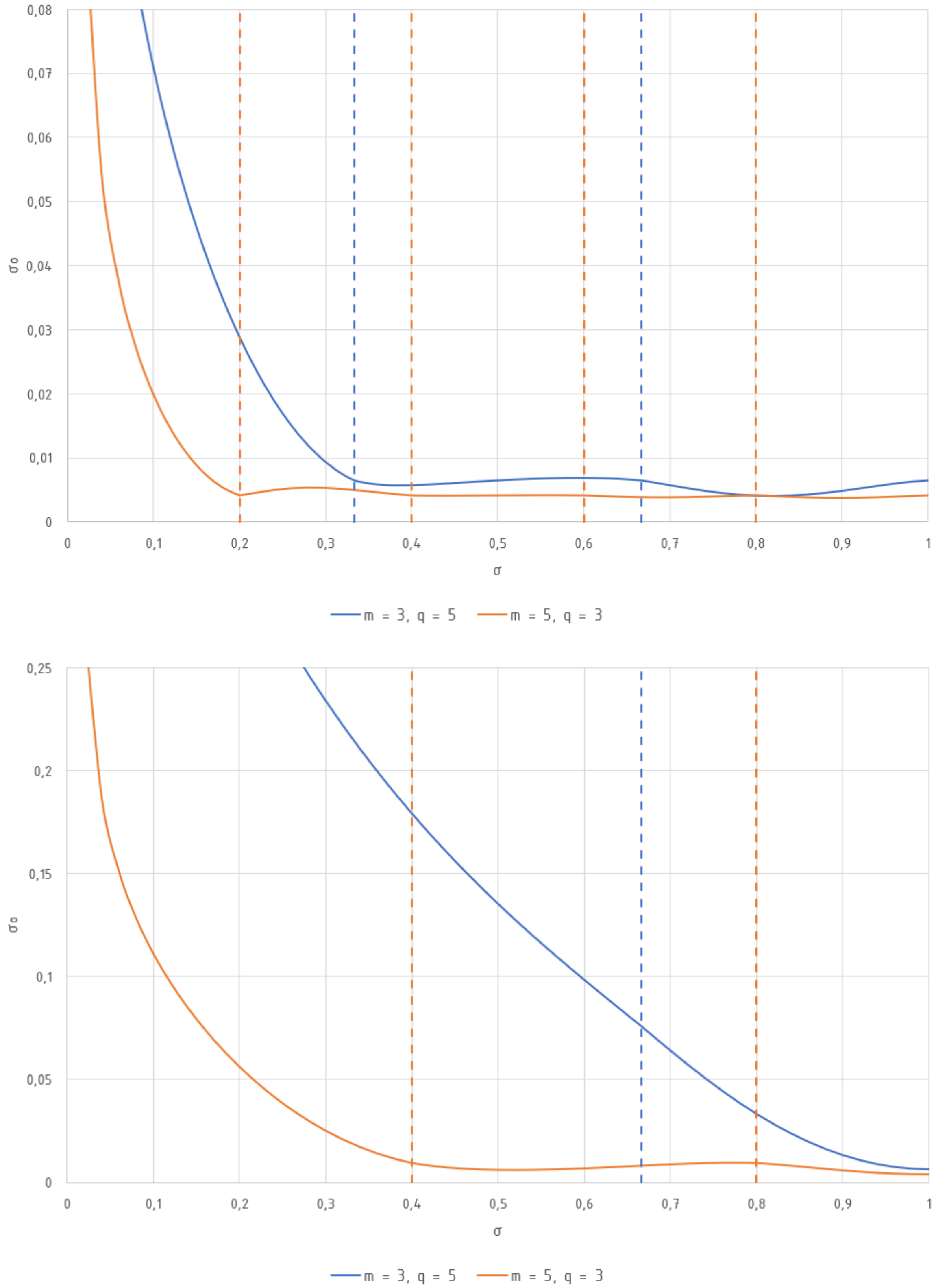

Figure 6.36: Correlation of the harmonic scattering coefficient σ_o of windings with normal zone span (top) and double zone span (bottom) for three and five phases with $m\,q = 15$.

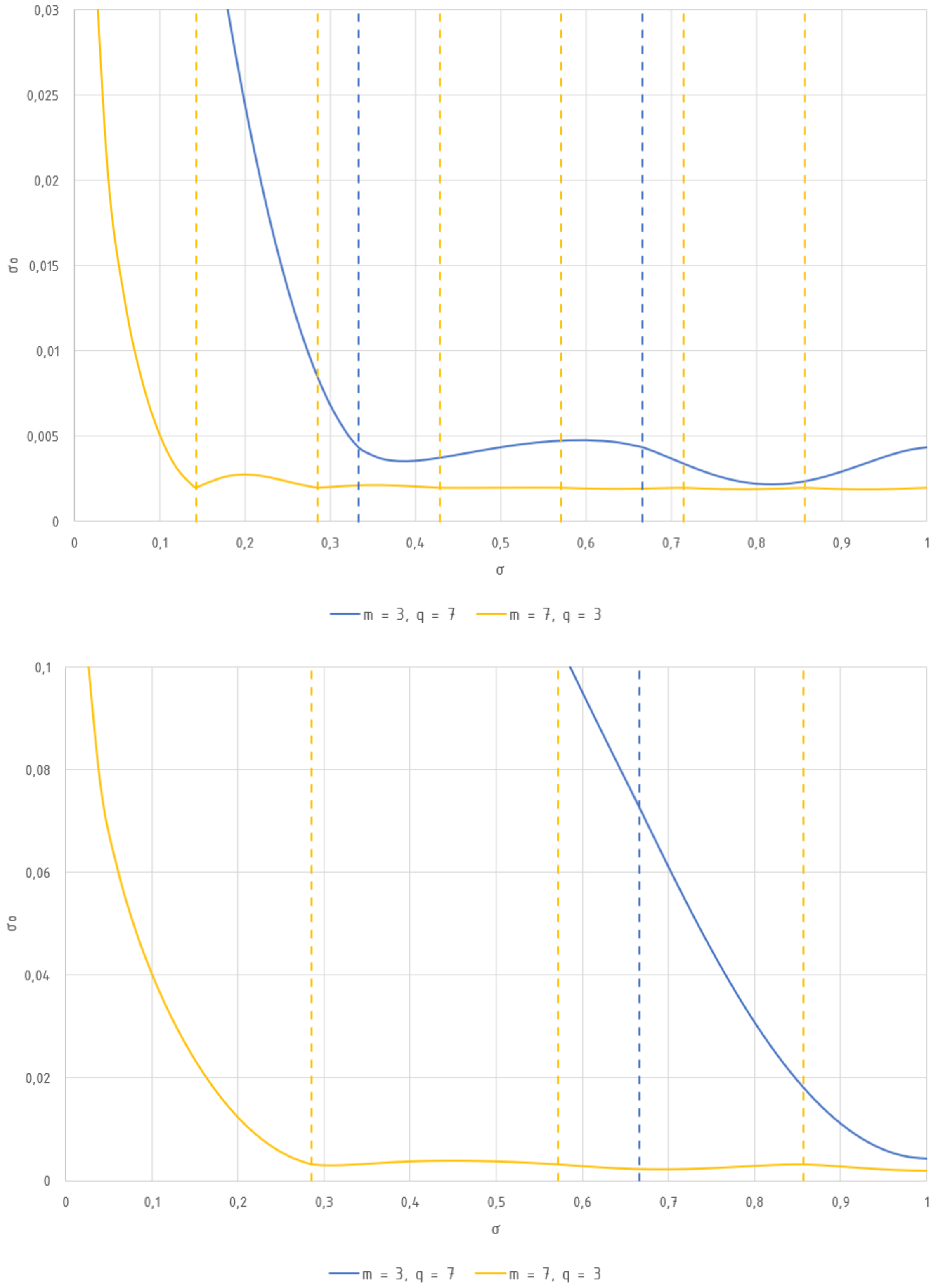

Figure 6.37: Correlation of the harmonic scattering coefficient σ_o of windings with normal zone span (top) and double zone span (bottom) for three and seven phases with $m\,q = 21$.

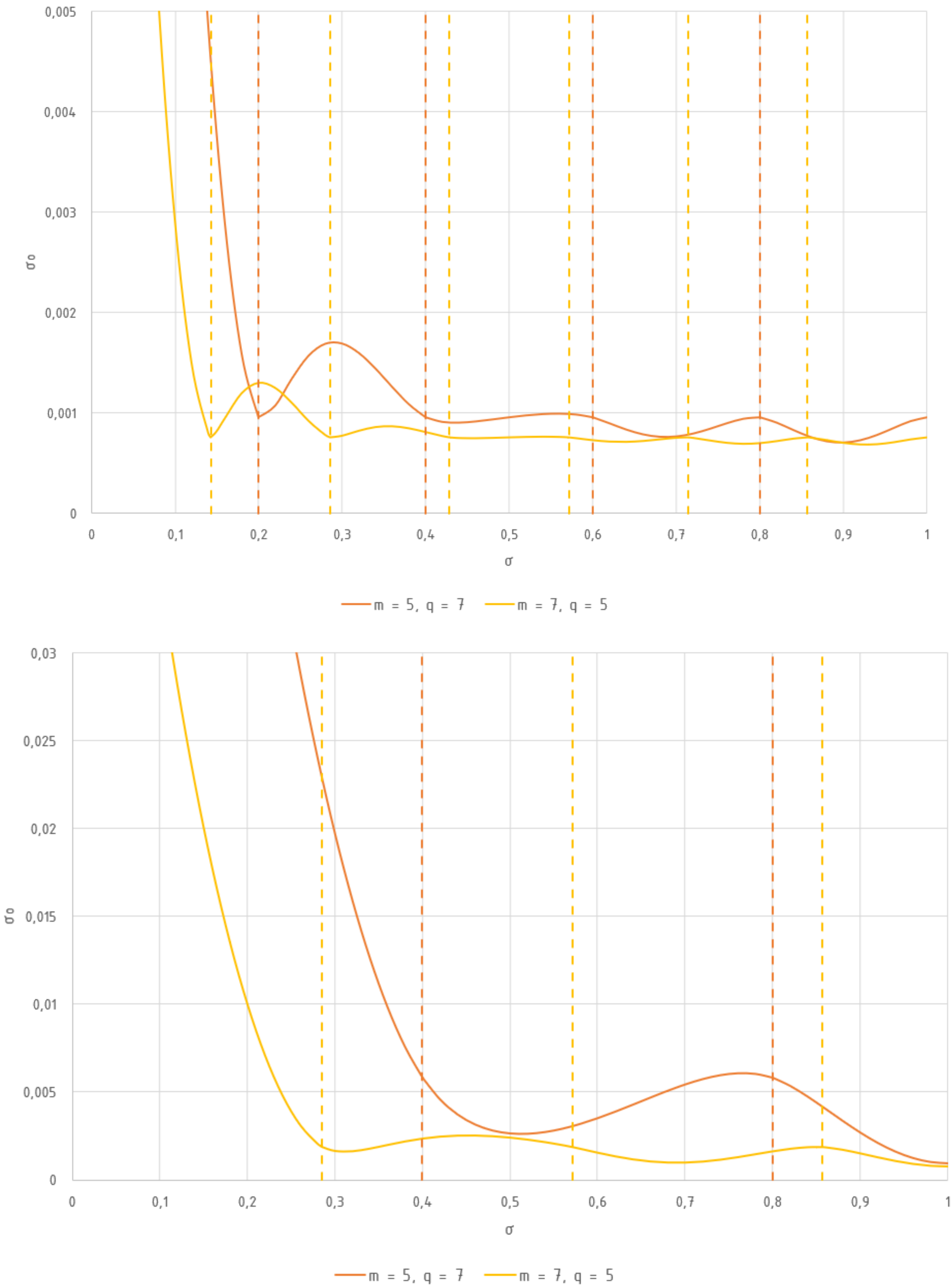

Figure 6.38: Correlation of the harmonic scattering coefficient σ_o of windings with normal zone span (top) and double zone span (bottom) for five and seven phases with $m\,q = 35$.

6.2 Fractional Slot Windings

In this chapter, double layer fractional slot windings with normal zone span and double zone span are evaluated for $m = \{2, 3, 5, 7\}$ phase systems. The number pool for possible numbers of slots per pole and phase has been defined for the numerator and denominator as follows:

$$q_n = \{2, 3, 5\} \quad , \quad q_z = \{3, 4, 5, 6, 7, 8, 9, 10, 11, 12, 13, 14, 15, 16, 17, 19, 21\}$$

A detailed evaluation of the harmonic wave scattering coefficients in tabular form for the respective possible slot numbers q and coil steps y_σ can be found in the appendix A.2. For each phase number, the two lowest possible numbers for q_n were evaluated.

6.2.1 Normal Zone Span

Winding with two Phases

According to the introduction, for two phase windings the denominators $q_n = 3$ and 5 are given for the number of slots per pole and phase. The evaluation of ten different slot numbers per denominator number q_n (see tables A.8 and A.9) results in up to 67 possible coil steps y_σ each. Figures 6.39 and 6.40 show the courses of the harmonic scattering coefficient.

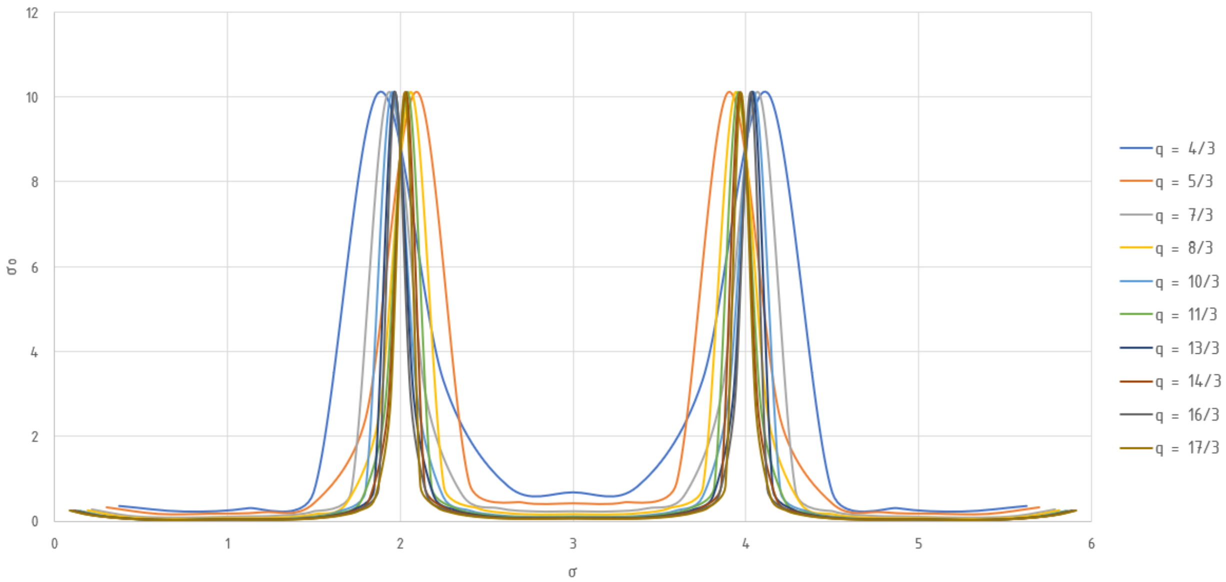

Figure 6.39: Courses of the harmonic scattering coefficient σ_o over the coil pitch $0 \leq \sigma \leq 6$ of a double layer fractional slot winding with normal zone span and $m = 2$ for several numbers of slots with $q_n = 3$.

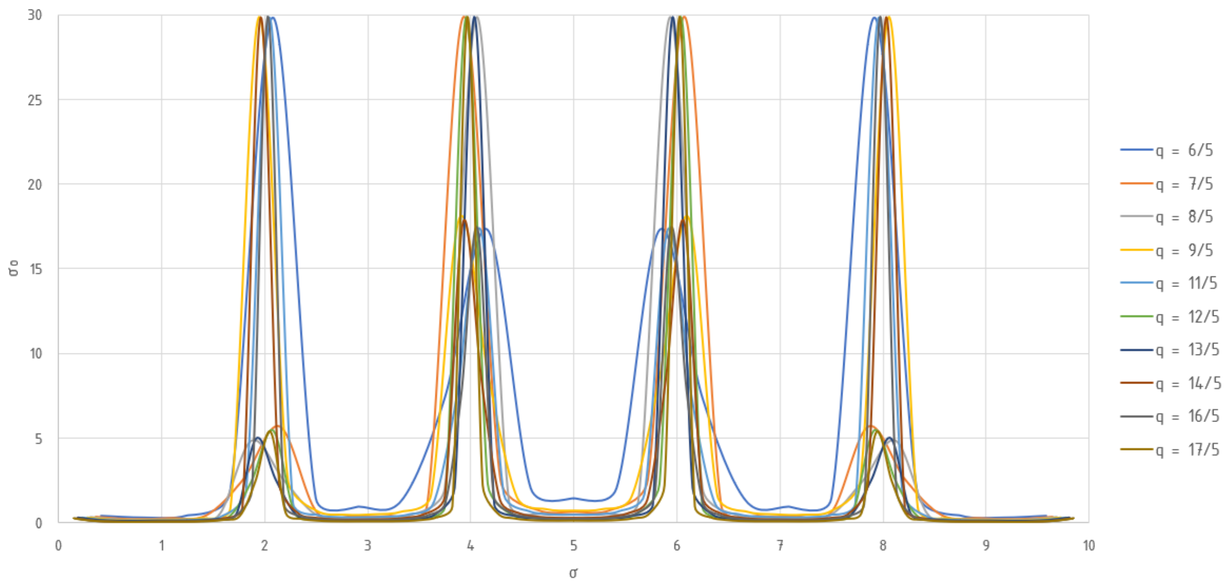

Figure 6.40: Courses of the harmonic scattering coefficient σ_o over the coil pitch $0 \leq \sigma \leq 10$ of a double layer fractional slot winding with normal zone span and $m = 2$ for several numbers of slots with $q_n = 5$.

The characteristics span a pitching range of $0 < \sigma < 2\,q_n$ and also exhibit a mirror symmetry at $\sigma = q_n$. In the area of those points of pitch, which represent a multiple of $\sigma = 2$, very high values of the harmonic scattering result since at these points practically no magnetic flux is covered by the coils. However, the exact points of the maxima are individual depending on the number of slots per pole and phase. In the variant with $q_n = 5$, it is also noticeable that the peaks of the harmonic scattering are not evenly distributed – either the maxima are at $\sigma = 2$ and 8, or at $\sigma = 4$ and 6.

The lowest achievable harmonic scattering coefficient in the observed range results in $\sigma_o = 0,015277$ for $q_n = 3$ and $\sigma_o = 0,040423$ at $q_n = 5$.

Winding with three Phases

For three phase windings the denominators $q_n = 2$ and 5 are given for the number of slots per pole and phase. The evaluation of ten different slot numbers per denominator number q_n (see tables A.10 and A.11) results in up to 62 possible coil steps y_σ for $q_n = 2$ and 101 for $q_n = 5$. Figures 6.41 and 6.42 show the courses of the harmonic scattering coefficient.

As in the previous sub section, very high values of the harmonic scattering result at points of a multiple of $\sigma = 2$. Again, for the variant with $q_n = 5$ the peaks of the harmonic scattering are not evenly distributed.

The lowest achievable harmonic scattering coefficient in the observed range results in $\sigma_o = 0,001189$ for $q_n = 2$ and $\sigma_o = 0,012652$ at $q_n = 5$. The maximum values of the harmonic scattering coefficient for windings with $q_n = 2$ are significantly lower, approximately $1 : 200$.

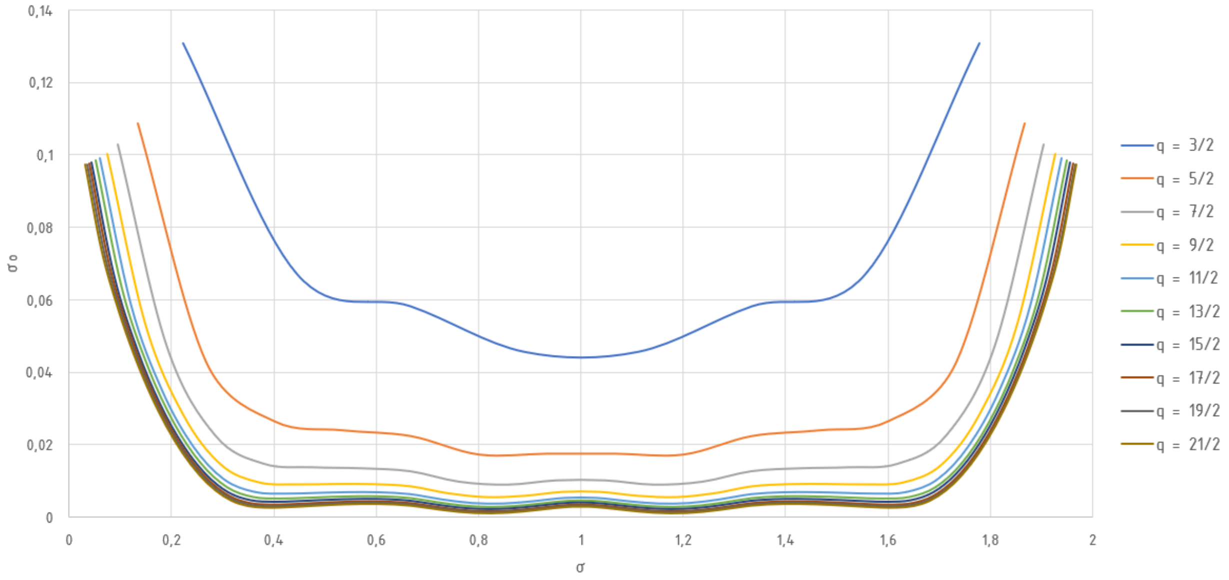

Figure 6.41: Courses of the harmonic scattering coefficient σ_o over the coil pitch $0 \leq \sigma \leq 2$ of a double layer fractional slot winding with normal zone span and $m = 3$ for several numbers of slots with $q_n = 2$.

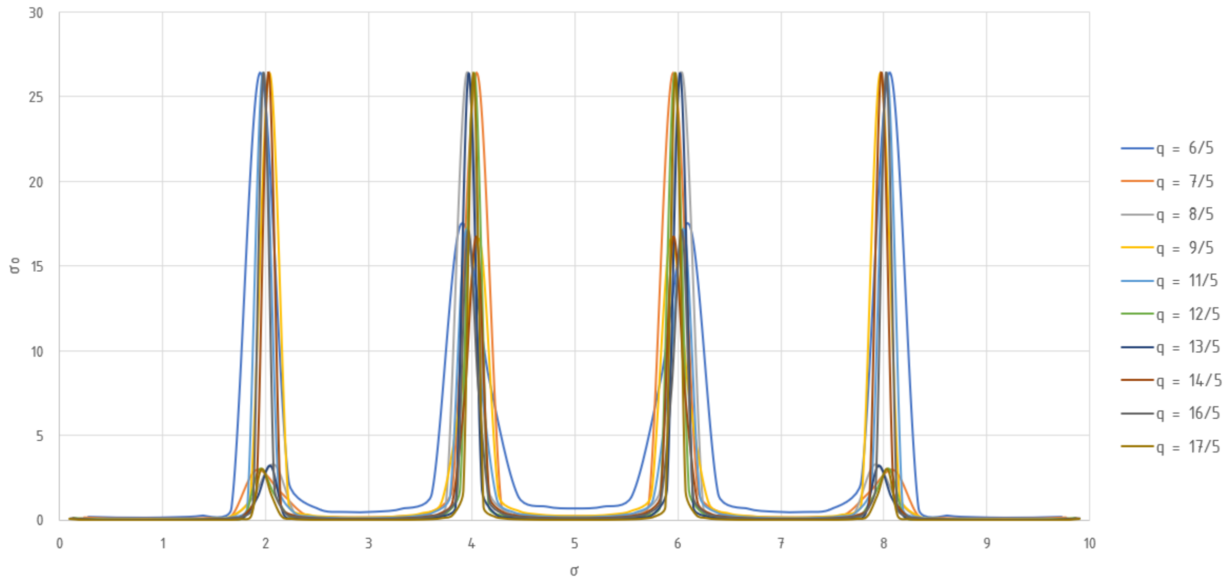

Figure 6.42: Courses of the harmonic scattering coefficient σ_o over the coil pitch $0 \leq \sigma \leq 10$ of a double layer fractional slot winding with normal zone span and $m = 3$ for several numbers of slots with $q_n = 5$.

Winding with five Phases

For five phase windings the denominators $q_n = 2$ and 3 are given for the number of slots per pole and phase. The evaluation of ten different slot numbers per denominator number

q_n (see tables A.12 and A.13) results in up to 104 possible coil steps y_σ for $qn = 2$ and 169 for $q_n = 3$. Figures 6.43 and 6.44 show the courses of the harmonic scattering coefficient.

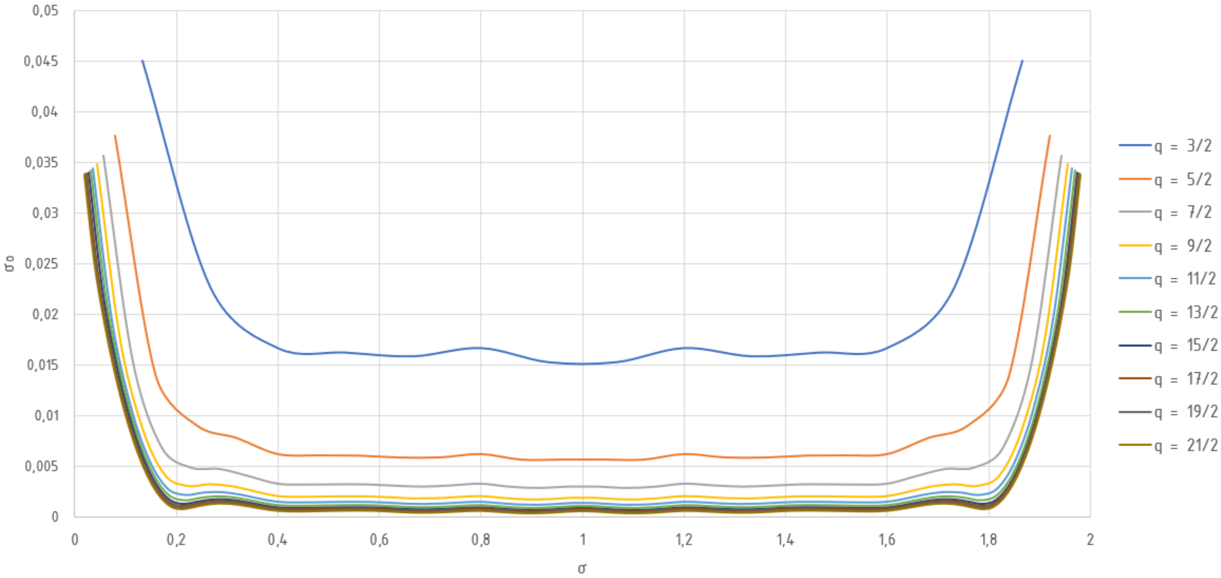

Figure 6.43: Courses of the harmonic scattering coefficient σ_o over the coil pitch $0 \leq \sigma \leq 2$ of a double layer fractional slot winding with normal zone span and $m = 5$ for several numbers of slots with $q_n = 2$.

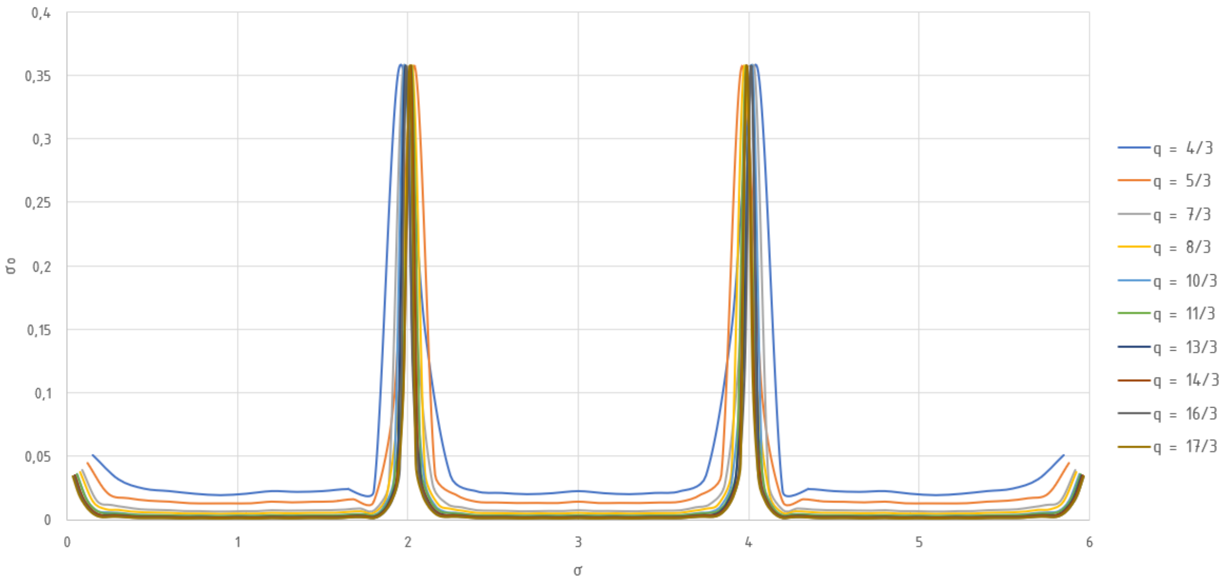

Figure 6.44: Courses of the harmonic scattering coefficient σ_o over the coil pitch $0 \leq \sigma \leq 6$ of a double layer fractional slot winding with normal zone span and $m = 5$ for several numbers of slots with $q_n = 3$.

Higher values, but much less than for windings with $m = 2$ and 3, of the harmonic scattering result at points of a multiple of $\sigma = 2$.

The lowest achievable harmonic scattering coefficient in the observed range results in $\sigma_o = 0,000333$ for $q_n = 2$ and $\sigma_o = 0,001098$ at $q_n = 3$. The maximum values of the harmonic scattering coefficient for windings with $q_n = 2$ are lower, approximately $1:8$.

Winding with seven Phases

Windings with seven phases can have the denominators $q_n = 2$ and 3 for the number of slots per pole and phase. The evaluation of ten different slot numbers per denominator number q_n (see tables A.14 and A.15) results in up to 146 possible coil steps y_σ for $qn = 2$ and 237 for $q_n = 3$. Figures 6.45 and 6.46 show the courses of the harmonic scattering coefficient.

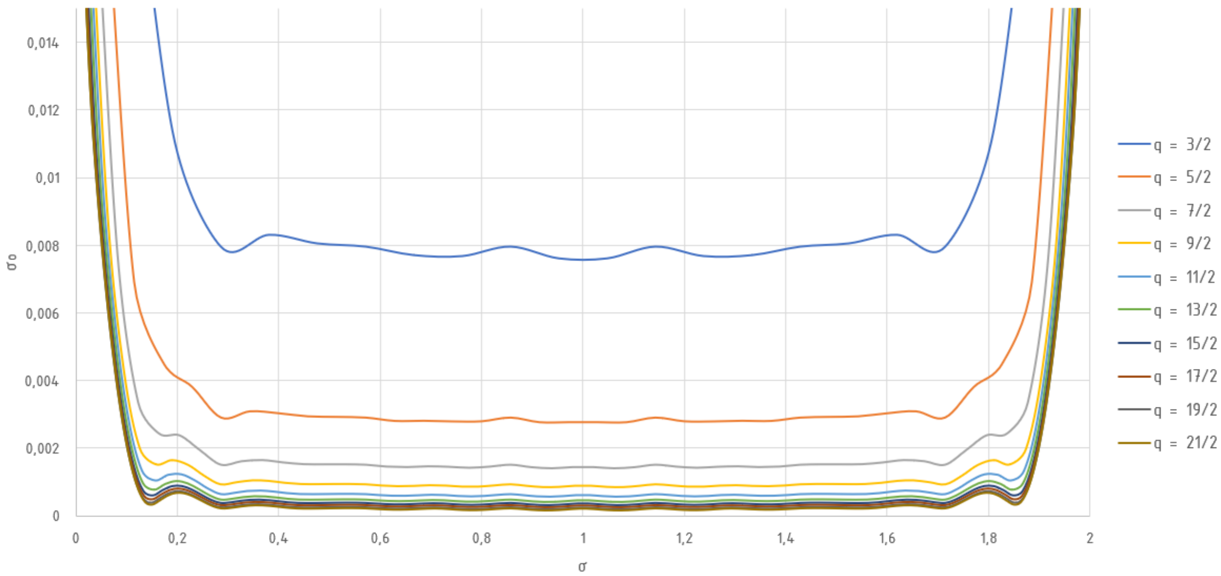

Figure 6.45: Courses of the harmonic scattering coefficient σ_o over the coil pitch $0 \leq \sigma \leq 2$ of a double layer fractional slot winding with normal zone span and $m = 7$ for several numbers of slots with $q_n = 2$.

Higher values of the harmonic scattering result at points of a multiple of $\sigma = 2$.

The lowest achievable harmonic scattering coefficient in the observed range results in $\sigma_o = 0,000160$ for $q_n = 2$ and $\sigma_o = 0,000541$ at $q_n = 3$. The maximum values of the harmonic scattering coefficient for windings with $q_n = 2$ are lower, approximately $1:7$.

6.2.2 Double Zone Span

Winding with three Phases

For three phase windings with double zone span the denominators $q_n = 2$ and 5 are given for the number of slots per pole and phase. The evaluation of ten different slot numbers

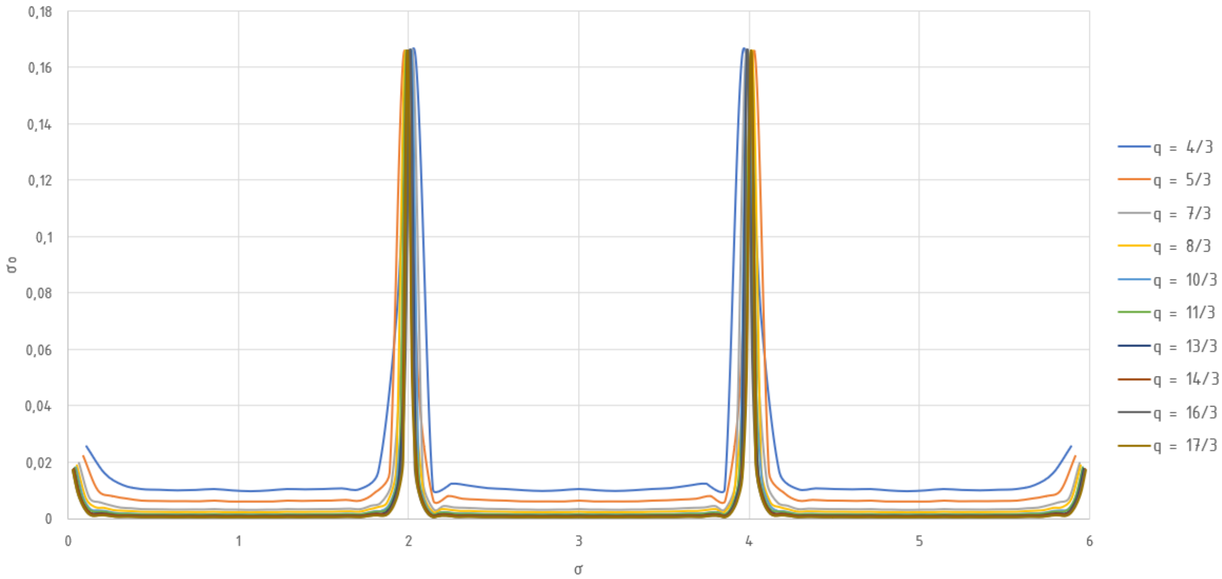

Figure 6.46: Courses of the harmonic scattering coefficient σ_o over the coil pitch $0 \leq \sigma \leq 6$ of a double layer fractional slot winding with normal zone span and $m = 7$ for several numbers of slots with $q_n = 3$.

per denominator number q_n (see tables A.16 and A.17) results in up to 62 possible coil steps y_σ for $qn = 2$ and 101 for $q_n = 5$. Figures 6.47 and 6.48 show the courses of the harmonic scattering coefficient.

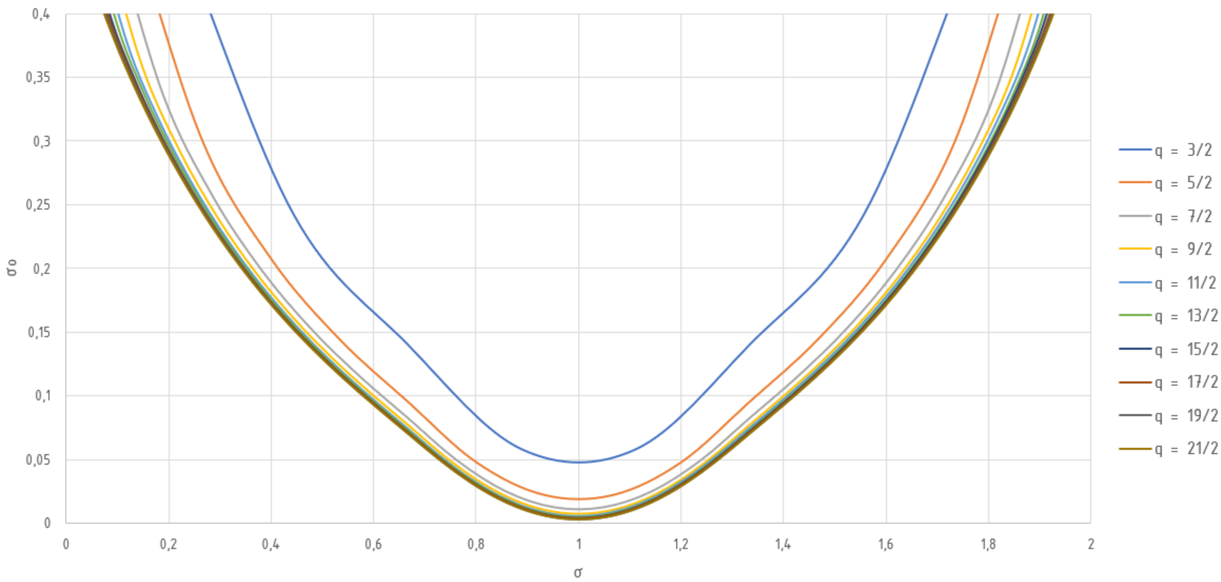

Figure 6.47: Courses of the harmonic scattering coefficient σ_o over the coil pitch $0 \leq \sigma \leq 2$ of a double layer fractional slot winding with double zone span and $m = 3$ for several numbers of slots with $q_n = 2$.

Compared to the version with normal zone span, $q_n = 2$ shows a course which falls

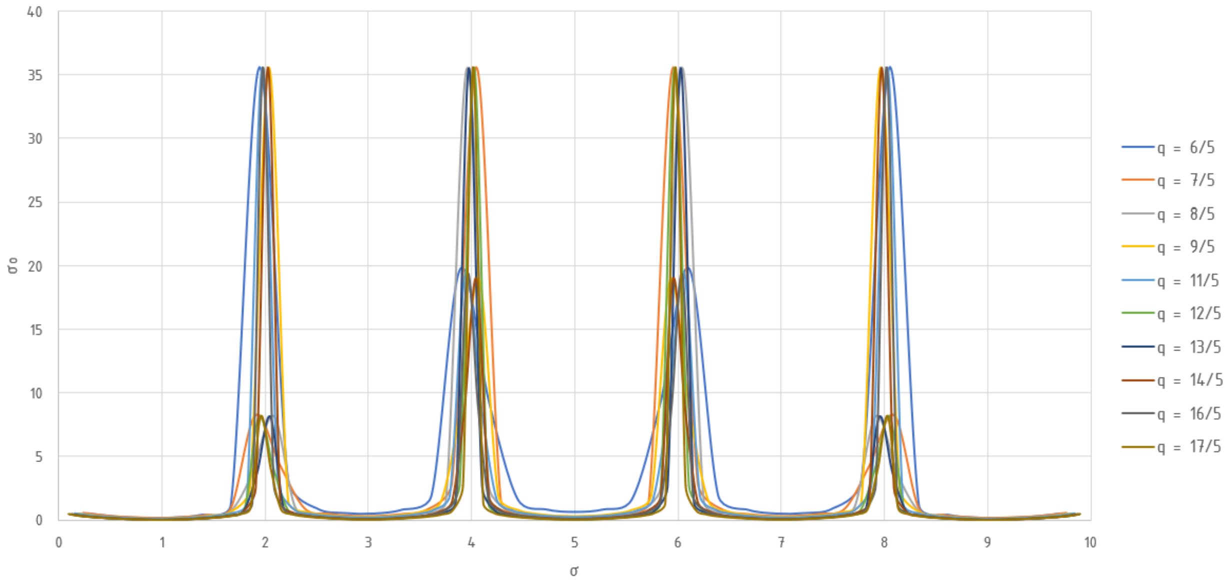

Figure 6.48: Courses of the harmonic scattering coefficient σ_o over the coil pitch $0 \leq \sigma \leq 6$ of a double layer fractional slot winding with double zone span and $m = 3$ for several numbers of slots with $q_n = 5$.

monotonously up to $\sigma = 1$ and then increases monotonously upwards. In the variant with $q_n = 5$, as with normal zone span, the peaks of the characteristics of the harmonic scattering are again not evenly distributed.

The lowest achievable harmonic scattering coefficient in the observed range results in $\sigma_o = 0,003307$ for $q_n = 2$ and $\sigma_o = 0,023604$ at $q_n = 5$. The maximum values of the harmonic scattering coefficient for windings with $q_n = 2$ are much lower, approximately $1 : 77$.

Winding with five Phases

For five phase windings with double zone span the denominators $q_n = 2$ and 3 are given for the number of slots per pole and phase. The evaluation of ten different slot numbers per denominator number q_n (see tables A.18 and A.19) results in up to 104 possible coil steps y_σ for $qn = 2$ and 169 for $q_n = 3$. Figures 6.49 and 6.50 show the courses of the harmonic scattering coefficient.

Higher values of the harmonic scattering result at points of a multiple of $\sigma = 2$, but much less than for windings with $m = 3$.

The lowest achievable harmonic scattering coefficient in the observed range results in $\sigma_o = 0,000573$ for $q_n = 2$ and $\sigma_o = 0,001443$ at $q_n = 3$. The maximum values of the harmonic scattering coefficient for windings with $q_n = 2$ are lower, approximately $1 : 20$.

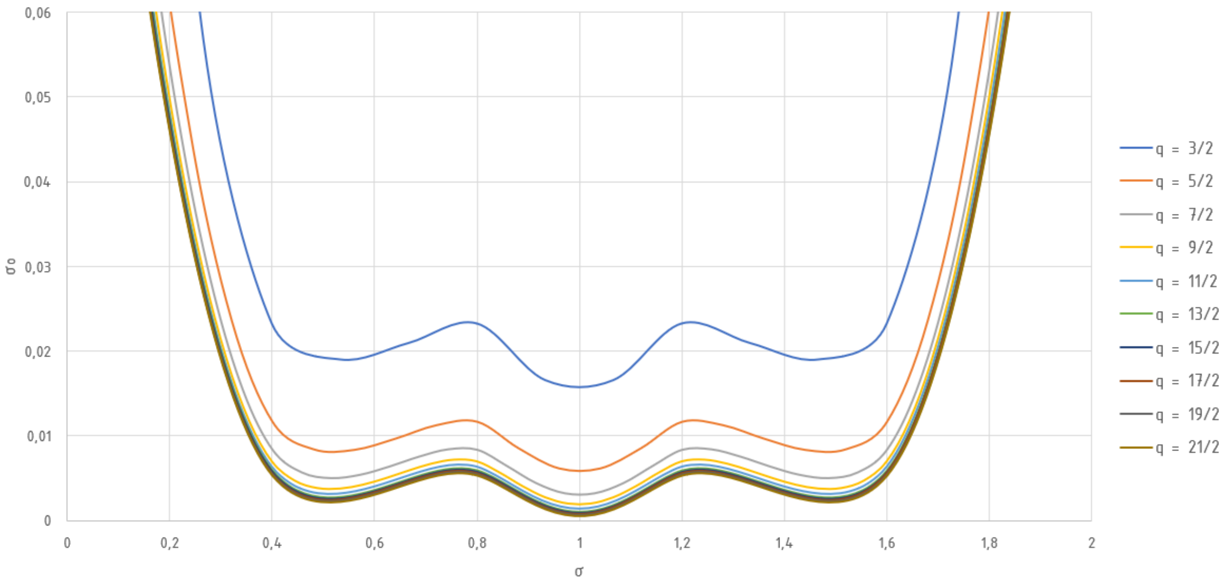

Figure 6.49: Courses of the harmonic scattering coefficient σ_o over the coil pitch $0 \leq \sigma \leq 2$ of a double layer fractional slot winding with double zone span and $m = 5$ for several numbers of slots with $q_n = 2$.

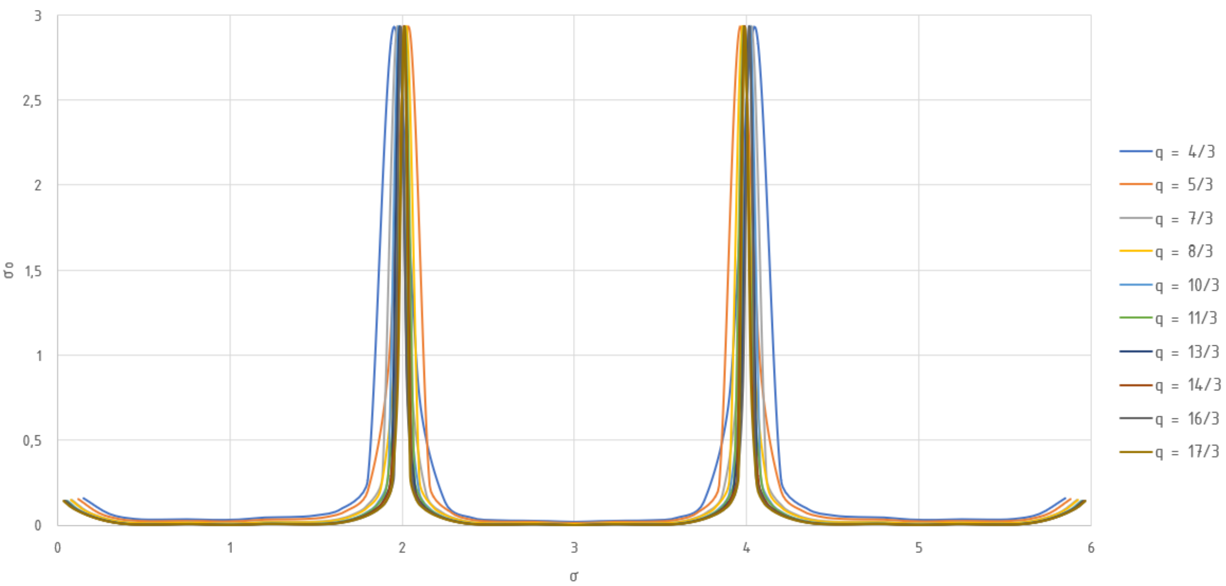

Figure 6.50: Courses of the harmonic scattering coefficient σ_o over the coil pitch $0 \leq \sigma \leq 6$ of a double layer fractional slot winding with double zone span and $m = 5$ for several numbers of slots with $q_n = 3$.

Winding with seven Phases

Windings with seven phases and double zone span can have the denominators $q_n = 2$ and 3 for the number of slots per pole and phase. The evaluation of ten different slot numbers per denominator number q_n (see tables A.20 and A.21) results in up to 146 possible coil steps y_σ for $qn = 2$ and 237 for $q_n = 3$. Figures 6.51 and 6.52 show the courses of the harmonic scattering coefficient.

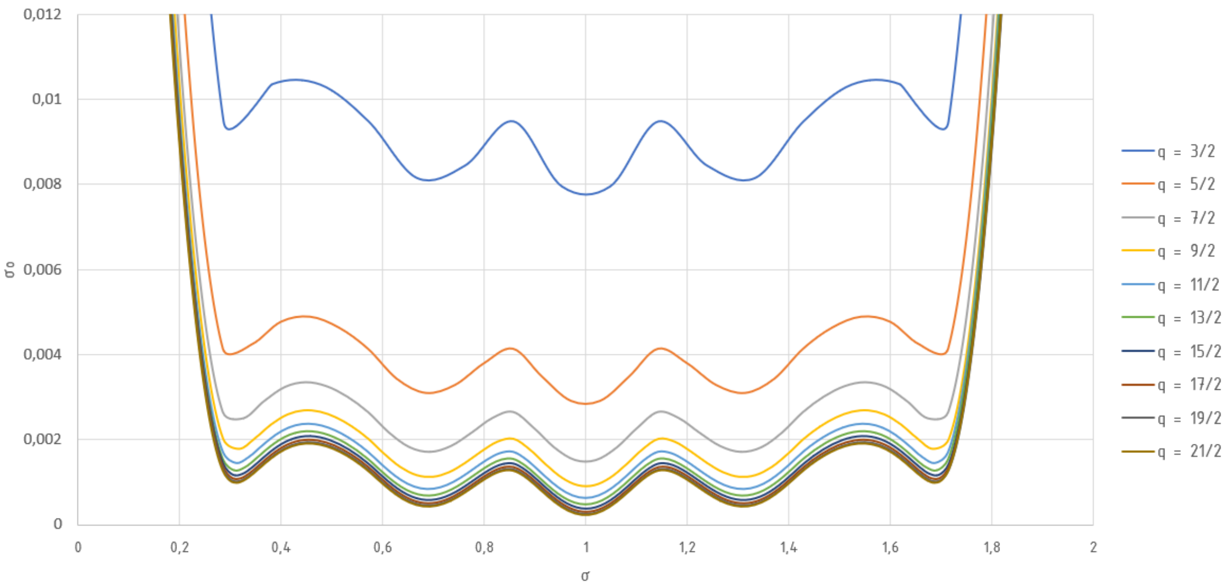

Figure 6.51: Courses of the harmonic scattering coefficient σ_o over the coil pitch $0 \leq \sigma \leq 2$ of a double layer fractional slot winding with double zone span and $m = 7$ for several numbers of slots with $q_n = 2$.

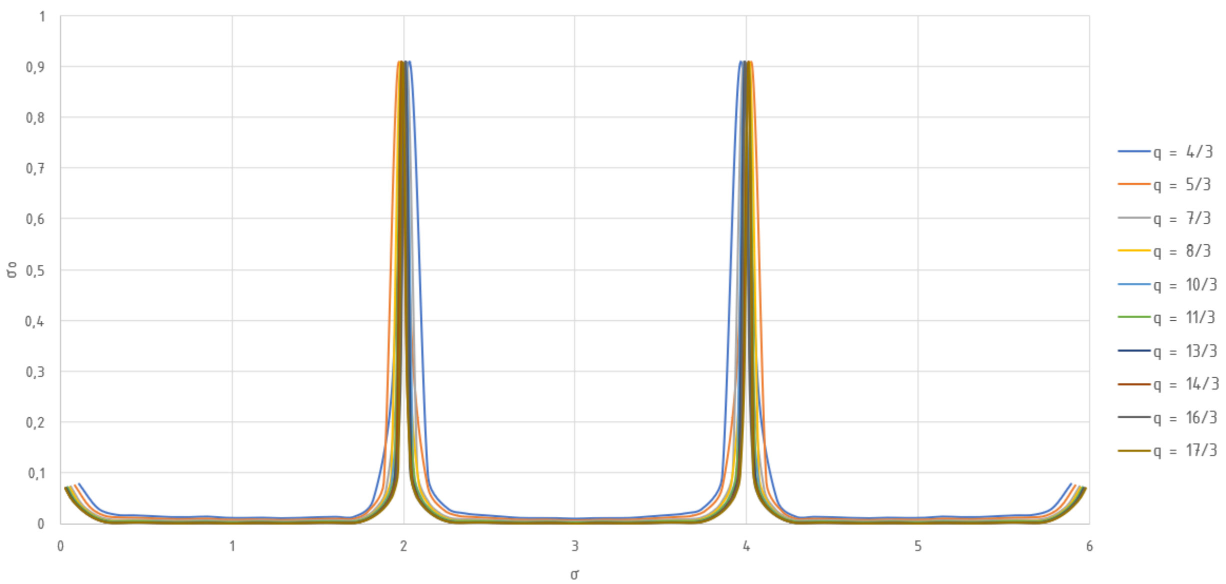

Figure 6.52: Courses of the harmonic scattering coefficient σ_o over the coil pitch $0 \leq \sigma \leq 6$ of a double layer fractional slot winding with double zone span and $m = 3$ for several numbers of slots with $q_n = 3$.

Again, higher values of the harmonic scattering result at points of a multiple of $\sigma = 2$.

The lowest achievable harmonic scattering coefficient in the observed range results in $\sigma_o = 0,000221$ for $q_n = 2$ and $\sigma_o = 0,000625$ at $q_n = 3$. The maximum values of the harmonic scattering coefficient for windings with $q_n = 2$ are lower, approximately $1 : 13$.

6.2.3 Correlation for a Constant Product of m q

The data basis for the correlations is again derived from the values calculated in the previous sub chapters (see also appendix tables). If possible, both normal zone span and double zone span windings are considered.

$\mathbf{m\,q = 18/5}$

The product $m\,q = 18/5$ allows combinations for $m = 2$ with $q = 9/5$ and $m = 3$ with $q = 6/5$. The graphs are shown in figure 6.53. Here both winding variants have nearly the same harmonic scattering factor. The two phase winding experiences higher peak values of σ_o for multiples of $\sigma = 2$.

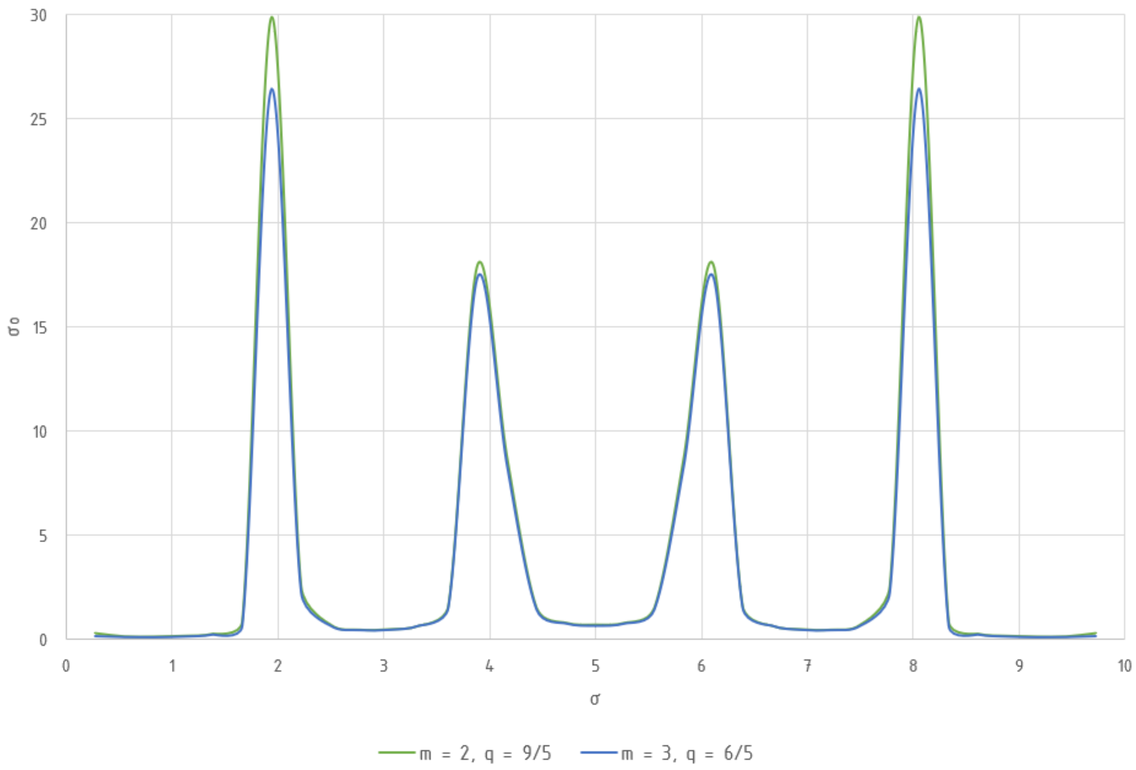

Figure 6.53: Correlation of the harmonic scattering coefficient σ_o of windings with two and three phases for $m\,q = 18/5$.

$\mathbf{m\,q = 20/3}$

The product $m\,q = 20/3$ allows combinations for $m = 2$ with $q = 10/3$ and $m = 5$ with $q = 4/3$. The graphs are shown in figure 6.54. Compared to the two phase winding, the five phase winding offers a significant reduction in harmonic scattering, especially at the points of multiples of $\sigma = 2$.

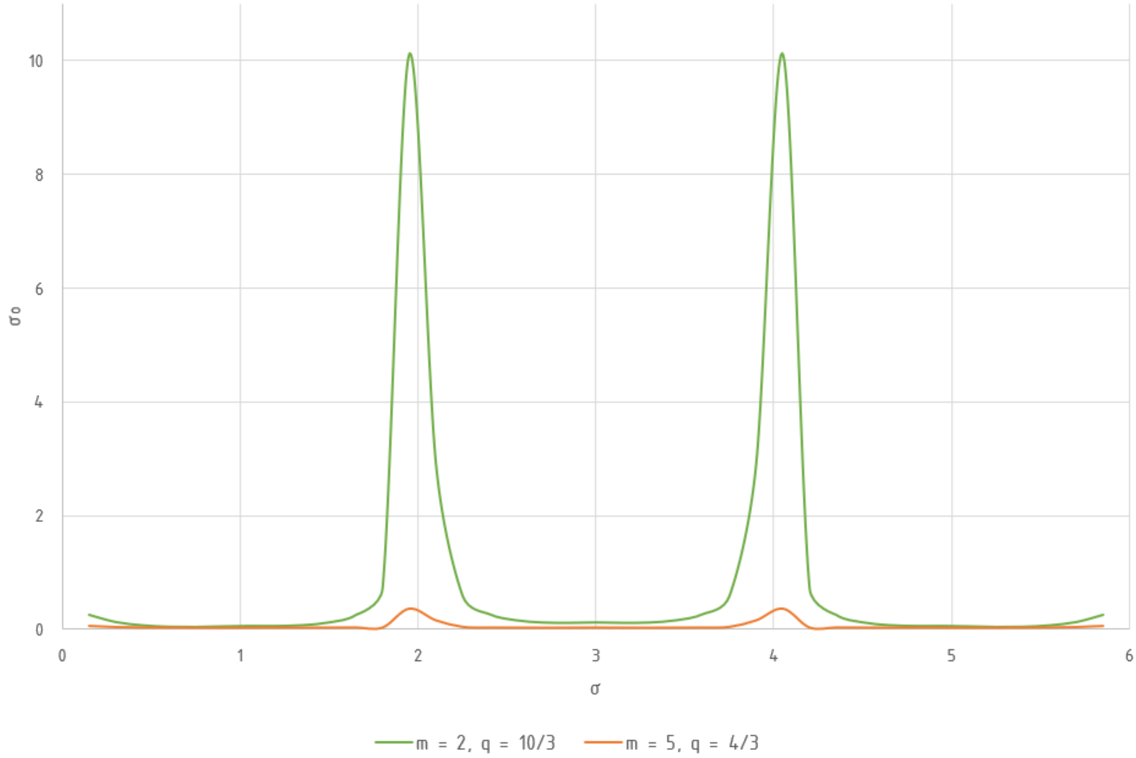

Figure 6.54: Correlation of the harmonic scattering coefficient σ_o of windings with two and five phases for $m\,q = 20/3$.

$\mathbf{m\,q = 15/2}$

The product $m\,q = 15/2$ allows combinations for $m = 3$ with $q = 5/2$ and $m = 5$ with $q = 3/2$, either with normal zone span or double zone span. The graphs are shown in figure 6.55. Whereas the variant with normal zone span has quite similar values of the harmonic scattering coefficients at pitches of $\sigma \approx 0,8$ and $\sigma \approx 1,2$, the same winding with double zone span has similar values at $\sigma \approx 1$. As in previous evaluations, σ_o is higher for windings with double zone span.

$\mathbf{m\,q = 28/3}$

The product $m\,q = 28/3$ allows combinations for $m = 2$ with $q = 14/3$ and $m = 7$ with $q = 4/3$. The graphs are shown in figure 6.56. Compared to the two phase winding, the seven phase winding offers a much stronger reduction of the peaks of the harmonic scattering at multiples of $\sigma = 2$ than five phase windings.

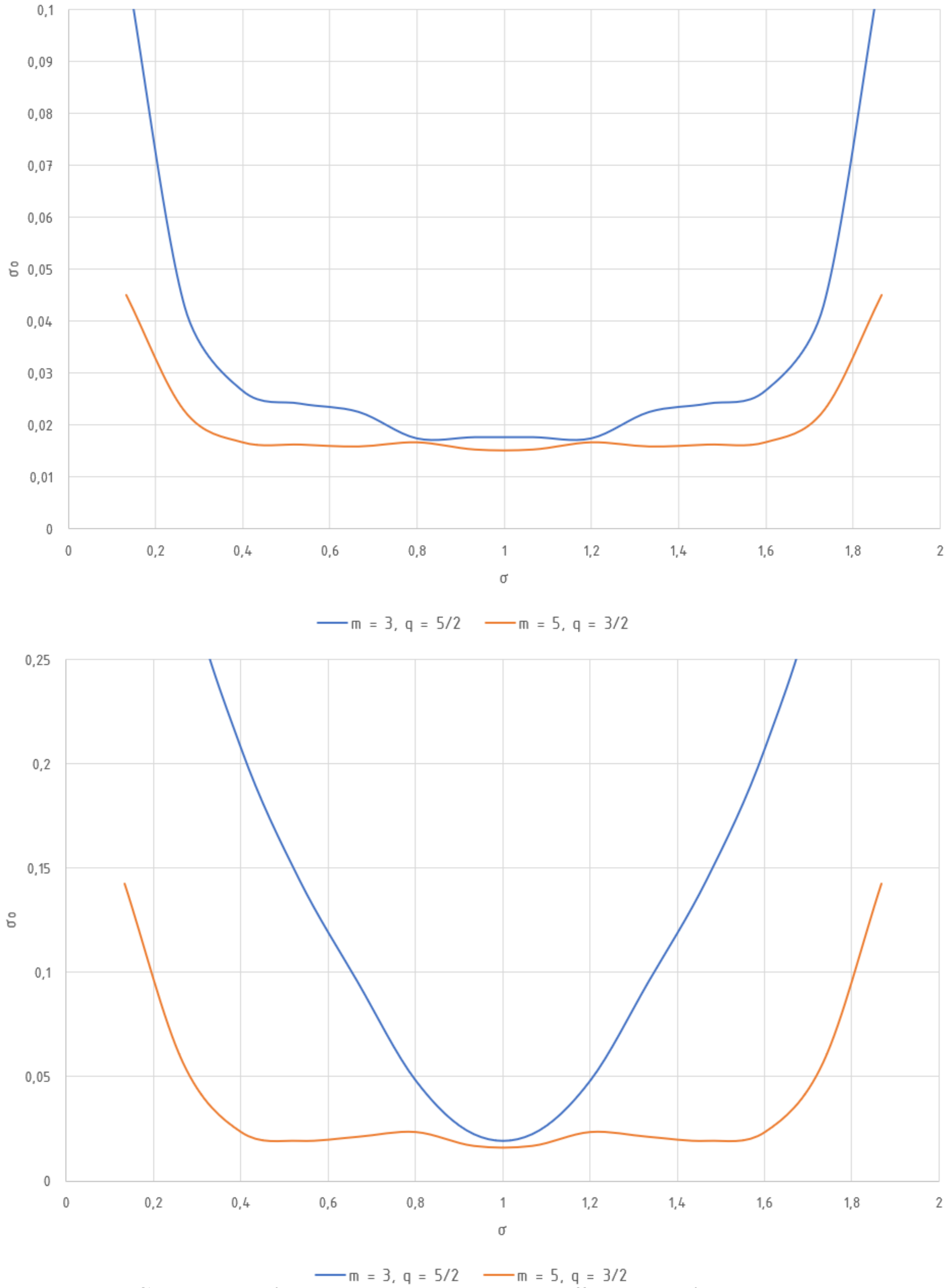

Figure 6.55: Correlation of the harmonic scattering coefficient σ_o of windings with normal zone span (top) and double zone span (bottom) and three and five phases for $m\,q = 15/2$.

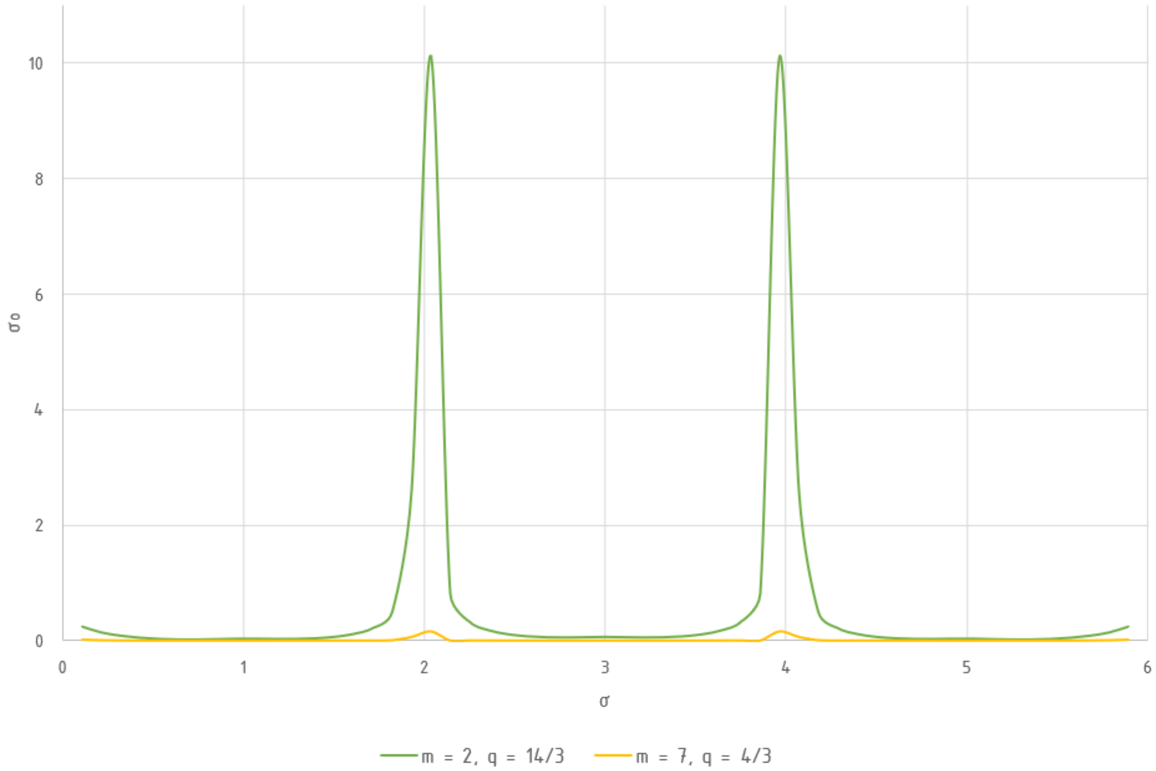

Figure 6.56: Correlation of the harmonic scattering coefficient σ_o of windings with two and seven phases for $m\,q = 28/3$.

$\mathbf{m\,q = 21/2}$

The product $m\,q = 21/2$ allows combinations for $m = 3$ with $q = 7/2$ and $m = 7$ with $q = 3/2$, either with normal zone span or double zone span. The graphs are shown in figure 6.57. The results are quite similar to $m\,q = 15/2$ and a lower harmonic scattering for the seven phase armature winding.

$\mathbf{m\,q = 105/2}$

The product $m\,q = 105/2$ allows combinations for $m = 5$ with $q = 21/2$ and $m = 7$ with $q = 15/2$, either with normal zone span or double zone span. The graphs are shown in figure 6.58. This comparison allows a fine scaling of the diagrams due to the low values of the harmonic scattering. Obviously, the courses for normal zone span (top of figure 6.58) show that the harmonic scattering of the seven phase winding is not always smaller for each pitch σ than that of the five phase winding. It is around the pitch of approximately $\sigma = 0,2$, $\sigma = 0,9$, $\sigma = 1,1$ and $\sigma = 1,8$.

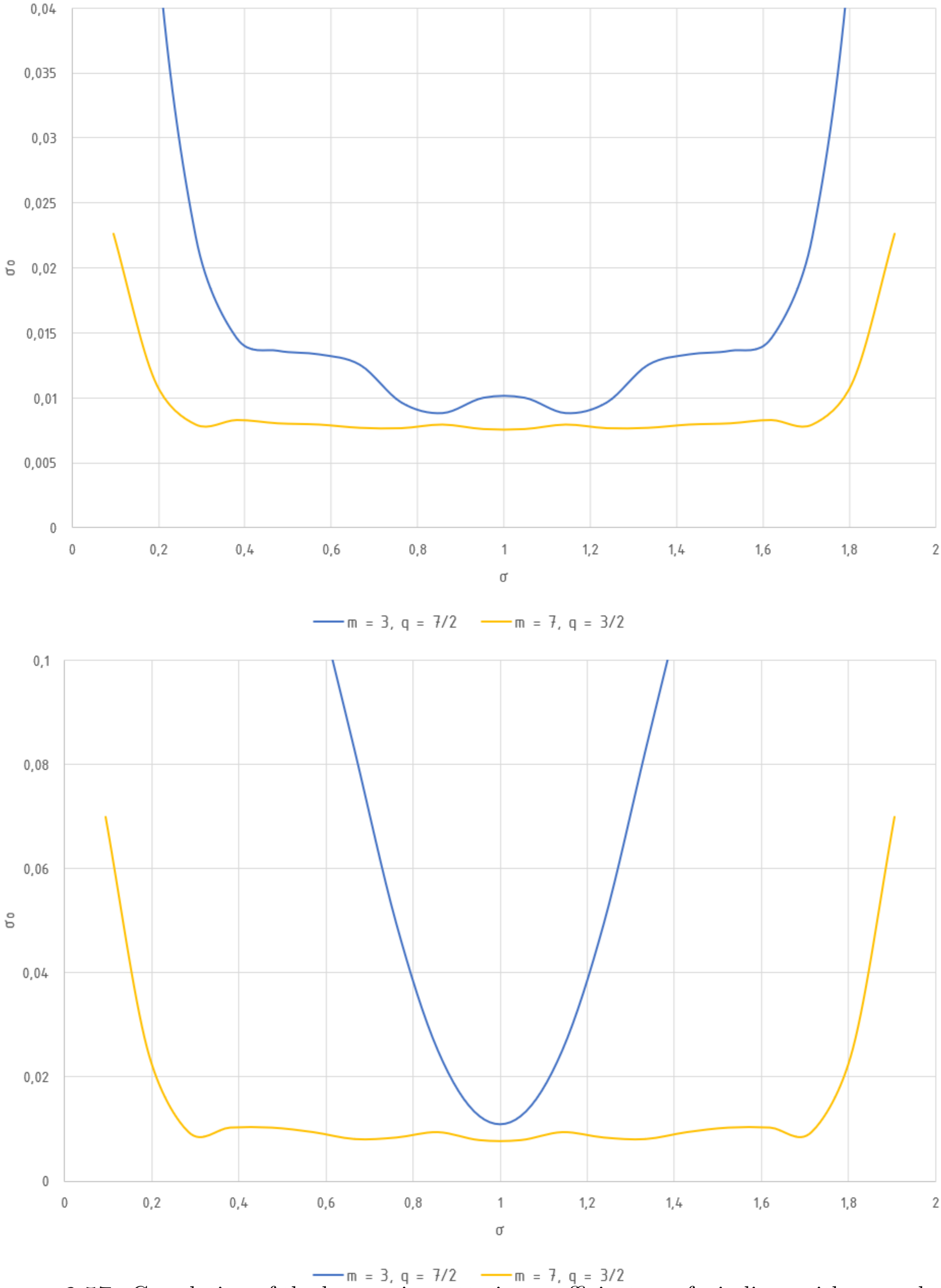

Figure 6.57: Correlation of the harmonic scattering coefficient σ_o of windings with normal zone span (top) and double zone span (bottom) and three and seven phases for $m\,q = 21/2$.

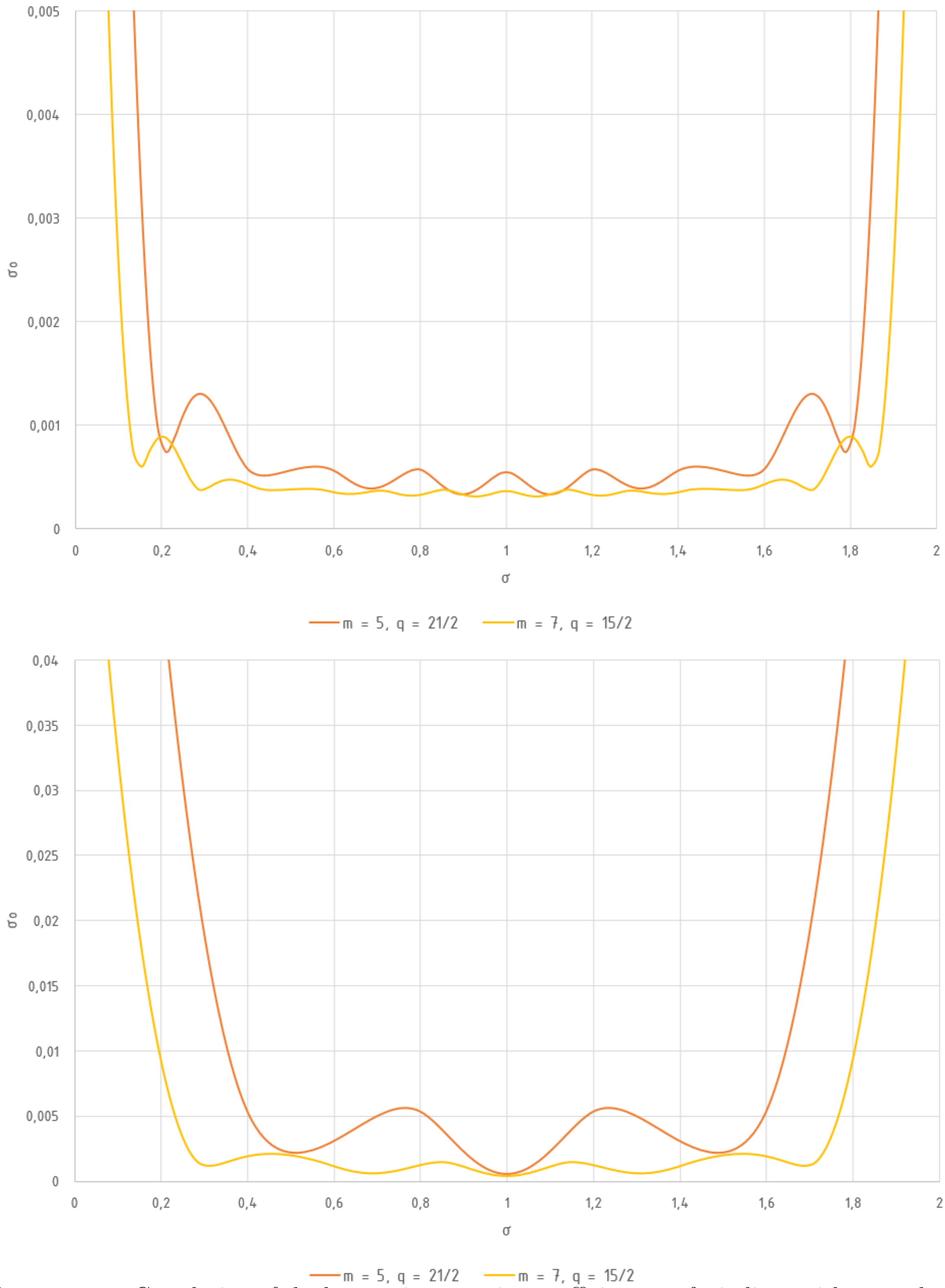

Figure 6.58: Correlation of the harmonic scattering coefficient σ_o of windings with normal zone span (top) and double zone span (bottom) and five and seven phases for $m\,q = 105/2$.

6.3 Tooth Coil Windings

Finally, selected double layer tooth coil windings are also investigated. The conditions laid down in chapter 2.5.4 shall be fulfilled for the realization of a coil as a tooth coil winding. The evaluation was also carried out again for the phase numbers $m = \{2, 3, 5, 7\}$, each for three slot numbers, which allow the calculation of the winding factor using the algorithm for fractional slot windings from chapter 5.2. A treatise on the winding factors of tooth coil windings using the finite elements method can be found in Maier et al. (2005). This approach is not considered further in this thesis.

Conversely, the advantage of the simple production of tooth coils is offset by large values of harmonic wave scattering (as shown in previous evaluations, the smaller the number of slots per pole and phase, the larger the harmonic scattering). Due to the fixed coil step of $y_\sigma = 1$ each number of slots per pole and phase q automatically has a fixed value of the pitch σ. The following treatise contain results of selected double layer tooth coil windings with respect to number of slots per pole and phase q as well as the corresponding values of the winding factor of the fundamental wave ξ_1 and the harmonic scattering coefficient σ_o. For some values of q there are also figures of the *Tingley-Scheme* of a base winding and the slot star and from which connections the *Görges Polygon* and its circulations can be derived. As the coil sides of a double layer tooth coil winding lie next to each other within a slot, RS describes the right coil side of a slot and LS the left coil side.

Winding with two Phases

Evaluated harmonic scattering coefficients for eight commonly used tooth coil windings for a number of phases $m = 2$ are shown in table 6.5. A detailed consideration is given to the number of slots per pole and phase $q = 5/7$. In addition to the *Tingley-Scheme* (figure 6.59) and the slot star, the *Görges Polygon* (figure 6.60) is also depicted.

Table 6.5: Evaluation of harmonic scattering coefficients of common tooth coil windings with $m = 2$.

q	σ	ξ_1	σ_o
2/3	3/4	0,853553	0,428769
2/5	5/4	0,853553	4,291739
3/5	5/6	0,879653	1,091371
3/7	7/6	0,879653	3,099087
4/7	7/8	0,888716	1,242336
5/7	7/10	0,805496	0,677071
4/9	9/8	0,888716	2,953833
5/9	9/10	0,892899	1,456665

	1	2	3	4	5	6	7	8	9	10
RS	-1	-2	1	-1	-2	2	-1	-2	2	-1
LS	1	1	2	-1	1	2	-2	1	2	-2

Figure 6.59: *Tingley-Scheme* of a tooth coil winding with $m = 2$ and $q = 5/7$.

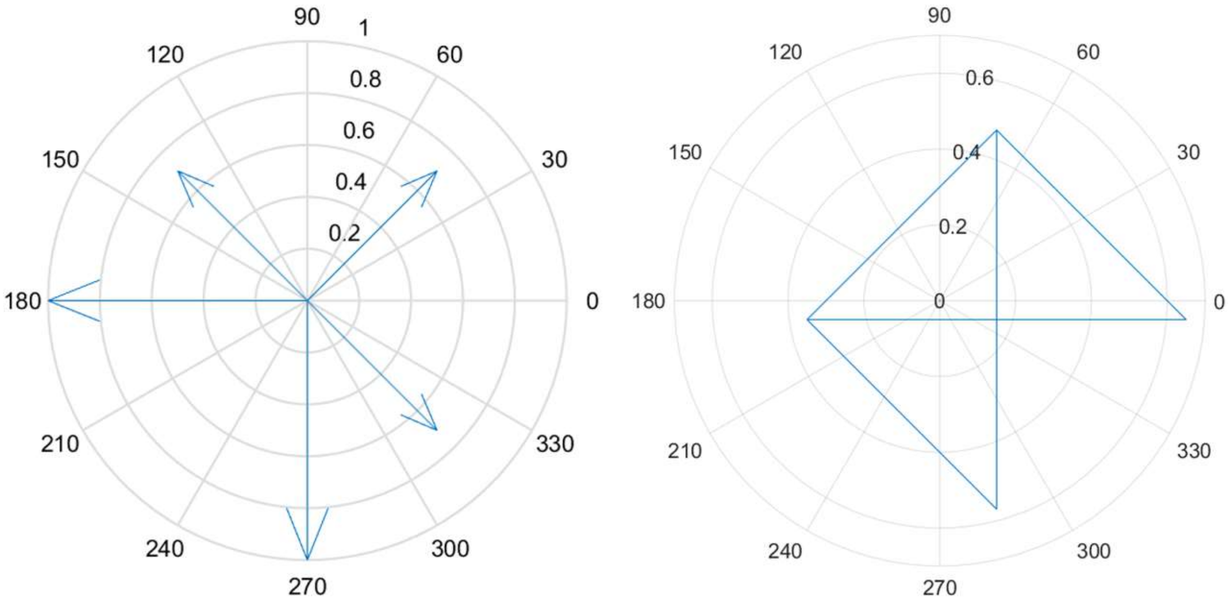

Figure 6.60: Slot star (left) and *Görges Polygon* (right) of a tooth coil winding with $m = 2$ and $q = 5/7$.

Winding with three Phases

Evaluated harmonic scattering coefficients for seven commonly used tooth coil windings for a number of phases $m = 3$ are shown in table 6.6. A detailed consideration is given to the number of slots per pole and phase $q = 1/4$ and $2/5$. In addition to the *Tingley-Scheme* (figures 6.61 and 6.63) and the slot star, the *Görges Polygon* (figures 6.62 and 6.64) is also depicted.

	1	2	3
RS	-1	-3	-2
LS	2	1	3

Figure 6.61: *Tingley-Scheme* of a tooth coil winding with $m = 3$ and $q = 1/4$.

Table 6.6: Evaluation of harmonic scattering coefficients of common tooth coil windings with $m = 3$.

$\mathbf{q}$	σ	ξ_1	σ_o
1/2	2/4	0,866025	0,462164
1/4	4/3	0,866025	4,848654
2/5	5/6	0,933013	0,749644
2/7	7/6	0,933013	2,857964
3/7	7/9	0,901912	0,834941
3/8	8/9	0,945214	1,182101
3/10	10/9	0,945214	2,409532

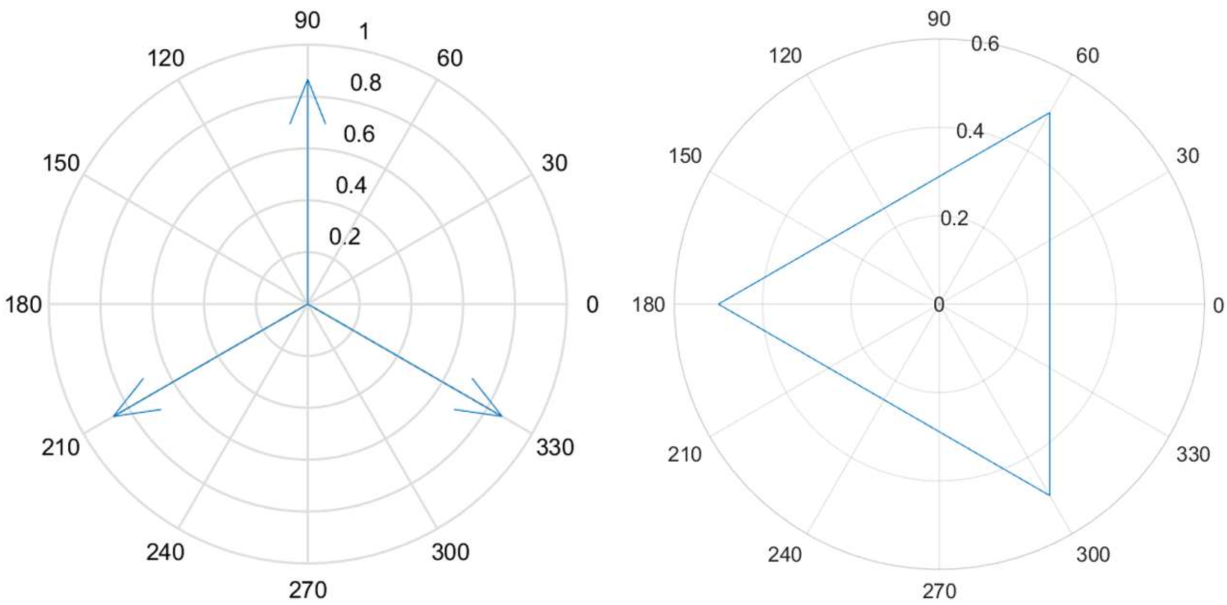

Figure 6.62: Slot star (left) and *Görges Polygon* (right) of a tooth coil winding with $m = 3$ and $q = 1/4$.

	1	2	3	4	5	6
RS	-1	-2	2	3	-3	-1
LS	1	1	2	-2	-3	3

Figure 6.63: *Tingley-Scheme* of a tooth coil winding with $m = 3$ and $q = 2/5$.

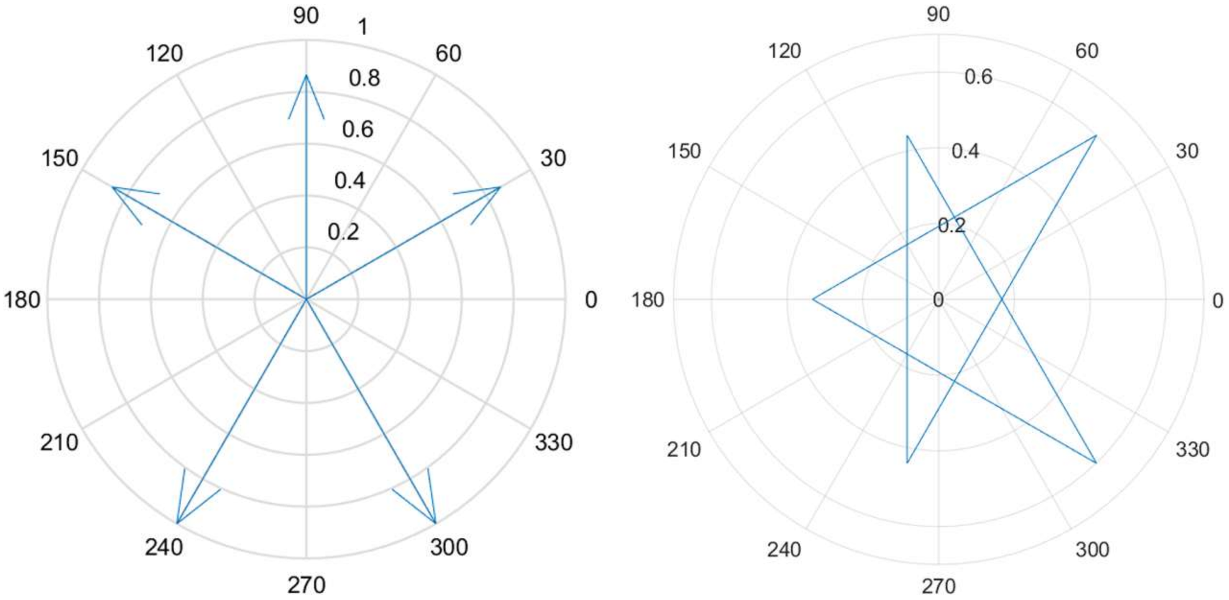

Figure 6.64: Slot star (left) and *Görges Polygon* (right) of a tooth coil winding with $m = 3$ and $q = 2/5$.

Winding with five Phases

Evaluated harmonic scattering coefficients for six commonly used tooth coil windings for a number of phases $m = 5$ are shown in table 6.7. A detailed consideration is given to the number of slots per pole and phase $q = 2/7$. In addition to the *Tingley-Scheme* (figure 6.65) and the slot star, the *Görges Polygon* (figure 6.66) is also depicted.

Table 6.7: Evaluation of harmonic scattering coefficients of common tooth coil windings with $m = 5$.

q	σ	ξ_1	σ_o
1/4	4/5	0,551057	0,745851
1/6	6/5	0,951057	2,928164
2/7	7/10	0,880037	0,528150
2/9	9/10	0,975528	1,016120
2/11	11/10	0,975528	2,137223
3/11	11/15	0,900237	0,626185

	1	2	3	4	5	6	7	8	9	10
RS	-1	5	2	-1	-3	2	4	-3	-5	4
LS	-4	1	-5	-2	1	3	-2	-4	3	5

Figure 6.65: *Tingley-Scheme* of a tooth coil winding with $m = 5$ and $q = 2/7$.

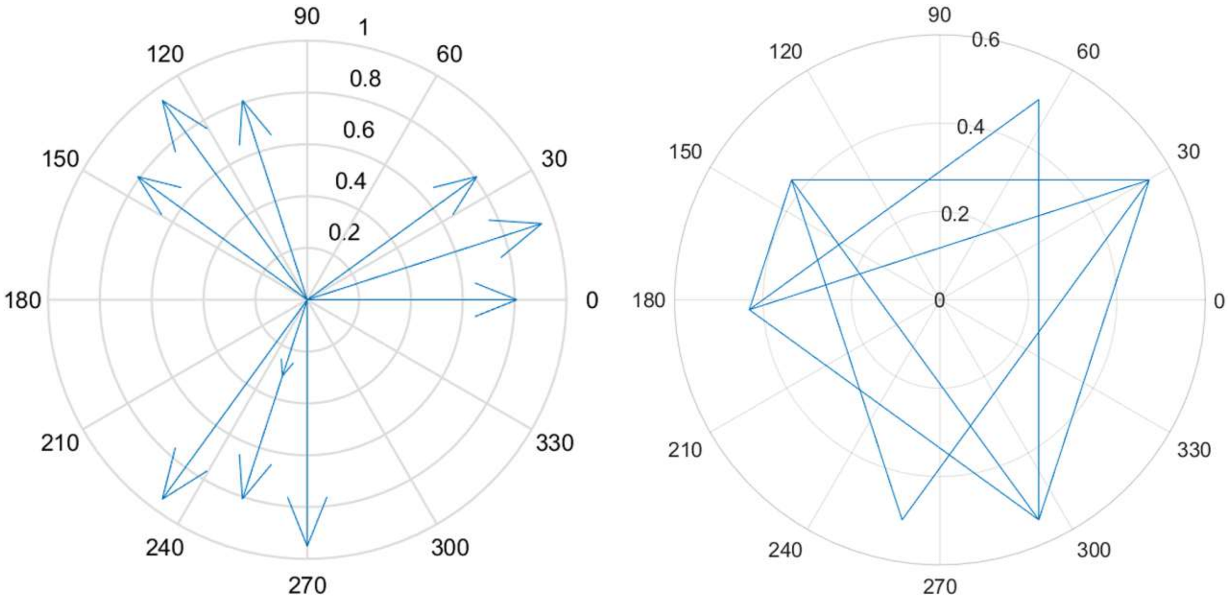

Figure 6.66: Slot star (left) and *Görges Polygon* (right) of a tooth coil winding with $m = 5$ and $q = 2/7$.

Winding with seven Phases

Evaluated harmonic scattering coefficients for five commonly used tooth coil windings for a number of phases $m = 7$ are shown in table 6.8. A detailed consideration is given to the number of slots per pole and phase $q = 2/11$. In addition to the *Tingley-Scheme* (figure 6.67) and the slot star, the *Görges Polygon* (figure 6.68) is also depicted.

Table 6.8: Evaluation of harmonic scattering coefficients of common tooth coil windings with $m = 7$.

q	σ	ξ_1	σ_o
1/5	5/7	0,551057	0,511840
1/6	6/7	0,951057	0,907222
1/8	8/7	0,880037	2,390616
1/9	9/7	0,975528	3,898362
2/11	11/14	0,975528	0,714343

	1	2	3	4	5	6	7	8	9	10	11	12	13	14
RS	-1	7	3	-2	-5	4	7	-6	-2	1	4	-3	-6	5
LS	-5	1	-7	-3	2	5	-4	-7	6	2	-1	-4	3	6

Figure 6.67: *Tingley-Scheme* of a tooth coil winding with $m = 7$ and $q = 2/11$.

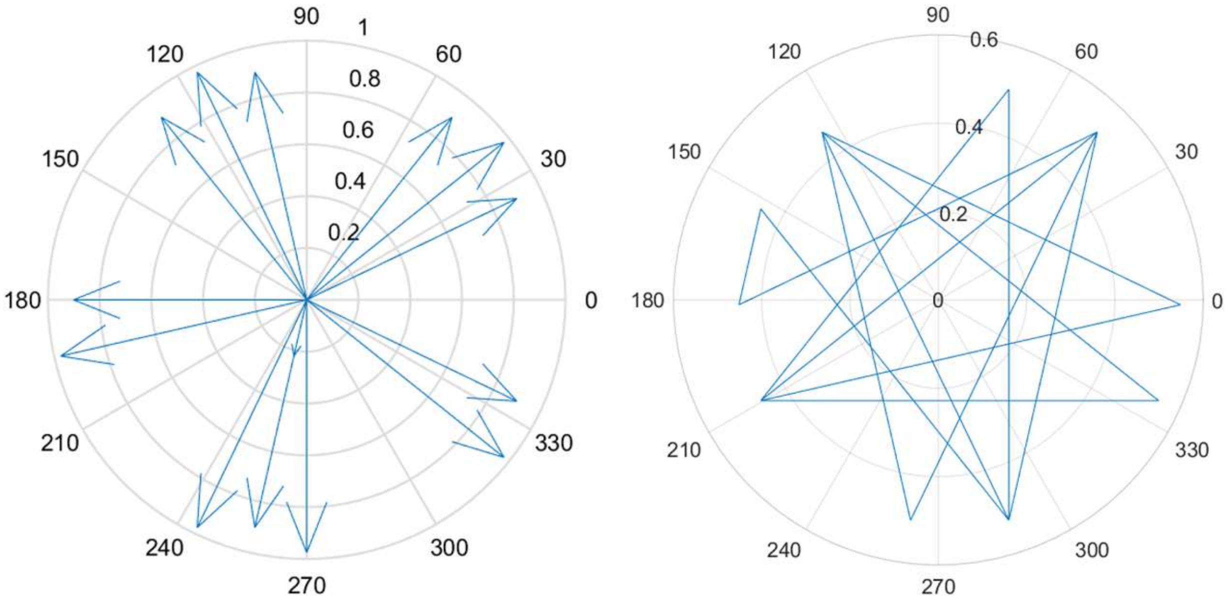

Figure 6.68: Slot star (left) and *Görges Polygon* (right) of a tooth coil winding with $m = 7$ and $q = 2/11$.

7 Conclusion

The presented work deals with the mathematical formulation of the harmonic scattering of electric machines. The main focus is set on windings for arbitrarily odd numbered phase systems. Due to their practical interest, windings of two phase systems are discussed as well. The aim was to establish a general and analytical way for describing such windings. This applies in particular to integer slot windings. For fractional slot windings only an algorithmic path was introduced.

On the basis of the fundamentals related to harmonic scattering, the basic possibilities for the design of alternating current armature windings are discussed. Particular attention is given to the terms of the number of layers, zone span, number of slots per pole and phase as well as coil pitch. In addition, an introduction to the distribution of the magnetomotive force along the air-gap of electrical machines and statements to the voltage phasor diagram within the windings are given.

In a separate chapter, the composition of the winding factor is thematized, which provides a significant proportion for harmonic scattering. Starting from a general definition, the coil voltages are described in dependence of the type and design of the winding, such as integer or fractional slot windings. Separate approaches in the mathematical formulation yield the winding factor also as far as harmonics are concerned. For the composition of the winding factor, the concepts such as the pitch factor, group factor and zone factor are introduced. In application of this thesis, the winding factor of the fundamental wave was always of interest for the further calculations of the work.

For the mathematical formulation of the harmonic scattering coefficient, several approaches from literature were compared and described in a uniform nomenclature. In addition to the already existing solutions in literature for selected short pitching areas for two phase and three phase windings, a generalized approach based on the *Görges Polygon* of the magnetomotive force in the slots is established. This is valid for all integer slot windings with odd phase numbers and for two phase windings, too. The formal connections are also usable for non-integer shortening steps of coils, which occur often in the design of ironless machines.

For the kind of fractional slot windings, an algorithmic solution method is used to determine the harmonic scattering coefficients. Using predefined values such as number of phases, zone span, number of slots per pole and phase as well as coil step, the algorithm determines the complex magnetomotive force of the slots based on the phase locations calculated by the *Tingley-Scheme*. This makes it easy to specify the *Görges Polygon*, which in turn is the prerequisite for calculating the harmonic scattering.

In the course of an evaluation, the odd numbers of phases three, five and seven were investigated as well as the even number of two phases due to the fairly wide usage in practice. In addition to the evaluation of the harmonic scattering for certain slot numbers, the corresponding, theoretically feasible pitch range was also investigated in the case of double layer windings. In order to be able to make comparisons between the different phase numbers with regard to the total number of slots, diagrams of integer slot windings and fractional slot windings were given for a constant value of the slots per base distribution. Finally, harmonic scattering coefficients for selected tooth coil windings with two and three phases were calculated via the algorithm.

When considering the results it became clear that a large number of slots per pole and phase on the one hand and an increase of the number of phases on the other hand have a significant effect on the reduction of the harmonic scattering. In the case of integer slot windings there are lower values of the harmonic scattering compared to fractional slot windings with a comparable total number of slots. Double layer fractional slot windings have the property that the coil sides of the upper layer are shifted to those of the lower layer precisely to an angle corresponding to one pole pitch. Considering the entire winding, this results in a greatly improved form of the induced voltages, which are quite similar to a time-harmonic shape. For this reason fractional slot windings are often preferred for generators despite the higher harmonic scattering. The special form of tooth coil windings as part of fractional slot windings is often used in machines with a relatively high number of poles, in particular with permanent magnet excited synchronous machines. Here, the disadvantage of the very strong harmonic scattering can be seen clearly.

The topic of harmonic scattering is receiving increasing attention in the design and pre-calculations of electric machines today. In addition to efficiency, it also manifests itself in the smooth running, e.g. resulting in reduced vibration torques, and above all in the noise environment of a poly-phase machine, especially important in vehicle drives. A correspondingly low harmonic scattering, possibly by machines with windings that have the possibility of switchable phase numbers, should have a positive influence on these parameters. The relationships in the field of harmonic scattering established in this thesis therefore form a basis for further considerations.

A Appendix

A.1 Harmonic Scattering Coeffficients of Double Layer Integer Slot Windings

The colors in the following list represent several pitching ranges:

normal zone span	double zone span
$0 \le y_\varepsilon \le q$	$0 \le y_\varepsilon \le q$
$q \le y_\varepsilon \le 2q$	$q \le y_\varepsilon \le 3q$
$2q \le y_\varepsilon \le 3q$	$3q \le y_\varepsilon \le 5q$
$3q \le y_\varepsilon \le 4q$	$5q \le y_\varepsilon \le 7q$
$4q \le y_\varepsilon \le 5q$	
$5q \le y_\varepsilon \le 6q$	
$6q \le y_\varepsilon \le 7q$	

The second list provides an overview of the tables with the harmonic scattering coefficients:

m	normal zone span	double zone span
2	A.1	-
3	A.2	A.5
5	A.3	A.6
7	A.4	A.7

Table A.1: Harmonic scattering coefficients σ_o for integer slot windings with $m = 2$ and normal zone span.

	q										
$\mathbf{y}_\varepsilon$	**1**	**2**	**3**	**4**	**5**	**6**	**7**	**8**	**9**	**10**	∞
0	0,233701	0,084028	0,046802	0,033008	0,026487	0,022908	0,020738	0,019324	0,018352	0,017656	0,014678
1	0,233701	0,058348	0,033383	0,025068	0,021289	0,019255	0,018034	0,017244	0,016704	0,016318	0,014678
2		0,084028	0,028437	0,017706	0,014695	0,013748	0,013477	0,013449	0,013511	0,013602	0,014678
3		0,233701	0,046802	0,018778	0,011567	0,009621	0,009323	0,009575	0,009997	0,010448	0,014678
4			0,101897	0,033008	0,014804	0,008896	0,007058	0,006749	0,007037	0,007546	0,014678
5			0,233701	0,064882	0,026487	0,012959	0,007711	0,005769	0,005266	0,005412	0,014678
6				0,122199	0,048621	0,022908	0,012055	0,007231	0,005163	0,004440	0,014678
7				0,233701	0,083959	0,039806	0,020738	0,011610	0,007105	0,004939	0,014678
8					0,138184	0,064946	0,034391	0,019324	0,011408	0,007165	0,014678
9					0,233701	0,100354	0,053732	0,030777	0,018352	0,011337	0,014678
10						0,150493	0,079725	0,046411	0,028216	0,017656	0,014678
11						0,233701	0,113968	0,066770	0,041292	0,026319	0,014678
12							0,160122	0,092618	0,057920	0,037531	0,014678
13							0,233701	0,125267	0,078536	0,051521	0,014678
14								0,167814	0,103767	0,068565	0,014678
15								0,233701	0,134722	0,089021	0,014678
16									0,174080	0,113422	0,014678
17									0,233701	0,142720	0,014678
18										0,179275	0,014678
19										0,233701	0,014678

Table A.2: Harmonic scattering coefficients σ_o for integer windings with $m = 3$ and normal zone span.

	q										
y$_\varepsilon$	**1**	**2**	**3**	**4**	**5**	**6**	**7**	**8**	**9**	**10**	**∞**
0	0,096623	0,028437	0,014061	0,008896	0,006481	0,005163	0,004366	0,003848	0,003493	0,003238	0,002151
1	0,096623	0,023542	0,011495	0,007375	0,005485	0,004463	0,003848	0,003450	0,003177	0,002982	0,002151
2	0,096623	0,028437	0,011090	0,006239	0,004366	0,003490	0,003025	0,002755	0,002587	0,002477	0,002151
3		0,028437	0,014061	0,006885	0,004114	0,002929	0,002382	0,002117	0,001987	0,001925	0,002151
4		0,028437	0,014290	0,008896	0,004995	0,003107	0,002200	0,001763	0,001559	0,001473	0,002151
5		0,096623	0,013736	0,009249	0,006481	0,003998	0,002577	0,001814	0,001417	0,001222	0,002151
6			0,014061	0,008896	0,006871	0,005163	0,003414	0,002280	0,001607	0,001226	0,002151
7			0,036492	0,008297	0,006694	0,005554	0,004366	0,003047	0,002104	0,001497	0,002151
8			0,096623	0,008896	0,006219	0,005493	0,004743	0,003848	0,002802	0,001997	0,002151
9				0,020618	0,005743	0,005163	0,004757	0,004207	0,003493	0,002632	0,002151
10				0,045903	0,006481	0,004695	0,004537	0,004268	0,003832	0,003238	0,002151
11				0,096623	0,013976	0,004367	0,004168	0,004128	0,003924	0,003558	0,002151
12					0,028906	0,005163	0,003752	0,003848	0,003841	0,003670	0,002151
13					0,053300	0,010520	0,003555	0,003485	0,003633	0,003630	0,002151
14					0,096623	0,020688	0,004366	0,003135	0,003336	0,003476	0,002151
15						0,036276	0,008471	0,003045	0,002998	0,003238	0,002151
16						0,058974	0,015980	0,003848	0,002714	0,002945	0,002151
17						0,096623	0,027135	0,007145	0,002708	0,002641	0,002151
18							0,042463	0,012991	0,003493	0,002419	0,002151
19							0,063396	0,021500	0,006232	0,002479	0,002151
20							0,096623	0,032889	0,010956	0,003238	0,002151
21								0,047615	0,017727	0,005572	0,002151
22								0,066917	0,026651	0,009499	0,002151
23								0,096623	0,037919	0,015054	0,002151
24									0,051931	0,022295	0,002151

Continued from table A.2.

					q						
$\mathbf{y}_\varepsilon$	**1**	**2**	**3**	**4**	**5**	**6**	**7**	**8**	**9**	**10**	∞
25									0,069778	0,031319	0,002151
26									0,096623	0,042296	0,002151
27										0,055580	0,002151
28										0,072144	0,002151
29										0,096623	0,002151

Table A.3: Harmonic scattering coefficients σ_o for integer slot windings with $m = 5$ and normal zone span.

	q										
y_ε	**1**	**2**	**3**	**4**	**5**	**6**	**7**	**8**	**9**	**10**	**∞**
0	0,033558	0,008900	0,004115	0,002424	0,001639	0,001211	0,000953	0,000786	0,000671	0,000588	0,000238
1	0,033558	0,008281	0,003790	0,002231	0,001512	0,001122	0,000887	0,000735	0,000630	0,000556	0,000238
2	0,033558	0,008900	0,003772	0,002105	0,001380	0,001005	0,000787	0,000649	0,000557	0,000493	0,000238
3	0,033558	0,008430	0,004115	0,002210	0,001369	0,000948	0,000715	0,000575	0,000486	0,000427	0,000238
4	0,033558	0,008900	0,003885	0,002424	0,001491	0,000988	0,000707	0,000542	0,000441	0,000376	0,000238
5		0,008900	0,003835	0,002298	0,001639	0,001102	0,000767	0,000562	0,000435	0,000354	0,000238
6		0,008900	0,004115	0,002182	0,001563	0,001211	0,000869	0,000629	0,000470	0,000365	0,000238
7		0,010709	0,004135	0,002237	0,001454	0,001163	0,000953	0,000718	0,000536	0,000408	0,000238
8		0,008900	0,004091	0,002424	0,001422	0,001071	0,000921	0,000786	0,000615	0,000472	0,000238
9		0,033558	0,004115	0,002455	0,001501	0,001011	0,000846	0,000764	0,000671	0,000541	0,000238
10			0,004954	0,002424	0,001639	0,001022	0,000781	0,000702	0,000656	0,000588	0,000238
11			0,005276	0,002382	0,001673	0,001104	0,000757	0,000639	0,000605	0,000578	0,000238
12			0,004115	0,002424	0,001656	0,001211	0,000789	0,000601	0,000547	0,000536	0,000238
13			0,011714	0,002923	0,001619	0,001245	0,000866	0,000601	0,000503	0,000484	0,000238
14			0,033558	0,003357	0,001589	0,001239	0,000953	0,000642	0,000485	0,000439	0,000238
15				0,003158	0,001211	0,000986	0,000712	0,000712	0,000499	0,000410	0,000238
16				0,002424	0,001980	0,001177	0,000986	0,000786	0,000543	0,000407	0,000238
17				0,006142	0,002356	0,001159	0,000967	0,000817	0,000607	0,000429	0,000238
18				0,015133	0,002474	0,001211	0,000938	0,000822	0,000671	0,000475	0,000238
19				0,033558	0,002120	0,001465	0,000910	0,000809	0,000701	0,000533	0,000238
20					0,001639	0,001777	0,000901	0,000786	0,000708	0,000588	0,000238
21					0,003875	0,001980	0,000953	0,000758	0,000700	0,000617	0,000238
22					0,009047	0,001917	0,001154	0,000736	0,000682	0,000626	0,000238
23					0,017832	0,001538	0,001413	0,000735	0,000659	0,000621	0,000238
24					0,033558	0,001211	0,001629	0,000786	0,000635	0,000608	0,000238

Continued from table A.3.

						q					
y_ε	**1**	**2**	**3**	**4**	**5**	**6**	**7**	**8**	**9**	**10**	**∞**
25						0,002725	0,001697	0,000950	0,000618	0,000588	0,000238
26						0,006154	0,001539	0,001169	0,000621	0,000566	0,000238
27						0,011691	0,001180	0,001375	0,000671	0,000546	0,000238
28						0,019903	0,000953	0,001497	0,000809	0,000534	0,000238
29						0,033558	0,002058	0,001473	0,000996	0,000541	0,000238
30							0,004525	0,001269	0,001186	0,000588	0,000238
31							0,008426	0,000945	0,001328	0,000708	0,000238
32							0,013928	0,000786	0,001376	0,000870	0,000238
33							0,021515	0,001635	0,001292	0,001043	0,000238
34							0,033558	0,003508	0,001071	0,001189	0,000238
35								0,006437	0,000784	0,001273	0,000238
36								0,010484	0,000671	0,001265	0,000238
37								0,015797	0,001349	0,001144	0,000238
38								0,022798	0,002827	0,000920	0,000238
39								0,033558	0,005120	0,000668	0,000238
40									0,008257	0,000588	0,000238
41									0,012296	0,001147	0,000238
42									0,017365	0,002348	0,000238
43									0,023839	0,004199	0,000238
44									0,033558	0,006716	0,000238
45										0,009925	0,000238
46										0,013878	0,000238
47										0,018691	0,000238
48										0,024700	0,000238
49										0,033558	0,000238

Table A.4: Harmonic scattering coefficients σ_o for integer slot windings with $m = 7$ and normal zone span.

	q										
y_ε	**1**	**2**	**3**	**4**	**5**	**6**	**7**	**8**	**9**	**10**	**∞**
0	0,016955	0,004369	0,001982	0,001142	0,000752	0,000541	0,000413	0,000330	0,000273	0,000233	0,000059
1	0,016955	0,004209	0,001897	0,001092	0,000720	0,000518	0,000396	0,000317	0,000263	0,000224	0,000059
2	0,016955	0,004369	0,001895	0,001061	0,000686	0,000488	0,000370	0,000295	0,000244	0,000208	0,000059
3	0,016955	0,004227	0,001982	0,001089	0,000685	0,000474	0,000352	0,000276	0,000226	0,000191	0,000059
4	0,016955	0,004369	0,001909	0,001142	0,000717	0,000486	0,000351	0,000269	0,000215	0,000179	0,000059
5	0,016955	0,001902	0,001902	0,001100	0,000752	0,000515	0,000368	0,000275	0,000214	0,000174	0,000059
6	0,016955	0,004369	0,001982	0,001070	0,000726	0,000541	0,000394	0,000292	0,000224	0,000177	0,000059
7		0,004369	0,001934	0,001092	0,000695	0,000523	0,000413	0,000315	0,000241	0,000189	0,000059
8		0,004369	0,001924	0,001142	0,000691	0,000496	0,000400	0,000315	0,000241	0,000189	0,000059
9		0,004617	0,001982	0,001116	0,000718	0,000482	0,000378	0,000321	0,000273	0,000222	0,000059
10		0,004369	0,001985	0,001092	0,000752	0,000489	0,000360	0,000302	0,000266	0,000205	0,000059
11		0,005529	0,001977	0,001104	0,000738	0,000515	0,000357	0,000284	0,000250	0,000227	0,000059
12		0,004369	0,001982	0,001142	0,000715	0,000541	0,000370	0,000276	0,000233	0,000213	0,000059
13		0,016955	0,002105	0,001148	0,000708	0,000532	0,000393	0,000279	0,000222	0,000198	0,000059
14			0,002124	0,001142	0,000725	0,000513	0,000413	0,000294	0,000220	0,000186	0,000059
15			0,001982	0,001134	0,000752	0,000500	0,000407	0,000314	0,000227	0,000180	0,000059
16			0,002496	0,001142	0,000759	0,000502	0,000392	0,000330	0,000242	0,000182	0,000059
17			0,002743	0,001218	0,000756	0,000519	0,000378	0,000326	0,000260	0,000191	0,000059
18			0,001982	0,001268	0,000749	0,000541	0,000373	0,000314	0,000273	0,000205	0,000059
19			0,005787	0,001225	0,000744	0,000547	0,000380	0,000301	0,000271	0,000221	0,000059
20			0,016955	0,001142	0,000752	0,000546	0,000395	0,000292	0,000261	0,000233	0,000059
21				0,001432	0,000805	0,000541	0,000413	0,000292	0,000249	0,000231	0,000059
22				0,001731	0,000854	0,000535	0,000420	0,000301	0,000239	0,000223	0,000059
23				0,001643	0,000858	0,000532	0,000419	0,000315	0,000235	0,000212	0,000059
24				0,001142	0,000804	0,000541	0,000416	0,000330	0,000238	0,000202	0,000059

Continued from table A.4.

											q
y_ε	**1**	**2**	**3**	**4**	**5**	**6**	**7**	**8**	**9**	**10**	∞
25				0,002966	0,000752	0,000581	0,000410	0,000336	0,000247	0,000196	0,000059
26				0,007534	0,000941	0,000624	0,000405	0,000337	0,000261	0,000196	0,000059
27				0,016955	0,001190	0,000644	0,000404	0,000335	0,000273	0,000200	0,000059
28					0,001295	0,000625	0,000413	0,000330	0,000279	0,000210	0,000059
29					0,001098	0,000573	0,000445	0,000325	0,000281	0,000221	0,000059
30					0,000752	0,000541	0,000482	0,000321	0,000279	0,000233	0,000059
31					0,001828	0,000675	0,000507	0,000321	0,000275	0,000238	0,000059
32					0,004436	0,000874	0,000508	0,000330	0,000271	0,000240	0,000059
33					0,008915	0,001024	0,000480	0,000356	0,000267	0,000239	0,000059
34					0,016955	0,001012	0,000434	0,000388	0,000264	0,000236	0,000059
35						0,000790	0,000413	0,000415	0,000265	0,000233	0,000059
36						0,000541	0,000515	0,000425	0,000273	0,000229	0,000059
37						0,001254	0,000676	0,000415	0,000295	0,000225	0,000059
38						0,002970	0,000826	0,000383	0,000323	0,000223	0,000059
39						0,005782	0,000892	0,000349	0,000225	0,000225	0,000059
40						0,009975	0,000816	0,000330	0,000364	0,000233	0,000059
41						0,016955	0,000599	0,000410	0,000364	0,000252	0,000059
42							0,000413	0,000543	0,000347	0,000276	0,000059
43							0,000924	0,000681	0,000316	0,000300	0,000059
44							0,002148	0,000776	0,000282	0,000317	0,000059
45							0,004121	0,000783	0,000273	0,000324	0,000059
46							0,006923	0,000674	0,000339	0,000317	0,000059
47							0,010800	0,000472	0,000450	0,000297	0,000059
48							0,016955	0,000330	0,000573	0,000266	0,000059
49								0,000716	0,000676	0,000238	0,000059
50								0,001638	0,000725	0,000233	0,000059

Continued from table A.4.

	q										
y_ε	**1**	**2**	**3**	**4**	**5**	**6**	**7**	**8**	**9**	**10**	**∞**
51								0,003112	0,000691	0,000288	0,000059
52								0,005168	0,000567	0,000382	0,000059
53								0,007878	0,000384	0,000492	0,000059
54								0,011457	0,000273	0,000593	0,000059
55								0,016955	0,000577	0,000661	0,000059
56									0,001299	0,000673	0,000059
57									0,002447	0,000614	0,000059
58									0,004035	0,000485	0,000059
59									0,006091	0,000321	0,000059
60									0,008680	0,000233	0,000059
61									0,011989	0,000478	0,000059
62									0,016955	0,001060	0,000059
63										0,001983	0,000059
64										0,003253	0,000059
65										0,004884	0,000059
66										0,006899	0,000059
67										0,009358	0,000059
68										0,012430	0,000059
69										0,016955	0,000059

Table A.5: Harmonic scattering coefficients σ_o for integer slot windings with $m = 3$ and double zone span.

	q										
$\mathbf{y}_\varepsilon$	**1**	**2**	**3**	**4**	**5**	**6**	**7**	**8**	**9**	**10**	∞
0	0,096623	0,028437	0,014061	0,008896	0,006481	0,005163	0,004366	0,003848	0,003493	0,003238	0,002151
1	0,218470	0,049786	0,022860	0,013711	0,009523	0,007261	0,005901	0,005020	0,004417	0,003986	0,002151
2	0,462164	0,110059	0,048538	0,027932	0,018559	0,013511	0,010482	0,008522	0,007180	0,006222	0,002151
3		0,175357	0,087544	0,050662	0,033257	0,023762	0,018030	0,014308	0,011756	0,009931	0,002151
4		0,273303	0,126989	0,079477	0,052852	0,037696	0,028389	0,022293	0,018092	0,015078	0,002151
5		0,462164	0,173800	0,108195	0,075710	0,054705	0,041281	0,032331	0,026105	0,021611	0,002151
6			0,234510	0,139679	0,098405	0,073655	0,056226	0,044184	0,035663	0,029453	0,002151
7			0,319171	0,176346	0,122406	0,092453	0,072413	0,057475	0,046566	0,038487	0,002151
8			0,462164	0,220639	0,148945	0,111957	0,088472	0,071605	0,058513	0,048546	0,002151
9				0,275773	0,179147	0,132891	0,104946	0,085629	0,071051	0,059385	0,002151
10				0,348053	0,214168	0,155903	0,122303	0,099913	0,083501	0,070655	0,002151
11				0,462164	0,255399	0,181608	0,140957	0,114776	0,096121	0,081850	0,002151
12					0,304953	0,210639	0,161291	0,130502	0,109139	0,093161	0,002151
13					0,367442	0,243717	0,183680	0,147353	0,122760	0,104755	0,002151
14					0,462164	0,281794	0,208506	0,165577	0,137172	0,116786	0,002151
15						0,326434	0,236190	0,185416	0,152550	0,129394	0,002151
16						0,381271	0,267244	0,207120	0,169063	0,142708	0,002151
17						0,462164	0,302380	0,230955	0,186879	0,156854	0,002151
18							0,342833	0,257230	0,206169	0,171953	0,002151
19							0,391605	0,286333	0,227112	0,188123	0,002151
20							0,462164	0,318831	0,249909	0,205488	0,002151
21								0,355737	0,274800	0,224174	0,002151
22								0,399612	0,302094	0,244322	0,002151
23								0,462164	0,332254	0,266088	0,002151
24									0,366144	0,289664	0,002151

Continued from table A.5.

						q					
$\mathbf{y}_\varepsilon$	**1**	**2**	**3**	**4**	**5**	**6**	**7**	**8**	**9**	**10**	∞
25									0,405994	0,315305	0,002151
26									0,462164	0,343404	0,002151
27										0,374709	0,002151
28										0,411198	0,002151
29										0,462164	0,002151

Table A.6: Harmonic scattering coefficients σ_o for integer slot windings with $m = 5$ and double zone span.

	q										
y_ε	**1**	**2**	**3**	**4**	**5**	**6**	**7**	**8**	**9**	**10**	∞
0	0,033558	0,008900	0,004115	0,002424	0,001639	0,001211	0,000953	0,000786	0,000671	0,000588	0,000238
1	0,045078	0,011019	0,004995	0,002907	0,001944	0,001422	0,001107	0,000903	0,000764	0,000664	0,000238
2	0,039639	0,015368	0,007253	0,004237	0,002812	0,002031	0,001558	0,001250	0,001038	0,000886	0,000238
3	0,045078	0,014363	0,009619	0,006033	0,004091	0,002967	0,002266	0,001802	0,001479	0,001247	0,000238
4	0,142674	0,012314	0,009513	0,007589	0,005510	0,004102	0,003164	0,002521	0,002065	0,001731	0,000238
5		0,011719	0,008336	0,007736	0,006646	0,005247	0,004155	0,003351	0,002759	0,002315	0,000238
6		0,015368	0,007021	0,007094	0,006875	0,006133	0,005102	0,004217	0,003516	0,002969	0,000238
7		0,033562	0,006244	0,006119	0,006524	0,006386	0,005823	0,005016	0,004276	0,003656	0,000238
8		0,070167	0,006692	0,005150	0,005848	0,006201	0,006079	0,005622	0,004963	0,004329	0,000238
9		0,142674	0,009619	0,004464	0,005047	0,005733	0,005993	0,005871	0,005484	0,004929	0,000238
10			0,018456	0,004332	0,004282	0,005111	0,005668	0,005847	0,005723	0,005385	0,000238
11			0,033669	0,005136	0,003691	0,004440	0,005191	0,005622	0,005739	0,005613	0,000238
12			0,056252	0,007589	0,003411	0,003809	0,004635	0,005256	0,005584	0,005656	0,000238
13			0,088773	0,013261	0,003608	0,003296	0,004061	0,004802	0,005303	0,005552	0,000238
14			0,142674	0,022277	0,004538	0,002980	0,003524	0,004305	0,004934	0,005335	0,000238
15				0,034851	0,006646	0,002949	0,003073	0,003806	0,004511	0,005034	0,000238
16				0,051346	0,010784	0,003324	0,002756	0,003338	0,004066	0,004678	0,000238
17				0,072477	0,017000	0,004286	0,002629	0,002937	0,003625	0,004288	0,000238
18				0,100098	0,025371	0,006133	0,002756	0,002633	0,003211	0,003886	0,000238
19				0,142674	0,036005	0,009377	0,003228	0,002462	0,002850	0,003491	0,000238
20					0,049068	0,014044	0,004182	0,002464	0,002562	0,003120	0,000238
21					0,064837	0,020167	0,005823	0,002693	0,002372	0,002792	0,000238
22					0,083856	0,027793	0,008487	0,003219	0,002308	0,002521	0,000238
23					0,107562	0,036985	0,012186	0,004145	0,002403	0,002325	0,000238
24					0,142674	0,047830	0,016939	0,005622	0,002698	0,002224	0,000238

Continued from table A.6.

	q										
y_ε	**1**	**2**	**3**	**4**	**5**	**6**	**7**	**8**	**9**	**10**	∞
25						0,060458	0,022771	0,007879	0,003251	0,002240	0,000238
26						0,075087	0,029710	0,010924	0,004142	0,002399	0,000238
27						0,092150	0,037797	0,014769	0,005484	0,002738	0,000238
28						0,112823	0,047082	0,019427	0,007441	0,003302	0,000238
29						0,142674	0,057636	0,024915	0,010018	0,004156	0,000238
30							0,069564	0,031255	0,013223	0,005385	0,000238
31							0,083042	0,038471	0,017065	0,007112	0,000238
32							0,098431	0,046597	0,021553	0,009340	0,000238
33							0,116723	0,055673	0,026700	0,012074	0,000238
34							0,142674	0,065759	0,032522	0,015320	0,000238
35								0,076939	0,039036	0,019084	0,000238
36								0,089364	0,046264	0,023376	0,000238
37								0,103339	0,054232	0,028204	0,000238
38								0,119726	0,062975	0,033579	0,000238
39								0,142674	0,072543	0,039515	0,000238
40									0,083007	0,046025	0,000238
41									0,094495	0,053130	0,000238
42									0,107276	0,060851	0,000238
43									0,122108	0,069217	0,000238
44									0,142674	0,078270	0,000238
45										0,088073	0,000238
46										0,098738	0,000238
47										0,110502	0,000238
48										0,124044	0,000238
49										0,142674	0,000238

Table A.7: Harmonic scattering coefficients σ_o for integer slot windings with $m = 7$ and double zone span.

	q										
$\mathbf{y}_\varepsilon$	**1**	**2**	**3**	**4**	**5**	**6**	**7**	**8**	**9**	**10**	∞
0	0,016955	0,004369	0,001982	0,001142	0,000752	0,000541	0,000413	0,000330	0,000273	0,000233	0,000059
1	0,019715	0,004881	0,002195	0,001259	0,000827	0,000592	0,000451	0,000359	0,000296	0,000251	0,000059
2	0,017596	0,005835	0,002722	0,001575	0,001035	0,000739	0,000559	0,000442	0,000362	0,000305	0,000059
3	0,019715	0,005267	0,003205	0,001980	0,001332	0,000959	0,000728	0,000574	0,000468	0,000392	0,000059
4	0,021295	0,004709	0,002987	0,002280	0,001642	0,001218	0,000936	0,000743	0,000607	0,000507	0,000059
5	0,019715	0,004903	0,002564	0,002181	0,001851	0,001461	0,001157	0,000933	0,000768	0,000643	0,000059
6	0,069934	0,005835	0,002265	0,001901	0,001803	0,001618	0,001353	0,001123	0,000938	0,000794	0,000059
7		0,006457	0,002276	0,001604	0,001613	0,001596	0,001477	0,001285	0,001102	0,000946	0,000059
8		0,006675	0,002634	0,001406	0,001373	0,001462	0,001469	0,001386	0,001238	0,001089	0,000059
9		0,006218	0,003205	0,001377	0,001154	0,001274	0,001373	0,001386	0,001323	0,001205	0,000059
10		0,005835	0,003622	0,001540	0,001007	0,001076	0,001224	0,001314	0,001328	0,001278	0,000059
11		0,014029	0,003878	0,001871	0,000967	0,000906	0,001055	0,001196	0,001274	0,001287	0,000059
12		0,032522	0,003905	0,002280	0,001049	0,000791	0,000892	0,001054	0,001179	0,001245	0,000059
13		0,069934	0,003632	0,002599	0,001247	0,000749	0,000755	0,000906	0,001059	0,001168	0,000059
14			0,003149	0,002830	0,001533	0,000790	0,000660	0,000769	0,000929	0,001067	0,000059
15			0,003205	0,002952	0,001851	0,000914	0,000619	0,000655	0,000800	0,000952	0,000059
16			0,006791	0,002932	0,002111	0,001111	0,000638	0,000575	0,000683	0,000834	0,000059
17			0,014072	0,002742	0,002314	0,001358	0,000719	0,000536	0,000586	0,000721	0,000059
18			0,025468	0,002403	0,002453	0,001618	0,000857	0,000542	0,000517	0,000620	0,000059
19			0,042184	0,002077	0,002514	0,001837	0,001042	0,000596	0,000480	0,000536	0,000059
20			0,069934	0,002280	0,002480	0,002017	0,001257	0,000695	0,000478	0,000475	0,000059
21				0,004416	0,002337	0,002154	0,001477	0,000834	0,000514	0,000440	0,000059
22				0,008519	0,002091	0,002243	0,001667	0,001006	0,000586	0,000434	0,000059
23				0,014662	0,001795	0,002273	0,001827	0,001195	0,000693	0,000457	0,000059
24				0,022990	0,001597	0,002234	0,001958	0,001386	0,000828	0,000511	0,000059

Continued from table A.7.

	q										
y_ε	**1**	**2**	**3**	**4**	**5**	**6**	**7**	**8**	**9**	**10**	**∞**
25				0,033823	0,001851	0,002121	0,002055	0,001553	0,000986	0,000593	0,000059
26				0,048051	0,003327	0,001933	0,002112	0,001698	0,001155	0,000701	0,000059
27				0,069934	0,006034	0,001693	0,002125	0,001820	0,001323	0,000831	0,000059
28					0,009993	0,001457	0,002086	0,001918	0,001473	0,000976	0,000059
29					0,015241	0,001350	0,001992	0,001987	0,001605	0,001128	0,000059
30					0,021841	0,001618	0,001843	0,002025	0,001719	0,001278	0,000059
31					0,029911	0,002728	0,001649	0,002028	0,001814	0,001414	0,000059
32					0,039699	0,004684	0,001436	0,001990	0,001888	0,001535	0,000059
33					0,051909	0,007494	0,001256	0,001910	0,001939	0,001641	0,000059
34					0,069934	0,011170	0,001211	0,001788	0,001964	0,001733	0,000059
35						0,015734	0,001477	0,001628	0,001960	0,001808	0,000059
36						0,021217	0,002359	0,001444	0,001924	0,001865	0,000059
37						0,027671	0,003859	0,001263	0,001855	0,001903	0,000059
38						0,035192	0,005981	0,001131	0,001752	0,001919	0,000059
39						0,043982	0,008729	0,001128	0,001618	0,001911	0,000059
40						0,054623	0,012112	0,001386	0,001460	0,001877	0,000059
41						0,069934	0,016143	0,002114	0,001294	0,001816	0,000059
42							0,020840	0,003314	0,001143	0,001727	0,000059
43							0,026229	0,004986	0,001049	0,001613	0,000059
44							0,032355	0,007134	0,001076	0,001477	0,000059
45							0,039295	0,009763	0,001323	0,001329	0,000059
46							0,047223	0,012876	0,001941	0,001182	0,000059
47							0,056632	0,016484	0,002931	0,001059	0,000059
48							0,069934	0,020596	0,004293	0,000995	0,000059
49								0,025227	0,006029	0,001043	0,000059
50								0,030402	0,008141	0,001278	0,000059

Continued from table A.7.

					q						
y_ε	**1**	**2**	**3**	**4**	**5**	**6**	**7**	**8**	**9**	**10**	**∞**
51								0,036156	0,010632	0,001814	0,000059
52								0,042557	0,013506	0,002650	0,000059
53								0,049755	0,016769	0,003787	0,000059
54								0,058177	0,020428	0,005226	0,000059
55								0,069934	0,024492	0,006968	0,000059
56									0,028974	0,009015	0,000059
57									0,033894	0,011369	0,000059
58									0,039284	0,014033	0,000059
59									0,045204	0,017011	0,000059
60									0,051783	0,020308	0,000059
61									0,059402	0,023930	0,000059
62									0,069934	0,027885	0,000059
63										0,032185	0,000059
64										0,036846	0,000059
65										0,041897	0,000059
66										0,047391	0,000059
67										0,053444	0,000059
68										0,060397	0,000059
69										0,069934	0,000059

A.2 Harmonic Scattering Coeffficients of Double Layer Fractional Slot Windings

The following list provides an overview of the tables with the harmonic scattering coefficients of fractional slot windings:

m	normal zone span	double zone span
2	A.8 and A.9	-
3	A.10 and A.11	A.16 and A.17
5	A.12 and A.13	A.18 and A.19
7	A.14 and A.15	A.20 and A.21

Table A.8: Harmonic scattering coefficients σ_o for fractional slot windings with $m = 2$, normal zone span and $q_n = 3$.

	q									
y_σ	**4/3**	**5/3**	**7/3**	**8/3**	**10/3**	**11/3**	**13/3**	**14/3**	**16/3**	**17/3**
1	0,369133	0,318328	0,276000	0,265925	0,254205	0,250616	0,245782	0,244109	0,241660	0,240748
2	0,237750	0,162411	0,125327	0,123212	0,127520	0,131189	0,139048	0,142879	0,150014	0,153283
3	0,317944	0,169840	0,081672	0,071117	0,069532	0,072805	0,081952	0,086942	0,096782	0,101471
4	0,690378	0,201613	0,087860	0,062294	0,044296	0,043321	0,047967	0,051907	0,060966	0,065681
5	10,103305	0,412930	0,107532	0,077082	0,041002	0,033656	0,030091	0,031476	0,037321	0,041076
6	3,328482	2,414552	0,126816	0,081217	0,050970	0,037875	0,024612	0,022482	0,023372	0,025423
7	0,833801	10,103305	0,232839	0,097202	0,059111	0,048160	0,028223	0,022421	0,017423	0,017249
8	0,690378	0,887518	0,690005	0,173408	0,057923	0,048654	0,036343	0,028332	0,017878	0,015277
9	0,833801	0,437489	10,103305	0,440139	0,071796	0,047457	0,040648	0,035524	0,022761	0,018070
10	3,328482	0,412930	3,015808	2,503442	0,120941	0,059778	0,037091	0,035273	0,029072	0,023650
11	10,103305	0,437489	0,615723	10,103305	0,251811	0,099334	0,037192	0,031534	0,031694	0,028895
12	0,690378	0,887518	0,301213	0,821030	0,717851	0,195108	0,048156	0,032077	0,028246	0,028491
13	0,317944	10,103305	0,227555	0,325285	10,103305	0,472240	0,077332	0,042136	0,025276	0,024690
14	0,237750	2,414552	0,232839	0,195818	2,910227	2,550941	0,138570	0,067176	0,026813	0,022175
15	0,369133	0,412930	0,227555	0,164895	0,586859	10,103305	0,275501	0,116914	0,035923	0,023980
16		0,201613	0,301213	0,173408	0,266139	0,812174	0,739728	0,218522	0,055943	0,032509
17		0,169840	0,615723	0,164895	0,158441	0,319610	10,103305	0,496603	0,092338	0,050383
18		0,162411	3,015808	0,195818	0,119233	0,173935	2,857515	2,580175	0,157899	0,081726
19		0,318328	10,103305	0,325285	0,113260	0,114200	0,583081	10,103305	0,295478	0,135485
20			0,690005	0,821030	0,120941	0,092690	0,268725	0,812813	0,755948	0,238336
21			0,232839	10,103305	0,113260	0,092175	0,154299	0,328029	10,103305	0,514843
22			0,126816	2,503442	0,119233	0,099334	0,100380	0,180379	2,825973	2,599924
23			0,107532	0,440139	0,158441	0,092175	0,075644	0,111878	0,584782	10,103305
24			0,087860	0,173408	0,266139	0,092690	0,068456	0,076886	0,277797	0,815417
25			0,081672	0,097202	0,586859	0,114200	0,071675	0,061138	0,163165	0,338023
26			0,125327	0,081217	2,910227	0,173935	0,077332	0,057907	0,104302	0,191970
27			0,276000	0,077082	10,103305	0,319610	0,071675	0,062068	0,071240	0,120993

Continued from table A.8.

	q									
y_σ	**4/3**	**5/3**	**7/3**	**8/3**	**10/3**	**11/3**	**13/3**	**14/3**	**16/3**	**17/3**
28				0,062294	0,717851	0,812174	0,068456	0,067176	0,053700	0,080417
29				0,071117	0,251811	10,103305	0,075644	0,062068	0,046807	0,056800
30				0,123212	0,120941	2,550941	0,100380	0,057907	0,047286	0,044518
31				0,265925	0,071796	0,472240	0,154299	0,061138	0,051856	0,040423
32					0,057923	0,195108	0,268725	0,076886	0,055943	0,042053
33					0,059111	0,099334	0,583081	0,111878	0,051856	0,046679
34					0,050970	0,059778	2,857515	0,180379	0,047286	0,050383
35					0,041002	0,047457	10,103305	0,328029	0,046807	0,046679
36					0,044296	0,048654	0,739728	0,812813	0,053700	0,042053
37					0,069532	0,048160	0,275501	10,103305	0,071240	0,040423
38					0,127520	0,037875	0,138570	2,580175	0,104302	0,044518
39					0,254205	0,033656	0,077332	0,496603	0,163165	0,056800
40						0,043321	0,048156	0,218522	0,277797	0,080417
41						0,072805	0,037192	0,116914	0,584782	0,120993
42						0,131189	0,037091	0,067176	2,825973	0,191970
43						0,250616	0,040648	0,042136	10,103305	0,338023
44							0,036343	0,032077	0,755948	0,815417
45							0,028223	0,031534	0,295478	10,103305
46							0,024612	0,035273	0,157899	2,599924
47							0,030091	0,035524	0,092338	0,514843
48							0,047967	0,028332	0,055943	0,238336
49							0,081952	0,022421	0,035923	0,135485
50							0,139048	0,022482	0,026813	0,081726
51							0,245782	0,031476	0,025276	0,050383
52								0,051907	0,028246	0,032509
53								0,086942	0,031694	0,023980
54								0,142879	0,029072	0,022175

Continued from table A.8.

	q									
y_σ	**4/3**	**5/3**	**7/3**	**8/3**	**10/3**	**11/3**	**13/3**	**14/3**	**16/3**	**17/3**
55								0,244109	0,022761	0,024690
56									0,017878	0,028491
57									0,017423	0,028895
58									0,023372	0,023650
59									0,037321	0,018070
60									0,060966	0,015277
61									0,096782	0,017249
62									0,150014	0,025423
63									0,241660	0,041076
64										0,065681
65										0,101471
66										0,153283
67										0,240748

Table A.9: Harmonic scattering coefficients σ_o for fractional slot windings with $m = 2$, normal zone span and $q_n = 5$.

	q									
y_σ	**6/5**	**7/5**	**8/5**	**9/5**	**11/5**	**12/5**	**13/5**	**14/5**	**16/5**	**17/5**
1	0,417917	0,365949	0,333462	0,311732	0,285289	0,276875	0,270374	0,265244	0,257764	0,254987
2	0,314118	0,224800	0,178674	0,153359	0,131343	0,127340	0,125705	0,125569	0,127824	0,129644
3	0,436452	0,286527	0,196758	0,143920	0,092934	0,081388	0,074756	0,071340	0,070251	0,071418
4	1,802488	0,445792	0,215042	0,180998	0,106912	0,084091	0,068456	0,058015	0,047255	0,045148
5	29,842514	2,544445	0,472539	0,280219	0,120869	0,104148	0,085094	0,068909	0,047055	0,040423
6	1,452177	5,693014	4,839069	0,874268	0,169466	0,107729	0,082596	0,080163	0,059063	0,049281
7	0,960105	0,657042	2,516459	29,842514	0,390674	0,166987	0,098319	0,087336	0,062481	0,058678
8	1,335407	0,394692	0,481576	2,560540	1,876466	0,407264	0,180143	0,133088	0,065727	0,054099
9	7,372257	0,425947	0,294327	0,718079	29,842514	2,466374	0,489111	0,282382	0,093475	0,059675
10	17,303301	0,989214	0,309166	0,474001	1,149920	5,453127	4,952955	0,904798	0,176261	0,091177
11	2,061140	29,842514	0,487662	0,495153	0,455504	0,573664	2,460506	29,842514	0,421754	0,175273
12	1,452177	2,520844	2,035049	0,666016	0,310676	0,231356	0,441733	2,357061	1,926581	0,423375
13	2,061140	0,771969	29,842514	1,611143	0,305181	0,148109	0,193576	0,598444	29,842514	2,446521
14	17,303301	0,657042	1,160023	17,992472	0,332994	0,140850	0,125219	0,302110	1,092937	5,363502
15	7,372257	0,771969	0,523892	8,715090	0,491835	0,142925	0,117446	0,211593	0,404788	0,570989
16	1,335407	2,520844	0,481576	1,520138	1,148070	0,172720	0,123407	0,195057	0,225250	0,228773
17	0,960105	29,842514	0,523892	0,806437	7,526924	0,315050	0,133713	0,208945	0,160750	0,122204
18	1,452177	0,989214	1,160023	0,718079	17,318349	0,951909	0,204119	0,228316	0,145406	0,081348
19	29,842514	0,425947	29,842514	0,806437	1,671526	29,842514	0,454237	0,312041	0,153770	0,071789
20	1,802488	0,394692	2,035049	1,520138	0,698895	2,282488	2,020360	0,567883	0,157935	0,077199
21	0,436452	0,657042	0,487662	8,715090	0,479184	0,567257	29,842514	1,553902	0,181293	0,076976
22	0,314118	5,693014	0,309166	17,992472	0,455504	0,292600	1,063492	17,784870	0,258244	0,077004
23	0,417917	2,544445	0,294327	1,611143	0,479184	0,226111	0,387159	8,380187	0,464821	0,097301
24		0,445792	0,481576	0,666016	0,698895	0,231356	0,225913	1,354632	1,155015	0,159539
25		0,286527	2,516459	0,495153	1,671526	0,226111	0,186119	0,591071	7,622637	0,323752
26		0,224800	4,839069	0,474001	17,318349	0,292600	0,193576	0,371811	17,356939	0,963474
27		0,365949	0,472539	0,718079	7,526924	0,567257	0,186119	0,305170	1,617127	29,842514

Continued from table A.9.

	q									
y$_\sigma$	**6/5**	**7/5**	**8/5**	**9/5**	**11/5**	**12/5**	**13/5**	**14/5**	**16/5**	**17/5**
28			0,215042	2,560540	1,148070	2,282488	0,225913	0,302110	0,623927	2,209071
29			0,196758	29,842514	0,491835	29,842514	0,387159	0,305170	0,352576	0,541680
30			0,178674	0,874268	0,332994	0,951909	1,063492	0,371811	0,253085	0,257325
31			0,333462	0,280219	0,305181	0,315050	29,842514	0,591071	0,223210	0,157223
32				0,180998	0,310676	0,172720	2,020360	1,354632	0,225250	0,120359
33				0,143920	0,455504	0,142925	0,454237	8,380187	0,223210	0,114859
34				0,153359	1,149920	0,140850	0,204119	17,784870	0,253085	0,122204
35				0,311732	29,842514	0,148109	0,133713	1,553902	0,352576	0,114859
36					1,876466	0,231356	0,123407	0,567883	0,623927	0,120359
37					0,390674	0,573664	0,117446	0,312041	1,617127	0,157223
38					0,169466	5,453127	0,125219	0,228316	17,356939	0,257325
39					0,120869	2,466374	0,193576	0,208945	7,622637	0,541680
40					0,106912	0,407264	0,441733	0,195057	1,155015	2,209071
41					0,092934	0,166987	2,460506	0,211593	0,464821	29,842514
42					0,131343	0,107729	4,952955	0,302110	0,258244	0,963474
43					0,285289	0,104148	0,489111	0,598444	0,181293	0,323752
44						0,084091	0,180143	2,357061	0,157935	0,159539
45						0,081388	0,098319	29,842514	0,153770	0,097301
46						0,127340	0,082596	0,904798	0,145406	0,077004
47						0,276875	0,085094	0,282382	0,160750	0,076976
48							0,068456	0,133088	0,225250	0,077199
49							0,074756	0,087336	0,404788	0,071789
50							0,125705	0,080163	1,092937	0,081348
51							0,270374	0,068909	29,842514	0,122204
52								0,058015	1,926581	0,228773
53								0,071340	0,421754	0,570989
54								0,125569	0,176261	5,363502

Continued from table A.9.

	q									
y_σ	**6/5**	**7/5**	**8/5**	**9/5**	**11/5**	**12/5**	**13/5**	**14/5**	**16/5**	**17/5**
55								0,265244	0,093475	2,446521
56									0,065727	0,423375
57									0,062481	0,175273
58									0,059063	0,091177
59									0,047055	0,059675
60									0,047255	0,054099
61									0,070251	0,058678
62									0,127824	0,049281
63									0,257764	0,040423
64										0,045148
65										0,071418
66										0,129644
67										0,254987

Table A.10: Harmonic scattering coefficients σ_o for fractional slot windings with $m = 3$, normal zone span and $q_n = 2$.

	q									
ys	**3/2**	**5/2**	**7/2**	**9/2**	**11/2**	**13/2**	**15/2**	**17/2**	**19/2**	**21/2**
1	0,130718	0,108737	0,102781	0,100343	0,099111	0,098404	0,097960	0,097664	0,097456	0,097305
2	0,067091	0,042947	0,047275	0,053410	0,058718	0,063040	0,066551	0,069432	0,071828	0,073847
3	0,058151	0,026551	0,022413	0,028292	0,035084	0,041199	0,046430	0,050863	0,054630	0,057855
4	0,045590	0,024051	0,014583	0,014412	0,019614	0,025650	0,031361	0,036474	0,040973	0,044919
5	0,045590	0,022457	0,013623	0,009530	0,010452	0,014837	0,020013	0,025105	0,029828	0,034113
6	0,058151	0,017361	0,013345	0,008980	0,006951	0,008194	0,011895	0,016328	0,020819	0,025104
7	0,067091	0,017600	0,012532	0,009083	0,006509	0,005470	0,006778	0,009940	0,013766	0,017730
8	0,130718	0,017600	0,009645	0,009046	0,006712	0,005048	0,004547	0,005829	0,008566	0,011900
9		0,017361	0,008825	0,008436	0,006913	0,005248	0,004121	0,003936	0,005159	0,007558
10		0,022457	0,010007	0,006501	0,006878	0,005525	0,004281	0,003502	0,003513	0,004668
11		0,024051	0,010007	0,005457	0,006360	0,005691	0,004569	0,003612	0,003072	0,003210
12		0,026551	0,008825	0,005809	0,004932	0,005625	0,004812	0,003882	0,003134	0,002766
13		0,042947	0,009645	0,006897	0,003907	0,005165	0,004926	0,004150	0,003372	0,002782
14		0,108737	0,012532	0,006897	0,003768	0,004044	0,004833	0,004342	0,003639	0,002985
15			0,013345	0,005809	0,004433	0,003101	0,004415	0,004411	0,003866	0,003239
16			0,013623	0,005457	0,005326	0,002725	0,003497	0,004297	0,004013	0,003476
17			0,014583	0,006501	0,005326	0,002988	0,002647	0,003914	0,004045	0,003661
18			0,022413	0,008436	0,004433	0,003701	0,002165	0,003139	0,003916	0,003770
19			0,047275	0,009046	0,003768	0,004423	0,002162	0,002375	0,003563	0,003773
20			0,102781	0,009083	0,003907	0,004423	0,002592	0,001855	0,002894	0,003635
21				0,008980	0,004932	0,003701	0,003267	0,001689	0,002205	0,003307
22				0,009530	0,006360	0,002988	0,003857	0,001889	0,001680	0,002719
23				0,014412	0,006878	0,002725	0,003857	0,002377	0,001418	0,002095
24				0,028292	0,006913	0,003101	0,003267	0,002991	0,001454	0,001582
25				0,053410	0,006712	0,004044	0,002592	0,003479	0,001759	0,001267
26				0,100343	0,006509	0,005165	0,002162	0,003479	0,002255	0,001189
27					0,006951	0,005625	0,002165	0,002991	0,002805	0,001347

Continued from table A.10.

	q									
ys	**3/2**	**5/2**	**7/2**	**9/2**	**11/2**	**13/2**	**15/2**	**17/2**	**19/2**	**21/2**
28					0,010452	0,005691	0,002647	0,002377	0,003214	0,001704
29					0,019614	0,005525	0,003497	0,001889	0,003214	0,002184
30					0,035084	0,005248	0,004415	0,001689	0,002805	0,002674
31					0,058718	0,005048	0,004833	0,001855	0,002255	0,003021
32					0,099111	0,005470	0,004926	0,002375	0,001759	0,003021
33						0,008194	0,004812	0,003139	0,001454	0,002674
34						0,014837	0,004569	0,003914	0,001418	0,002184
35						0,025650	0,004281	0,004297	0,001680	0,001704
36						0,041199	0,004121	0,004411	0,002205	0,001347
37						0,063040	0,004547	0,004342	0,002894	0,001189
38						0,098404	0,006778	0,004150	0,003563	0,001267
39							0,011895	0,003882	0,003916	0,001582
40							0,020013	0,003612	0,004045	0,002095
41							0,031361	0,003502	0,004013	0,002719
42							0,046430	0,003936	0,003866	0,003307
43							0,066551	0,005829	0,003639	0,003635
44							0,097960	0,009940	0,003372	0,003773
45								0,016328	0,003134	0,003770
46								0,025105	0,003072	0,003661
47								0,036474	0,003513	0,003476
48								0,050863	0,005159	0,003239
49								0,069432	0,008566	0,002985
50								0,097664	0,013766	0,002782
51									0,020819	0,002766
52									0,029828	0,003210
53									0,040973	0,004668
54									0,054630	0,007558

Continued from table A.10.

	q									
ys	**3/2**	**5/2**	**7/2**	**9/2**	**11/2**	**13/2**	**15/2**	**17/2**	**19/2**	**21/2**
55									0,071828	0,011900
56									0,097456	0,017730
57										0,025104
58										0,034113
59										0,044919
60										0,057855
61										0,073847
62										0,097305

Table A.11: Harmonic scattering coefficients σ_o for fractional slot windings with $m = 3$, normal zone span and $q_n = 5$.

	q									
$\mathbf{y}_\sigma$	**6/5**	**7/5**	**8/5**	**9/5**	**11/5**	**12/5**	**13/5**	**14/5**	**16/5**	**17/5**
1	0,165984	0,147074	0,135000	0,126812	0,116721	0,113481	0,110968	0,108978	0,106067	0,104984
2	0,123786	0,087376	0,068006	0,057278	0,048076	0,046519	0,045994	0,046119	0,047450	0,048403
3	0,116019	0,077781	0,060185	0,052980	0,039483	0,032199	0,027793	0,025270	0,023595	0,023769
4	0,145210	0,077751	0,052668	0,050475	0,037493	0,029632	0,025510	0,023801	0,019653	0,017062
5	0,241424	0,077892	0,059982	0,054366	0,034440	0,027614	0,024317	0,023448	0,019265	0,016203
6	0,666016	0,109240	0,064793	0,061877	0,036686	0,024968	0,020779	0,021953	0,018868	0,015842
7	26,415568	0,224837	0,089188	0,083274	0,042033	0,027813	0,021278	0,021174	0,017022	0,014738
8	2,263828	2,938505	0,172720	0,128989	0,048895	0,026379	0,024013	0,024196	0,016442	0,012652
9	0,666016	1,650329	1,310916	0,277023	0,068414	0,028717	0,022804	0,025861	0,018673	0,012995
10	0,454347	0,309584	3,302085	1,517340	0,101980	0,036492	0,026330	0,028429	0,020589	0,014930
11	0,468922	0,185443	0,348855	26,415568	0,196256	0,047614	0,032552	0,036768	0,021187	0,013986
12	0,666016	0,150576	0,172720	0,936851	0,706183	0,078020	0,041949	0,048087	0,025102	0,013394
13	1,532017	0,163187	0,129885	0,357361	26,415568	0,249870	0,066803	0,068164	0,032722	0,015487
14	17,416943	0,224837	0,118481	0,232496	1,993398	3,005725	0,193409	0,117038	0,041679	0,018998
15	8,326486	0,406603	0,127686	0,189612	0,471420	1,551407	1,353375	0,305116	0,057427	0,022125
16	1,436133	1,769237	0,172720	0,188353	0,240416	0,263429	3,224629	1,588262	0,093266	0,027270
17	0,774745	26,415568	0,281331	0,207353	0,168946	0,114227	0,325202	26,415568	0,212247	0,039966
18	0,666016	0,858932	0,801762	0,277023	0,138868	0,078020	0,124085	0,879945	0,735044	0,089928
19	0,774745	0,343182	26,415568	0,443334	0,129499	0,063325	0,077095	0,301176	26,415568	0,269808
20	1,436133	0,236815	1,844823	1,045186	0,136760	0,053458	0,059942	0,164746	1,907019	3,035528
21	8,326486	0,224837	0,424779	7,196864	0,152292	0,052483	0,051024	0,117038	0,436730	1,514970
22	17,416943	0,236815	0,234374	16,574919	0,196256	0,055611	0,045123	0,094862	0,200267	0,259604
23	1,532017	0,343182	0,177066	1,494567	0,281969	0,060936	0,046223	0,081987	0,124564	0,107263
24	0,666016	0,858932	0,172720	0,595225	0,505793	0,078020	0,047835	0,077295	0,093266	0,059563
25	0,468922	26,415568	0,177066	0,372081	1,426444	0,103551	0,052692	0,080219	0,077194	0,044133
26	0,454347	1,769237	0,234374	0,290486	17,110354	0,162720	0,066803	0,083615	0,067244	0,036908
27	0,666016	0,406603	0,424779	0,277023	7,915342	0,365380	0,086309	0,094010	0,061660	0,032454

Continued from table A.11.

	q									
y_σ	**6/5**	**7/5**	**8/5**	**9/5**	**11/5**	**12/5**	**13/5**	**14/5**	**16/5**	**17/5**
28	2,263828	0,224837	1,844823	0,290486	1,205895	1,738976	0,127457	0,117038	0,061829	0,027910
29	26,415568	0,163187	26,415568	0,372081	0,509349	26,415568	0,246558	0,153233	0,065057	0,026073
30	0,666016	0,150576	0,801762	0,595225	0,313966	0,816940	0,791054	0,225458	0,067873	0,027301
31	0,241424	0,185443	0,281331	1,494567	0,235639	0,264025	26,415568	0,404406	0,076411	0,028571
32	0,145210	0,309584	0,172720	16,574919	0,200937	0,146744	1,790481	1,048323	0,093266	0,028943
33	0,116019	1,650329	0,127686	7,196864	0,196256	0,104999	0,386789	7,299100	0,117404	0,032468
34	0,123786	2,938505	0,118481	1,045186	0,200937	0,084870	0,173048	16,648969	0,160341	0,039966
35	0,165984	0,224837	0,129885	0,443334	0,235639	0,076277	0,111561	1,452261	0,249838	0,048187
36		0,109240	0,172720	0,277023	0,313966	0,078020	0,085389	0,527040	0,490552	0,061435
37		0,077892	0,348855	0,207353	0,509349	0,076277	0,070580	0,288861	1,419051	0,087722
38		0,077751	3,302085	0,188353	1,205895	0,084870	0,064962	0,197309	17,010748	0,155618
39		0,077781	1,310916	0,189612	7,915342	0,104999	0,066803	0,153270	7,782806	0,368211
40		0,087376	0,172720	0,232496	17,110354	0,146744	0,064962	0,127962	1,163287	1,734344
41		0,147074	0,089188	0,357361	1,426444	0,264025	0,070580	0,117327	0,464653	26,415568
42			0,064793	0,936851	0,505793	0,816940	0,085389	0,117038	0,259904	0,811832
43			0,059982	26,415568	0,281969	26,415568	0,111561	0,117327	0,177623	0,259934
44			0,052668	1,517340	0,196256	1,738976	0,173048	0,127962	0,136608	0,127458
45			0,060185	0,277023	0,152292	0,365380	0,386789	0,153270	0,113171	0,082269
46			0,068006	0,128989	0,136760	0,162720	1,790481	0,197309	0,098545	0,062310
47			0,135000	0,083274	0,129499	0,103551	26,415568	0,288861	0,092917	0,051444
48				0,061877	0,138868	0,078020	0,791054	0,527040	0,093266	0,043982
49				0,054366	0,168946	0,060936	0,246558	1,452261	0,092917	0,039113
50				0,050475	0,240416	0,055611	0,127457	16,648969	0,098545	0,038400
51				0,052980	0,471420	0,052483	0,086309	7,299100	0,113171	0,039966
52				0,057278	1,993398	0,053458	0,066803	1,048323	0,136608	0,038400
53				0,126812	26,415568	0,063325	0,052692	0,404406	0,177623	0,039113
54					0,706183	0,078020	0,047835	0,225458	0,259904	0,043982

Continued from table A.11.

	q									
y_σ	**6/5**	**7/5**	**8/5**	**9/5**	**11/5**	**12/5**	**13/5**	**14/5**	**16/5**	**17/5**
55					0,196256	0,114227	0,046223	0,153233	0,464653	0,051444
56					0,101980	0,263429	0,045123	0,117038	1,163287	0,062310
57					0,068414	1,551407	0,051024	0,094010	7,782806	0,082269
58					0,048895	3,005725	0,059942	0,083615	17,010748	0,127458
59					0,042033	0,249870	0,077095	0,080219	1,419051	0,259934
60					0,036686	0,078020	0,124085	0,077295	0,490552	0,811832
61					0,034440	0,047614	0,325202	0,081987	0,249838	26,415568
62					0,037493	0,036492	3,224629	0,094862	0,160341	1,734344
63					0,039483	0,028717	1,353375	0,117038	0,117404	0,368211
64					0,048076	0,026379	0,193409	0,164746	0,093266	0,155618
65					0,116721	0,027813	0,066803	0,301176	0,076411	0,087722
66						0,024968	0,041949	0,879945	0,067873	0,061435
67						0,027614	0,032552	26,415568	0,065057	0,048187
68						0,029632	0,026330	1,588262	0,061829	0,039966
69						0,032199	0,022804	0,305116	0,061660	0,032468
70						0,046519	0,024013	0,117038	0,067244	0,028943
71						0,113481	0,021278	0,068164	0,077194	0,028571
72							0,020779	0,048087	0,093266	0,027301
73							0,024317	0,036768	0,124564	0,026073
74							0,025510	0,028429	0,200267	0,027910
75							0,027793	0,025861	0,436730	0,032454
76							0,045994	0,024196	1,907019	0,036908
77							0,110968	0,021174	26,415568	0,044133
78								0,021953	0,735044	0,059563
79								0,023448	0,212247	0,107263
80								0,023801	0,093266	0,259604
81								0,025270	0,057427	1,514970

Continued from table A.11.

	q									
y_σ	**6/5**	**7/5**	**8/5**	**9/5**	**11/5**	**12/5**	**13/5**	**14/5**	**16/5**	**17/5**
82								0,046119	0,041679	3,035528
83								0,108978	0,032722	0,269808
84									0,025102	0,089928
85									0,021187	0,039966
86									0,020589	0,027270
87									0,018673	0,022125
88									0,016442	0,018998
89									0,017022	0,015487
90									0,018868	0,013394
91									0,019265	0,013986
92									0,019653	0,014930
93									0,023595	0,012995
94									0,047450	0,012652
95									0,106067	0,014738
96										0,015842
97										0,016203
98										0,017062
99										0,023769
100										0,048403
101										0,104984

Table A.12: Harmonic scattering coefficients σ_o for fractional slot windings with $m = 5$, normal zone span and $q_n = 2$.

	q									
y_σ	**3/2**	**5/2**	**7/2**	**9/2**	**11/2**	**13/2**	**15/2**	**17/2**	**19/2**	**21/2**
1	0,044976	0,037649	0,035643	0,034819	0,034402	0,034162	0,034012	0,033911	0,033841	0,033790
2	0,022659	0,013942	0,015547	0,017812	0,019766	0,021353	0,022640	0,023694	0,024569	0,025306
3	0,016600	0,009012	0,006869	0,008828	0,011244	0,013451	0,015349	0,016962	0,018333	0,019507
4	0,016158	0,007721	0,004858	0,004162	0,005808	0,007899	0,009929	0,011766	0,013391	0,014820
5	0,015791	0,006144	0,004712	0,003067	0,002841	0,004174	0,005926	0,007708	0,009388	0,010924
6	0,016600	0,006015	0,004002	0,003230	0,002138	0,002098	0,003184	0,004652	0,006201	0,007709
7	0,015208	0,005991	0,003253	0,003025	0,002373	0,001595	0,001637	0,002536	0,003777	0,005126
8	0,015208	0,005804	0,003170	0,002518	0,002416	0,001830	0,001252	0,001331	0,002088	0,003149
9	0,016600	0,005816	0,003191	0,002062	0,002163	0,001987	0,001464	0,001021	0,001118	0,001764
10	0,015791	0,006144	0,003188	0,001991	0,001776	0,001910	0,001669	0,001206	0,000859	0,000963
11	0,016158	0,005592	0,003061	0,002013	0,001459	0,001658	0,001702	0,001426	0,001018	0,000741
12	0,016600	0,005603	0,002967	0,002040	0,001393	0,001351	0,001569	0,001524	0,001235	0,000876
13	0,022659	0,005603	0,003089	0,002032	0,001409	0,001112	0,001336	0,001481	0,001371	0,001083
14	0,044976	0,005592	0,003253	0,001936	0,001439	0,001051	0,001085	0,001327	0,001391	0,001239
15		0,006144	0,002956	0,001831	0,001458	0,001058	0,000895	0,001116	0,001306	0,001302
16		0,005816	0,002834	0,001847	0,001445	0,001086	0,000837	0,000906	0,001149	0,001272
17		0,005804	0,002972	0,001969	0,001368	0,001111	0,000838	0,000749	0,000960	0,001166
18		0,005991	0,002972	0,002062	0,001272	0,001123	0,000860	0,000695	0,000780	0,001013
19		0,006015	0,002834	0,001874	0,001243	0,001107	0,000886	0,000691	0,000647	0,000844
20		0,006144	0,002956	0,001733	0,001299	0,001042	0,000906	0,000708	0,000596	0,000688
21		0,007721	0,003253	0,001759	0,001402	0,000957	0,000912	0,000732	0,000588	0,000573
22		0,009012	0,003089	0,001891	0,001459	0,000910	0,000894	0,000754	0,000601	0,000524
23		0,013942	0,002967	0,001891	0,001327	0,000924	0,000838	0,000768	0,000621	0,000513
24		0,037649	0,003061	0,001759	0,001197	0,000991	0,000763	0,000770	0,000643	0,000522
25			0,003188	0,001733	0,001162	0,001075	0,000710	0,000752	0,000661	0,000540
26			0,003191	0,001874	0,001234	0,001112	0,000700	0,000702	0,000672	0,000560
27			0,003170	0,002062	0,001344	0,001013	0,000735	0,000636	0,000670	0,000579

Continued from table A.12.

					q					
$\mathbf{y}_\sigma$	**3/2**	**5/2**	**7/2**	**9/2**	**11/2**	**13/2**	**15/2**	**17/2**	**19/2**	**21/2**
28			0,003253	0,001969	0,001344	0,000899	0,000802	0,000582	0,000651	0,000593
29			0,004002	0,001847	0,001234	0,000839	0,000869	0,000559	0,000607	0,000601
30			0,004712	0,001831	0,001162	0,000858	0,000895	0,000571	0,000548	0,000597
31			0,004858	0,001936	0,001197	0,000940	0,000817	0,000615	0,000496	0,000578
32			0,006869	0,002032	0,001327	0,001030	0,000718	0,000677	0,000465	0,000538
33			0,015547	0,002040	0,001459	0,001030	0,000649	0,000732	0,000463	0,000485
34			0,035643	0,002013	0,001402	0,000940	0,000635	0,000749	0,000488	0,000435
35				0,001991	0,001299	0,000858	0,000679	0,000686	0,000534	0,000401
36				0,002062	0,001243	0,000839	0,000759	0,000600	0,000590	0,000389
37				0,002518	0,001272	0,000899	0,000832	0,000530	0,000635	0,000400
38				0,003025	0,001368	0,001013	0,000832	0,000498	0,000647	0,000432
39				0,003230	0,001445	0,001112	0,000759	0,000512	0,000595	0,000478
40				0,003067	0,001458	0,001075	0,000679	0,000566	0,000520	0,000527
41				0,004162	0,001439	0,000991	0,000635	0,000640	0,000452	0,000565
42				0,008828	0,001409	0,000924	0,000649	0,000701	0,000410	0,000573
43				0,017812	0,001393	0,000910	0,000718	0,000701	0,000404	0,000528
44				0,034819	0,001459	0,000957	0,000817	0,000640	0,000433	0,000463
45					0,001776	0,001042	0,000895	0,000566	0,000490	0,000399
46					0,002163	0,001107	0,000869	0,000512	0,000557	0,000352
47					0,002416	0,001123	0,000802	0,000498	0,000608	0,000333
48					0,002373	0,001111	0,000735	0,000530	0,000608	0,000343
49					0,002138	0,001086	0,000700	0,000600	0,000557	0,000381
50					0,002841	0,001058	0,000710	0,000686	0,000490	0,000437
51					0,005808	0,001051	0,000763	0,000749	0,000433	0,000497
52					0,011244	0,001112	0,000838	0,000732	0,000404	0,000541
53					0,019766	0,001351	0,000894	0,000677	0,000410	0,000541
54					0,034402	0,001658	0,000912	0,000615	0,000452	0,000497

Continued from table A.12.

	q									
y_σ	3/2	5/2	7/2	9/2	11/2	13/2	15/2	17/2	19/2	21/2
55						0,001910	0,000906	0,000571	0,000520	0,000437
56						0,001987	0,000886	0,000559	0,000595	0,000381
57						0,001830	0,000860	0,000582	0,000647	0,000343
58						0,001595	0,000838	0,000636	0,000635	0,000333
59						0,002098	0,000837	0,000702	0,000590	0,000352
60						0,004174	0,000895	0,000752	0,000534	0,000399
61						0,007899	0,001085	0,000770	0,000488	0,000463
62						0,013451	0,001336	0,000768	0,000463	0,000528
63						0,021353	0,001569	0,000754	0,000465	0,000573
64						0,034162	0,001702	0,000732	0,000496	0,000565
65							0,001669	0,000708	0,000548	0,000527
66							0,001464	0,000691	0,000607	0,000478
67							0,001252	0,000695	0,000651	0,000432
68							0,001637	0,000749	0,000670	0,000400
69							0,003184	0,000906	0,000672	0,000389
70							0,005926	0,001116	0,000661	0,000401
71							0,009929	0,001327	0,000643	0,000435
72							0,015349	0,001481	0,000621	0,000485
73							0,022640	0,001524	0,000601	0,000538
74							0,034012	0,001426	0,000588	0,000578
75								0,001206	0,000596	0,000597
76								0,001021	0,000647	0,000601
77								0,001331	0,000780	0,000593
78								0,002536	0,000960	0,000579
79								0,004652	0,001149	0,000560
80								0,007708	0,001306	0,000540
81								0,011766	0,001391	0,000522

Continued from table A.12.

	q									
y_σ	**3/2**	**5/2**	**7/2**	**9/2**	**11/2**	**13/2**	**15/2**	**17/2**	**19/2**	**21/2**
82								0,016962	0,001371	0,000513
83								0,023694	0,001235	0,000524
84								0,033911	0,001018	0,000573
85									0,000859	0,000688
86									0,001118	0,000844
87									0,002088	0,001013
88									0,003777	0,001166
89									0,006201	0,001272
90									0,009388	0,001302
91									0,013391	0,001239
92									0,018333	0,001083
93									0,024569	0,000876
94									0,033841	0,000741
95										0,000963
96										0,001764
97										0,003149
98										0,005126
99										0,007709
100										0,010924
101										0,014820
102										0,019507
103										0,025306
104										0,033790

Table A.13: Harmonic scattering coefficients σ_o for fractional slot windings with $m = 5$, normal zone span and $q_n = 3$.

	q									
$\mathbf{y}_\sigma$	**4/3**	**5/3**	**7/3**	**8/3**	**10/3**	**11/3**	**13/3**	**14/3**	**16/3**	**17/3**
1	0,050736	0,044511	0,039129	0,037820	0,036283	0,035810	0,035170	0,034947	0,034622	0,034500
2	0,031708	0,020498	0,014889	0,014674	0,015591	0,016276	0,017698	0,018378	0,019631	0,020200
3	0,024329	0,016745	0,011547	0,008564	0,007152	0,007430	0,008679	0,009443	0,011011	0,011776
4	0,022356	0,014808	0,009714	0,007999	0,005984	0,004729	0,004266	0,004568	0,005640	0,006291
5	0,020261	0,014048	0,008159	0,006676	0,005665	0,004830	0,003687	0,003032	0,002880	0,003145
6	0,019159	0,012805	0,007723	0,006051	0,004785	0,004370	0,003808	0,003273	0,002522	0,002137
7	0,020282	0,012646	0,007427	0,005845	0,004116	0,003650	0,003477	0,003230	0,002768	0,002385
8	0,022356	0,012690	0,006773	0,005660	0,003950	0,003327	0,002914	0,002822	0,002732	0,002525
9	0,021749	0,012737	0,006730	0,005168	0,003871	0,003249	0,002525	0,002352	0,002410	0,002362
10	0,022356	0,014048	0,006380	0,005111	0,003753	0,003205	0,002433	0,002141	0,002007	0,002017
11	0,023973	0,013474	0,006411	0,005089	0,003423	0,003112	0,002412	0,002098	0,001741	0,001678
12	0,022356	0,013944	0,006722	0,004860	0,003327	0,002838	0,002389	0,002094	0,001675	0,001521
13	0,357147	0,014199	0,006739	0,005117	0,003415	0,002736	0,002315	0,002079	0,001671	0,001490
14	0,149808	0,015947	0,007427	0,005063	0,003238	0,002814	0,002108	0,002014	0,001676	0,001496
15	0,034565	0,014048	0,007110	0,005134	0,003100	0,002803	0,001999	0,001833	0,001664	0,001505
16	0,022356	0,096158	0,007211	0,005660	0,003266	0,002604	0,002036	0,001726	0,001608	0,001495
17	0,020917	0,357147	0,007389	0,005402	0,003404	0,002621	0,002118	0,001745	0,001461	0,001443
18	0,019928	0,035305	0,007477	0,005383	0,003273	0,002823	0,002008	0,001831	0,001358	0,001310
19	0,020720	0,019659	0,007923	0,005626	0,003408	0,002779	0,001860	0,001820	0,001349	0,001211
20	0,022356	0,014048	0,008796	0,005660	0,003753	0,002679	0,001874	0,001664	0,001416	0,001192
21	0,020720	0,013377	0,007427	0,005715	0,003590	0,002825	0,002031	0,001598	0,001480	0,001247
22	0,019928	0,012961	0,028336	0,006399	0,003493	0,003112	0,002108	0,001686	0,001402	0,001320
23	0,020917	0,013037	0,357147	0,006874	0,003637	0,002976	0,001984	0,001835	0,001273	0,001309
24	0,022356	0,012939	0,132892	0,005660	0,003747	0,002862	0,001953	0,001803	0,001224	0,001187
25	0,034565	0,014048	0,027519	0,018958	0,003753	0,002943	0,002104	0,001687	0,001292	0,001098
26	0,149808	0,012939	0,012375	0,102017	0,003763	0,003101	0,002315	0,001683	0,001422	0,001109
27	0,357147	0,013037	0,009687	0,357147	0,004004	0,003121	0,002222	0,001831	0,001471	0,001209

Continued from table A.13.

	q									
$\mathbf{y}_\sigma$	**4/3**	**5/3**	**7/3**	**8/3**	**10/3**	**11/3**	**13/3**	**14/3**	**16/3**	**17/3**
28	0,022356	0,012961	0,007427	0,037535	0,004614	0,003101	0,002106	0,002014	0,001370	0,001322
29	0,023973	0,013377	0,007104	0,012835	0,004622	0,003130	0,002112	0,001935	0,001293	0,001297
30	0,022356	0,014048	0,006962	0,008859	0,003753	0,003520	0,002240	0,001821	0,001326	0,001194
31	0,021749	0,019659	0,006611	0,007229	0,010669	0,004010	0,002323	0,001801	0,001464	0,001137
32	0,022356	0,035305	0,006674	0,005660	0,033841	0,003872	0,002326	0,001897	0,001608	0,001182
33	0,020282	0,357147	0,006859	0,005443	0,357147	0,003112	0,002303	0,002013	0,001551	0,001314
34	0,019159	0,096158	0,006845	0,005375	0,126877	0,008420	0,002304	0,002034	0,001449	0,001443
35	0,020261	0,014048	0,007427	0,005206	0,029802	0,024037	0,002473	0,002014	0,001401	0,001393
36	0,022356	0,015947	0,006845	0,005053	0,011564	0,105075	0,002904	0,001988	0,001445	0,001297
37	0,024329	0,014199	0,006859	0,005265	0,006364	0,357147	0,003171	0,002017	0,001554	0,001241
38	0,031708	0,013944	0,006674	0,005140	0,005679	0,040402	0,002878	0,002282	0,001622	0,001264
39	0,050736	0,013474	0,006611	0,005209	0,004696	0,015474	0,002315	0,002675	0,001629	0,001356
40		0,014048	0,006962	0,005660	0,003753	0,006696	0,005790	0,002846	0,001608	0,001446
41		0,012737	0,007104	0,005209	0,003601	0,005077	0,014722	0,002509	0,001582	0,001469
42		0,012690	0,007427	0,005140	0,003580	0,004668	0,037552	0,002014	0,001587	0,001456
43		0,012646	0,009687	0,005265	0,003535	0,003866	0,357147	0,004905	0,001720	0,001429
44		0,012805	0,012375	0,005053	0,003338	0,003112	0,123811	0,012068	0,002042	0,001408
45		0,014048	0,027519	0,005206	0,003257	0,002988	0,032235	0,027747	0,002333	0,001438
46		0,014808	0,132892	0,005375	0,003403	0,002983	0,014189	0,106935	0,002357	0,001638
47		0,016745	0,357147	0,005443	0,003466	0,002968	0,006466	0,357147	0,001984	0,001951
48		0,020498	0,028336	0,005660	0,003322	0,002860	0,003911	0,042563	0,001608	0,002187
49		0,044511	0,007427	0,007229	0,003463	0,002711	0,003787	0,018585	0,003728	0,002156
50			0,008796	0,008859	0,003753	0,002754	0,003463	0,008733	0,008743	0,001777
51			0,007923	0,012835	0,003463	0,002906	0,002853	0,004169	0,018081	0,001443
52			0,007477	0,037535	0,003322	0,002814	0,002315	0,003318	0,040140	0,003288
53			0,007389	0,357147	0,003466	0,002718	0,002212	0,003318	0,357147	0,007587
54			0,007211	0,102017	0,003403	0,002871	0,002214	0,003011	0,121957	0,015236

Continued from table A.13.

	q									
y_σ	**4/3**	**5/3**	**7/3**	**8/3**	**10/3**	**11/3**	**13/3**	**14/3**	**16/3**	**17/3**
55			0,007110	0,018958	0,003257	0,003112	0,002223	0,002474	0,034184	0,030465
56			0,007427	0,005660	0,003338	0,002871	0,002193	0,002014	0,016918	0,108181
57			0,006739	0,006874	0,003535	0,002718	0,002058	0,001921	0,008580	0,357147
58			0,006722	0,006399	0,003580	0,002814	0,001956	0,001927	0,004196	0,044165
59			0,006411	0,005715	0,003601	0,002906	0,001993	0,001944	0,002675	0,021224
60			0,006380	0,005660	0,003753	0,002754	0,002118	0,001934	0,002728	0,011318
61			0,006730	0,005626	0,004696	0,002711	0,002142	0,001852	0,002710	0,005723
62			0,006773	0,005383	0,005679	0,002860	0,002005	0,001726	0,002406	0,002887
63			0,007427	0,005402	0,006364	0,002968	0,001987	0,001698	0,001967	0,002360
64			0,007723	0,005660	0,011564	0,002983	0,002142	0,001784	0,001608	0,002500
65			0,008159	0,005134	0,029802	0,002988	0,002315	0,001890	0,001525	0,002455
66			0,009714	0,005063	0,126877	0,003112	0,002142	0,001820	0,001529	0,002161
67			0,011547	0,005117	0,357147	0,003866	0,001987	0,001703	0,001550	0,001763
68			0,014889	0,004860	0,033841	0,004668	0,002005	0,001714	0,001559	0,001443
69			0,039129	0,005089	0,010669	0,005077	0,002142	0,001864	0,001532	0,001365
70				0,005111	0,003753	0,006696	0,002118	0,002014	0,001430	0,001369
71				0,005168	0,004622	0,015474	0,001993	0,001864	0,001333	0,001392
72				0,005660	0,004614	0,040402	0,001956	0,001714	0,001317	0,001407
73				0,005845	0,004004	0,357147	0,002058	0,001703	0,001386	0,001395
74				0,006051	0,003763	0,105075	0,002193	0,001820	0,001484	0,001329
75				0,006676	0,003753	0,024037	0,002223	0,001890	0,001491	0,001223
76				0,007999	0,003747	0,008420	0,002214	0,001784	0,001376	0,001171
77				0,008564	0,003637	0,003112	0,002212	0,001698	0,001308	0,001199
78				0,014674	0,003493	0,003872	0,002315	0,001726	0,001356	0,001286
79				0,037820	0,003590	0,004010	0,002853	0,001852	0,001493	0,001361
80					0,003753	0,003520	0,003463	0,001934	0,001608	0,001306
81					0,003408	0,003130	0,003787	0,001944	0,001493	0,001197

Continued from table A.13.

					q					
y_σ	**4/3**	**5/3**	**7/3**	**8/3**	**10/3**	**11/3**	**13/3**	**14/3**	**16/3**	**17/3**
82					0,003273	0,003101	0,003911	0,001927	0,001356	0,001152
83					0,003404	0,003121	0,006466	0,001921	0,001308	0,001211
84					0,003266	0,003101	0,014189	0,002014	0,001376	0,001342
85					0,003100	0,002943	0,032235	0,002474	0,001491	0,001443
86					0,003238	0,002862	0,123811	0,003011	0,001484	0,001342
87					0,003415	0,002976	0,357147	0,003318	0,001386	0,001211
88					0,003327	0,003112	0,037552	0,003318	0,001317	0,001152
89					0,003423	0,002825	0,014722	0,004169	0,001333	0,001197
90					0,003753	0,002679	0,005790	0,008733	0,001430	0,001306
91					0,003871	0,002779	0,002315	0,018585	0,001532	0,001361
92					0,003950	0,002823	0,002878	0,042563	0,001559	0,001286
93					0,004116	0,002621	0,003171	0,357147	0,001550	0,001199
94					0,004785	0,002604	0,002904	0,106935	0,001529	0,001171
95					0,005665	0,002803	0,002473	0,027747	0,001525	0,001223
96					0,005984	0,002814	0,002304	0,012068	0,001608	0,001329
97					0,007152	0,002736	0,002303	0,004905	0,001967	0,001395
98					0,015591	0,002838	0,002326	0,002014	0,002406	0,001407
99					0,036283	0,003112	0,002323	0,002509	0,002710	0,001392
100						0,003205	0,002240	0,002846	0,002728	0,001369
101						0,003249	0,002112	0,002675	0,002675	0,001365
102						0,003327	0,002106	0,002282	0,004196	0,001443
103						0,003650	0,002222	0,002017	0,008580	0,001763
104						0,004370	0,002315	0,001988	0,016918	0,002161
105						0,004830	0,002104	0,002014	0,034184	0,002455
106						0,004729	0,001953	0,002034	0,121957	0,002500
107						0,007430	0,001984	0,002013	0,357147	0,002360
108						0,016276	0,002108	0,001897	0,040140	0,002887

Continued from table A.13.

					q					
y_σ	**4/3**	**5/3**	**7/3**	**8/3**	**10/3**	**11/3**	**13/3**	**14/3**	**16/3**	**17/3**
109						0,035810	0,002031	0,001801	0,018081	0,005723
110							0,001874	0,001821	0,008743	0,011318
111							0,001860	0,001935	0,003728	0,021224
112							0,002008	0,002014	0,001608	0,044165
113							0,002118	0,001831	0,001984	0,357147
114							0,002036	0,001683	0,002357	0,108181
115							0,001999	0,001687	0,002333	0,030465
116							0,002108	0,001803	0,002042	0,015236
117							0,002315	0,001835	0,001720	0,007587
118							0,002389	0,001686	0,001587	0,003288
119							0,002412	0,001598	0,001582	0,001443
120							0,002433	0,001664	0,001608	0,001777
121							0,002525	0,001820	0,001629	0,002156
122							0,002914	0,001831	0,001622	0,002187
123							0,003477	0,001745	0,001554	0,001951
124							0,003808	0,001726	0,001445	0,001638
125							0,003687	0,001833	0,001401	0,001438
126							0,004266	0,002014	0,001449	0,001408
127							0,008679	0,002079	0,001551	0,001429
128							0,017698	0,002094	0,001608	0,001456
129							0,035170	0,002098	0,001464	0,001469
130								0,002141	0,001326	0,001446
131								0,002352	0,001293	0,001356
132								0,002822	0,001370	0,001264
133								0,003230	0,001471	0,001241
134								0,003273	0,001422	0,001297
135								0,003032	0,001292	0,001393

Continued from table A.13.

					q					
y_σ	**4/3**	**5/3**	**7/3**	**8/3**	**10/3**	**11/3**	**13/3**	**14/3**	**16/3**	**17/3**
136								0,004568	0,001224	0,001443
137								0,009443	0,001273	0,001314
138								0,018378	0,001402	0,001182
139								0,034947	0,001480	0,001137
140									0,001416	0,001194
141									0,001349	0,001297
142									0,001358	0,001322
143									0,001461	0,001209
145									0,001664	0,001098
146									0,001676	0,001187
147									0,001671	0,001309
148									0,001675	0,001320
149									0,001741	0,001247
150									0,002007	0,001192
151									0,002410	0,001211
152									0,002732	0,001310
153									0,002768	0,001443
154									0,002522	0,001495
155									0,002880	0,001505
156									0,005640	0,001496
157									0,011011	0,001490
158									0,019631	0,001521
159									0,034622	0,001678
160										0,002017
161										0,002362
162										0,002525
163										0,002385

Continued from table A.13.

	q									
$\mathbf{y}_{\sigma}$	**4/3**	**5/3**	**7/3**	**8/3**	**10/3**	**11/3**	**13/3**	**14/3**	**16/3**	**17/3**
164										0,002137
165										0,003145
166										0,006291
167										0,011776
168										0,020200
169										0,034500

Table A.14: Harmonic scattering coefficients σ_o for fractional slot windings with $m = 7$, normal zone span and $q_n = 2$.

	q									
$\mathbf{y}_\sigma$	**3/2**	**5/2**	**7/2**	**9/2**	**11/2**	**13/2**	**15/2**	**17/2**	**19/2**	**21/2**
1	0,022667	0,019007	0,018001	0,017588	0,017379	0,017259	0,017183	0,017133	0,017097	0,017072
2	0,011374	0,006915	0,007736	0,008898	0,009900	0,010713	0,011373	0,011913	0,012361	0,012738
3	0,007957	0,004535	0,003351	0,004325	0,005552	0,006678	0,007648	0,008472	0,009173	0,009774
4	0,008305	0,003817	0,002436	0,001994	0,002800	0,003854	0,004884	0,005820	0,006649	0,007379
5	0,008051	0,002906	0,002380	0,001527	0,001335	0,001979	0,002855	0,003757	0,004610	0,005392
6	0,007957	0,003092	0,001935	0,001652	0,001052	0,000965	0,001484	0,002213	0,002993	0,003757
7	0,007705	0,003034	0,001512	0,001509	0,001221	0,000774	0,000736	0,001161	0,001774	0,002450
8	0,007677	0,002943	0,001615	0,001187	0,001232	0,000943	0,000597	0,000585	0,000939	0,001460
9	0,007957	0,002927	0,001649	0,000938	0,001057	0,001029	0,000753	0,000478	0,000480	0,000779
10	0,007609	0,002906	0,001580	0,001000	0,000814	0,000961	0,000873	0,000617	0,000394	0,000404
11	0,007609	0,002808	0,001529	0,001055	0,000648	0,000790	0,000875	0,000749	0,000517	0,000333
12	0,007957	0,002812	0,001524	0,001039	0,000686	0,000602	0,000774	0,000795	0,000651	0,000440
13	0,007677	0,002793	0,001524	0,000982	0,000741	0,000481	0,000620	0,000750	0,000723	0,000571
14	0,007705	0,002797	0,001512	0,000946	0,000754	0,000505	0,000469	0,000641	0,000719	0,000658
15	0,007957	0,002906	0,001458	0,000943	0,000724	0,000555	0,000376	0,000504	0,000650	0,000682
16	0,008051	0,002769	0,001442	0,000947	0,000679	0,000581	0,000392	0,000380	0,000542	0,000648
17	0,008305	0,002771	0,001465	0,000948	0,000651	0,000573	0,000434	0,000306	0,000422	0,000570
18	0,007957	0,002771	0,001451	0,000938	0,000648	0,000542	0,000465	0,000316	0,000318	0,000467
19	0,011374	0,002769	0,001422	0,000902	0,000651	0,000504	0,000472	0,000352	0,000256	0,000361
20	0,022667	0,002906	0,001456	0,000882	0,000656	0,000482	0,000456	0,000384	0,000263	0,000272
21		0,002797	0,001512	0,000891	0,000656	0,000478	0,000426	0,000399	0,000293	0,000221
22		0,002793	0,001440	0,000911	0,000648	0,000481	0,000394	0,000395	0,000325	0,000224
23		0,002812	0,001407	0,000900	0,000621	0,000485	0,000376	0,000376	0,000344	0,000250
24		0,002808	0,001442	0,000870	0,000602	0,000489	0,000371	0,000348	0,000349	0,000280
25		0,002906	0,001442	0,000870	0,000600	0,000488	0,000373	0,000321	0,000339	0,000302
26		0,002927	0,001407	0,000905	0,000615	0,000481	0,000377	0,000305	0,000318	0,000311
27		0,002943	0,001440	0,000938	0,000630	0,000460	0,000381	0,000300	0,000293	0,000309

Continued from table A.14.

					q					
y_σ	**3/2**	**5/2**	**7/2**	**9/2**	**11/2**	**13/2**	**15/2**	**17/2**	**19/2**	**21/2**
28		0,003034	0,001512	0,000893	0,000621	0,000442	0,000384	0,000301	0,000269	0,000296
29		0,003092	0,001456	0,000856	0,000594	0,000436	0,000383	0,000304	0,000255	0,000275
30		0,002906	0,001422	0,000862	0,000582	0,000442	0,000376	0,000309	0,000250	0,000252
31		0,003817	0,001451	0,000895	0,000596	0,000457	0,000359	0,000312	0,000250	0,000232
32		0,004535	0,001465	0,000895	0,000626	0,000469	0,000343	0,000314	0,000253	0,000219
33		0,006915	0,001442	0,000862	0,000648	0,000461	0,000334	0,000312	0,000257	0,000214
34		0,019007	0,001458	0,000856	0,000617	0,000438	0,000335	0,000306	0,000261	0,000214
35			0,001512	0,000893	0,000583	0,000422	0,000345	0,000291	0,000263	0,000216
36			0,001524	0,000938	0,000573	0,000422	0,000358	0,000277	0,000264	0,000219
37			0,001524	0,000905	0,000591	0,000440	0,000367	0,000267	0,000263	0,000223
38			0,001529	0,000870	0,000619	0,000466	0,000360	0,000265	0,000256	0,000226
39			0,001580	0,000870	0,000619	0,000481	0,000341	0,000270	0,000244	0,000228
40			0,001649	0,000900	0,000591	0,000458	0,000324	0,000280	0,000231	0,000228
41			0,001615	0,000911	0,000573	0,000429	0,000318	0,000292	0,000221	0,000226
42			0,001512	0,000891	0,000583	0,000412	0,000325	0,000299	0,000217	0,000221
43			0,001935	0,000882	0,000617	0,000416	0,000344	0,000293	0,000219	0,000210
44			0,002380	0,000902	0,000648	0,000437	0,000365	0,000277	0,000226	0,000198
45			0,002436	0,000938	0,000626	0,000460	0,000376	0,000260	0,000236	0,000189
46			0,003351	0,000948	0,000596	0,000460	0,000358	0,000251	0,000246	0,000183
47			0,007736	0,000947	0,000582	0,000437	0,000333	0,000251	0,000252	0,000182
48			0,018001	0,000943	0,000594	0,000416	0,000315	0,000262	0,000246	0,000186
49				0,000946	0,000621	0,000412	0,000310	0,000280	0,000232	0,000194
50				0,000982	0,000630	0,000429	0,000321	0,000297	0,000216	0,000204
51				0,001039	0,000615	0,000458	0,000341	0,000306	0,000205	0,000213
52				0,001055	0,000600	0,000481	0,000360	0,000292	0,000202	0,000217
53				0,001000	0,000602	0,000466	0,000360	0,000270	0,000207	0,000212
54				0,000938	0,000621	0,000440	0,000341	0,000252	0,000219	0,000200

Continued from table A.14.

				q						
y_σ	**3/2**	**5/2**	**7/2**	**9/2**	**11/2**	**13/2**	**15/2**	**17/2**	**19/2**	**21/2**
55				0,001187	0,000648	0,000422	0,000321	0,000243	0,000235	0,000185
56				0,001509	0,000656	0,000422	0,000310	0,000245	0,000250	0,000174
57				0,001652	0,000656	0,000438	0,000315	0,000259	0,000256	0,000168
58				0,001527	0,000651	0,000461	0,000333	0,000278	0,000245	0,000168
59				0,001994	0,000648	0,000469	0,000358	0,000293	0,000226	0,000176
60				0,004325	0,000651	0,000457	0,000376	0,000293	0,000209	0,000188
61				0,008898	0,000679	0,000442	0,000365	0,000278	0,000198	0,000203
62				0,017588	0,000724	0,000436	0,000344	0,000259	0,000195	0,000216
63					0,000754	0,000442	0,000325	0,000245	0,000202	0,000221
64					0,000741	0,000460	0,000318	0,000243	0,000216	0,000211
65					0,000686	0,000481	0,000324	0,000252	0,000233	0,000195
66					0,000648	0,000488	0,000341	0,000270	0,000247	0,000179
67					0,000814	0,000489	0,000360	0,000292	0,000247	0,000166
68					0,001057	0,000485	0,000367	0,000306	0,000233	0,000160
69					0,001232	0,000481	0,000358	0,000297	0,000216	0,000163
70					0,001221	0,000478	0,000345	0,000280	0,000202	0,000172
71					0,001052	0,000482	0,000335	0,000262	0,000195	0,000186
72					0,001335	0,000504	0,000334	0,000251	0,000198	0,000201
73					0,002800	0,000542	0,000343	0,000251	0,000209	0,000213
74					0,005552	0,000573	0,000359	0,000260	0,000226	0,000213
75					0,009900	0,000581	0,000376	0,000277	0,000245	0,000201
76					0,017379	0,000555	0,000383	0,000293	0,000256	0,000186
77						0,000505	0,000384	0,000299	0,000250	0,000172
78						0,000481	0,000381	0,000292	0,000235	0,000163
79						0,000602	0,000377	0,000280	0,000219	0,000160
80						0,000790	0,000373	0,000270	0,000207	0,000166
81						0,000961	0,000371	0,000265	0,000202	0,000179

Continued from table A.14.

					q					
y_σ	**3/2**	**5/2**	**7/2**	**9/2**	**11/2**	**13/2**	**15/2**	**17/2**	**19/2**	**21/2**
82						0,001029	0,000376	0,000267	0,000205	0,000195
83						0,000943	0,000394	0,000277	0,000216	0,000211
84						0,000774	0,000426	0,000291	0,000232	0,000221
85						0,000965	0,000456	0,000306	0,000246	0,000216
86						0,001979	0,000472	0,000312	0,000252	0,000203
87						0,003854	0,000465	0,000314	0,000246	0,000188
88						0,006678	0,000434	0,000312	0,000236	0,000176
89						0,010713	0,000392	0,000309	0,000226	0,000168
90						0,017259	0,000376	0,000304	0,000219	0,000168
91							0,000469	0,000301	0,000217	0,000174
92							0,000620	0,000300	0,000221	0,000185
93							0,000774	0,000305	0,000231	0,000200
94							0,000875	0,000321	0,000244	0,000212
95							0,000873	0,000348	0,000256	0,000217
96							0,000753	0,000376	0,000263	0,000213
97							0,000597	0,000395	0,000264	0,000204
98							0,000736	0,000399	0,000263	0,000194
99							0,001484	0,000384	0,000261	0,000186
100							0,002855	0,000352	0,000257	0,000182
101							0,004884	0,000316	0,000253	0,000183
102							0,007648	0,000306	0,000250	0,000189
103							0,011373	0,000380	0,000250	0,000198
104							0,017183	0,000504	0,000255	0,000210
105								0,000641	0,000269	0,000221
106								0,000750	0,000293	0,000226
107								0,000795	0,000318	0,000228
108								0,000749	0,000339	0,000228

Continued from table A.14.

	q									
y_σ	**3/2**	**5/2**	**7/2**	**9/2**	**11/2**	**13/2**	**15/2**	**17/2**	**19/2**	**21/2**
109								0,000617	0,000349	0,000226
110								0,000478	0,000344	0,000223
111								0,000585	0,000325	0,000219
112								0,001161	0,000293	0,000216
113								0,002213	0,000263	0,000214
114								0,003757	0,000256	0,000214
115								0,005820	0,000318	0,000219
116								0,008472	0,000422	0,000232
117								0,011913	0,000542	0,000252
118								0,017133	0,000650	0,000275
119									0,000719	0,000296
120									0,000723	0,000309
121									0,000651	0,000311
122									0,000517	0,000302
123									0,000394	0,000280
124									0,000480	0,000250
125									0,000939	0,000224
126									0,001774	0,000221
127									0,002993	0,000272
128									0,004610	0,000361
129									0,006649	0,000467
130									0,009173	0,000570
131									0,012361	0,000648
132									0,017097	0,000682
133										0,000658
134										0,000571
135										0,000440

Continued from table A.14.

	q									
$\mathbf{y}_\sigma$	**3/2**	**5/2**	**7/2**	**9/2**	**11/2**	**13/2**	**15/2**	**17/2**	**19/2**	**21/2**
136										0,000333
137										0,000404
138										0,000779
139										0,001460
140										0,002450
141										0,003757
142										0,005392
143										0,007379
144										0,009774
145										0,012738
146										0,017072

Table A.15: Harmonic scattering coefficients σ_o for fractional slot windings with $m = 7$, normal zone span and $q_n = 3$.

	q									
y_σ	**4/3**	**5/3**	**7/3**	**8/3**	**10/3**	**11/3**	**13/3**	**14/3**	**16/3**	**17/3**
1	0,025535	0,022436	0,019747	0,019092	0,018322	0,018085	0,017764	0,017652	0,017489	0,017428
2	0,015956	0,010264	0,007396	0,007285	0,007756	0,008107	0,008837	0,009186	0,009829	0,010121
3	0,011783	0,008187	0,005856	0,004282	0,003503	0,003630	0,004251	0,004637	0,005433	0,005823
4	0,010367	0,007285	0,004791	0,004008	0,003035	0,002349	0,002056	0,002193	0,002718	0,003043
5	0,010112	0,006572	0,003945	0,003213	0,002856	0,002455	0,001862	0,001491	0,001363	0,001481
6	0,009895	0,006456	0,003731	0,002978	0,002312	0,002156	0,001948	0,001676	0,001264	0,001037
7	0,010041	0,006369	0,003417	0,002834	0,001970	0,001724	0,001724	0,001632	0,001428	0,001224
8	0,010367	0,006378	0,003362	0,002610	0,001946	0,001623	0,001377	0,001363	0,001386	0,001297
9	0,009877	0,006341	0,003334	0,002574	0,001842	0,001613	0,001190	0,001088	0,001170	0,001175
10	0,009597	0,006572	0,003260	0,002560	0,001703	0,001522	0,001206	0,001030	0,000925	0,000951
11	0,009874	0,006257	0,003270	0,002525	0,001677	0,001410	0,001188	0,001053	0,000805	0,000758
12	0,010367	0,006251	0,003303	0,002492	0,001673	0,001389	0,001113	0,001032	0,000827	0,000718
13	0,010253	0,006245	0,003296	0,002535	0,001664	0,001388	0,001031	0,000964	0,000842	0,000749
14	0,010367	0,006265	0,003417	0,002501	0,001623	0,001385	0,001014	0,000894	0,000814	0,000758
15	0,010593	0,006572	0,003252	0,002516	0,001605	0,001363	0,001014	0,000878	0,000756	0,000729
16	0,010367	0,006459	0,003250	0,002610	0,001635	0,001331	0,001015	0,000879	0,000700	0,000675
17	0,016304	0,006555	0,003171	0,002483	0,001645	0,001340	0,001009	0,000882	0,000686	0,000625
18	0,071015	0,006594	0,003168	0,002466	0,001611	0,001371	0,000982	0,000880	0,000687	0,000612
19	0,165809	0,006832	0,003251	0,002481	0,001643	0,001347	0,000960	0,000863	0,000691	0,000612
20	0,010367	0,006572	0,003256	0,002417	0,001703	0,001325	0,000968	0,000837	0,000692	0,000617
21	0,012267	0,009480	0,003417	0,002478	0,001620	0,001360	0,000993	0,000831	0,000687	0,000619
22	0,011562	0,016492	0,003354	0,002472	0,001586	0,001410	0,000996	0,000849	0,000666	0,000617
23	0,010686	0,165809	0,003376	0,002487	0,001620	0,001342	0,000964	0,000870	0,000646	0,000604
24	0,010367	0,045490	0,003411	0,002610	0,001585	0,001304	0,000961	0,000852	0,000643	0,000582
25	0,009935	0,006572	0,003424	0,002559	0,001544	0,001329	0,000996	0,000825	0,000657	0,000571
26	0,009683	0,008211	0,003490	0,002556	0,001581	0,001341	0,001031	0,000829	0,000677	0,000577
27	0,009929	0,007241	0,003587	0,002605	0,001621	0,001290	0,000981	0,000863	0,000677	0,000595

Continued from table A.15.

	q									
y_σ	**4/3**	**5/3**	**7/3**	**8/3**	**10/3**	**11/3**	**13/3**	**14/3**	**16/3**	**17/3**
28	0,010367	0,006957	0,003417	0,002610	0,001592	0,001288	0,000943	0,000894	0,000650	0,000610
29	0,009929	0,006698	0,004607	0,002617	0,001622	0,001339	0,000950	0,000850	0,000635	0,000596
30	0,009683	0,006572	0,005829	0,002718	0,001703	0,001334	0,000982	0,000813	0,000647	0,000571
31	0,009935	0,006317	0,012958	0,002757	0,001671	0,001311	0,000962	0,000813	0,000678	0,000561
32	0,010367	0,006277	0,062963	0,002610	0,001651	0,001343	0,000923	0,000842	0,000700	0,000576
33	0,010686	0,006291	0,165809	0,003453	0,001681	0,001410	0,000921	0,000851	0,000667	0,000605
34	0,011562	0,006281	0,013344	0,004272	0,001702	0,001383	0,000959	0,000813	0,000632	0,000625
35	0,012267	0,006572	0,003417	0,005948	0,001703	0,001360	0,000983	0,000792	0,000622	0,000595
36	0,010367	0,006281	0,004515	0,017779	0,001703	0,001377	0,000956	0,000810	0,000642	0,000562
37	0,165809	0,006291	0,003998	0,165809	0,001740	0,001409	0,000948	0,000849	0,000668	0,000549
38	0,071015	0,006277	0,003879	0,048254	0,001822	0,001412	0,000982	0,000846	0,000656	0,000563
39	0,016304	0,006317	0,003740	0,008960	0,001802	0,001408	0,001031	0,000820	0,000622	0,000590
40	0,010367	0,006572	0,003532	0,002610	0,001703	0,001412	0,001013	0,000817	0,000606	0,000596
41	0,010593	0,006698	0,003468	0,003539	0,002205	0,001471	0,000989	0,000850	0,000620	0,000568
42	0,010367	0,006957	0,003417	0,003244	0,002749	0,001531	0,000990	0,000894	0,000653	0,000542
43	0,010253	0,007241	0,003284	0,002893	0,002983	0,001495	0,001017	0,000878	0,000669	0,000541
44	0,010367	0,008211	0,003273	0,002909	0,005387	0,001410	0,001033	0,000855	0,000647	0,000565
45	0,009874	0,006572	0,003192	0,002760	0,014212	0,001813	0,001033	0,000851	0,000629	0,000595
46	0,009597	0,045490	0,003202	0,002672	0,060094	0,002276	0,001028	0,000871	0,000635	0,000593
47	0,009877	0,165809	0,003266	0,002643	0,165809	0,002440	0,001028	0,000894	0,000666	0,000570
48	0,010367	0,016492	0,003265	0,002610	0,016137	0,003069	0,001055	0,000898	0,000700	0,000556
49	0,010041	0,009480	0,003417	0,002510	0,004987	0,007304	0,001116	0,000894	0,000690	0,000565
50	0,009895	0,006572	0,003265	0,002498	0,001703	0,019303	0,001141	0,000888	0,000669	0,000595
51	0,010112	0,006832	0,003266	0,002489	0,002369	0,165809	0,001091	0,000893	0,000659	0,000625
52	0,010367	0,006594	0,003202	0,002439	0,002355	0,049704	0,001031	0,000935	0,000668	0,000616
53	0,011783	0,006555	0,003192	0,002499	0,001983	0,011521	0,001313	0,000988	0,000690	0,000596
54	0,015956	0,006459	0,003273	0,002475	0,001936	0,003931	0,001675	0,000999	0,000704	0,000584

Continued from table A.15.

	q									
y_σ	**4/3**	**5/3**	**7/3**	**8/3**	**10/3**	**11/3**	**13/3**	**14/3**	**16/3**	**17/3**
55	0,025535	0,006572	0,003284	0,002493	0,001949	0,001410	0,001851	0,000945	0,000705	0,000589
56		0,006265	0,003417	0,002610	0,001854	0,001988	0,001819	0,000894	0,000700	0,000608
57		0,006245	0,003468	0,002493	0,001758	0,002060	0,002973	0,001134	0,000695	0,000626
58		0,006251	0,003532	0,002475	0,001735	0,001746	0,006733	0,001456	0,000696	0,000630
59		0,006257	0,003740	0,002499	0,001724	0,001562	0,015499	0,001640	0,000718	0,000628
60		0,006572	0,003879	0,002439	0,001703	0,001613	0,058632	0,001585	0,000765	0,000622
61		0,006341	0,003998	0,002489	0,001636	0,001583	0,165809	0,001885	0,000800	0,000619
62		0,006378	0,004515	0,002498	0,001616	0,001490	0,018022	0,004083	0,000792	0,000624
63		0,006369	0,003417	0,002510	0,001633	0,001443	0,007033	0,008907	0,000738	0,000655
64		0,006456	0,013344	0,002610	0,001591	0,001433	0,002667	0,020439	0,000700	0,000700
65		0,006572	0,165809	0,002643	0,001562	0,001427	0,001031	0,165809	0,000884	0,000726
66		0,007285	0,062963	0,002672	0,001601	0,001410	0,001469	0,050588	0,001148	0,000711
67		0,008187	0,012958	0,002760	0,001627	0,001354	0,001640	0,013400	0,001339	0,000658
68		0,010264	0,005829	0,002909	0,001592	0,001333	0,001453	0,005765	0,001340	0,000625
69		0,022436	0,004607	0,002893	0,001627	0,001349	0,001197	0,002251	0,001231	0,000787
70			0,003417	0,003244	0,001703	0,001344	0,001168	0,000894	0,001901	0,001027
71			0,003587	0,003539	0,001627	0,001299	0,001211	0,001280	0,004034	0,001216
72			0,003490	0,002610	0,001592	0,001306	0,001191	0,001479	0,008138	0,001244
73			0,003424	0,008960	0,001627	0,001351	0,001120	0,001350	0,016523	0,001118
74			0,003411	0,048254	0,001601	0,001333	0,001063	0,001104	0,057747	0,001286
75			0,003376	0,165809	0,001562	0,001309	0,001050	0,000987	0,165809	0,002643
76			0,003354	0,017779	0,001591	0,001347	0,001048	0,001034	0,019337	0,005398
77			0,003417	0,005948	0,001633	0,001410	0,001045	0,001051	0,008741	0,010267
78			0,003256	0,004272	0,001616	0,001347	0,001031	0,001010	0,004147	0,021276
79			0,003251	0,003453	0,001636	0,001309	0,000989	0,000945	0,001686	0,165809
80			0,003168	0,002610	0,001703	0,001333	0,000967	0,000913	0,000700	0,051181
81			0,003171	0,002757	0,001724	0,001351	0,000974	0,000907	0,001005	0,014778

Continued from table A.15.

					q					
y_σ	**4/3**	**5/3**	**7/3**	**8/3**	**10/3**	**11/3**	**13/3**	**14/3**	**16/3**	**17/3**
82			0,003250	0,002718	0,001735	0,001306	0,000991	0,000907	0,001230	0,007372
83			0,003252	0,002617	0,001758	0,001299	0,000964	0,000906	0,001191	0,003591
84			0,003417	0,002610	0,001854	0,001344	0,000931	0,000894	0,000997	0,001480
85			0,003296	0,002605	0,001949	0,001349	0,000937	0,000857	0,000811	0,000625
86			0,003303	0,002556	0,001936	0,001333	0,000973	0,000835	0,000788	0,000898
87			0,003270	0,002559	0,001983	0,001354	0,000986	0,000839	0,000834	0,001129
88			0,003260	0,002610	0,002355	0,001410	0,000952	0,000856	0,000847	0,001125
89			0,003334	0,002487	0,002369	0,001427	0,000947	0,000852	0,000815	0,000961
90			0,003362	0,002472	0,001703	0,001433	0,000986	0,000817	0,000761	0,000771
91			0,003417	0,002478	0,004987	0,001443	0,001031	0,000803	0,000720	0,000687
92			0,003731	0,002417	0,016137	0,001490	0,000986	0,000825	0,000711	0,000726
93			0,003945	0,002481	0,165809	0,001583	0,000947	0,000858	0,000711	0,000759
94			0,004791	0,002466	0,060094	0,001613	0,000952	0,000844	0,000713	0,000751
95			0,005856	0,002483	0,014212	0,001562	0,000986	0,000815	0,000711	0,000710
96			0,007396	0,002610	0,005387	0,001746	0,000973	0,000816	0,000700	0,000661
97			0,019747	0,002516	0,002983	0,002060	0,000937	0,000855	0,000671	0,000637
98				0,002501	0,002749	0,001988	0,000931	0,000894	0,000650	0,000632
99				0,002535	0,002205	0,001410	0,000964	0,000855	0,000648	0,000634
100				0,002492	0,001703	0,003931	0,000991	0,000816	0,000662	0,000636
101				0,002525	0,001802	0,011521	0,000974	0,000815	0,000674	0,000635
102				0,002560	0,001822	0,049704	0,000967	0,000844	0,000656	0,000625
103				0,002574	0,001740	0,165809	0,000989	0,000858	0,000626	0,000598
104				0,002610	0,001703	0,019303	0,001031	0,000825	0,000617	0,000578
105				0,002834	0,001703	0,007304	0,001045	0,000803	0,000634	0,000574
106				0,002978	0,001702	0,003069	0,001048	0,000817	0,000663	0,000586
107				0,003213	0,001681	0,002440	0,001050	0,000852	0,000670	0,000601
108				0,004008	0,001651	0,002276	0,001063	0,000856	0,000642	0,000597

Continued from table A.15.

					q					
y_σ	**4/3**	**5/3**	**7/3**	**8/3**	**10/3**	**11/3**	**13/3**	**14/3**	**16/3**	**17/3**
109				0,004282	0,001671	0,001813	0,001120	0,000839	0,000624	0,000568
110				0,007285	0,001703	0,001410	0,001191	0,000835	0,000636	0,000549
111				0,019092	0,001622	0,001495	0,001211	0,000857	0,000671	0,000553
112					0,001592	0,001531	0,001168	0,000894	0,000700	0,000577
113					0,001621	0,001471	0,001197	0,000906	0,000671	0,000601
114					0,001581	0,001412	0,001453	0,000907	0,000636	0,000591
115					0,001544	0,001408	0,001640	0,000907	0,000624	0,000564
116					0,001585	0,001412	0,001469	0,000913	0,000642	0,000551
117					0,001620	0,001409	0,001031	0,000945	0,000670	0,000565
118					0,001586	0,001377	0,002667	0,001010	0,000663	0,000599
119					0,001620	0,001360	0,007033	0,001051	0,000634	0,000625
120					0,001703	0,001383	0,018022	0,001034	0,000617	0,000599
121					0,001643	0,001410	0,165809	0,000987	0,000626	0,000565
122					0,001611	0,001343	0,058632	0,001104	0,000656	0,000551
123					0,001645	0,001311	0,015499	0,001350	0,000674	0,000564
124					0,001635	0,001334	0,006733	0,001479	0,000662	0,000591
125					0,001605	0,001339	0,002973	0,001280	0,000648	0,000601
126					0,001623	0,001288	0,001819	0,000894	0,000650	0,000577
127					0,001664	0,001290	0,001851	0,002251	0,000671	0,000553
128					0,001673	0,001341	0,001675	0,005765	0,000700	0,000549
129					0,001677	0,001329	0,001313	0,013400	0,000711	0,000568
130					0,001703	0,001304	0,001031	0,050588	0,000713	0,000597
131					0,001842	0,001342	0,001091	0,165809	0,000711	0,000601
132					0,001946	0,001410	0,001141	0,020439	0,000711	0,000586
133					0,001970	0,001360	0,001116	0,008907	0,000720	0,000574
134					0,002312	0,001325	0,001055	0,004083	0,000761	0,000578
135					0,002856	0,001347	0,001028	0,001885	0,000815	0,000598

Continued from table A.15.

	q									
y_σ	**4/3**	**5/3**	**7/3**	**8/3**	**10/3**	**11/3**	**13/3**	**14/3**	**16/3**	**17/3**
136					0,003035	0,001371	0,001028	0,001585	0,000847	0,000625
137					0,003503	0,001340	0,001033	0,001640	0,000834	0,000635
138					0,007756	0,001331	0,001033	0,001456	0,000788	0,000636
139					0,018322	0,001363	0,001017	0,001134	0,000811	0,000634
140						0,001385	0,000990	0,000894	0,000997	0,000632
141						0,001388	0,000989	0,000945	0,001191	0,000637
142						0,001389	0,001013	0,000999	0,001230	0,000661
143						0,001410	0,001031	0,000988	0,001005	0,000710
144						0,001522	0,000982	0,000935	0,000700	0,000751
145						0,001613	0,000948	0,000893	0,001686	0,000759
146						0,001623	0,000956	0,000888	0,004147	0,000726
147						0,001724	0,000983	0,000894	0,008741	0,000687
148						0,002156	0,000959	0,000898	0,019337	0,000771
149						0,002455	0,000921	0,000894	0,165809	0,000961
150						0,002349	0,000923	0,000871	0,057747	0,001125
151						0,003630	0,000962	0,000851	0,016523	0,001129
152						0,008107	0,000982	0,000855	0,008138	0,000898
153						0,018085	0,000950	0,000878	0,004034	0,000625
154							0,000943	0,000894	0,001901	0,001480
155							0,000981	0,000850	0,001231	0,003591
156							0,001031	0,000817	0,001340	0,007372
157							0,000996	0,000820	0,001339	0,014778
158							0,000961	0,000846	0,001148	0,051181
159							0,000964	0,000849	0,000884	0,165809
160							0,000996	0,000810	0,000700	0,021276
161							0,000993	0,000792	0,000738	0,010267
162							0,000968	0,000813	0,000792	0,005398

Continued from table A.15.

	q									
y_σ	**4/3**	**5/3**	**7/3**	**8/3**	**10/3**	**11/3**	**13/3**	**14/3**	**16/3**	**17/3**
163							0,000960	0,000851	0,000800	0,002643
164							0,000982	0,000842	0,000765	0,001286
165							0,001009	0,000813	0,000718	0,001118
166							0,001015	0,000813	0,000696	0,001244
167							0,001014	0,000850	0,000695	0,001216
168							0,001014	0,000894	0,000700	0,001027
169							0,001031	0,000863	0,000705	0,000787
170							0,001113	0,000829	0,000704	0,000625
171							0,001188	0,000825	0,000690	0,000658
172							0,001206	0,000852	0,000668	0,000711
173							0,001190	0,000870	0,000659	0,000726
174							0,001377	0,000849	0,000669	0,000700
175							0,001724	0,000831	0,000690	0,000655
176							0,001948	0,000837	0,000700	0,000624
177							0,001862	0,000863	0,000666	0,000619
178							0,002056	0,000880	0,000635	0,000622
179							0,004251	0,000882	0,000629	0,000628
180							0,008837	0,000879	0,000647	0,000630
181							0,017764	0,000878	0,000669	0,000626
182								0,000894	0,000653	0,000608
183								0,000964	0,000620	0,000589
184								0,001032	0,000606	0,000584
185								0,001053	0,000622	0,000596
186								0,001030	0,000656	0,000616
187								0,001088	0,000668	0,000625
188								0,001363	0,000642	0,000595
189								0,001632	0,000622	0,000565

Continued from table A.15.

				q						
$\mathbf{y}_\sigma$	**4/3**	**5/3**	**7/3**	**8/3**	**10/3**	**11/3**	**13/3**	**14/3**	**16/3**	**17/3**
190								0,001676	0,000632	0,000556
191								0,001491	0,000667	0,000570
192								0,002193	0,000700	0,000593
193								0,004637	0,000678	0,000595
194								0,009186	0,000647	0,000565
195								0,017652	0,000635	0,000541
196									0,000650	0,000542
197									0,000677	0,000568
198									0,000677	0,000596
199									0,000657	0,000590
200									0,000643	0,000563
201									0,000646	0,000549
202									0,000666	0,000562
203									0,000687	0,000595
204									0,000692	0,000625
205									0,000691	0,000605
206									0,000687	0,000576
207									0,000686	0,000561
208									0,000700	0,000571
209									0,000756	0,000596
210									0,000814	0,000610
211									0,000842	0,000595
212									0,000827	0,000577
213									0,000805	0,000571
214									0,000925	0,000582
215									0,001170	0,000604

Continued from table A.15.

	q									
y_σ	**4/3**	**5/3**	**7/3**	**8/3**	**10/3**	**11/3**	**13/3**	**14/3**	**16/3**	**17/3**
216									0,001386	0,000617
217									0,001428	0,000619
218									0,001264	0,000617
219									0,001363	0,000612
220									0,002718	0,000612
221									0,005433	0,000625
222									0,009829	0,000675
223									0,017489	0,000729
224										0,000758
225										0,000749
226										0,000718
227										0,000758
228										0,000951
229										0,001175
230										0,001297
231										0,001224
232										0,001037
233										0,001481
234										0,003043
235										0,005823
236										0,010121
237										0,017428

Table A.16: Harmonic scattering coefficients σ_o for fractional slot windings with $m = 3$, double zone span and $q_n = 2$.

	q									
$\mathbf{y}_\sigma$	**3/2**	**5/2**	**7/2**	**9/2**	**11/2**	**13/2**	**15/2**	**17/2**	**19/2**	**21/2**
1	0,462164	0,462164	0,462164	0,462164	0,462164	0,462164	0,462164	0,462164	0,462164	0,462164
2	0,241897	0,298991	0,335162	0,358628	0,374894	0,386787	0,395848	0,402973	0,408722	0,413455
3	0,140271	0,207426	0,257014	0,291548	0,316461	0,335152	0,349650	0,361206	0,370625	0,378446
4	0,058151	0,144476	0,199003	0,239269	0,269458	0,292693	0,311043	0,325867	0,338076	0,348297
5	0,058151	0,095559	0,153390	0,196463	0,229818	0,256121	0,277265	0,294575	0,308979	0,321137
6	0,140271	0,048172	0,115855	0,160577	0,195744	0,224057	0,247201	0,266395	0,282531	0,296264
7	0,241897	0,022457	0,082664	0,129828	0,166101	0,195684	0,220220	0,240819	0,258308	0,273313
8	0,462164	0,022457	0,049521	0,102625	0,139997	0,170402	0,195880	0,217501	0,236029	0,252050
9		0,048172	0,025159	0,077283	0,116610	0,147702	0,173823	0,196171	0,215482	0,232303
10		0,095559	0,012532	0,051793	0,095103	0,127107	0,153732	0,176599	0,196489	0,213929
11		0,144476	0,012532	0,030688	0,074544	0,108138	0,135307	0,158574	0,178893	0,196805
12		0,207426	0,025159	0,015955	0,053824	0,090282	0,118247	0,141896	0,162547	0,180819
13		0,298991	0,049521	0,008436	0,035593	0,072963	0,102239	0,126364	0,147310	0,165864
14		0,462164	0,082664	0,008436	0,021208	0,055503	0,086941	0,111769	0,133040	0,151837
15			0,115855	0,015955	0,011354	0,039585	0,071969	0,097893	0,119593	0,138634
16			0,153390	0,030688	0,006360	0,026162	0,056880	0,084494	0,106819	0,126152
17			0,199003	0,051793	0,006360	0,015775	0,042807	0,071304	0,094555	0,114281
18			0,257014	0,077283	0,011354	0,008724	0,030442	0,058018	0,082627	0,102908
19			0,335162	0,102625	0,021208	0,005165	0,020212	0,045432	0,070837	0,091911
20			0,462164	0,129828	0,035593	0,005165	0,012374	0,034066	0,058967	0,081156
21				0,160577	0,053824	0,008724	0,007081	0,024258	0,047600	0,070497
22				0,196463	0,074544	0,015775	0,004415	0,016225	0,037132	0,059770
23				0,239269	0,095103	0,026162	0,004415	0,010105	0,027835	0,049414
24				0,291548	0,116610	0,039585	0,007081	0,005985	0,019891	0,039740
25				0,358628	0,139997	0,055503	0,012374	0,003914	0,013424	0,030967
26				0,462164	0,166101	0,072963	0,020212	0,003914	0,008516	0,023249
27					0,195744	0,090282	0,030442	0,005985	0,005218	0,016696

Continued from table A.16.

	q									
$\mathbf{y}_\sigma$	**3/2**	**5/2**	**7/2**	**9/2**	**11/2**	**13/2**	**15/2**	**17/2**	**19/2**	**21/2**
28					0,229818	0,108138	0,042807	0,010105	0,003563	0,011383
29					0,269458	0,127107	0,056880	0,016225	0,003563	0,007360
30					0,316461	0,147702	0,071969	0,024258	0,005218	0,004661
31					0,374894	0,170402	0,086941	0,034066	0,008516	0,003307
32					0,462164	0,195684	0,102239	0,045432	0,013424	0,003307
33						0,224057	0,118247	0,058018	0,019891	0,004661
34						0,256121	0,135307	0,071304	0,027835	0,007360
35						0,292693	0,153732	0,084494	0,037132	0,011383
36						0,335152	0,173823	0,097893	0,047600	0,016696
37						0,386787	0,195880	0,111769	0,058967	0,023249
38						0,462164	0,220220	0,126364	0,070837	0,030967
39							0,247201	0,141896	0,082627	0,039740
40							0,277265	0,158574	0,094555	0,049414
41							0,311043	0,176599	0,106819	0,059770
42							0,349650	0,196171	0,119593	0,070497
43							0,395848	0,217501	0,133040	0,081156
44							0,462164	0,240819	0,147310	0,091911
45								0,266395	0,162547	0,102908
46								0,294575	0,178893	0,114281
47								0,325867	0,196489	0,126152
48								0,361206	0,215482	0,138634
49								0,402973	0,236029	0,151837
50								0,462164	0,258308	0,165864
51									0,282531	0,180819
52									0,308979	0,196805
53									0,338076	0,213929
54									0,370625	0,232303

Continued from table A.16.

					q					
y_σ	**3/2**	**5/2**	**7/2**	**9/2**	**11/2**	**13/2**	**15/2**	**17/2**	**19/2**	**21/2**
55									0,408722	0,252050
56									0,462164	0,273313
57										0,296264
58										0,321137
59										0,348297
60										0,378446
61										0,413455
62										0,462164

Table A.17: Harmonic scattering coefficients σ_o for fractional slot windings with $m = 3$, double zone span and $q_n = 5$.

	q									
y_σ	**6/5**	**7/5**	**8/5**	**9/5**	**11/5**	**12/5**	**13/5**	**14/5**	**16/5**	**17/5**
1	0,554646	0,529432	0,513333	0,502416	0,488962	0,484642	0,481290	0,478637	0,474756	0,473312
2	0,301226	0,292244	0,292156	0,296018	0,307855	0,314233	0,320475	0,326452	0,337421	0,342399
3	0,190421	0,185560	0,187407	0,193378	0,210538	0,219872	0,229113	0,238061	0,254729	0,262392
4	0,216785	0,129073	0,110277	0,123764	0,145211	0,155558	0,165750	0,175694	0,194545	0,203371
5	0,448328	0,181689	0,099241	0,085684	0,091181	0,104962	0,116857	0,127766	0,147821	0,157167
6	1,221355	0,359714	0,167838	0,104352	0,059723	0,062239	0,071623	0,086036	0,109080	0,119107
7	35,554090	0,866418	0,313941	0,186443	0,062912	0,045234	0,043505	0,052474	0,073032	0,085014
8	3,153964	8,189844	0,680899	0,323643	0,103657	0,057753	0,038854	0,037044	0,044622	0,053341
9	0,943686	4,300658	3,621831	0,647771	0,180039	0,100014	0,059073	0,042496	0,029786	0,031988
10	0,572267	0,883963	8,177781	2,485548	0,287618	0,166054	0,103130	0,069407	0,030414	0,023604
11	0,538871	0,452435	0,998303	35,554090	0,504725	0,257136	0,162736	0,116160	0,046974	0,028997
12	0,851129	0,288645	0,465900	1,465083	1,274910	0,425768	0,244119	0,173499	0,078829	0,048110
13	1,954020	0,282488	0,287826	0,617281	35,554090	0,922877	0,385932	0,252626	0,122597	0,079727
14	19,719060	0,438697	0,202988	0,376554	2,886166	8,155943	0,750333	0,387172	0,172565	0,119504
15	9,362763	0,800452	0,219120	0,259590	0,831100	4,102814	3,706750	0,706690	0,239742	0,164942
16	1,688147	2,860148	0,342113	0,219354	0,456996	0,857983	8,153363	2,533183	0,345182	0,224423
17	0,859256	35,554090	0,573565	0,261738	0,302888	0,445484	1,002527	35,554090	0,557196	0,313212
18	0,666016	1,323665	1,402350	0,400606	0,213883	0,286669	0,488226	1,432869	1,313392	0,476676
19	0,859256	0,519559	35,554090	0,662021	0,162662	0,197768	0,310751	0,620763	35,554090	0,960405
20	1,688147	0,295711	2,647209	1,454223	0,157497	0,132221	0,215704	0,386192	2,804248	8,147197
21	9,362763	0,224837	0,709735	8,563008	0,201326	0,096705	0,151329	0,270357	0,828566	4,029940
22	19,719060	0,295711	0,366351	18,867300	0,299079	0,095032	0,101950	0,197798	0,475328	0,867984
23	1,954020	0,519559	0,220661	1,888446	0,450743	0,127842	0,078344	0,142822	0,326409	0,476351
24	0,851129	1,323665	0,172720	0,794628	0,776064	0,193936	0,082531	0,106099	0,240013	0,324454
25	0,538871	35,554090	0,220661	0,475356	1,883600	0,279480	0,114764	0,093013	0,180842	0,238026
26	0,572267	2,860148	0,366351	0,324151	19,400169	0,426975	0,173179	0,105082	0,134137	0,179229
27	0,943686	0,800452	0,709735	0,277023	9,029760	0,780931	0,244984	0,143179	0,097717	0,134006

Continued from table A.17.

	q									
y_σ	**6/5**	**7/5**	**8/5**	**9/5**	**11/5**	**12/5**	**13/5**	**14/5**	**16/5**	**17/5**
28	3,153964	0,438697	2,647209	0,324151	1,559927	2,748073	0,358002	0,207083	0,077380	0,094033
29	35,554090	0,282488	35,554090	0,475356	0,721776	35,554090	0,587656	0,289842	0,074850	0,064557
30	1,221355	0,288645	1,402350	0,794628	0,442399	1,336066	1,388071	0,422658	0,090756	0,048896
31	0,448328	0,452435	0,573565	1,888446	0,304683	0,549450	35,554090	0,688631	0,125276	0,048016
32	0,216785	0,883963	0,342113	18,867300	0,222845	0,325594	2,632055	1,478996	0,177238	0,062065
33	0,190421	4,300658	0,219120	8,563008	0,196256	0,215499	0,740284	8,609484	0,240195	0,090512
34	0,301226	8,189844	0,202988	1,454223	0,222845	0,143082	0,404466	18,936798	0,330525	0,131048
35	0,554646	0,866418	0,287826	0,662021	0,304683	0,094519	0,263569	1,888218	0,482264	0,175851
36		0,359714	0,465900	0,400606	0,442399	0,078020	0,181307	0,803362	0,803693	0,233287
37		0,181689	0,998303	0,261738	0,721776	0,094519	0,120406	0,480378	1,893374	0,316628
38		0,129073	8,177781	0,219354	1,559927	0,143082	0,080396	0,328079	19,297827	0,459113
39		0,185560	3,621831	0,259590	9,029760	0,215499	0,066803	0,237283	8,928389	0,797053
40		0,292244	0,680899	0,376554	19,400169	0,325594	0,080396	0,171143	1,555782	2,713307
41		0,529432	0,313941	0,617281	1,883600	0,549450	0,120406	0,130561	0,737480	35,554090
42			0,167838	1,465083	0,776064	1,336066	0,181307	0,117038	0,461964	1,355382
43			0,099241	35,554090	0,450743	35,554090	0,263569	0,130561	0,324172	0,587609
44			0,110277	2,485548	0,299079	2,748073	0,404466	0,171143	0,239583	0,371171
45			0,187407	0,647771	0,201326	0,780931	0,740284	0,237283	0,179207	0,263349
46			0,292156	0,323643	0,157497	0,426975	2,632055	0,328079	0,131958	0,194851
47			0,513333	0,186443	0,162662	0,279480	35,554090	0,480378	0,102967	0,144803
48				0,104352	0,213883	0,193936	1,388071	0,803362	0,093266	0,103148
49				0,085684	0,302888	0,127842	0,587656	1,888218	0,102967	0,068866
50				0,123764	0,456996	0,095032	0,358002	18,936798	0,131958	0,047275
51				0,193378	0,831100	0,096705	0,244984	8,609484	0,179207	0,039966
52				0,296018	2,886166	0,132221	0,173179	1,478996	0,239583	0,047275
53				0,502416	35,554090	0,197768	0,114764	0,688631	0,324172	0,068866
54					1,274910	0,286669	0,082531	0,422658	0,461964	0,103148

Continued from table A.17.

					q					
y_σ	**6/5**	**7/5**	**8/5**	**9/5**	**11/5**	**12/5**	**13/5**	**14/5**	**16/5**	**17/5**
55					0,504725	0,445484	0,078344	0,289842	0,737480	0,144803
56					0,287618	0,857983	0,101950	0,207083	1,555782	0,194851
57					0,180039	4,102814	0,151329	0,143179	8,928389	0,263349
58					0,103657	8,155943	0,215704	0,105082	19,297827	0,371171
59					0,062912	0,922877	0,310751	0,093013	1,893374	0,587609
60					0,059723	0,425768	0,488226	0,106099	0,803693	1,355382
61					0,091181	0,257136	1,002527	0,142822	0,482264	35,554090
62					0,145211	0,166054	8,153363	0,197798	0,330525	2,713307
63					0,210538	0,100014	3,706750	0,270357	0,240195	0,797053
64					0,307855	0,057753	0,750333	0,386192	0,177238	0,459113
65					0,488962	0,045234	0,385932	0,620763	0,125276	0,316628
66						0,062239	0,244119	1,432869	0,090756	0,233287
67						0,104962	0,162736	35,554090	0,074850	0,175851
68						0,155558	0,103130	2,533183	0,077380	0,131048
69						0,219872	0,059073	0,706690	0,097717	0,090512
70						0,314233	0,038854	0,387172	0,134137	0,062065
71						0,484642	0,043505	0,252626	0,180842	0,048016
72							0,071623	0,173499	0,240013	0,048896
73							0,116857	0,116160	0,326409	0,064557
74							0,165750	0,069407	0,475328	0,094033
75							0,229113	0,042496	0,828566	0,134006
76							0,320475	0,037044	2,804248	0,179229
77							0,481290	0,052474	35,554090	0,238026
78								0,086036	1,313392	0,324454
79								0,127766	0,557196	0,476351
80								0,175694	0,345182	0,867984
81								0,238061	0,239742	4,029940

Continued from table A.17.

	q									
y$_\sigma$	**6/5**	**7/5**	**8/5**	**9/5**	**11/5**	**12/5**	**13/5**	**14/5**	**16/5**	**17/5**
82								0,326452	0,172565	8,147197
83								0,478637	0,122597	0,960405
84									0,078829	0,476676
85									0,046974	0,313212
86									0,030414	0,224423
87									0,029786	0,164942
88									0,044622	0,119504
89									0,073032	0,079727
90									0,109080	0,048110
91									0,147821	0,028997
92									0,194545	0,023604
93									0,254729	0,031988
94									0,337421	0,053341
95									0,474756	0,085014
96										0,119107
97										0,157167
98										0,203371
99										0,262392
100										0,342399
101										0,473312

Table A.18: Harmonic scattering coefficients σ_o for fractional slot windings with $m = 5$, double zone span and $q_n = 2$.

	q									
$\mathbf{y}_\sigma$	**3/2**	**5/2**	**7/2**	**9/2**	**11/2**	**13/2**	**15/2**	**17/2**	**19/2**	**21/2**
1	0,142674	0,142674	0,142674	0,142674	0,142674	0,142674	0,142674	0,142674	0,142674	0,142674
2	0,056760	0,080693	0,095075	0,104182	0,110404	0,114908	0,118316	0,120982	0,123124	0,124882
3	0,023285	0,045649	0,065112	0,078643	0,088309	0,095495	0,101027	0,105411	0,108966	0,111905
4	0,019033	0,023679	0,043049	0,058566	0,070301	0,079303	0,086375	0,092057	0,096713	0,100594
5	0,020968	0,011652	0,026730	0,042332	0,055087	0,065259	0,073438	0,080115	0,085650	0,090303
6	0,023285	0,008410	0,015317	0,029321	0,042183	0,052966	0,061885	0,069299	0,075523	0,080807
7	0,016600	0,008337	0,008389	0,019215	0,031347	0,042231	0,051554	0,059471	0,066216	0,072002
8	0,016600	0,009656	0,005720	0,011829	0,022430	0,032937	0,042349	0,050551	0,057658	0,063829
9	0,023285	0,011245	0,005050	0,007039	0,015335	0,025006	0,034209	0,042488	0,049807	0,056248
10	0,020968	0,011652	0,005448	0,004772	0,009993	0,018381	0,027085	0,035244	0,042629	0,049233
11	0,019033	0,008546	0,006423	0,003888	0,006355	0,013018	0,020944	0,028787	0,036101	0,042763
12	0,023285	0,006144	0,007577	0,003829	0,004386	0,008886	0,015756	0,023096	0,030202	0,036821
13	0,056760	0,006144	0,008445	0,004287	0,003433	0,005960	0,011499	0,018151	0,024916	0,031394
14	0,142674	0,008546	0,008389	0,005056	0,003133	0,004222	0,008156	0,013936	0,020230	0,026468
15		0,011652	0,006503	0,005950	0,003274	0,003261	0,005712	0,010437	0,016130	0,022035
16		0,011245	0,004477	0,006763	0,003715	0,002830	0,004157	0,007643	0,012609	0,018085
17		0,009656	0,003253	0,007239	0,004348	0,002773	0,003217	0,005547	0,009656	0,014610
18		0,008337	0,003253	0,007039	0,005073	0,002986	0,002713	0,004141	0,007265	0,011604
19		0,008410	0,004477	0,005723	0,005781	0,003394	0,002530	0,003232	0,005431	0,009061
20		0,011652	0,006503	0,004130	0,006342	0,003932	0,002586	0,002689	0,004148	0,006977
21		0,023679	0,008389	0,002802	0,006600	0,004539	0,002824	0,002424	0,003275	0,005346
22		0,045649	0,008445	0,002062	0,006355	0,005152	0,003198	0,002372	0,002715	0,004166
23		0,080693	0,007577	0,002062	0,005358	0,005697	0,003665	0,002485	0,002395	0,003332
24		0,142674	0,006423	0,002802	0,004087	0,006086	0,004187	0,002728	0,002266	0,002765
25			0,005448	0,004130	0,002877	0,006216	0,004723	0,003070	0,002287	0,002411
26			0,005050	0,005723	0,001954	0,005960	0,005226	0,003483	0,002430	0,002226
27			0,005720	0,007039	0,001459	0,005165	0,005643	0,003940	0,002669	0,002179

Continued from table A.18.

	q									
y_σ	**3/2**	**5/2**	**7/2**	**9/2**	**11/2**	**13/2**	**15/2**	**17/2**	**19/2**	**21/2**
28			0,008389	0,007239	0,001459	0,004126	0,005914	0,004413	0,002983	0,002243
29			0,015317	0,006763	0,001954	0,003065	0,005966	0,004872	0,003353	0,002400
30			0,026730	0,005950	0,002877	0,002141	0,005712	0,005281	0,003759	0,002631
31			0,043049	0,005056	0,004087	0,001467	0,005054	0,005602	0,004182	0,002922
32			0,065112	0,004287	0,005358	0,001112	0,004186	0,005789	0,004599	0,003257
33			0,095075	0,003829	0,006355	0,001112	0,003260	0,005791	0,004987	0,003622
34			0,142674	0,003888	0,006600	0,001467	0,002394	0,005547	0,005320	0,004003
35				0,004772	0,006342	0,002141	0,001674	0,004987	0,005567	0,004384
36				0,007039	0,005781	0,003065	0,001161	0,004247	0,005695	0,004748
37				0,011829	0,005073	0,004126	0,000895	0,003437	0,005664	0,005075
38				0,019215	0,004348	0,005165	0,000895	0,002643	0,005431	0,005346
39				0,029321	0,003715	0,005960	0,001161	0,001933	0,004944	0,005537
40				0,042332	0,003274	0,006216	0,001674	0,001359	0,004303	0,005621
41				0,058566	0,003133	0,006086	0,002394	0,000956	0,003589	0,005568
42				0,078643	0,003433	0,005697	0,003260	0,000749	0,002868	0,005346
43				0,104182	0,004386	0,005152	0,004186	0,000749	0,002192	0,004917
44				0,142674	0,006355	0,004539	0,005054	0,000956	0,001605	0,004354
45					0,009993	0,003932	0,005712	0,001359	0,001137	0,003719
46					0,015335	0,003394	0,005966	0,001933	0,000813	0,003064
47					0,022430	0,002986	0,005914	0,002643	0,000647	0,002431
48					0,031347	0,002773	0,005643	0,003437	0,000647	0,001855
49					0,042183	0,002830	0,005226	0,004247	0,000813	0,001362
50					0,055087	0,003261	0,004723	0,004987	0,001137	0,000975
51					0,070301	0,004222	0,004187	0,005547	0,001605	0,000709
52					0,088309	0,005960	0,003665	0,005791	0,002192	0,000573
53					0,110404	0,008886	0,003198	0,005789	0,002868	0,000573
54					0,142674	0,013018	0,002824	0,005602	0,003589	0,000709

Continued from table A.18.

					q					
y_σ	**3/2**	**5/2**	**7/2**	**9/2**	**11/2**	**13/2**	**15/2**	**17/2**	**19/2**	**21/2**
55						0,018381	0,002586	0,005281	0,004303	0,000975
56						0,025006	0,002530	0,004872	0,004944	0,001362
57						0,032937	0,002713	0,004413	0,005431	0,001855
58						0,042231	0,003217	0,003940	0,005664	0,002431
59						0,052966	0,004157	0,003483	0,005695	0,003064
60						0,065259	0,005712	0,003070	0,005567	0,003719
61						0,079303	0,008156	0,002728	0,005320	0,004354
62						0,095495	0,011499	0,002485	0,004987	0,004917
63						0,114908	0,015756	0,002372	0,004599	0,005346
64						0,142674	0,020944	0,002424	0,004182	0,005568
65							0,027085	0,002689	0,003759	0,005621
66							0,034209	0,003232	0,003353	0,005537
67							0,042349	0,004141	0,002983	0,005346
68							0,051554	0,005547	0,002669	0,005075
69							0,061885	0,007643	0,002430	0,004748
70							0,073438	0,010437	0,002287	0,004384
71							0,086375	0,013936	0,002266	0,004003
72							0,101027	0,018151	0,002395	0,003622
73							0,118316	0,023096	0,002715	0,003257
74							0,142674	0,028787	0,003275	0,002922
75								0,035244	0,004148	0,002631
76								0,042488	0,005431	0,002400
77								0,050551	0,007265	0,002243
78								0,059471	0,009656	0,002179
79								0,069299	0,012609	0,002226
80								0,080115	0,016130	0,002411
81								0,092057	0,020230	0,002765

Continued from table A.18.

	q									
y_σ	**3/2**	**5/2**	**7/2**	**9/2**	**11/2**	**13/2**	**15/2**	**17/2**	**19/2**	**21/2**
82								0,105411	0,024916	0,003332
83								0,120982	0,030202	0,004166
84								0,142674	0,036101	0,005346
85									0,042629	0,006977
86									0,049807	0,009061
87									0,057658	0,011604
88									0,066216	0,014610
89									0,075523	0,018085
90									0,085650	0,022035
91									0,096713	0,026468
92									0,108966	0,031394
93									0,123124	0,036821
94									0,142674	0,042763
95										0,049233
96										0,056248
97										0,063829
98										0,072002
99										0,080807
100										0,090303
101										0,100594
102										0,111905
103										0,124882
104										0,142674

Table A.19: Harmonic scattering coefficients σ_o for fractional slot windings with $m = 5$, double zone span and $q_n = 3$.

	q									
$\mathbf{y}_\sigma$	**4/3**	**5/3**	**7/3**	**8/3**	**10/3**	**11/3**	**13/3**	**14/3**	**16/3**	**17/3**
1	0,161665	0,154783	0,148832	0,147385	0,145686	0,145163	0,144455	0,144210	0,143850	0,143715
2	0,069442	0,072759	0,083299	0,088090	0,096019	0,099261	0,104628	0,106863	0,110650	0,112265
3	0,039707	0,036806	0,047348	0,053709	0,065140	0,070043	0,078383	0,081928	0,088017	0,090644
4	0,036002	0,025687	0,025995	0,031236	0,042777	0,048217	0,057919	0,062181	0,069660	0,072942
5	0,037967	0,024482	0,015862	0,017736	0,026644	0,031733	0,041541	0,046064	0,054240	0,057908
6	0,034425	0,026185	0,013327	0,012098	0,015852	0,019795	0,028600	0,032986	0,041253	0,045076
7	0,036207	0,025733	0,013665	0,010710	0,009962	0,012001	0,018765	0,022643	0,030446	0,034209
8	0,048208	0,022866	0,015103	0,011207	0,007822	0,008127	0,011837	0,014855	0,021666	0,025168
9	0,050853	0,025882	0,016044	0,012490	0,007481	0,006710	0,007695	0,009504	0,014810	0,017858
10	0,060937	0,033816	0,014062	0,013527	0,008102	0,006591	0,005814	0,006513	0,009808	0,012212
11	0,101476	0,035035	0,011737	0,012851	0,009174	0,007209	0,005188	0,005143	0,006610	0,008182
12	0,267229	0,037803	0,011907	0,010428	0,010196	0,008189	0,005318	0,004731	0,004931	0,005732
13	2,928164	0,049061	0,015001	0,009086	0,010515	0,009160	0,005914	0,004921	0,004183	0,004436
14	0,758374	0,087289	0,019245	0,009930	0,009204	0,009655	0,006755	0,005494	0,004039	0,003878
15	0,137765	0,201293	0,019653	0,012794	0,007242	0,009036	0,007624	0,006276	0,004302	0,003815
16	0,048208	0,919813	0,019228	0,016168	0,005947	0,007292	0,008258	0,007094	0,004834	0,004094
17	0,032135	2,928164	0,019993	0,016548	0,005943	0,005687	0,008316	0,007743	0,005522	0,004604
18	0,029724	0,233811	0,023989	0,015974	0,007327	0,004921	0,007349	0,007963	0,006252	0,005252
19	0,027114	0,080083	0,035502	0,015835	0,009685	0,005292	0,005827	0,007420	0,006891	0,005942
20	0,022356	0,033816	0,062880	0,017318	0,011992	0,006751	0,004451	0,006111	0,007280	0,006565
21	0,027114	0,022971	0,119369	0,022144	0,012325	0,008894	0,003641	0,004701	0,007220	0,006994
22	0,029724	0,021040	0,279224	0,034602	0,011755	0,010874	0,003610	0,003623	0,006457	0,007069
23	0,032135	0,021229	2,928164	0,059319	0,011040	0,011212	0,004390	0,003130	0,005255	0,006592
24	0,048208	0,016952	0,790367	0,105198	0,010764	0,010721	0,005838	0,003334	0,004025	0,005563
25	0,137765	0,014048	0,174964	0,212559	0,011486	0,009992	0,007614	0,004214	0,003046	0,004376
26	0,758374	0,016952	0,078497	0,887704	0,014015	0,009477	0,009132	0,005621	0,002495	0,003306
27	2,928164	0,021229	0,038454	2,928164	0,020033	0,009576	0,009461	0,007250	0,002463	0,002543

Continued from table A.19.

	q									
$\mathbf{y}_\sigma$	**4/3**	**5/3**	**7/3**	**8/3**	**10/3**	**11/3**	**13/3**	**14/3**	**16/3**	**17/3**
28	0,267229	0,021040	0,019245	0,259496	0,031951	0,010765	0,009101	0,008606	0,002962	0,002200
29	0,101476	0,022971	0,013235	0,110417	0,051267	0,013854	0,008433	0,008935	0,003931	0,002327
30	0,060937	0,033816	0,011861	0,057910	0,081791	0,020587	0,007750	0,008638	0,005227	0,002915
31	0,050853	0,080083	0,012423	0,030575	0,136315	0,032239	0,007296	0,008030	0,006610	0,003896
32	0,048208	0,233811	0,013215	0,016168	0,287847	0,049987	0,007303	0,007353	0,007719	0,005134
33	0,036207	2,928164	0,012069	0,011135	2,928164	0,076634	0,008057	0,006809	0,008037	0,006416
34	0,034425	0,919813	0,008858	0,009786	0,804228	0,120656	0,010014	0,006579	0,007836	0,007432
35	0,037967	0,201293	0,007427	0,010144	0,194939	0,221007	0,014038	0,006864	0,007336	0,007745
36	0,036002	0,087289	0,008858	0,011085	0,102060	0,873846	0,021177	0,007943	0,006710	0,007585
37	0,039707	0,049061	0,012069	0,011409	0,061147	2,928164	0,031787	0,010289	0,006103	0,007138
38	0,069442	0,037803	0,013215	0,009372	0,036700	0,273258	0,046542	0,014803	0,005637	0,006553
39	0,161665	0,035035	0,012423	0,006744	0,021139	0,129652	0,066882	0,022020	0,005433	0,005953
40		0,033816	0,011861	0,005660	0,011992	0,078988	0,096485	0,032240	0,005626	0,005446
41		0,025882	0,013235	0,006744	0,008245	0,050210	0,147870	0,046013	0,006399	0,005128
42		0,022866	0,019245	0,009372	0,006994	0,031243	0,293414	0,064457	0,008048	0,005105
43		0,025733	0,038454	0,011409	0,007053	0,018582	2,928164	0,090259	0,011084	0,005505
44		0,026185	0,078497	0,011085	0,007795	0,010874	0,811952	0,131637	0,016062	0,006519
45		0,024482	0,174964	0,010144	0,008703	0,007498	0,206984	0,226787	0,023104	0,008452
46		0,025687	0,790367	0,009786	0,009171	0,006252	0,117690	0,866128	0,032411	0,011833
47		0,036806	2,928164	0,011135	0,008361	0,006177	0,078511	2,928164	0,044325	0,016945
48		0,072759	0,279224	0,016168	0,006249	0,006764	0,053976	0,281732	0,059494	0,023893
49		0,154783	0,119369	0,030575	0,004440	0,007630	0,036574	0,142274	0,079304	0,032849
50			0,062880	0,057910	0,003753	0,008364	0,023883	0,094088	0,107347	0,044099
51			0,035502	0,110417	0,004440	0,008442	0,014897	0,066276	0,155985	0,058166
52			0,023989	0,259496	0,006249	0,007140	0,009132	0,046856	0,297226	0,076125
53			0,019993	2,928164	0,008361	0,005203	0,006327	0,032388	2,928164	0,100584
54			0,019228	0,887704	0,009171	0,003677	0,005128	0,021550	0,816873	0,139601

Continued from table A.19.

	q									
y_σ	**4/3**	**5/3**	**7/3**	**8/3**	**10/3**	**11/3**	**13/3**	**14/3**	**16/3**	**17/3**
55			0,019653	0,212559	0,008703	0,003112	0,004877	0,013730	0,214986	0,230902
56			0,019245	0,105198	0,007795	0,003677	0,005212	0,008606	0,128560	0,861211
57			0,015001	0,059319	0,007053	0,005203	0,005888	0,005999	0,091304	2,928164
58			0,011907	0,034602	0,006994	0,007140	0,006683	0,004812	0,067744	0,287457
59			0,011737	0,022144	0,008245	0,008442	0,007346	0,004488	0,050408	0,151098
60			0,014062	0,017318	0,011992	0,008364	0,007563	0,004714	0,036909	0,105103
61			0,016044	0,015835	0,021139	0,007630	0,006919	0,005284	0,026267	0,078654
62			0,015103	0,015974	0,036700	0,006764	0,005409	0,006021	0,018010	0,059820
63			0,013665	0,016548	0,061147	0,006177	0,003841	0,006738	0,011878	0,045200
64			0,013327	0,016168	0,102060	0,006252	0,002719	0,007212	0,007719	0,033499
65			0,015862	0,012794	0,194939	0,007498	0,002315	0,007158	0,005441	0,024124
66			0,025995	0,009930	0,804228	0,010874	0,002719	0,006208	0,004295	0,016764
67			0,047348	0,009086	2,928164	0,018582	0,003841	0,004742	0,003873	0,011236
68			0,083299	0,010428	0,287847	0,031243	0,005409	0,003338	0,003934	0,007432
69			0,148832	0,012851	0,136315	0,050210	0,006919	0,002361	0,004322	0,005278
70				0,013527	0,081791	0,078988	0,007563	0,002014	0,004914	0,004149
71				0,012490	0,051267	0,129652	0,007346	0,002361	0,005592	0,003687
72				0,011207	0,031951	0,273258	0,006683	0,003338	0,006232	0,003680
73				0,010710	0,020033	2,928164	0,005888	0,004742	0,006682	0,003988
74				0,012098	0,014015	0,873846	0,005212	0,006208	0,006755	0,004504
75				0,017736	0,011486	0,221007	0,004877	0,007158	0,006217	0,005132
76				0,031236	0,010764	0,120656	0,005128	0,007212	0,005066	0,005773
77				0,053709	0,011040	0,076634	0,006327	0,006738	0,003764	0,006310
78				0,088090	0,011755	0,049987	0,009132	0,006021	0,002631	0,006605
79				0,147385	0,012325	0,032239	0,014897	0,005284	0,001873	0,006486
80					0,011992	0,020587	0,023883	0,004714	0,001608	0,005739
81					0,009685	0,013854	0,036574	0,004488	0,001873	0,004585

Continued from table A.19.

	q									
y_σ	**4/3**	**5/3**	**7/3**	**8/3**	**10/3**	**11/3**	**13/3**	**14/3**	**16/3**	**17/3**
82					0,007327	0,010765	0,053976	0,004812	0,002631	0,003375
83					0,005943	0,009576	0,078511	0,005999	0,003764	0,002352
84					0,005947	0,009477	0,117690	0,008606	0,005066	0,001678
85					0,007242	0,009992	0,206984	0,013730	0,006217	0,001443
86					0,009204	0,010721	0,811952	0,021550	0,006755	0,001678
87					0,010515	0,011212	2,928164	0,032388	0,006682	0,002352
88					0,010196	0,010874	0,293414	0,046856	0,006232	0,003375
89					0,009174	0,008894	0,147870	0,066276	0,005592	0,004585
90					0,008102	0,006751	0,096485	0,094088	0,004914	0,005739
91					0,007481	0,005292	0,066882	0,142274	0,004322	0,006486
92					0,007822	0,004921	0,046542	0,281732	0,003934	0,006605
93					0,009962	0,005687	0,031787	2,928164	0,003873	0,006310
94					0,015852	0,007292	0,021177	0,866128	0,004295	0,005773
95					0,026644	0,009036	0,014038	0,226787	0,005441	0,005132
96					0,042777	0,009655	0,010014	0,131637	0,007719	0,004504
97					0,065140	0,009160	0,008057	0,090259	0,011878	0,003988
98					0,096019	0,008189	0,007303	0,064457	0,018010	0,003680
99					0,145686	0,007209	0,007296	0,046013	0,026267	0,003687
100						0,006591	0,007750	0,032240	0,036909	0,004149
101						0,006710	0,008433	0,022020	0,050408	0,005278
102						0,008127	0,009101	0,014803	0,067744	0,007432
103						0,012001	0,009461	0,010289	0,091304	0,011236
104						0,019795	0,009132	0,007943	0,128560	0,016764
105						0,031733	0,007614	0,006864	0,214986	0,024124
106						0,048217	0,005838	0,006579	0,816873	0,033499
107						0,070043	0,004390	0,006809	2,928164	0,045200
108						0,099261	0,003610	0,007353	0,297226	0,059820

Continued from table A.19.

					q					
y_σ	**4/3**	**5/3**	**7/3**	**8/3**	**10/3**	**11/3**	**13/3**	**14/3**	**16/3**	**17/3**
109						0,145163	0,003641	0,008030	0,155985	0,078654
110							0,004451	0,008638	0,107347	0,105103
111							0,005827	0,008935	0,079304	0,151098
112							0,007349	0,008606	0,059494	0,287457
113							0,008316	0,007250	0,044325	2,928164
114							0,008258	0,005621	0,032411	0,861211
115							0,007624	0,004214	0,023104	0,230902
116							0,006755	0,003334	0,016062	0,139601
117							0,005914	0,003130	0,011084	0,100584
118							0,005318	0,003623	0,008048	0,076125
119							0,005188	0,004701	0,006399	0,058166
120							0,005814	0,006111	0,005626	0,044099
121							0,007695	0,007420	0,005433	0,032849
122							0,011837	0,007963	0,005637	0,023893
123							0,018765	0,007743	0,006103	0,016945
124							0,028600	0,007094	0,006710	0,011833
125							0,041541	0,006276	0,007336	0,008452
126							0,057919	0,005494	0,007836	0,006519
127							0,078383	0,004921	0,008037	0,005505
128							0,104628	0,004731	0,007719	0,005105
129							0,144455	0,005143	0,006610	0,005128
130								0,006513	0,005227	0,005446
131								0,009504	0,003931	0,005953
132								0,014855	0,002962	0,006553
133								0,022643	0,002463	0,007138
134								0,032986	0,002495	0,007585
135								0,046064	0,003046	0,007745

Continued from table A.19.

					q					
y_σ	**4/3**	**5/3**	**7/3**	**8/3**	**10/3**	**11/3**	**13/3**	**14/3**	**16/3**	**17/3**
136								0,062181	0,004025	0,007432
137								0,081928	0,005255	0,006416
138								0,106863	0,006457	0,005134
139								0,144210	0,007220	0,003896
140									0,007280	0,002915
141									0,006891	0,002327
142									0,006252	0,002200
143									0,005522	0,002543
144									0,004834	0,003306
145									0,004302	0,004376
146									0,004039	0,005563
147									0,004183	0,006592
148									0,004931	0,007069
149									0,006610	0,006994
150									0,009808	0,006565
151									0,014810	0,005942
152									0,021666	0,005252
153									0,030446	0,004604
154									0,041253	0,004094
155									0,054240	0,003815
156									0,069660	0,003878
157									0,088017	0,004436
158									0,110650	0,005732
159									0,143850	0,008182
160										0,012212
161										0,017858
162										0,025168

Continued from table A.19.

	q									
y_σ	**4/3**	**5/3**	**7/3**	**8/3**	**10/3**	**11/3**	**13/3**	**14/3**	**16/3**	**17/3**
163										0,034209
164										0,045076
165										0,057908
166										0,072942
167										0,090644
168										0,112265
169										0,143715

Table A.20: Harmonic scattering coefficients σ_o for fractional slot windings with $m = 7$, double zone span and $q_n = 2$.

	q									
y_σ	**3/2**	**5/2**	**7/2**	**9/2**	**11/2**	**13/2**	**15/2**	**17/2**	**19/2**	**21/2**
1	0,069934	0,069934	0,069934	0,069934	0,069934	0,069934	0,069934	0,069934	0,069934	0,069934
2	0,025575	0,037990	0,045451	0,050163	0,053375	0,055698	0,057452	0,058823	0,059924	0,060827
3	0,009486	0,020058	0,030024	0,037007	0,041999	0,045709	0,048563	0,050822	0,052653	0,054166
4	0,010358	0,009252	0,018771	0,026688	0,032724	0,037367	0,041015	0,043946	0,046347	0,048347
5	0,010351	0,004133	0,010666	0,018420	0,024917	0,030139	0,034351	0,037793	0,040647	0,043047
6	0,009486	0,004237	0,005344	0,011924	0,018351	0,023838	0,028410	0,032224	0,035430	0,038154
7	0,008156	0,004767	0,002644	0,007067	0,012922	0,018378	0,023120	0,027174	0,030640	0,033619
8	0,008449	0,004886	0,002496	0,003782	0,008573	0,013712	0,018440	0,022611	0,026247	0,029415
9	0,009486	0,004630	0,002901	0,002030	0,005268	0,009810	0,014346	0,018512	0,022232	0,025526
10	0,007957	0,004133	0,003231	0,001794	0,002988	0,006652	0,010821	0,014864	0,018584	0,021941
11	0,007957	0,003423	0,003343	0,002051	0,001719	0,004226	0,007854	0,011657	0,015294	0,018653
12	0,009486	0,003093	0,003250	0,002374	0,001455	0,002524	0,005436	0,008882	0,012355	0,015656
13	0,008449	0,003281	0,003006	0,002604	0,001603	0,001539	0,003561	0,006535	0,009761	0,012945
14	0,008156	0,003792	0,002644	0,002699	0,001870	0,001272	0,002225	0,004611	0,007510	0,010517
15	0,009486	0,004133	0,002167	0,002667	0,002117	0,001345	0,001427	0,003107	0,005597	0,008369
16	0,010351	0,003477	0,001817	0,002533	0,002289	0,001551	0,001165	0,002021	0,004021	0,006499
17	0,010358	0,002906	0,001705	0,002316	0,002370	0,001779	0,001187	0,001352	0,002781	0,004904
18	0,009486	0,002906	0,001841	0,002030	0,002365	0,001973	0,001341	0,001099	0,001873	0,003584
19	0,025575	0,003477	0,002155	0,001672	0,002287	0,002109	0,001539	0,001086	0,001299	0,002537
20	0,069934	0,004133	0,002499	0,001364	0,002147	0,002179	0,001729	0,001198	0,001058	0,001763
21		0,003792	0,002644	0,001176	0,001956	0,002187	0,001885	0,001363	0,001020	0,001261
22		0,003281	0,002271	0,001137	0,001719	0,002141	0,001996	0,001539	0,001098	0,001031
23		0,003093	0,001806	0,001244	0,001433	0,002047	0,002058	0,001699	0,001234	0,000976
24		0,003423	0,001512	0,001462	0,001167	0,001912	0,002074	0,001829	0,001391	0,001027
25		0,004133	0,001512	0,001732	0,000967	0,001743	0,002046	0,001922	0,001544	0,001137
26		0,004630	0,001806	0,001961	0,000859	0,001539	0,001981	0,001977	0,001680	0,001274
27		0,004886	0,002271	0,002030	0,000851	0,001301	0,001883	0,001996	0,001790	0,001417

Continued from table A.20.

					q					
y_σ	**3/2**	**5/2**	**7/2**	**9/2**	**11/2**	**13/2**	**15/2**	**17/2**	**19/2**	**21/2**
28		0,004767	0,002644	0,001782	0,000939	0,001071	0,001757	0,001981	0,001870	0,001551
29		0,004237	0,002499	0,001429	0,001104	0,000879	0,001605	0,001935	0,001920	0,001668
30		0,004133	0,002155	0,001117	0,001314	0,000746	0,001427	0,001862	0,001940	0,001762
31		0,009252	0,001841	0,000938	0,001527	0,000681	0,001223	0,001766	0,001933	0,001833
32		0,020058	0,001705	0,000938	0,001686	0,000688	0,001021	0,001648	0,001901	0,001878
33		0,037990	0,001817	0,001117	0,001719	0,000763	0,000843	0,001510	0,001846	0,001899
34		0,069934	0,002167	0,001429	0,001539	0,000893	0,000703	0,001352	0,001771	0,001897
35			0,002644	0,001782	0,001265	0,001062	0,000611	0,001173	0,001677	0,001875
36			0,003006	0,002030	0,000987	0,001245	0,000572	0,000994	0,001567	0,001833
37			0,003250	0,001961	0,000767	0,001412	0,000587	0,000830	0,001441	0,001773
38			0,003343	0,001732	0,000648	0,001525	0,000651	0,000692	0,001299	0,001698
39			0,003231	0,001462	0,000648	0,001539	0,000758	0,000588	0,001140	0,001609
40			0,002901	0,001244	0,000767	0,001401	0,000897	0,000524	0,000980	0,001506
41			0,002496	0,001137	0,000987	0,001183	0,001053	0,000501	0,000829	0,001390
42			0,002644	0,001176	0,001265	0,000944	0,001208	0,000519	0,000696	0,001261
43			0,005344	0,001364	0,001539	0,000728	0,001341	0,000576	0,000588	0,001118
44			0,010666	0,001672	0,001719	0,000566	0,001424	0,000667	0,000510	0,000973
45			0,018771	0,002030	0,001686	0,000481	0,001427	0,000784	0,000465	0,000833
46			0,030024	0,002316	0,001527	0,000481	0,001315	0,000917	0,000452	0,000707
47			0,045451	0,002533	0,001314	0,000566	0,001138	0,001056	0,000472	0,000600
48			0,069934	0,002667	0,001104	0,000728	0,000933	0,001187	0,000523	0,000515
49				0,002699	0,000939	0,000944	0,000734	0,001293	0,000601	0,000455
50				0,002604	0,000851	0,001183	0,000563	0,001355	0,000701	0,000423
51				0,002374	0,000859	0,001401	0,000440	0,001352	0,000817	0,000417
52				0,002051	0,000967	0,001539	0,000376	0,001259	0,000941	0,000439
53				0,001794	0,001167	0,001525	0,000376	0,001111	0,001063	0,000485
54				0,002030	0,001433	0,001412	0,000440	0,000935	0,001173	0,000553

Continued from table A.20.

	q									
y_σ	**3/2**	**5/2**	**7/2**	**9/2**	**11/2**	**13/2**	**15/2**	**17/2**	**19/2**	**21/2**
55				0,003782	0,001719	0,001245	0,000563	0,000755	0,001259	0,000640
56				0,007067	0,001956	0,001062	0,000734	0,000589	0,001306	0,000741
57				0,011924	0,002147	0,000893	0,000933	0,000453	0,001299	0,000851
58				0,018420	0,002287	0,000763	0,001138	0,000356	0,001220	0,000963
59				0,026688	0,002365	0,000688	0,001315	0,000306	0,001095	0,001070
60				0,037007	0,002370	0,000681	0,001427	0,000306	0,000942	0,001164
61				0,050163	0,002289	0,000746	0,001424	0,000356	0,000781	0,001234
62				0,069934	0,002117	0,000879	0,001341	0,000453	0,000625	0,001270
63					0,001870	0,001071	0,001208	0,000589	0,000487	0,001261
64					0,001603	0,001301	0,001053	0,000755	0,000375	0,001193
65					0,001455	0,001539	0,000897	0,000935	0,000297	0,001084
66					0,001719	0,001743	0,000758	0,001111	0,000256	0,000951
67					0,002988	0,001912	0,000651	0,001259	0,000256	0,000806
68					0,005268	0,002047	0,000587	0,001352	0,000297	0,000662
69					0,008573	0,002141	0,000572	0,001355	0,000375	0,000527
70					0,012922	0,002187	0,000611	0,001293	0,000487	0,000411
71					0,018351	0,002179	0,000703	0,001187	0,000625	0,000318
72					0,024917	0,002109	0,000843	0,001056	0,000781	0,000254
73					0,032724	0,001973	0,001021	0,000917	0,000942	0,000221
74					0,041999	0,001779	0,001223	0,000784	0,001095	0,000221
75					0,053375	0,001551	0,001427	0,000667	0,001220	0,000254
76					0,069934	0,001345	0,001605	0,000576	0,001299	0,000318
77						0,001272	0,001757	0,000519	0,001306	0,000411
78						0,001539	0,001883	0,000501	0,001259	0,000527
79						0,002524	0,001981	0,000524	0,001173	0,000662
80						0,004226	0,002046	0,000588	0,001063	0,000806
81						0,006652	0,002074	0,000692	0,000941	0,000951

Continued from table A.20.

	q									
y_σ	3/2	5/2	7/2	9/2	11/2	13/2	15/2	17/2	19/2	21/2
82						0,009810	0,002058	0,000830	0,000817	0,001084
83						0,013712	0,001996	0,000994	0,000701	0,001193
84						0,018378	0,001885	0,001173	0,000601	0,001261
85						0,023838	0,001729	0,001352	0,000523	0,001270
86						0,030139	0,001539	0,001510	0,000472	0,001234
87						0,037367	0,001341	0,001648	0,000452	0,001164
88						0,045709	0,001187	0,001766	0,000465	0,001070
89						0,055698	0,001165	0,001862	0,000510	0,000963
90						0,069934	0,001427	0,001935	0,000588	0,000851
91							0,002225	0,001981	0,000696	0,000741
92							0,003561	0,001996	0,000829	0,000640
93							0,005436	0,001977	0,000980	0,000553
94							0,007854	0,001922	0,001140	0,000485
95							0,010821	0,001829	0,001299	0,000439
96							0,014346	0,001699	0,001441	0,000417
97							0,018440	0,001539	0,001567	0,000423
98							0,023120	0,001363	0,001677	0,000455
99							0,028410	0,001198	0,001771	0,000515
100							0,034351	0,001086	0,001846	0,000600
101							0,041015	0,001099	0,001901	0,000707
102							0,048563	0,001352	0,001933	0,000833
103							0,057452	0,002021	0,001940	0,000973
104							0,069934	0,003107	0,001920	0,001118
105								0,004611	0,001870	0,001261
106								0,006535	0,001790	0,001390
107								0,008882	0,001680	0,001506
108								0,011657	0,001544	0,001609

Continued from table A.20.

	q									
y_σ	3/2	5/2	7/2	9/2	11/2	13/2	15/2	17/2	19/2	21/2
109								0,014864	0,001391	0,001698
110								0,018512	0,001234	0,001773
111								0,022611	0,001098	0,001833
112								0,027174	0,001020	0,001875
113								0,032224	0,001058	0,001897
114								0,037793	0,001299	0,001899
116								0,050822	0,002781	0,001833
117								0,058823	0,004021	0,001762
118								0,069934	0,005597	0,001668
119									0,007510	0,001551
120									0,009761	0,001417
121									0,012355	0,001274
122									0,015294	0,001137
123									0,018584	0,001027
124									0,022232	0,000976
125									0,026247	0,001031
126									0,030640	0,001261
127									0,035430	0,001763
128									0,040647	0,002537
129									0,046347	0,003584
130									0,052653	0,004904
131									0,059924	0,006499
132									0,069934	0,008369
133										0,010517
134										0,012945
135										0,015656
136										0,018653

Continued from table A.20.

	q									
$\mathbf{y}_\sigma$	**3/2**	**5/2**	**7/2**	**9/2**	**11/2**	**13/2**	**15/2**	**17/2**	**19/2**	**21/2**
137										0,021941
138										0,025526
139										0,029415
140										0,033619
141										0,038154
142										0,043047
143										0,048347
144										0,054166
145										0,060827
146										0,069934

Table A.21: Harmonic scattering coefficients σ_o for fractional slot windings with $m = 7$, double zone span and $q_n = 3$.

	q									
$\mathbf{y}_\sigma$	**4/3**	**5/3**	**7/3**	**8/3**	**10/3**	**11/3**	**13/3**	**14/3**	**16/3**	**17/3**
1	0,078961	0,075700	0,072871	0,072182	0,071372	0,071122	0,070784	0,070667	0,070495	0,070431
2	0,031740	0,033572	0,039173	0,041695	0,045851	0,047544	0,050339	0,051501	0,053466	0,054303
3	0,018315	0,015925	0,020875	0,024102	0,029979	0,032513	0,036829	0,038665	0,041817	0,043177
4	0,016979	0,012427	0,010576	0,012944	0,018618	0,021369	0,026326	0,028516	0,032369	0,034063
5	0,015409	0,011864	0,006738	0,006863	0,010687	0,013135	0,018011	0,020298	0,024466	0,026346
6	0,013595	0,010925	0,006664	0,005405	0,005802	0,007460	0,011592	0,013742	0,017874	0,019808
7	0,013511	0,009707	0,006724	0,005541	0,003798	0,004190	0,006933	0,008721	0,012486	0,014347
8	0,014572	0,008871	0,006421	0,005632	0,003745	0,003250	0,003962	0,005167	0,008240	0,009909
9	0,012215	0,009253	0,005846	0,005427	0,004020	0,003367	0,002643	0,003044	0,005104	0,006458
10	0,011864	0,009937	0,005066	0,004992	0,004159	0,003631	0,002538	0,002332	0,003053	0,003975
11	0,012359	0,008390	0,004578	0,004389	0,004086	0,003762	0,002779	0,002374	0,002078	0,002446
12	0,011342	0,007746	0,004671	0,003804	0,003838	0,003716	0,003021	0,002621	0,001936	0,001866
13	0,011995	0,008372	0,005175	0,003601	0,003461	0,003519	0,003148	0,002843	0,002109	0,001849
14	0,013351	0,008062	0,005520	0,003827	0,002968	0,003207	0,003142	0,002962	0,002347	0,002041
15	0,014052	0,007353	0,004698	0,004281	0,002547	0,002799	0,003020	0,002965	0,002540	0,002266
16	0,014572	0,007662	0,004012	0,004532	0,002366	0,002368	0,002806	0,002866	0,002649	0,002445
17	0,046240	0,008786	0,003989	0,003886	0,002461	0,002087	0,002517	0,002684	0,002667	0,002547
18	0,249569	0,009517	0,004517	0,003251	0,002766	0,002028	0,002155	0,002434	0,002604	0,002569
19	0,907222	0,009594	0,004816	0,003065	0,003120	0,002185	0,001811	0,002123	0,002473	0,002517
20	0,091084	0,009937	0,004328	0,003385	0,003265	0,002487	0,001580	0,001785	0,002285	0,002404
21	0,032488	0,026504	0,003905	0,003898	0,002832	0,002795	0,001505	0,001516	0,002048	0,002238
22	0,020934	0,081067	0,003980	0,003856	0,002312	0,002906	0,001589	0,001366	0,001761	0,002028
23	0,017319	0,907222	0,004584	0,003404	0,001993	0,002539	0,001800	0,001356	0,001476	0,001775
24	0,014572	0,308782	0,005224	0,003056	0,002001	0,002069	0,002073	0,001477	0,001249	0,001499
25	0,011930	0,071174	0,005622	0,003085	0,002308	0,001733	0,002310	0,001693	0,001113	0,001257
26	0,011615	0,028886	0,005658	0,003532	0,002737	0,001650	0,002378	0,001948	0,001083	0,001084
27	0,011471	0,015848	0,005291	0,004146	0,002931	0,001836	0,002102	0,002156	0,001156	0,001000

Continued from table A.21.

	q									
y_σ	**4/3**	**5/3**	**7/3**	**8/3**	**10/3**	**11/3**	**13/3**	**14/3**	**16/3**	**17/3**
28	0,010367	0,013281	0,005520	0,004576	0,002682	0,002205	0,001718	0,002209	0,001315	0,001010
29	0,011471	0,011587	0,012528	0,004779	0,002319	0,002560	0,001385	0,001965	0,001526	0,001107
30	0,011615	0,009937	0,028588	0,004657	0,002065	0,002574	0,001203	0,001616	0,001744	0,001272
31	0,011930	0,008153	0,064567	0,004271	0,002051	0,002304	0,001214	0,001294	0,001908	0,001476
32	0,014572	0,007691	0,261343	0,004532	0,002309	0,001979	0,001408	0,001088	0,001940	0,001678
33	0,017319	0,008066	0,907222	0,009747	0,002762	0,001757	0,001726	0,001042	0,001744	0,001823
34	0,020934	0,007258	0,100338	0,020950	0,003192	0,001732	0,002047	0,001162	0,001452	0,001848
35	0,032488	0,006572	0,043788	0,041834	0,003499	0,001932	0,002187	0,001416	0,001158	0,001670
36	0,091084	0,007258	0,021562	0,094035	0,003655	0,002313	0,002046	0,001731	0,000932	0,001401
37	0,907222	0,008066	0,010979	0,907222	0,003606	0,002737	0,001783	0,001989	0,000814	0,001122
38	0,249569	0,007691	0,008001	0,297084	0,003332	0,003059	0,001520	0,002018	0,000824	0,000894
39	0,046240	0,008153	0,007452	0,079325	0,002982	0,003269	0,001343	0,001848	0,000957	0,000755
40	0,014572	0,009937	0,006998	0,039500	0,003265	0,003333	0,001307	0,001597	0,001187	0,000726
41	0,014052	0,011587	0,006336	0,020916	0,006535	0,003214	0,001431	0,001359	0,001464	0,000810
42	0,013351	0,013281	0,005520	0,010969	0,013073	0,002917	0,001700	0,001199	0,001710	0,000992
43	0,011995	0,015848	0,004527	0,006889	0,023616	0,002608	0,002055	0,001159	0,001819	0,001239
44	0,011342	0,028886	0,004034	0,006233	0,040467	0,002906	0,002381	0,001258	0,001734	0,001498
45	0,012359	0,071174	0,004140	0,006051	0,074439	0,005630	0,002634	0,001486	0,001544	0,001694
46	0,011864	0,308782	0,004525	0,005717	0,266447	0,010947	0,002803	0,001801	0,001321	0,001728
47	0,012215	0,907222	0,004471	0,005193	0,907222	0,019254	0,002870	0,002126	0,001122	0,001614
48	0,014572	0,081067	0,003759	0,004532	0,105747	0,031602	0,002808	0,002386	0,000988	0,001425
49	0,013511	0,026504	0,003417	0,003719	0,053281	0,051651	0,002606	0,002580	0,000946	0,001216
50	0,013595	0,009937	0,003759	0,003239	0,031691	0,100897	0,002305	0,002693	0,001009	0,001033
51	0,015409	0,009594	0,004471	0,003220	0,018756	0,907222	0,002072	0,002708	0,001174	0,000909
52	0,016979	0,009517	0,004525	0,003533	0,010559	0,292017	0,002378	0,002605	0,001421	0,000866
53	0,018315	0,008786	0,004140	0,003818	0,005940	0,084575	0,004377	0,002385	0,001710	0,000916
54	0,031740	0,007662	0,004034	0,003468	0,004462	0,048087	0,008135	0,002096	0,001974	0,001058

Continued from table A.21.

	q									
$\mathbf{y}_\sigma$	**4/3**	**5/3**	**7/3**	**8/3**	**10/3**	**11/3**	**13/3**	**14/3**	**16/3**	**17/3**
55	0,078961	0,007353	0,004527	0,002870	0,004335	0,030130	0,013790	0,001900	0,002188	0,001277
56		0,008062	0,005520	0,002610	0,004401	0,018631	0,021639	0,002209	0,002351	0,001542
57		0,008372	0,006336	0,002870	0,004337	0,010953	0,032415	0,003966	0,002451	0,001806
58		0,007746	0,006998	0,003468	0,004104	0,006233	0,048402	0,007215	0,002478	0,002025
59		0,008390	0,007452	0,003818	0,003736	0,004117	0,080377	0,012046	0,002416	0,002199
60		0,009937	0,008001	0,003533	0,003265	0,003785	0,269291	0,018636	0,002261	0,002324
61		0,009253	0,010979	0,003220	0,002682	0,003880	0,907222	0,027381	0,002027	0,002388
62		0,008871	0,021562	0,003239	0,002258	0,003947	0,109071	0,039322	0,001769	0,002382
63		0,009707	0,043788	0,003719	0,002108	0,003870	0,059602	0,058085	0,001635	0,002294
64		0,010925	0,100338	0,004532	0,002229	0,003652	0,039529	0,105097	0,001940	0,002124
65		0,011864	0,907222	0,005193	0,002520	0,003324	0,026879	0,907222	0,003340	0,001891
66		0,012427	0,261343	0,005717	0,002788	0,002906	0,017825	0,289191	0,005855	0,001652
67		0,015925	0,064567	0,006051	0,002737	0,002393	0,011244	0,088016	0,009526	0,001544
68		0,033572	0,028588	0,006233	0,002291	0,001995	0,006700	0,054074	0,014427	0,001848
69		0,075700	0,012528	0,006889	0,001868	0,001811	0,003993	0,037375	0,020695	0,003116
70			0,005520	0,010969	0,001703	0,001858	0,003025	0,026144	0,028627	0,005365
71			0,005291	0,020916	0,001868	0,002084	0,002954	0,017839	0,038946	0,008623
72			0,005658	0,039500	0,002291	0,002371	0,003115	0,011627	0,053922	0,012940
73			0,005622	0,079325	0,002737	0,002538	0,003248	0,007165	0,084313	0,018407
74			0,005224	0,297084	0,002788	0,002329	0,003272	0,004291	0,271102	0,025200
75			0,004584	0,907222	0,002520	0,001905	0,003178	0,002921	0,907222	0,033709
76			0,003980	0,094035	0,002229	0,001546	0,002986	0,002666	0,111295	0,044964
77			0,003905	0,041834	0,002108	0,001410	0,002716	0,002785	0,063991	0,062574
78			0,004328	0,020950	0,002258	0,001546	0,002378	0,002958	0,045295	0,107923
79			0,004816	0,009747	0,002682	0,001905	0,001968	0,003060	0,033384	0,907222
80			0,004517	0,004532	0,003265	0,002329	0,001619	0,003058	0,024490	0,287390
81			0,003989	0,004271	0,003736	0,002538	0,001407	0,002956	0,017514	0,090414

Continued from table A.21.

					q					
y_σ	**4/3**	**5/3**	**7/3**	**8/3**	**10/3**	**11/3**	**13/3**	**14/3**	**16/3**	**17/3**
82			0,004012	0,004657	0,004104	0,002371	0,001358	0,002771	0,012034	0,058376
83			0,004698	0,004779	0,004337	0,002084	0,001464	0,002520	0,007854	0,042846
84			0,005520	0,004576	0,004401	0,001858	0,001680	0,002209	0,004873	0,032246
85			0,005175	0,004146	0,004335	0,001811	0,001931	0,001835	0,003036	0,024088
86			0,004671	0,003532	0,004462	0,001995	0,002106	0,001508	0,002311	0,017568
87			0,004578	0,003085	0,005940	0,002393	0,002058	0,001290	0,002232	0,012355
88			0,005066	0,003056	0,010559	0,002906	0,001751	0,001211	0,002382	0,008291
89			0,005846	0,003404	0,018756	0,003324	0,001395	0,001270	0,002565	0,005289
90			0,006421	0,003856	0,031691	0,003652	0,001129	0,001440	0,002693	0,003301
91			0,006724	0,003898	0,053281	0,003870	0,001031	0,001671	0,002740	0,002301
92			0,006664	0,003385	0,105747	0,003947	0,001129	0,001887	0,002704	0,002072
93			0,006738	0,003065	0,907222	0,003880	0,001395	0,001988	0,002596	0,002162
94			0,010576	0,003251	0,266447	0,003785	0,001751	0,001843	0,002426	0,002343
95			0,020875	0,003886	0,074439	0,004117	0,002058	0,001533	0,002206	0,002505
96			0,039173	0,004532	0,040467	0,006233	0,002106	0,001210	0,001940	0,002605
97			0,072871	0,004281	0,023616	0,010953	0,001931	0,000977	0,001624	0,002629
98				0,003827	0,013073	0,018631	0,001680	0,000894	0,001334	0,002580
99				0,003601	0,006535	0,030130	0,001464	0,000977	0,001117	0,002469
100				0,003804	0,003265	0,048087	0,001358	0,001210	0,001001	0,002305
101				0,004389	0,002982	0,084575	0,001407	0,001533	0,000991	0,002097
102				0,004992	0,003332	0,292017	0,001619	0,001843	0,001082	0,001848
103				0,005427	0,003606	0,907222	0,001968	0,001988	0,001249	0,001554
104				0,005632	0,003655	0,100897	0,002378	0,001887	0,001456	0,001279
105				0,005541	0,003499	0,051651	0,002716	0,001671	0,001651	0,001066
106				0,005405	0,003192	0,031602	0,002986	0,001440	0,001768	0,000938
107				0,006863	0,002762	0,019254	0,003178	0,001270	0,001724	0,000904
108				0,012944	0,002309	0,010947	0,003272	0,001211	0,001498	0,000962

Continued from table A.21.

	q									
y_σ	**4/3**	**5/3**	**7/3**	**8/3**	**10/3**	**11/3**	**13/3**	**14/3**	**16/3**	**17/3**
109				0,024102	0,002051	0,005630	0,003248	0,001290	0,001210	0,001097
110				0,041695	0,002065	0,002906	0,003115	0,001508	0,000946	0,001281
111				0,072182	0,002319	0,002608	0,002954	0,001835	0,000765	0,001479
112					0,002682	0,002917	0,003025	0,002209	0,000700	0,001639
113					0,002931	0,003214	0,003993	0,002520	0,000765	0,001702
114					0,002737	0,003333	0,006700	0,002771	0,000946	0,001592
115					0,002308	0,003269	0,011244	0,002956	0,001210	0,001355
116					0,002001	0,003059	0,017825	0,003058	0,001498	0,001083
117					0,001993	0,002737	0,026879	0,003060	0,001724	0,000844
118					0,002312	0,002313	0,039529	0,002958	0,001768	0,000682
119					0,002832	0,001932	0,059602	0,002785	0,001651	0,000625
120					0,003265	0,001732	0,109071	0,002666	0,001456	0,000682
121					0,003120	0,001757	0,907222	0,002921	0,001249	0,000844
122					0,002766	0,001979	0,269291	0,004291	0,001082	0,001083
123					0,002461	0,002304	0,080377	0,007165	0,000991	0,001355
124					0,002366	0,002574	0,048402	0,011627	0,001001	0,001592
125					0,002547	0,002560	0,032415	0,017839	0,001117	0,001702
126					0,002968	0,002205	0,021639	0,026144	0,001334	0,001639
127					0,003461	0,001836	0,013790	0,037375	0,001624	0,001479
128					0,003838	0,001650	0,008135	0,054074	0,001940	0,001281
129					0,004086	0,001733	0,004377	0,088016	0,002206	0,001097
130					0,004159	0,002069	0,002378	0,289191	0,002426	0,000962
131					0,004020	0,002539	0,002072	0,907222	0,002596	0,000904
132					0,003745	0,002906	0,002305	0,105097	0,002704	0,000938
133					0,003798	0,002795	0,002606	0,058085	0,002740	0,001066
134					0,005802	0,002487	0,002808	0,039322	0,002693	0,001279
135					0,010687	0,002185	0,002870	0,027381	0,002565	0,001554

Continued from table A.21.

					q					
y_σ	**4/3**	**5/3**	**7/3**	**8/3**	**10/3**	**11/3**	**13/3**	**14/3**	**16/3**	**17/3**
136					0,018618	0,002028	0,002803	0,018636	0,002382	0,001848
137					0,029979	0,002087	0,002634	0,012046	0,002232	0,002097
138					0,045851	0,002368	0,002381	0,007215	0,002311	0,002305
139					0,071372	0,002799	0,002055	0,003966	0,003036	0,002469
140						0,003207	0,001700	0,002209	0,004873	0,002580
141						0,003519	0,001431	0,001900	0,007854	0,002629
142						0,003716	0,001307	0,002096	0,012034	0,002605
143						0,003762	0,001343	0,002385	0,017514	0,002505
144						0,003631	0,001520	0,002605	0,024490	0,002343
145						0,003367	0,001783	0,002708	0,033384	0,002162
146						0,003250	0,002046	0,002693	0,045295	0,002072
147						0,004190	0,002187	0,002580	0,063991	0,002301
148						0,007460	0,002047	0,002386	0,111295	0,003301
149						0,013135	0,001726	0,002126	0,907222	0,005289
150						0,021369	0,001408	0,001801	0,271102	0,008291
151						0,032513	0,001214	0,001486	0,084313	0,012355
152						0,047544	0,001203	0,001258	0,053922	0,017568
153						0,071122	0,001385	0,001159	0,038946	0,024088
154							0,001718	0,001199	0,028627	0,032246
155							0,002102	0,001359	0,020695	0,042846
156							0,002378	0,001597	0,014427	0,058376
157							0,002310	0,001848	0,009526	0,090414
158							0,002073	0,002018	0,005855	0,287390
159							0,001800	0,001989	0,003340	0,907222
160							0,001589	0,001731	0,001940	0,107923
161							0,001505	0,001416	0,001635	0,062574
162							0,001580	0,001162	0,001769	0,044964

Continued from table A.21.

					q					
y$_\sigma$	**4/3**	**5/3**	**7/3**	**8/3**	**10/3**	**11/3**	**13/3**	**14/3**	**16/3**	**17/3**
163							0,001811	0,001042	0,002027	0,033709
164							0,002155	0,001088	0,002261	0,025200
165							0,002517	0,001294	0,002416	0,018407
166							0,002806	0,001616	0,002478	0,012940
167							0,003020	0,001965	0,002451	0,008623
168							0,003142	0,002209	0,002351	0,005365
169							0,003148	0,002156	0,002188	0,003116
170							0,003021	0,001948	0,001974	0,001848
171							0,002779	0,001693	0,001710	0,001544
172							0,002538	0,001477	0,001421	0,001652
173							0,002643	0,001356	0,001174	0,001891
174							0,003962	0,001366	0,001009	0,002124
175							0,006933	0,001516	0,000946	0,002294
176							0,011592	0,001785	0,000988	0,002382
177							0,018011	0,002123	0,001122	0,002388
178							0,026326	0,002434	0,001321	0,002324
179							0,036829	0,002684	0,001544	0,002199
180							0,050339	0,002866	0,001734	0,002025
181							0,070784	0,002965	0,001819	0,001806
182								0,002962	0,001710	0,001542
183								0,002843	0,001464	0,001277
184								0,002621	0,001187	0,001058
185								0,002374	0,000957	0,000916
186								0,002332	0,000824	0,000866
187								0,003044	0,000814	0,000909
188								0,005167	0,000932	0,001033
189								0,008721	0,001158	0,001216

Continued from table A.21.

					q					
y_σ	**4/3**	**5/3**	**7/3**	**8/3**	**10/3**	**11/3**	**13/3**	**14/3**	**16/3**	**17/3**
190								0,013742	0,001452	0,001425
191								0,020298	0,001744	0,001614
192								0,028516	0,001940	0,001728
193								0,038665	0,001908	0,001694
194								0,051501	0,001744	0,001498
195								0,070667	0,001526	0,001239
196									0,001315	0,000992
197									0,001156	0,000810
198									0,001083	0,000726
199									0,001113	0,000755
200									0,001249	0,000894
201									0,001476	0,001122
202									0,001761	0,001401
203									0,002048	0,001670
204									0,002285	0,001848
205									0,002473	0,001823
206									0,002604	0,001678
207									0,002667	0,001476
208									0,002649	0,001272
209									0,002540	0,001107
210									0,002347	0,001010
211									0,002109	0,001000
212									0,001936	0,001084
213									0,002078	0,001257
214									0,003053	0,001499
215									0,005104	0,001775
216									0,008240	0,002028

Continued from table A.21.

	q									
y_σ	**4/3**	**5/3**	**7/3**	**8/3**	**10/3**	**11/3**	**13/3**	**14/3**	**16/3**	**17/3**
217									0,012486	0,002238
218									0,017874	0,002404
219									0,024466	0,002517
220									0,032369	0,002569
221									0,041817	0,002547
222									0,053466	0,002445
223									0,070495	0,002266
224										0,002041
225										0,001849
226										0,001866
227										0,002446
228										0,003975
229										0,006458
230										0,009909
231										0,014347
232										0,019808
233										0,026346
234										0,034063
235										0,043177
236										0,054303
237										0,070431

Literature

Baffrey, R.
1926. Über den einfluß der schrittverkürzung auf die Überlastungsfähigkeit von drehstrommotoren. *Archiv für Elektrotechnik*, 16.

Di Tommaso, A., M. Caruso, F. Genduso, R. Miceli, and G. Galluzzo
2018. A general mathematical formulation for the determination of differential leakage factors in electrical machines with symmetrical and asymmetrical full or dead-coil multiphase windings. *IEEE Transactions on Industry Applications*, PP:1–1.

Heiles, F.
1953. *Wicklungen elektrischer Maschinen und ihre Herstellung*.

Heller, F. and W. Kauders
1935. Das görgessche durchflutungspolygon. *Archiv für Elektrotechnik*, 29:599–616.

Königshofer, T.
1956. *Die Wicklungen elektrischer Maschinen*.

Krall, R.
2015. *Permanentmagneterregte Mehrphasen-Synchronmaschine in Zahnspulenausführung einschließlich des phasendezimierten Betriebs*. PhD thesis.

Krondl, M.
1928. La dispersion differentielle dans les machines d'induction. *Revue Generale de l'Electricite*.

Kucera, J. and J. Hapl
1956. *Wicklungen der Wechselstrommaschinen*. VEB Verlag Technik Berlin.

Liwschitz, M.
1946. Differential leakage of a fractional-slot winding. *Electrical Engineering*, 65:314–320.

Liwschitz, M.
1949. Differential leakage of the different patterns of a fractional slot winding. *Transactions of the American Institute of Electrical Engineers*, 68:1129–1132.

Maier, G., H. Kofler, and J. P. Bacher
2005. The use of pitch factor in calculations of ac-machines with concentrated windings. *2005 European Conference on Power Electronics and Applications*, Pp. 5 pp.–P.5.

Müller, G., K. Vogt, and B. Ponick
2007. *Berechnung elektrischer Maschinen*.

Prechtl, A.
1994. *Vorlesungen über die Grundlagen der Elektrotechnik.*
Pyrhönen, J., T. Jokinen, and V. Hrabovcová
2008. *Design of Rotating Electrical Machines.*
Rader, G. F.
2013. *Entwicklung eines Berechnungsprogramms für die Erstauslegung von PSM mit vergrabenen Magneten und Oberflächenmagneten.*
Raskop, F.
1964. *Der Katechismus für die Ankerwickelei.*
Richter, R.
1952. *Lehrbuch der Wicklungen elektrischer Maschinen.*
Richter, R.
1954. *Elektrischer Maschinen, Vierter Band, Die Induktionsmaschinen.*
Schmidt, E.
2020. *Skriptum zum Seminar Elektrische Maschinen, Vertiefung, TU Wien.*
Schmidt, E.
2021. *Skriptum zur Vorlesung Elektrische Maschinen, TU Wien.*
Schuisky, W.
1960. *Berechnung elektrischer Maschinen.*
Sequenz, H.
1950. *Die Wicklungen elektrischer Maschinen.*